UNIVERSITY OF CALIFORNIA

Los Angeles

Transcriptional Regulation of Hemato-vascular Lineage Specification during Embryogenesis

A dissertation submitted in partial satisfaction of the

requirements for the degree Doctor of Philosophy

in Molecular, Cell and Developmental Biology

by

Dan Duan

2016

ABSTRACT OF THE DISSERTATION

Transcriptional Regulation of Hemato-vascular Lineage Specification

during Embryogenesis

by

Dan Duan

Doctor of Philosophy in Molecular, Cell and Developmental Biology

University of California, Los Angeles, 2016

Professor Hanna K.A. Mikkola, Chair

Cardiovascular and blood are the first functioning organ systems that need to be established during embryogenesis. Although individual regulators governing blood, vascular and heart development have been identified, we lack understanding of how these factors cooperate to enable precisely timed fate choices. Here, genetically modified mouse embryonic stem cells and embryoid body differentiation system were used to investigate how lineage specifying transcription factors (SCL, GATA1, GATA2, ETV2) exploit epigenetic landscape to regulate gene expression during mesoderm diversification to hemato-vascular and cardiac lineages. Our lab previously showed that transcription factor SCL specifies hematopoiesis and represses cardiogenesis during embryogenesis. In this thesis work, we determined that SCL directly binds to enhancers of both hematopoietic and cardiac genes that were epigenetically primed for

activation in mesoderm prior to SCL binding. The repression of cardiac fate was not caused by SCL dependent recruitment of co-repressors but possibly by SCL blocking the activation of these genes by cardiac transcription factors. Moreover, ChIP-seq, RNA-seq and functional analysis showed that SCL complex partners GATA1 and GATA2 are critical for SCL mediated endothelial to hematopoietic cell transition, but are dispensable for cardiac suppression by SCL. Finally, we demonstrated that SCL activates hematopoiesis and represses ectopic cardiogenesis in hemogenic endothelium independent of its upstream transcription factor ETV2. However, ETV2 cooperates with SCL in the activation of key hemato-vascular genes by establishing chromatin accessibility at its binding sites.

These data have increased our understanding of the transcriptional events regulating specification of mesodermal cells to hemato-vascular and cardiac fates, and provides new insights to the basic mechanisms of cardiovascular lineage choice. This knowledge may help develop better protocols for hematopoietic, endothelial and cardiac cell generation *in vitro* and thereby advance cell-based therapies for blood and cardiovascular disease.

The dissertation of Dan Duan is approved.

Luisa M. Iruela-Arispe

Siavash K. Kurdistani

Shuo Lin

Hanna K.A. Mikkola, Committee Chair

University of California, Los Angeles

2016

DEDICATION

This work is dedicated to my Mom Rui Zhang, and my Grandma Lianfang Li whose love, support and understanding made all of this possible,

and

to Dr. Hanna K.A. Mikkola whose mentorship and encouragement were indispensable to accomplish this work.

TABLE OF CONTENTS

LIST OF FIGURES

LIST OF ABBREVIATIONS

ESCs: Embryonic stem cells

iPSCs: Induced pluripotent stem cells

ICM: Inner cell mass

LIF: Leukemia inhibitory factor

MEFs: Mouse embryonic fibroblasts

HSCs: Hematopoietic stem cells

MSCs: Mesenchymal stem cells

EBs: Embryoid bodies

ChIP: Chromatin immunoprecipitation

VEGF: Vascular endothelial growth factor

HSPCs: Hematopoietic stem or progenitor cells

HSCs: Hematopoietic stem cells

AGM: Aorta-gonad-mesonephros region

ETS: E-twenty-six specific sequence

bHLH: Basic helix-loop-helix

EHT: Endothelial-to-hematopoietic transition

ATAC: Assay for transposase-accessible chromatin

PRC2: Polycomb-repressive complex 2

Acknowledgements

Chapter 2 was originally published in *The EMBO Journal*. Org, T. *, **Duan, D.** *, Ferrari, R., Montel-Hagen, A., Van Handel, B., Kerenyi, M. A., Sasidharan, R., Rubbi, L., Fujiwara, Y., Pellegrini, M., Orkin, S. H., Kurdistani, S. K., Mikkola, H. K. (2015). Scl binds to primed enhancers in mesoderm to regulate hematopoietic and cardiac fate divergence. *The EMBO Journal*. doi:10.15252/embj.201490542 * denotes equal contribution. ©EMBO

Chapter 3 is a version of **Duan, D.**, Org, T., Mikkola, H.K. ETV2 cooperates with SCL for timely gene activation during hemogenic endothelium specification. (in preparation)

Appendix was originally published in *Blood*. He, H., Xu, J., Warren, C. M., **Duan, D.**, Li, X., Wu, L., & Iruela-Arispe, M. L. (2012). Endothelial cells provide an instructive niche for the differentiation and functional polarization of M2-like macrophages. Blood, 120(15), 3152–62. doi:10.1182/blood-2012-04-422758 ©the American Society of Hematology.

I would like to thank Dr. Kouskoff (University of Manchester, United Kingdom) for kindly sharing *Etv2*^{KO}iSCL, *Etv2*^{KO}iETV2 ES cell lines for the work of Chapter 3. I would also like to thank the UCLA BSCRC Flow Cytometry Core for the assistance in FACS sorting and the UCLA Stem Cells Sequencing core for the assistance in ChIP sequencing, RNA sequencing and ATAC sequencing.

I would like to acknowledge our funding sources for this work. This work was funded by the California Institute for Regenerative Medicine (CIRM) New Faculty Award (RN1-00557), the Eli and Edythe Broad Center of Regenerative Medicine and Stem Cell Research at UCLA Research Award, American Heart Association (#14GRNT20480340), and Leukemia Lymphoma

Society Scholar Award (20103778) to H.K.A.M. D.D was supported by the government of P.R.C through the State Scholarship Fund (File No.2011624028) and 2016 UCLA Dissertation Year Fellowship. T.O was supported by Leukemia Lymphoma Society postdoctoral fellowship (57537-13) and by the European Union through the European Social Fund (Mobilitas Grant No. MJD284). A.M.H was supported by a fellowship from HFSP and American Society of Hematology. B.V.H was supported by the NIH/NHLBI T32 HL69766.

Biographical Sketch:

DAN DUAN

EDUCATION

09/07 – 07/11 B.S. in Life Science (National Key Courses), Sichuan University, China

PUBLICATIONS

Duan D, Org T, Mikkola, HK. ETV2 cooperates with SCL for timely gene activation during hemogenic endothelium specification. (in preparation)

Org T*, **Duan D***, Ferrari R, Montel-Hagen A, Van Handel B, Kerenyi MA, Sasidharan R, Rubbi L, Fujiwara Y, Pellegrini M, Orkin SH, Kurdistani SK, Mikkola, HK. 2015 Jan 6. Scl binds to primed enhancers in mesoderm to regulate hematopoietic and cardiac fate divergence. EMBO J. * denotes equal contribution.

He H, Xu J, Warren CM, **Duan D**, Li X, Wu L, Iruela-Arispe ML. 2012. Endothelial cells provide an instructive niche for the differentiation and functional polarization of M2-like macrophages. Blood 120:3152–62.

Wang H, Zuo B, Wang H, Ren L, Yang P, Zeng M, **Duan D**, Liu C, Li M. 2012. CGK733 enhances multinucleated cell formation and cytotoxicity induced by taxol in Chk1-deficient HBV-positive hepatocellular carcinoma cells. Biochem. Biophys. Res. Commun. 422:103–8.

Ou L, **Duan D**, Wu J, Nice E, Huang C. 2012. The application of high throughput siRNA screening technology to study host-pathogen interactions. Comb. Chem. High Throughput Screen. 15:299–305.

HONORS & AWARDS

UCLA Dissertation Year Fellowship 2015-2016

Graduate Fellowship from Chinese Scholarship Council 2011-2015

Travel Award granted by the International Society Hematology and Stem Cells for the Annual Meeting in Vienna, Austria Aug 2013

Travel Award granted by American Society of Hematology for the Annual Meeting in Atlanta, GA, United States Dec 2012

UCLA Cross-Disciplinary Scholars in Science and Technology Award for research Sept 2010

Sichuan University Excellent Student Award 2008-2011

National Scholarship 2008

INTERNATIONAL CONFERENCE PRESENTATIONS

"ETV2 and SCL cooperate to specify hemogenic endothelium and override cardiac fate choice during mesoderm". Poster presented at **Annual Meeting of International Society for Stem Cell Research (ISSCR), San Francisco, United States** June 2016

"Scl specifies hemogenic endothelium and represses cardiac fate independent of Etv2". Poster presented at **Keystone Symposia Conference, Hematopoiesis, Keystone, CO, United States,** Feb 2015

"Scl specifies hematopoietic fate and overrides cardiac fate in embryonic endothelium independent of Etv2". Poster presented at **Gordon Research Conferences, Vascular Cell Biology, Ventura, CA, United States** Jan 2015

"Scl represses cardiogenesis via distant enhancers during hemogenic endothelium specification". Talk presented at Plenary Session of **Annual Meeting of International Society for Hematology and Stem Cells (ISEH), Vienna, Austria** Sept 2013

"Scl/Tal1 Directly Activates Hematopoiesis and Represses Cardiogenesis during Mesodermal Diversification". Poster presented at **Annual Meeting of American Society of Hematology (ASH), Atlanta, GA, United States** Dec 2012

WORK & EXTRACURRICULARS

Graduate Industry Consultant Dec 2015-June 2016
UCLA Career Center
Helped build and deliver professional development curriculum and services specifically for Master's & PhD students. Organized employer information sessions, recruitment events and work on employer and alumni outreach.

Group Leader July 2014/2015
Cross-disciplinary Scholars in Science and Technology (CSST), UCLA
Led group discussion for the summer program of CSST and led the group of reviewers to pre-select candidates for the program interview

Teaching Assistant for MCDB 138: Developmental Biology Mar-June 2013
Department of Molecular, Cell and Developmental Biology, UCLA, Lecturer: Dr. Volker Hartenstein
Gave independent lectures and held office hours on developmental biology

Teaching Assistant for MCDB 168: Stem Cell Biology Mar-June 2014
Department of Molecular, Cell and Developmental Biology, UCLA, Lecturer: Dr. Leanne Jones
Led discussions on research papers about stem cell biology

Chapter 1:

Introduction

Preface

Pluripotent stem cells have the theoretical capacity to generate differentiated cells of any tissue, thus they hold immense potential in cell-based therapy to replenish an injured or diseased tissue. The sources for pluripotent stem cells include embryonic stem cells (ESCs) and induced pluripotent stem cells (iPSCs). ESCs serve as a good model to study the developmental process of cell type specific differentiation because they can be maintained and expanded in culture and further differentiate into multiple tissue specific cells. However, immunocompatible match with the recipients still need to be found when using general ESC-derived cells for regenerative treatment. Over the past decade, induced pluripotent stem cells (iPSCs) were reprogrammed from unipotent differentiated cells and regained pluripotency with the ability to generate multiple cell types. iPSCs are regarded as a promising resource for cell therapy since host-donor immune rejection can be overcome by patient specific iPSCs. Although various cell types such as hematopoietic, endothelial and cardiac cells can be differentiated from iPSCs (Itzhaki et al., 2011; Adams et al., 2013; Menon et al., 2015), fully functional and long lasting cells cannot be generated to replace the diseased tissue. Thus it is critical to understand how these cells are made during development.

Cardiovascular and blood systems are closely related both functionally and by their developmental origin. Malfunction in these organ systems during development or post-natal life is life-threatening, and thus they are important targets for cell based therapies. In the embryo, the specification of cardiovascular system starts during gastrulation. Blood vessels, hematopoietic cells and heart are all derived from lateral plate mesoderm (Kattman et al., 2006; Fehling et al., 2003; Chan et al., 2013). These fates first diverge when hemato-vascular mesoderm (or hemangioblasts) is separated from cardiac mesoderm. Thus, understanding how mesodermal

lineages diverge during embryogenesis to generate cardiovascular or hematopoietic stem/progenitor cells is an important step in advancing cell-based therapies for blood and cardiovascular disease.

Lineage specific regulators activate respective lineage programs for cell fate determination. However, how these regulators cooperate with each other to guide multipotent mesodermal cells to commit to hemato-vascular or cardiac fate is largely unknown. Moreover, the epigenetic landscape provides the platform for the lineage specification factors to activate or repress respective genes. Despite the critical role of epigenetic regulatory machinery, it is not known which factors establish and modify the epigenetic landscape necessary for lineage specification. Thus, there are important unanswered questions that require further investigation to improve the differentiation and reprogramming protocols for generating functional hematopoietic and endothelial cells for therapeutic application:

- How do the hematopoietic fate and cardiac fate diverge during mesoderm specification?
- How do the lineage specific transcriptional regulators specify endothelial and hematopoietic cells from cardiovascular mesoderm?
- How is the epigenetic landscape defined or exploited by lineage specific factors during mesoderm diversification?

1.1 Embryonic stem cells and embryoid body differentiation

1.1.1 ES cells and iPSC derived cells for regenerative medicine.

Embryonic stem cells (ESCs) are derived from the inner cell mass (ICM) of a pre-implantation embryo (Thomson et al., 1998). They can proliferate indefinitely and be maintained undifferentiated *in vitro* with leukemia inhibitory factor (LIF) (mouse ES cells) or bFGF (human ES cells) or by being cultured on a layer of mitotically inactivated mouse embryonic fibroblasts (MEFs) (Reubinoff et al., 2000). They are pluripotent cells that can generate cells of all three germ layers, and have the potential to differentiate into all types of cells in the body. However, the use of ESCs for regenerative medicine has been debatable due to potential ethical concerns with destroying the pre-implantation embryos for ES cell generation, and the additional challenges of immunocompatibility during transplantation. A novel technology was developed over the past 10 years to reprogram differentiated adult cells, such as fibroblasts, blood cells, etc. back to ES cell like stage. These induced pluripotent stem cells can be generated by ectopic expression of transcription factors, RNA molecules or chemicals that govern pluripotent state (Takahashi et al., 2006; Huangfu et al., 2008; Wesemann et al., 2012; Bao et al., 2013). In contrast to adult stem cells, such as bone marrow hematopoietic stem cells (HSCs) and mesenchymal stem cells (MSCs), which lose their differentiation and proliferation capacity after sustained culture (de Peppo et al., 2010), both ESCs and iPSCs can be maintained in culture and differentiated to desired lineage specific progenitors or precursors to replenish injured tissues. Thus, ESCs and iPSCs hold tremendous potential in cell therapy for regenerative medicine.

1.1.2 Embryoid bodies (EBs) recapitulate early development *in vitro*

In addition to promising regenerative application, ESCs can be used to gain insight of molecular regulation of early embryonic development due to their capability to recapitulate differentiation

process occurring during embryogenesis, which is difficult to assess *in vivo*, especially in human. In the absence of LIF (mouse) or bFGF (human), ESCs differentiate into multicellular aggregates known as embryoid bodies (EBs), which serve as a physiological *in vitro* model for the *in vivo* germ layer formation (Doss et al., 2012). All three germ layers, ectoderm, mesoderm and endoderm as well as their subsequent derivatives can be generated during EB differentiation (Stevens, 1960) (Figure 1.1). For example, mesodermal cells that express Flk1, indicating the formation of cardiovascular mesoderm, are generated from EBs by day 3. Later, EBs start to beat spontaneously, indicating that cardiomyocytes have been produced. In addition, flow cytometry analysis of cell surface markers shows that blood cells can be generated as well. Thus, ES cell derived EBs are appropriate tools for studying mesoderm diversification during early development.

Compared to *in vivo* study of embryonic development, the ESC system provides the possibility to produce sufficient number of lineage specific cells for subsequent molecular assays, such as gene expression and ChIP-sequencing analysis. Moreover, it is relatively easy to genetically modify ESCs to investigate the function of a given gene, or generate reporter cell lines to understand the spatial and temporal expression of a certain factor and thus better study its potential function during development (Doss et al., 2012; Gadue et al., 2005). Thus ESC derived EBs serve as a platform for developmental biology to discover novel regulatory mechanisms during differentiation.

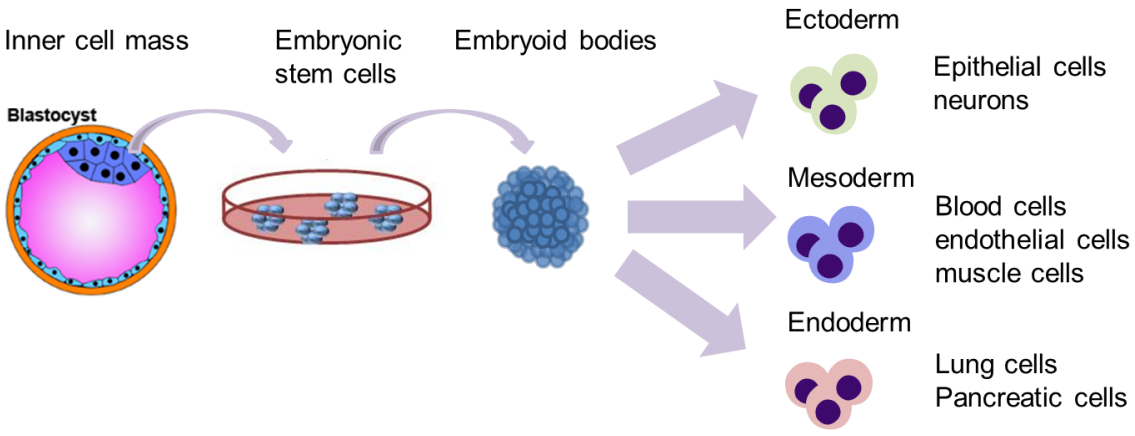

Figure 1.1 ES cells derivation and EBs differentiation

Embryonic stem cells are derived from the inner cell mass of the blastocyst. They can be maintained in culture and form embryoid bodies. EBs can differentiate into cells of three germ layers, endoderm, mesoderm and ectoderm, which further generate differentiated cells of the respective lineages.

1.2 Hemato-vascular development

1.2.1 Mesoderm diversification

Gastrulation gives rise to the three primary germ layers of an embryo: ectoderm, mesoderm and endoderm. All organs and tissues develop from these three germ layers. During embryonic development, mesoderm specification is initiated with formation of a primitive streak on the surface of the epiblast and creates a mesodermal layer between the endoderm and the ectoderm (Gilbert, 2000a). Mesoderm is composed of three important components: the paraxial mesoderm, the intermediate mesoderm and the lateral plate mesoderm. The paraxial mesoderm forms the somites, which give rise to skeletal muscle, cartilage and bone, as well as dermis of skin. The intermediate mesoderm, which connects the paraxial with the lateral plate mesoderm, differentiates into kidneys, gonads and the adrenal glands. The lateral plate mesoderm gives rise

to the vascular system, heart and blood (Gilbert, 2000b). Lineage specific transcription factors are responsible for activating designated programs driving the differentiation of a particular cell fate. For example, ETV2, TAL1/SCL and GATA2 are critical for hemato-vascular development (Sumanas et al., 2008; Kataoka et al., 2011a) and HAND1, HAND2, GATA4 and GATA6 are indispensable for cardiac differentiation (Niu et al., 2008).

During vertebrate embryonic development, the nascent mesodermal cells of primitive streak are specified into cardiovascular precursors that express Flk1, the vascular endothelial growth factor receptor 2 (VEGFR2) (Fehling, 2003). $Flk1^{+}$ mesoderm further gives rise to 2 groups of cells: hemangioblasts, the assumptive common progenitor for both endothelial and hematopoietic cells, and cardiac progenitors, capable of differentiating to cardiac cells (Figure 1.2). VEGF signaling is considered to initiate the specification of cardiovascular mesoderm through Flk1 (Fehling, 2003). Indeed, mouse embryos deficient of Flk1 completely lack hematopoietic and endothelial cells due to inability of the mesoderm to migrate to a correct location (Shalaby et al., 1995). In zebrafish, the deficiency of Flk1 results in less significant hemato-vascular defect (Habeck et al., 2002; Covassin et al., 2006; Bahary et al., 2007), whereas a mutation of the gene functioning upstream of Flk1, called *cloche*, results in impaired hemato-vascular specification (Stainier et al., 1995; Liao et al., 1998).

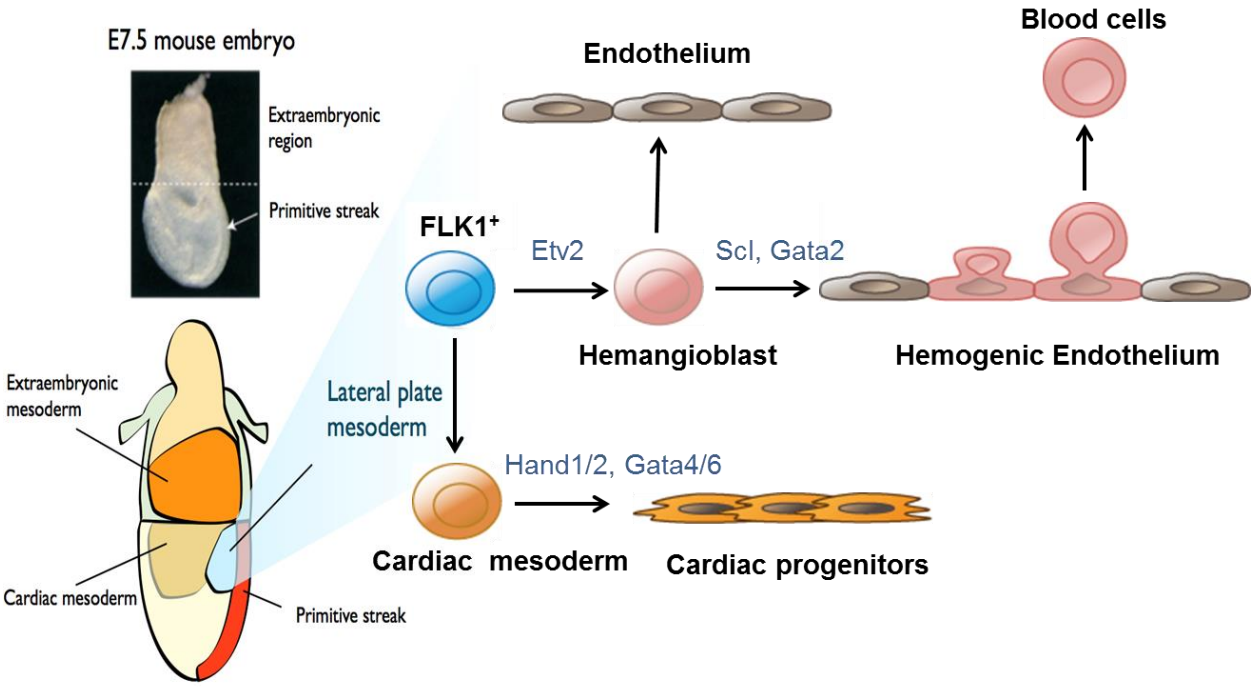

Figure 1.2 Mesoderm diversification

Mesoderm is formed during gastrulation. The lateral plate mesoderm marked by Flk1 gives rise to hemangioblasts, which generates endothelial cells and hematopoietic cells, and cardiac mesoderm which differentiates to cardiac cells.

1.2.2 Vascular development

One of the first organ systems to develop in embryo is the vasculature, which provides nutrition for other organogenesis. As early as day 7.5 of mouse embryonic development at gastrulation stage, early vasculature is found in the extraembryonic yolk sac blood island (Choi, 2002), which subsequently form the vascular network called primary plexus. This is followed by vascular remodeling which leads to the formation of complex vasculature in the yolk sac. In the embryo proper, blood vessel formation is initiated from angioblasts (Flamme et al., 1997) which establishes the vasculature such as dorsal aorta, vitelline vessels as well as primary vascular

network in lungs, spleen and heart (Risau, 1997). These vessels are lined by endothelial cells and further specified into arteries, veins and capillaries depending on the presence of smooth muscle cells and extracellular matrix surrounding them. Two major processes have been identified for vasculature formation: 1. Vasculogenesis, which is a *de novo* process where vessels are directly formed by endothelial cells differentiated from angiogenic precursors. 2. Angiogenesis, where new blood vessels are branching out from the preexisting ones by expansion of endothelial cells (Poole and Coffin, 1989; Flamme et al., 1997). During vascular specification, multiple master regulators have been identified. For example, ETV2 is the critical transcription factor for vascular development, in the absence of which the hemangioblasts will fail to form (Lee et al., 2008; Ferdous et al., 2009). Although SCL is not required for vasculogenesis, it has been shown that large vessels are missing and the vasculature in SCL deficient yolk sac is disorganized, indicating its role in vascular remodeling (Robb et al., 1995; Shivdasani et al., 1995; Porcher et al., 1996).

1.2.3 Hematopoietic development

Embryonic hematopoiesis generates both differentiated blood cells for the embryo's immediate needs, as well as hematopoietic stem cells that sustain life-long need for blood cells. This process occurs in three waves. The first wave is called primitive hematopoiesis, which originates from the blood island of yolk sac at mouse embryonic day E7.5 and produces primitive erythroid cells, macrophages and megakaryocytes. These cells meet the immediate needs of the embryos for oxygen and nutrition but do not last into adulthood. The primitive erythroid cells enter circulation with an intact nucleus and enucleate only later in development. The second wave, also called transient definitive wave, of hematopoiesis starts right after the primitive wave at around E8.25, generating multipotent myeloid and erythroid progenitors that give rise to

definitive myeloid and red blood cells (Mikkola et al., 2003). However, these precursors lack robust lymphoid potential and cannot self-renew. The last wave, known as the long-term definitive wave, generates self-renewing, multipotent hematopoietic stem cells (HSCs) that are capable of differentiating into erythroid, myeloid and lymphoid cells. HSCs arise from specialized endothelium, called hemogenic endothelium, of ventral wall of dorsal aorta and other major arteries (Bertrand et al., 2010; Boisset et al., 2010) in multiple anatomic locations including the aorta-gonad-mesonephros region (AGM) (Kyba et al., 2002; Galic et al., 2006), yolk sac (de Bruijn et al., 2000), and the placenta (Rhodes et al., 2008). The definitive wave does not emerge until E10.5 (Kumaravelu et al., 2002). Once emerged, HSCs will migrate to fetal liver for active expansion until later when they move to bone marrow and acquire quiescence (Kim et al., 2007) (Figure 1.3).

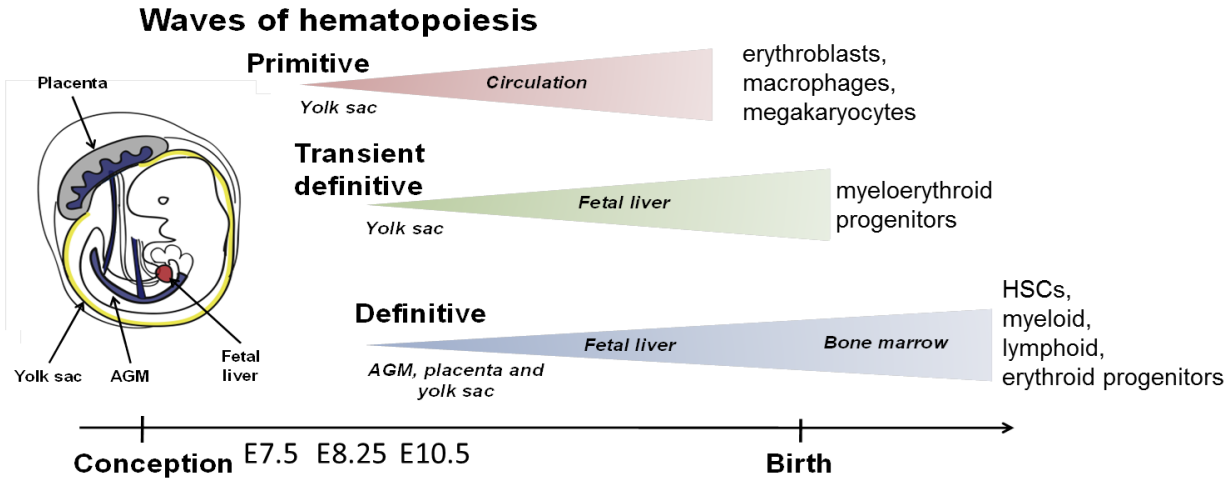

Figure 1.3 Waves of embryonic hematopoiesis

The primitive wave starts in E7.5 mouse yolk sac and produces primitive red blood cells, macrophages and megakaryocytes, which enter into circulation. The transient definitive wave generates myelo-erythroid progenitor cells in the E8.25 yolk sac, which migrate to fetal liver for

further differentiation. The definitive wave produces multipotent, self-renewing hematopoietic stem cells from AGM, yolk sac and placenta from E10.5. These cells migrate to the fetal liver for expansion, and eventually reside in the bone marrow.

1.3 ETV2/ER71/ETSRP in hemato-vascular development

The first transcription factor indispensable for the generation of endothelial and hematopoietic progenitors is ETV2/ER71/ETSRP. ETV2 is an E-twenty-six specific sequence (ETS) transcription factor harboring a conserved ETS DNA binding domain (Hollenhorst et al., 2004) and binds to GGA(A/T) consensus DNA regions (Lelièvre et al., 2001; Sharrocks, 2001). Unlike the other ETS family members, such as FLI1, ETS1 and PU.1 which are continuously required for hemato-vascular development (Hollenhorst et al., 2004; Dejana et al., 2007; Randi et al., 2009; Ciau-Uitz et al., 2013; Findlay et al., 2013), ETV2 is only transiently expressed during a short developmental window (Ferdous et al., 2009; Kataoka et al., 2011b; Lee et al., 2008). The expression of ETV2 first appears in E7.0 to E7.5 mesodermal cells during gastrulation (Figure 1.4). Shortly after, ETV2 expression is detected in large vessels including dorsal aorta, cardinal vein as well as endocardium. Similarly, during ES cell differentiation, ETV2 expression starts from EB day 3 and ceases around day 5 (Lee et al., 2008).

ETV2 resides on top of the transcription factor hierarchy required for hemato-vascular development, and specifies the mesodermal precursor that gives rise to hematopoietic and endothelial progenitors, called as the hemangioblast, from $Flk1^{+}PDGFRa^{+}$ primitive mesoderm (Kataoka et al., 2011; Sakurai et al., 2006). ETV2 also marks hemogenic endothelium at the onset of blood development (Wareing et al., 2012). ETV2 deficient embryos die around E9.0 due to complete failure of vasculature and blood development (Lee et al., 2008). In agreement of its

role in endothelial and hematopoietic development, overexpression of *Etv2* leads to expansion of hematopoietic and vascular endothelial area (Lee et al., 2008). In addition, ectopic induction of *Etv2* in differentiating mouse ESCs increases hemo-angiogenic mesoderm population (Liu et al., 2013). ETV2 is known to interact with other proteins to form complex for targeted gene activation. FOXC2, GATA2 and OVOL2 have all been shown to interact with ETV2 and promote gene expression for endothelial and hematopoietic differentiation (Dejana et al., 2007; Sharrocks, 2001; Verger and Duterque-Coquillaud, 2002; Kim et al., 2014; Shi et al., 2014). Moreover, ETV2 CHIP-seq data shows that ETV2 directly binds to the promoter and enhancers of its regulated targets and activates the downstream genes. Among them are critical hematopoietic regulators *Scl*, *Gata2*, *Meis1* as well as vascular endothelial factors *Fli1*, *Sox7*, *Flt4*, *Dll4* (Liu et al., 2015).

In addition to specifying hemato-vascular lineages during development, presence of ETV2 has been shown to correlate with repression of cardiogenesis. Lack of ETV2 in mouse embryos leads to expansion of $Flk1^{+}PDGFRa^{+}$ cardiogenic mesoderm as well as upregulation of cardiac genes (Lee et al., 2008; Liu et al., 2012). Furthermore, vascular endothelial and endocardial progenitors ectopically differentiate into cardiomyocytes in ETV2 deficient zebrafish embryos (Palencia-Desai et al., 2011; Liu et al., 2013). On the other hand, failure to repress ETV2 expression in fish embryos results in expansion of endocardial cells at expense of myocardial population (Schupp et al., 2014). These results imply that ETV2 expression demarcates the divergence of cardiomyocytic and endocardial/endothelial fates.

Moreover, ETV2 is a potent reprogramming factor able to convert non-endothelial to endothelial cells, which is promising as a cell based therapeutic reagent for treating cardiovascular diseases. By overexpressing ETV2 alone, human dermal fibroblasts can be reprogrammed into endothelial

cells (Morita et al., 2015). Similarly, skeletal muscle can be converted into endothelial cells in zebrafish (Veldman et al., 2013).

1.4 SCL and its complex in hematopoietic development

As the direct downstream target of ETV2, the basic helix–loop–helix transcription factor SCL/*Tal1,* which binds to the conserved DNA motif of E-BOX (CANNTG), is also critical for the development of the hematopoietic system. SCL is first expressed in mouse embryos at day E7.5, localizing at the sites of hematopoiesis in both extraembryonic tissues such as the blood islands of the yolk sac, placenta, as well as the embryo proper including dorsal aorta, and even endocardium (Kallianpur et al., 1994). SCL expression is also found in multiple hematopoietic cell types such as HSCs, erythroid and megakaryocytic cells, and its expression is highly conserved across vertebrates (Barton et al., 2001; Göttgens et al., 2002). SCL deficient mouse embryos die by E9.5 with a complete absence of hematopoietic cells, whereas the endothelial population is present (Robb et al., 1995; Shivdasani et al., 1995). However, vascular abnormalities of vitelline artery and vein (Visvader et al., 1998) were observed in the absence of SCL, suggesting that SCL has a role in vasculogenesis. Moreover, the expression of multiple important hematopoietic genes such as *Gata1,* critical for red blood cell development (Fujiwara et al., 2004), *Pu.1*, essential for myeloid development, and *Runx1* which is critical for HSC emergence from hemogenic endothelial cells (Lancrin et al., 2009), are dependent on SCL.

Ectopic induction of SCL expression in ETV2 deficient mesoderm has been shown to restore hemangioblast development, based on flow cytometry and methylcellulose assays (Kataoka et al., 2011; Wareing et al., 2012). Like ETV2, SCL is also required during a specific developmental window for hematopoiesis. By inducing SCL expression from E7 to E8.5 (EB differentiation day 2-4) in the SCL deficient embryos, hemogenic endothelial cells could be

rescued, but not if it was induced at later stages (Endoh et al., 2002). Moreover, when SCL is deleted by TIE2-Cre, which is expressed shortly after SCL in endothelial and hemogenic endothelial cells, HSC population is intact in the fetal liver, indicating that SCL is no longer essential for HSC development, but continues to be required for erythroid and megakaryocytic differentiation (Schlaeger et al., 2005; Chan et al., 2007; Souroullas et al., 2009). Another bHLH transcription factor LYL1 is redundant with SCL in HSC maintenance.

Given the critical function of SCL in hematopoietic development, it is perhaps surprising that direct DNA binding by SCL is not required for hematopoietic specification (Porcher et al., 1999; Kassouf et al., 2008). Hematopoietic regulators are rather activated by SCL centered protein complex. SCL forms a heterodimer with ubiquitously expressed bHLH factor E2A/E47 which is then bridged by the molecule LMO2 and LDB1 to form the core complex (SCL:E47:LMO2:LDB1). Both LMO2 and LDB1 are critical for SCL mediated regulation of hematopoiesis. In the absence of LMO2 or LDB1, hematopoietic cells cannot be generated even when SCL is present (Schlaeger et al., 2004; Mukhopadhyay et al., 2003; Lécuyer et al., 2007; Warren et al., 1994). Furthermore, the core complex of SCL recruits additional partners for specific functions. For example, in erythroid cells, LMO2 recruits hematopoietic-specific transcription factor GATA1 for gene activation (Wadman et al., 1997; Kassouf et al., 2010). GATA2 also interacts with SCL for hematopoietic gene activation during hematopoietic stem/progenitor cell development (Wilson et al., 2010). A combination of cofactors and chromatin remodelers ETO2, mSin3A, P300, PCAF, and LSD1 all could be recruited for the activation or repression of specific genes during specification of erythropoiesis (Schuh et al., 2005; Li et al., 2012).

In addition to establishing hematopoietic lineages by promoting the formation of hemogenic

endothelium, SCL is also found to be critical for repression of ectopic cardiogenesis during development (Figure 1.4). Overexpression of *Scl* in ES cells result in expansion of hematopoietic cells while the expression of cardiac markers and the formation of beating cardiomyocytes is compromised (Ismailoglu et al., 2008). Moreover, our lab showed that *Scl* deficient mouse embryos turn on ectopic cardiac program in the hemogenic tissue yolk sac and endocardium, with generation of $CD31^{+}PDGFRa^{+}$ cardiac progenitors and beating cardiomyocytes (Van Handel et al., 2012). In agreement with its temporal role during development, timely deletion of SCL starting at E 7.5, but not at E 8.5, results in ectopic cardiogenesis in yolk sac (Van Handel et al., 2012). These data suggest that the cardiac fate repression role of SCL in hemogenic tissues is also required for a limited developmental window. However, the mechanism of repressing cardiogenesis mediated by SCL is not clear.

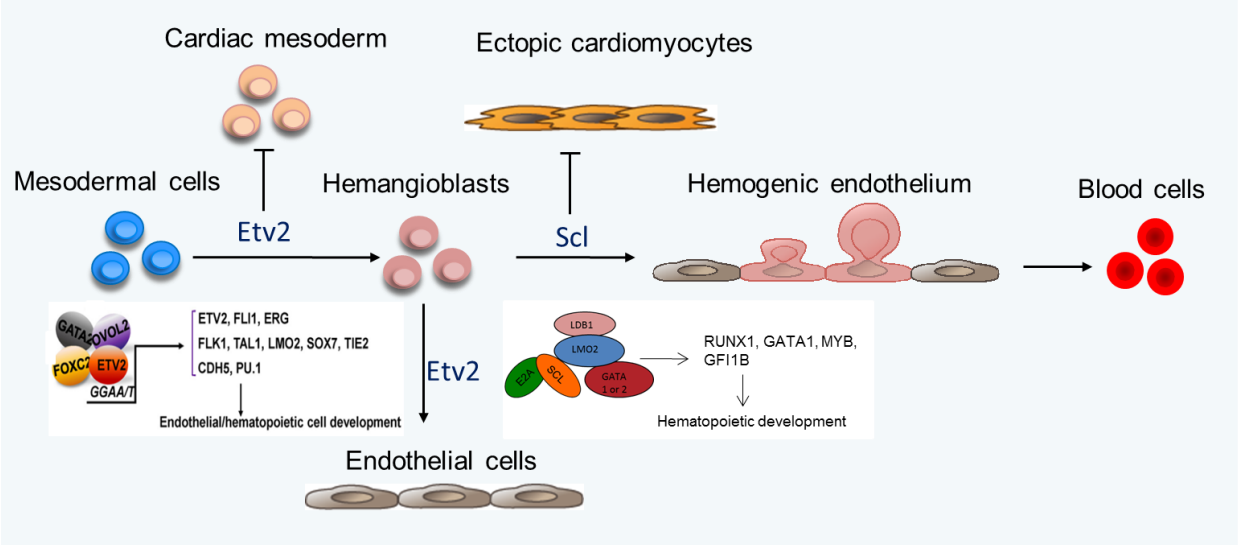

Figure 1.4 ETV2 and SCL in hemato-vascular development

ETV2 forms an activation complex with FOXC2, GATA2, and OVOL2 to activate endothelial/hematopoietic program for hemangioblasts and endothelial specification. ETV2 is also shown to repress cardiac mesoderm formation. SCL activates hematopoietic genes while repressing ectopic cardiogenesis. SCL acts in a complex containing E2A, LDB1, LMO2 and

GATA2.

1.5 Hemogenic endothelium

Given the close functional and anatomical relation of endothelial cells and hematopoietic cells, it has been postulated that HSCs are generated from endothelial precursors. Recent studies have now proven that multipotent hematopoietic stem or progenitor cells (HSPCs) are indeed generated directly from endothelial cells lining the blood vessels. Specialized endothelial cells that acquire hematopoietic potential to give rise to HSPCs during development in vertebrates are called "hemogenic endothelium". Hemogenic endothelium exists transiently in the AGM (Godin et al., 1993; Cumano et al., 1996; Medvinsky and Dzierzak, 1996; Gritz and Hirschi, 2016), vasculature of yolk sac (Samokhvalov et al., 2007; Dzierzak and Speck, 2008), placenta (Gekas et al., 2005), umbilical arteries (de Bruijn et al., 2000; Zovein et al., 2010; Gordon-Keylock et al., 2013) and even endocardium (Nakano et al., 2013). Multiple real-time imaging and lineage tracing studies have documented the emergence of hematopoietic cells from the ventral wall of dorsal aorta in mice and zebrafish (Kissa and Herbomel, 2010; Boisset et al., 2010; Bertrand et al., 2010). Although critical for hematopoietic system, endothelial cells that are capable of generating hematopoietic cells only constitute a very small (around 1-3%) and transient fraction of the endothelial population (Goldie et al., 2008; Marcelo et al., 2013). Hemogenic endothelium harbors both endothelial and hematopoietic markers including but not limited to CD31, TIE2, CD41, VE-cadherin and Flk1 (Sánchez et al., 1996; Yoder et al., 1997; North et al., 2002; Taoudi et al., 2005; Taoudi and Medvinsky 2007; Taoudi et al., 2008; Medvinsky et al., 2011).

The process when HSPCs emerge from hemogenic endothelium is known as the endothelial-to-hematopoietic transition (EHT) (Lancrin et al., 2009) (Figure 1.5). This event is precisely regulated by transcription factors as well as cell-cell interactions and signaling in the

microenvironment. Specific transcriptional regulators are critical for the specification of hemogenic endothelium as well as EHT process. As mentioned before, the helix-loop-helix transcription factor SCL and its complex partners (GATA2, LMO2) are critical for hematopoietic specification, in the absence of which both primitive and definitive hematopoiesis are impaired, and hemogenic endothelium is not specified (Van Handel et al., 2012; Minegishi et al., 1999; Ling et al., 2004; Yamada et al., 1998; Yamada et al., 2000). SCL's downstream transcription factor RUNX1 (AML1) is an essential regulator of EHT during hematopoiesis, and its deficiency prevents blood formation from hemogenic endothelium (Lacaud et al., 2002; Liakhovitskaia et al., 2014). RUNX1 is precisely required during the process of EHT to increase hematopoietic gene expression and repress endothelial program, but not after EHT (Rybtsov et al., 2011). In addition, GFI1/ GFI1B, the downstream targets of RUNX1, are responsible for the morphological change and release of round blood cells from flattened endothelial cells (Lancrin et al., 2012). Recently, the arterial regulator SOX17 is shown to be important for the repression of hematopoietic program to ensure the expansion and maturation of hemogenic endothelium that will give rise to HSPCs. It is then downregulated by RUNX1 in the hemogenic endothelium for the generation of hematopoietic cells via the EHT process (Clarke et al., 2013; Nakajima-Takagi et al., 2013; Bos et al., 2015).

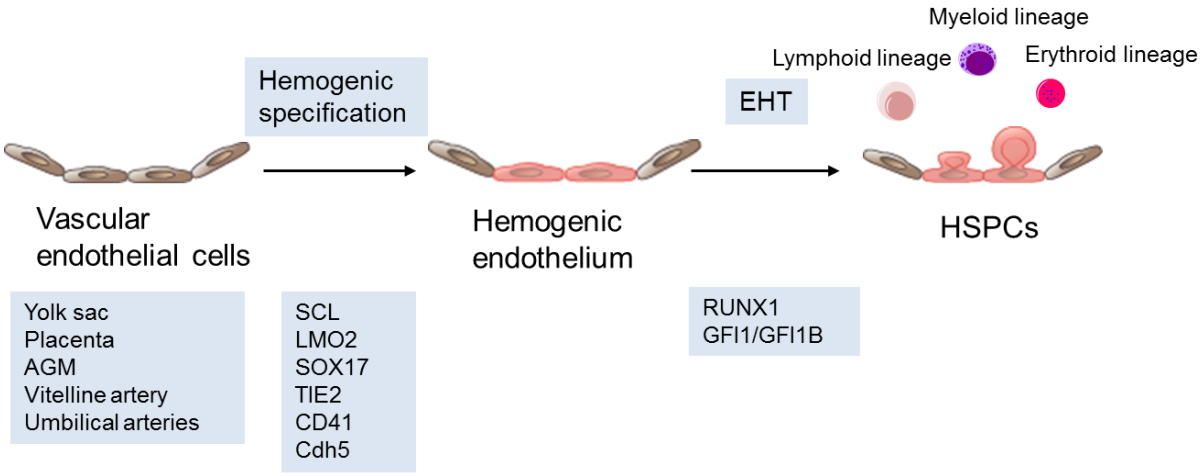

Figure 1.5 Hemogenic endothelium specification and endothelial to hematopoietic transition (EHT)

A subset of endothelial cells lining the large vessels in midgestation mouse embryos can be specified to hemogenic endothelial cells, which then give rise to hematopoietic stem/progenitor cells (HSPCs) through the process of endothelial to hematopoietic transition (EHT)

1.6 Dynamic epigenetic landscape during specification

1.6.1 Epigenetic modification

During lineage specification, lineage specific genes need to be activated while the alternative cell fate program has to be silenced. Epigenetic landscape where the chromatin or DNA is non-hereditarily modified at certain regulatory sites of genes is critical for cell fate determination. Two major epigenetic modifications that can control the expression of genes at the transcriptional level are histone modifications and DNA methylation. Genomic DNA in eukaryotic nuclei is packed into a compact structure, called chromatin, with histone protein H2A, H2B, H3 and H4. The lysine residues on these histones can be modified with mono-methylation,

tri-methylation, acetylation, etc. These modifications have been demonstrated to control the accessibility of the chromatin for transcription factors, thus regulating gene expression (Martin and Zhang, 2005). In contrast to modification at protein level, DNA methylation occurs at selected CpG islands around the regulatory DNA regions and is known to permanently silence gene expression (Lister et al., 2009).

Overall, active genes generally harbor H3K4me3 at promoters, and H3K4me1, H3K4me2 and H3K27ac at enhancers, while repressed genes can contain H3K27me3, H3K9me3 and/or DNA methylation. Recently, it has been reported that during development, the regulatory sites of critical developmental genes are enriched for both H3K4me3 (active mark) and H3K27me3 (repressive mark). These genes are silent in ES cells but become activated during differentiation (Azuara et al., 2006; Bernstein et al., 2006; Pan et al., 2007; Zhao et al., 2007) and their "poised" epigenetic state facilitates lineage specific transcription factor binding during differentiation (Szutorisz and Dillon, 2005). As lineage specific genes become active during differentiation, they lose the repressive H3K27me3 marks while maintaining H3K4me3 on their regulatory regions. In contrast, the pluripotent genes and alternative lineage specific genes gradually lose H3K4me3 while maintaining H3K27me3 and become silenced (Wamstad et al., 2012; Paige et al., 2012).

Epigenetic landscape establishes and maintains a permissive environment for lineage specific transcription factors to bind and specify certain cell fate (Szutorisz et al., 2005; Xu et al., 2011). The presence of H3K4me1 and H3K4me2 has been shown to facilitate the binding of 'pioneer factors', which further open up the chromatin for full activation by transcription factors (Zaret and Carroll, 2011). Moreover, when DNA is accessible, the histones around are typically marked by H3K4me1 and H3K27ac. A couple of methods are used to detect the accessibility of

chromatin such as DNase I, MNase and ATAC, where specific enzyme (DNase, nuclease, transposase) is used to access and cut the open chromatin followed by deep sequencing.

1.6.2 Epigenetic modification at enhancers

Enhancers are important cis-regulatory elements for gene activation. Enhancer sequences contain DNA motifs, which serve as binding sites for sequence-specific transcription factors (Figure 1.6). They typically locate far away from transcription start site. Enhancers can activate transcription independent of the location, distance or orientation relative to the gene promoters (Banerji et al., 1981). Sometimes enhancers could even induce the transcription of genes located in a different chromosome (Geyer et al., 1990; Lomvardas et al., 2006). Active enhancers are typically at open chromatin where the DNA is accessible and the histones around which are marked by H3K4me1 and H3K27ac.

Two complimentary hypotheses have been proposed by which enhancers regulate transcription: chromatin looping formation with promoter and enhancer RNA. Experimental evidence by fluorescence *in situ* hybridization (FISH) and, more recently, by chromosome conformation capture (3C) (Dekker et al., 2002) suggest that physical association of distant enhancers to promoter is required for the recruitment of RNA polymerase II and initiation of transcription (Bulger and Groudine, 1999; Engel and Tanimoto, 2000; West, 2005). Recently, it has been reported that the transcription of the enhancer, product of which called enhancer RNA, is also shown to be positively correlated with mRNA level and likely has a role in transcription regulation (Lei and Corces, 2006; Yao et al., 2010).

1.6.3 Epigenetic modulators

H3K4 methylation marks are shown to be deposited by several H3K4 methyltransferases that belong to the MLL family (Ruthenburg et al., 2007). As for the removal of the H3K4 methylation for the gene which become repressed, several members of the JmjC-domain-containing family of demethylases, especially LSD1 can demethylate mono- and di-methylated lysines (Shi et al., 2004; Klose et al., 2007). LSD1 has also been shown to assist in downregulating pluripotent gene expression by demethylating H3K4 at the regulatory regions during differentiation (Whyte et al., 2012).

The Polycomb-repressive complex 2 (PRC2), which mediates H3K27me3 modification contain EZH1 or EZH2, SUZ12 and EED. It has been shown that PRC2 plays an important role in suppressing developmental gene expression to maintain the pluripotent state of ES cells by mediating H3K27 methylation at the regulatory domains (Boyer et al., 2006; Lee et al., 2006). Next generation sequencing analysis (ChIP-seq, RNA-seq) revealed that PRC complex is enriched in high H3K27me3 regulatory region and modulates the expression of developmental regulators (Boyer et al., 2006; Lee et al., 2006). Moreover, PRC2 deficient mouse ES cells failed to deposit H3K27me3 and resulted in ectopic induction of key developmental genes (Azuara et al., 2006). Embryos lacking EZH2, the histone methyltransferase catalytic subunit of PRC2, are not able to form the primitive streak from gastrulation (Lachner et al., 2001). Similarly, deletion of the other core components of PRC2, such as SUZ12 and EED also leads to early developmental defect (Faust et al., 1995; Pasini et al., 2004; Chen and Dent, 2014).

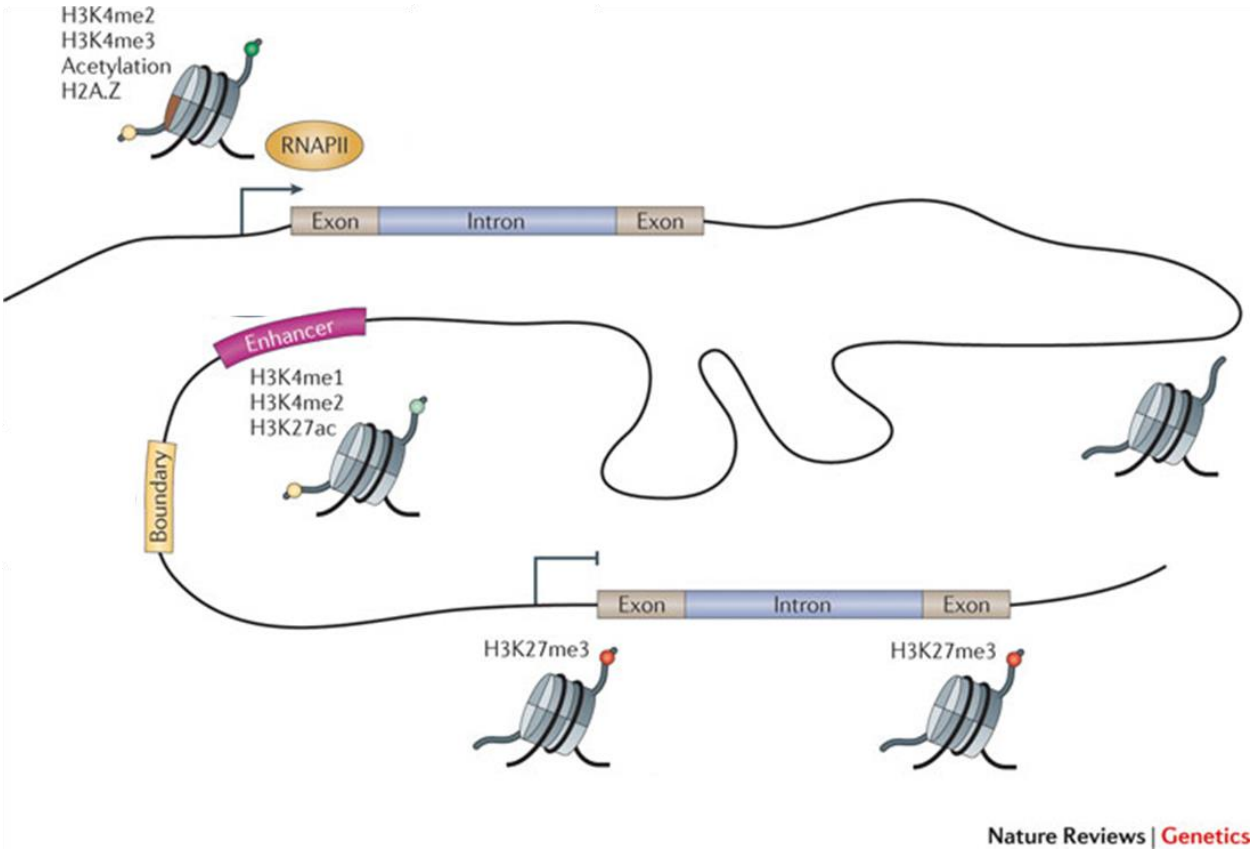

Figure 1.6 Epigenetic landscape for gene expression

Promoters, gene bodies, and an enhancer are indicated on a schematic genomic region. Active promoters are commonly marked by H3K4me2/3 and acetylation. Repressed genes are marked by H3K27me3. Enhancer is enriched for H3K4me1, H3K4me2, and H3K27ac. The active enhancer can form loop with the promoter to recruit RNA polymerase II for gene activation. Adapted from (Zhou et al., 2011)

Aims of this dissertation

Given that both SCL and ETV2 have been identified as critical players during mesoderm specification to hemato-vascular lineages and repression of ectopic cardiogenesis, we utilized ESCs and EB differentiation system to understand how SCL and ETV2 co-regulate cell fate at transcriptional and epigenetic level.

Aim1: To assess how SCL regulates gene expression and exploits the epigenetic landscape to mediate hematopoietic vs. cardiac fate choice during mesoderm specification

Previous studies have shown that SCL is critical for hematopoietic gene activation and cardiac gene repression during mesoderm diversification (Van Handel et al., 2012). The requirement for SCL only for a short developmental window to repress ectopic cardiogenesis in endothelial cells also implies dynamic changes in the epigenetic landscape. ChIP-sequencing for SCL was conducted to identify whether SCL directly regulates both fates by binding to their regulatory regions. ChIP-sequencing of multiple histone marks was performed in WT and SCL deficient ESC derived mesodermal cells to understand how SCL modifies and exploits the epigenetic landscape for cell fate determination.

Aim2: To investigate the function of SCL's complex partners GATA1 and GATA2 in hemato-vascular specification and cardiac repression

In the absence of GATA1 and 2, hematopoietic progenitors in mouse embryos are dramatically reduced, which is similar to SCL deficient mouse phenotype (Porcher et al., 1996; Robb et al., 1996; Shivdasani et al., 1995; Robb et al., 1995). GATA 1 and GATA 2 are induced by SCL, and form a complex with SCL in hematopoietic cells to activate gene expression (Wilson et al.,

2010). To understand whether GATA1 and GATA2 are required for hematopoietic vs. cardiac fate choice, endothelial cells derived from WT, *Scl*^{KO} and *Gata1&2*^{KO} ESCs were subjected to RNA sequencing and functional assays for endothelial cell differentiation potential.

Aim3: To define the function of SCL's upstream transcription factor ETV2 in hemato-vascular specification and cardiac repression

Apart from SCL, so far, the only hemato-vascular transcription factor that shows cardiac derepression phenotype in loss of function studies is ETV2/ER71/ETSRP(Liu et al., 2012; Palencia-Desai et al., 2011). ETV2 is essential for generating endothelial cells as well as activating SCL, and thereby distinguishes the hemato-vascular branch from cardiac mesoderm. To understand whether ETV2 is directly involved in cardiac repression and how ETV2 regulates the hemato-vascular program, functional rescue assays and RNA sequencing were performed in ESC derived EBs and endothelial cells by overexpressing SCL in ETV2 deficient cells. Analysis of ETV2 and SCL binding and ATAC sequencing was used to elucidate the role of ETV2 in the establishment of epigenetic landscape in the genes it activates.

Aim 1 and Aim 2 are addressed in Chapter 2, which was published in EMBO Journal in 2015. Aim 3 is addressed in Chapter 3, which was under preparation for submission.

Bibliography

Adams WJ, Zhang Y, Cloutier J, Kuchimanchi P, Newton G, Sehrawat S, Aird WC, Mayadas TN, Luscinskas FW, García-Cardeña G. 2013. Functional vascular endothelium derived from human induced pluripotent stem cells. Stem cell reports 1:105–13.

Azuara V, Perry P, Sauer S, Spivakov M, Jørgensen HF, John RM, Gouti M, Casanova M, Warnes G, Merkenschlager M, et al., 2006. Chromatin signatures of pluripotent cell lines. Nat. Cell Biol. 8:532–8.

Bahary N, Goishi K, Stuckenholz C, Weber G, Leblanc J, Schafer CA, Berman SS, Klagsbrun M, Zon LI. 2007. Duplicate VegfA genes and orthologues of the KDR receptor tyrosine kinase family mediate vascular development in the zebrafish. Blood 110:3627–36.

Banerji J, Rusconi S, Schaffner W. 1981. Expression of a beta-globin gene is enhanced by remote SV40 DNA sequences. Cell 27:299–308.

Bao X, Zhu X, Liao B, Benda C, Zhuang Q, Pei D, Qin B, Esteban MA. 2013. MicroRNAs in somatic cell reprogramming. Curr. Opin. Cell Biol. 25:208–14.

Barton LM, Gottgens B, Gering M, Gilbert JG, Grafham D, Rogers J, Bentley D, Patient R, Green AR. 2001. Regulation of the stem cell leukemia (SCL) gene: a tale of two fishes. Proc. Natl. Acad. Sci. U. S. A. 98:6747–52.

Bernstein BE, Mikkelsen TS, Xie X, Kamal M, Huebert DJ, Cuff J, Fry B, Meissner A, Wernig M, Plath K, et al., 2006. A bivalent chromatin structure marks key developmental genes in embryonic stem cells. Cell 125:315–26.

Bertrand JY, Chi NC, Santoso B, Teng S, Stainier DYR, Traver D. 2010a. Haematopoietic stem cells derive directly from aortic endothelium during development. Nature 464:108–11.

Boisset J-C, van Cappellen W, Andrieu-Soler C, Galjart N, Dzierzak E, Robin C. 2010. In vivo imaging of haematopoietic cells emerging from the mouse aortic endothelium. Nature 464:116–20.

Bos FL, Hawkins JS, Zovein AC. 2015. Single-cell resolution of morphological changes in hemogenic endothelium. Development 142:2719–24.

Boyer LA, Plath K, Zeitlinger J, Brambrink T, Medeiros LA, Lee TI, Levine SS, Wernig M, Tajonar A, Ray MK, et al., 2006. Polycomb complexes repress developmental regulators in murine embryonic stem cells. Nature 441:349–53.

de Bruijn MF, Speck NA, Peeters MC, Dzierzak E. 2000. Definitive hematopoietic stem cells first develop within the major arterial regions of the mouse embryo. EMBO J. 19:2465–74.

Bulger M, Groudine M. 1999. Looping versus linking: toward a model for long-distance gene activation. Genes Dev. 13:2465–2477.

Chan WYI, Follows GA, Lacaud G, Pimanda JE, Landry J-R, Kinston S, Knezevic K, Piltz S, Donaldson IJ, Gambardella L, et al., 2007. The paralogous hematopoietic regulators Lyl1 and Scl are coregulated by Ets and GATA factors, but Lyl1 cannot rescue the early Scl-/- phenotype. Blood 109:1908–16.

Chen T, Dent SYR. 2014. Chromatin modifiers and remodellers: regulators of cellular differentiation. Nat. Rev. Genet. 15:93–106.

Choi K. 2002. The hemangioblast: a common progenitor of hematopoietic and endothelial cells. J. Hematother. Stem Cell Res. 11:91–101.

Ciau-Uitz A, Wang L, Patient R, Liu F. 2013. ETS transcription factors in hematopoietic stem cell development. Blood Cells. Mol. Dis. 51:248–55.

Clarke RL, Yzaguirre AD, Yashiro-Ohtani Y, Bondue A, Blanpain C, Pear WS, Speck NA, Keller G. 2013. The expression of Sox17 identifies and regulates haemogenic endothelium. Nat. Cell Biol. 15:502–10.

Covassin LD, Villefranc JA, Kacergis MC, Weinstein BM, Lawson ND. 2006. Distinct genetic interactions between multiple Vegf receptors are required for development of different blood vessel types in zebrafish. Proc. Natl. Acad. Sci. U. S. A. 103:6554–9.

Cumano A, Dieterlen-Lievre F, Godin I. 1996. Lymphoid potential, probed before circulation in mouse, is restricted to caudal intraembryonic splanchnopleura. Cell 86:907–16.

Dejana E, Taddei A, Randi AM. 2007. Foxs and Ets in the transcriptional regulation of endothelial cell differentiation and angiogenesis. Biochim. Biophys. Acta 1775:298–312.

Dekker J, Rippe K, Dekker M, Kleckner N. 2002. Capturing chromosome conformation. Science 295:1306–11.

Doss MX, Gaspar JA, Winkler J, Hescheler J, Schulz H, Sachinidis A. 2012. Specific gene signatures and pathways in mesodermal cells and their derivatives derived from embryonic stem cells. Stem Cell Rev. 8:43–54.

Doss MX, Koehler CI, Gissel C, Hescheler J, Sachinidis A. Embryonic stem cells: a promising tool for cell replacement therapy. J. Cell. Mol. Med. 8:465–73.

Dzierzak E, Speck NA. 2008. Of lineage and legacy: the development of mammalian hematopoietic stem cells. Nat. Immunol. 9:129–36.

Endoh M, Ogawa M, Orkin S, Nishikawa S. 2002. SCL/tal-1-dependent process determines a competence to select the definitive hematopoietic lineage prior to endothelial differentiation. EMBO J. 21:6700–8.

Engel JD, Tanimoto K. 2000. Looping, Linking, and Chromatin Activity. Cell 100:499–502.

Faust C, Schumacher A, Holdener B, Magnuson T. 1995. The eed mutation disrupts anterior mesoderm production in mice. Development 121:273–85.

Fehling HJ. 2003. Tracking mesoderm induction and its specification to the hemangioblast during embryonic stem cell differentiation. Development 130:4217–4227.

Ferdous A, Caprioli A, Iacovino M, Martin CM, Morris J, Richardson JA, Latif S, Hammer RE, Harvey RP, Olson EN, et al., 2009. Nkx2-5 transactivates the Ets-related protein 71 gene and specifies an endothelial/endocardial fate in the developing embryo. Proc. Natl. Acad. Sci. U. S.

A. 106:814–9.

Findlay VJ, LaRue AC, Turner DP, Watson PM, Watson DK. 2013. Understanding the role of ETS-mediated gene regulation in complex biological processes. Adv. Cancer Res. 119:1–61.

Flamme I, Frölich T, Risau W. 1997. Molecular mechanisms of vasculogenesis and embryonic angiogenesis. J. Cell. Physiol. 173:206–10.

Fujiwara Y, Chang AN, Williams AM, Orkin SH. 2004. Functional overlap of GATA-1 and GATA-2 in primitive hematopoietic development. Blood 103:583–5.

Gadue P, Huber TL, Nostro MC, Kattman S, Keller GM. 2005. Germ layer induction from embryonic stem cells. Exp. Hematol. 33:955–64.

Galic Z, Kitchen SG, Kacena A, Subramanian A, Burke B, Cortado R, Zack JA. 2006. T lineage differentiation from human embryonic stem cells. Proc. Natl. Acad. Sci. U. S. A. 103:11742–7.

Gekas C, Dieterlen-Lièvre F, Orkin SH, Mikkola HKA. 2005. The placenta is a niche for hematopoietic stem cells. Dev. Cell 8:365–75.

Geyer PK, Green MM, Corces VG. 1990. Tissue-specific transcriptional enhancers may act in trans on the gene located in the homologous chromosome: the molecular basis of transvection in Drosophila. EMBO J. 9:2247–56.

Gilbert SF. 2000a. Paraxial Mesoderm: The Somites and Their Derivatives.

Gilbert SF. 2000b. Developmental Biology.

Godin IE, Garcia-Porrero JA, Coutinho A, Dieterlen-Lièvre F, Marcos MA. 1993. Para-aortic splanchnopleura from early mouse embryos contains B1a cell progenitors. Nature 364:67–70.

Goldie LC, Lucitti JL, Dickinson ME, Hirschi KK. 2008. Cell signaling directing the formation and function of hemogenic endothelium during murine embryogenesis. Blood 112:3194–204.

Gordon-Keylock S, Sobiesiak M, Rybtsov S, Moore K, Medvinsky A. 2013. Mouse

extraembryonic arterial vessels harbor precursors capable of maturing into definitive HSCs. Blood 122:2338–45.

Göttgens B, Nastos A, Kinston S, Piltz S, Delabesse ECM, Stanley M, Sanchez M-J, Ciau-Uitz A, Patient R, Green AR. 2002. Establishing the transcriptional programme for blood: the SCL stem cell enhancer is regulated by a multiprotein complex containing Ets and GATA factors. EMBO J. 21:3039–50.

Gritz E, Hirschi KK. 2016. Specification and function of hemogenic endothelium during embryogenesis. Cell. Mol. Life Sci. 73:1547–67.

Habeck H, Odenthal J, Walderich B, Maischein H, Schulte-Merker S. 2002. Analysis of a zebrafish VEGF receptor mutant reveals specific disruption of angiogenesis. Curr. Biol. 12:1405–12.

Van Handel B, Montel-Hagen A, Sasidharan R, Nakano H, Ferrari R, Boogerd CJ, Schredelseker J, Wang Y, Hunter S, Org T, et al., 2012. Scl represses cardiomyogenesis in prospective hemogenic endothelium and endocardium. Cell 150:590–605.

Hollenhorst PC, Jones DA, Graves BJ. 2004. Expression profiles frame the promoter specificity dilemma of the ETS family of transcription factors. Nucleic Acids Res. 32:5693–702.

Huangfu D, Maehr R, Guo W, Eijkelenboom A, Snitow M, Chen AE, Melton DA. 2008. Induction of pluripotent stem cells by defined factors is greatly improved by small-molecule compounds. Nat. Biotechnol. 26:795–7.

Ismailoglu I, Yeamans G, Daley GQ, Perlingeiro RCR, Kyba M. 2008. Mesodermal patterning activity of SCL. Exp. Hematol. 36:1593–603.

Itzhaki I, Maizels L, Huber I, Zwi-Dantsis L, Caspi O, Winterstern A, Feldman O, Gepstein A, Arbel G, Hammerman H, et al., 2011. Modelling the long QT syndrome with induced pluripotent stem cells. Nature 471:225–9.

Kallianpur AR, Jordan JE, Brandt SJ. 1994. The SCL/TAL-1 gene is expressed in progenitors of

both the hematopoietic and vascular systems during embryogenesis. Blood 83:1200–8.

Kassouf MT, Chagraoui H, Vyas P, Porcher C. 2008. Differential use of SCL/TAL-1 DNA-binding domain in developmental hematopoiesis. Blood 112:1056–67.

Kassouf MT, Hughes JR, Taylor S, McGowan SJ, Soneji S, Green AL, Vyas P, Porcher C. 2010. Genome-wide identification of TAL1's functional targets: insights into its mechanisms of action in primary erythroid cells. Genome Res. 20:1064–83.

Kataoka H, Hayashi M, Nakagawa R, Tanaka Y, Izumi N, Nishikawa S, Jakt ML, Tarui H, Nishikawa S-I. 2011a. Etv2/ER71 induces vascular mesoderm from Flk1+PDGFRα+ primitive mesoderm. Blood 118:6975–86.

Kattman SJ, Huber TL, Keller GM. 2006. Multipotent flk-1+ cardiovascular progenitor cells give rise to the cardiomyocyte, endothelial, and vascular smooth muscle lineages. Dev. Cell 11:723–32.

Kim I, Saunders TL, Morrison SJ. 2007. Sox17 dependence distinguishes the transcriptional regulation of fetal from adult hematopoietic stem cells. Cell 130:470–83.

Kim JY, Lee RH, Kim TM, Kim D-W, Jeon Y-J, Huh S-H, Oh S-Y, Kyba M, Kataoka H, Choi K, et al., 2014. OVOL2 is a critical regulator of ER71/ETV2 in generating FLK1+, hematopoietic, and endothelial cells from embryonic stem cells. Blood 124:2948–52.

Kissa K, Herbomel P. 2010. Blood stem cells emerge from aortic endothelium by a novel type of cell transition. Nature 464:112–5.

Klose RJ, Gardner KE, Liang G, Erdjument-Bromage H, Tempst P, Zhang Y. 2007. Demethylation of Histone H3K36 and H3K9 by Rph1: a Vestige of an H3K9 Methylation System in Saccharomyces cerevisiae? Mol. Cell. Biol. 27:3951–3961.

Kumaravelu P, Hook L, Morrison AM, Ure J, Zhao S, Zuyev S, Ansell J, Medvinsky A. 2002. Quantitative developmental anatomy of definitive haematopoietic stem cells/long-term repopulating units (HSC/RUs): role of the aorta-gonad-mesonephros (AGM) region and the yolk

sac in colonisation of the mouse embryonic liver. Development 129:4891–9.

Kyba M, Perlingeiro RCR, Daley GQ. 2002. HoxB4 confers definitive lymphoid-myeloid engraftment potential on embryonic stem cell and yolk sac hematopoietic progenitors. Cell 109:29–37.

Lacaud G, Gore L, Kennedy M, Kouskoff V, Kingsley P, Hogan C, Carlsson L, Speck N, Palis J, Keller G. 2002. Runx1 is essential for hematopoietic commitment at the hemangioblast stage of development in vitro. Blood 100:458–66.

Lachner M, O'Carroll D, Rea S, Mechtler K, Jenuwein T. 2001. Methylation of histone H3 lysine 9 creates a binding site for HP1 proteins. Nature 410:116–20.

Lancrin C, Mazan M, Stefanska M, Patel R, Lichtinger M, Costa G, Wilson NK, Mo T, Bonifer C, Go B, et al., 2012. GFI1 and GFI1B control the loss of endothelial identity of hemogenic endothelium during hematopoietic commitment. 120:314–322.

Lancrin C, Sroczynska P, Stephenson C, Allen T, Kouskoff V, Lacaud G. 2009. The haemangioblast generates haematopoietic cells through a haemogenic endothelium stage. Nature 457:892–5.

Lécuyer E, Larivière S, Sincennes M-C, Haman A, Lahlil R, Todorova M, Tremblay M, Wilkes BC, Hoang T. 2007. Protein stability and transcription factor complex assembly determined by the SCL-LMO2 interaction. J. Biol. Chem. 282:33649–58.

Lee D, Park C, Lee H, Lugus JJ, Kim SH, Arentson E, Chung YS, Gomez G, Kyba M, Lin S, et al., 2008. ER71 acts downstream of BMP, Notch, and Wnt signaling in blood and vessel progenitor specification. Cell Stem Cell 2:497–507.

Lee TI, Jenner RG, Boyer LA, Guenther MG, Levine SS, Kumar RM, Chevalier B, Johnstone SE, Cole MF, Isono K, et al., 2006. Control of developmental regulators by Polycomb in human embryonic stem cells. Cell 125:301–13.

Lei EP, Corces VG. 2006. RNA interference machinery influences the nuclear organization of a

chromatin insulator. Nat. Genet. 38:936–941.

Lelièvre E, Lionneton F, Soncin F, Vandenbunder B. 2001. The Ets family contains transcriptional activators and repressors involved in angiogenesis. Int. J. Biochem. Cell Biol. 33:391–407.

Li Y, Deng C, Hu X, Patel B, Fu X, Qiu Y, Brand M, Zhao K, Huang S. 2012. Dynamic interaction between TAL1 oncoprotein and LSD1 regulates TAL1 function in hematopoiesis and leukemogenesis. Oncogene 31:5007–18.

Liakhovitskaia A, Rybtsov S, Smith T, Batsivari A, Rybtsova N, Rode C, de Bruijn M, Buchholz F, Gordon-Keylock S, Zhao S, et al., 2014. Runx1 is required for progression of CD41+ embryonic precursors into HSCs but not prior to this. Development 141:3319–23.

Liao EC, Paw BH, Oates AC, Pratt SJ, Postlethwait JH, Zon LI. 1998. SCL/Tal-1 transcription factor acts downstream of cloche to specify hematopoietic and vascular progenitors in zebrafish. Genes Dev. 12:621–6.

Ling K-W, Ottersbach K, van Hamburg JP, Oziemlak A, Tsai F-Y, Orkin SH, Ploemacher R, Hendriks RW, Dzierzak E. 2004. GATA-2 plays two functionally distinct roles during the ontogeny of hematopoietic stem cells. J. Exp. Med. 200:871–82.

Lister R, Pelizzola M, Dowen RH, Hawkins RD, Hon G, Tonti-Filippini J, Nery JR, Lee L, Ye Z, Ngo Q-M, et al., 2009. Human DNA methylomes at base resolution show widespread epigenomic differences. Nature 462:315–22.

Liu F, Bhang SH, Arentson E, Sawada A, Kim CK, Kang I, Yu J, Sakurai N, Kim SH, Yoo JJW, et al., 2013. Enhanced hemangioblast generation and improved vascular repair and regeneration from embryonic stem cells by defined transcription factors. Stem cell reports 1:166–82.

Liu F, Kang I, Park C, Chang L-W, Wang W, Lee D, Lim D-S, Vittet D, Nerbonne JM, Choi K. 2012. ER71 specifies Flk-1+ hemangiogenic mesoderm by inhibiting cardiac mesoderm and Wnt signaling. Blood 119:3295–305.

Liu F, Li D, Yu YYL, Kang I, Cha M-J, Kim JY, Park C, Watson DK, Wang T, Choi K. 2015. Induction of hematopoietic and endothelial cell program orchestrated by ETS transcription factor ER71/ETV2. EMBO Rep. 16:654–69.

Lomvardas S, Barnea G, Pisapia DJ, Mendelsohn M, Kirkland J, Axel R. 2006. Interchromosomal interactions and olfactory receptor choice. Cell 126:403–13.

Marcelo KL, Sills TM, Coskun S, Vasavada H, Sanglikar S, Goldie LC, Hirschi KK. 2013. Hemogenic endothelial cell specification requires c-Kit, Notch signaling, and p27-mediated cell-cycle control. Dev. Cell 27:504–15.

Martin C, Zhang Y. 2005. The diverse functions of histone lysine methylation. Nat. Rev. Mol. Cell Biol. 6:838–49.

Medvinsky A, Dzierzak E. 1996. Definitive hematopoiesis is autonomously initiated by the AGM region. Cell 86:897–906.

Medvinsky A, Rybtsov S, Taoudi S. 2011. Embryonic origin of the adult hematopoietic system: advances and questions. Development 138:1017–31.

Menon T, Firth AL, Scripture-Adams DD, Galic Z, Qualls SJ, Gilmore WB, Ke E, Singer O, Anderson LS, Bornzin AR, et al., 2015. Lymphoid regeneration from gene-corrected SCID-X1 subject-derived iPSCs. Cell Stem Cell 16:367–72.

Mikkola HKA, Fujiwara Y, Schlaeger TM, Traver D, Orkin SH. 2003. Expression of CD41 marks the initiation of definitive hematopoiesis in the mouse embryo. Blood 101:508–16.

Minegishi N, Ohta J, Yamagiwa H, Suzuki N, Kawauchi S, Zhou Y, Takahashi S, Hayashi N, Engel JD, Yamamoto M. 1999. The mouse GATA-2 gene is expressed in the para-aortic splanchnopleura and aorta-gonads and mesonephros region. Blood 93:4196–207.

Morita R, Suzuki M, Kasahara H, Shimizu N, Shichita T, Sekiya T, Kimura A, Sasaki K, Yasukawa H, Yoshimura A. 2015. ETS transcription factor ETV2 directly converts human fibroblasts into functional endothelial cells. Proc. Natl. Acad. Sci. U. S. A. 112:160–5.

Mukhopadhyay M, Teufel A, Yamashita T, Agulnick AD, Chen L, Downs KM, Schindler A, Grinberg A, Huang S-P, Dorward D, et al., 2003. Functional ablation of the mouse Ldb1 gene results in severe patterning defects during gastrulation. Development 130:495–505.

Nakajima-Takagi Y, Osawa M, Oshima M, Takagi H, Miyagi S, Endoh M, Endo TA, Takayama N, Eto K, Toyoda T, et al., 2013. Role of SOX17 in hematopoietic development from human embryonic stem cells. Blood 121:447–58.

Nakano H, Liu X, Arshi A, Nakashima Y, van Handel B, Sasidharan R, Harmon AW, Shin J-H, Schwartz RJ, Conway SJ, et al., 2013. Haemogenic endocardium contributes to transient definitive haematopoiesis. Nat. Commun. 4:1564.

Niu Z, Iyer D, Conway SJ, Martin JF, Ivey K, Srivastava D, Nordheim A, Schwartz RJ. 2008. Serum response factor orchestrates nascent sarcomerogenesis and silences the biomineralization gene program in the heart. Proc. Natl. Acad. Sci. U. S. A. 105:17824–9.

North TE, de Bruijn MFTR, Stacy T, Talebian L, Lind E, Robin C, Binder M, Dzierzak E, Speck NA. 2002. Runx1 expression marks long-term repopulating hematopoietic stem cells in the midgestation mouse embryo. Immunity 16:661–72.

Paige SL, Thomas S, Stoick-Cooper CL, Wang H, Maves L, Sandstrom R, Pabon L, Reinecke H, Pratt G, Keller G, et al., 2012. A temporal chromatin signature in human embryonic stem cells identifies regulators of cardiac development. Cell 151:221–32.

Palencia-Desai S, Kohli V, Kang J, Chi NC, Black BL, Sumanas S. 2011. Vascular endothelial and endocardial progenitors differentiate as cardiomyocytes in the absence of Etsrp/Etv2 function. Development 138:4721–32.

Pan G, Tian S, Nie J, Yang C, Ruotti V, Wei H, Jonsdottir GA, Stewart R, Thomson JA. 2007. Whole-genome analysis of histone H3 lysine 4 and lysine 27 methylation in human embryonic stem cells. Cell Stem Cell 1:299–312.

Pasini D, Bracken AP, Jensen MR, Lazzerini Denchi E, Helin K. 2004. Suz12 is essential for mouse development and for EZH2 histone methyltransferase activity. EMBO J. 23:4061–71.

de Peppo GM, Svensson S, Lennerås M, Synnergren J, Stenberg J, Strehl R, Hyllner J, Thomsen P, Karlsson C. 2010. Human embryonic mesodermal progenitors highly resemble human mesenchymal stem cells and display high potential for tissue engineering applications. Tissue Eng. Part A 16:2161–82.

Poole TJ, Coffin JD. 1989. Vasculogenesis and angiogenesis: two distinct morphogenetic mechanisms establish embryonic vascular pattern. J. Exp. Zool. 251:224–31.

Porcher C, Liao EC, Fujiwara Y, Zon LI, Orkin SH. 1999. Specification of hematopoietic and vascular development by the bHLH transcription factor SCL without direct DNA binding. Development 126:4603–15.

Porcher C, Swat W, Rockwell K, Fujiwara Y, Alt FW, Orkin SH. 1996. The T cell leukemia oncoprotein SCL/tal-1 is essential for development of all hematopoietic lineages. Cell 86:47–57.

Randi AM, Sperone A, Dryden NH, Birdsey GM. 2009. Regulation of angiogenesis by ETS transcription factors. Biochem. Soc. Trans. 37:1248–53.

Reubinoff BE, Pera MF, Fong CY, Trounson A, Bongso A. 2000. Embryonic stem cell lines from human blastocysts: somatic differentiation in vitro. Nat. Biotechnol. 18:399–404.

Rhodes KE, Gekas C, Wang Y, Lux CT, Francis CS, Chan DN, Conway S, Orkin SH, Yoder MC, Mikkola HKA. 2008. The emergence of hematopoietic stem cells is initiated in the placental vasculature in the absence of circulation. Cell Stem Cell 2:252–63.

Risau W. 1997. Mechanisms of angiogenesis. Nature 386:671–4.

Robb L, Elwood NJ, Elefanty AG, Köntgen F, Li R, Barnett LD, Begley CG. 1996. The scl gene product is required for the generation of all hematopoietic lineages in the adult mouse. EMBO J. 15:4123–9.

Robb L, Lyons I, Li R, Hartley L, Köntgen F, Harvey RP, Metcalf D, Begley CG. 1995. Absence of yolk sac hematopoiesis from mice with a targeted disruption of the scl gene. Proc. Natl. Acad. Sci. U. S. A. 92:7075–9.

Ruthenburg AJ, Allis CD, Wysocka J. 2007. Methylation of lysine 4 on histone H3: intricacy of writing and reading a single epigenetic mark. Mol. Cell 25:15–30.

Rybtsov S, Sobiesiak M, Taoudi S, Souilhol C, Senserrich J, Liakhovitskaia A, Ivanovs A, Frampton J, Zhao S, Medvinsky A. 2011. Hierarchical organization and early hematopoietic specification of the developing HSC lineage in the AGM region. J. Exp. Med. 208:1305–15.

Sakurai H, Era T, Jakt LM, Okada M, Nakai S, Nishikawa S, Nishikawa S. 2006. In vitro modeling of paraxial and lateral mesoderm differentiation reveals early reversibility. Stem Cells 24:575–86.

Samokhvalov IM, Samokhvalova NI, Nishikawa S. 2007. Cell tracing shows the contribution of the yolk sac to adult haematopoiesis. Nature 446:1056–61.

Sánchez MJ, Holmes A, Miles C, Dzierzak E. 1996. Characterization of the first definitive hematopoietic stem cells in the AGM and liver of the mouse embryo. Immunity 5:513–25.

Schlaeger TM, Mikkola HKA, Gekas C, Helgadottir HB, Orkin SH. 2005. Tie2Cre-mediated gene ablation defines the stem-cell leukemia gene (SCL/tal1)-dependent window during hematopoietic stem-cell development. Blood 105:3871–4.

Schlaeger TM, Schuh A, Flitter S, Fisher A, Mikkola H, Orkin SH, Vyas P, Porcher C. 2004. Decoding hematopoietic specificity in the helix-loop-helix domain of the transcription factor SCL/Tal-1. Mol. Cell. Biol. 24:7491–502.

Schuh AH, Tipping AJ, Clark AJ, Hamlett I, Guyot B, Iborra FJ, Rodriguez P, Strouboulis J, Enver T, Vyas P, et al., 2005. ETO-2 associates with SCL in erythroid cells and megakaryocytes and provides repressor functions in erythropoiesis. Mol. Cell. Biol. 25:10235–50.

Schupp M-O, Waas M, Chun C-Z, Ramchandran R. 2014. Transcriptional inhibition of etv2 expression is essential for embryonic cardiac development. Dev. Biol. 393:71–83.

Shalaby F, Rossant J, Yamaguchi TP, Gertsenstein M, Wu XF, Breitman ML, Schuh AC. 1995. Failure of blood-island formation and vasculogenesis in Flk-1-deficient mice. Nature 376:62–6.

Sharrocks AD. 2001. The ETS-domain transcription factor family. Nat. Rev. Mol. Cell Biol. 2:827–37.

Shi X, Richard J, Zirbes KM, Gong W, Lin G, Kyba M, Thomson JA, Koyano-Nakagawa N, Garry DJ. 2014. Cooperative interaction of Etv2 and Gata2 regulates the development of endothelial and hematopoietic lineages. Dev. Biol. 389:208–18.

Shi Y, Lan F, Matson C, Mulligan P, Whetstine JR, Cole PA, Casero RA, Shi Y. 2004. Histone demethylation mediated by the nuclear amine oxidase homolog LSD1. Cell 119:941–53.

Shivdasani RA, Mayer EL, Orkin SH. 1995. Absence of blood formation in mice lacking the T-cell leukaemia oncoprotein tal-1/SCL. Nature 373:432–4.

Souroullas GP, Salmon JM, Sablitzky F, Curtis DJ, Goodell MA. 2009. Adult hematopoietic stem and progenitor cells require either Lyl1 or Scl for survival. Cell Stem Cell 4:180–6.

Stainier DY, Weinstein BM, Detrich HW, Zon LI, Fishman MC. 1995. Cloche, an early acting zebrafish gene, is required by both the endothelial and hematopoietic lineages. Development 121:3141–50.

Stevens LC. 1960. Embryonic potency of embryoid bodies derived from a transplantable testicular teratoma of the mouse. Dev. Biol. 2:285–97.

Sumanas S, Gomez G, Zhao Y, Park C, Choi K, Lin S. 2008. Interplay among Etsrp/ER71, Scl, and Alk8 signaling controls endothelial and myeloid cell formation. Blood 111:4500–10.

Szutorisz H, Canzonetta C, Georgiou A, Chow C-M, Tora L, Dillon N. 2005. Formation of an active tissue-specific chromatin domain initiated by epigenetic marking at the embryonic stem cell stage. Mol. Cell. Biol. 25:1804–20.

Szutorisz H, Dillon N. 2005. The epigenetic basis for embryonic stem cell pluripotency. Bioessays 27:1286–93.

Takahashi K, Yamanaka S. 2006. Induction of pluripotent stem cells from mouse embryonic and

adult fibroblast cultures by defined factors. Cell 126:663–76.

Taoudi S, Gonneau C, Moore K, Sheridan JM, Blackburn CC, Taylor E, Medvinsky A. 2008. Extensive hematopoietic stem cell generation in the AGM region via maturation of VE-cadherin+CD45+ pre-definitive HSCs. Cell Stem Cell 3:99–108.

Taoudi S, Medvinsky A. 2007. Functional identification of the hematopoietic stem cell niche in the ventral domain of the embryonic dorsal aorta. Proc. Natl. Acad. Sci. U. S. A. 104:9399–403.

Taoudi S, Morrison AM, Inoue H, Gribi R, Ure J, Medvinsky A. 2005. Progressive divergence of definitive haematopoietic stem cells from the endothelial compartment does not depend on contact with the foetal liver. Development 132:4179–91.

Thomson JA, Itskovitz-Eldor J, Shapiro SS, Waknitz MA, Swiergiel JJ, Marshall VS, Jones JM. 1998. Embryonic stem cell lines derived from human blastocysts. Science 282:1145–7.

Veldman MB, Zhao C, Gomez GA, Lindgren AG, Huang H, Yang H, Yao S, Martin BL, Kimelman D, Lin S. 2013. Transdifferentiation of fast skeletal muscle into functional endothelium in vivo by transcription factor Etv2. PLoS Biol. 11:e1001590.

Verger A, Duterque-Coquillaud M. 2002. When Ets transcription factors meet their partners. Bioessays 24:362–70.

Visvader JE, Fujiwara Y, Orkin SH. 1998. Unsuspected role for the T-cell leukemia protein SCL/tal-1 in vascular development. Genes Dev. 12:473–479.

Wadman IA, Osada H, Grütz GG, Agulnick AD, Westphal H, Forster A, Rabbitts TH. 1997. The LIM-only protein Lmo2 is a bridging molecule assembling an erythroid, DNA-binding complex which includes the TAL1, E47, GATA-1 and Ldb1/NLI proteins. EMBO J. 16:3145–57.

Wamstad JA, Alexander JM, Truty RM, Shrikumar A, Li F, Eilertson KE, Ding H, Wylie JN, Pico AR, Capra JA, et al., 2012. Dynamic and coordinated epigenetic regulation of developmental transitions in the cardiac lineage. Cell 151:206–20.

Wareing S, Eliades A, Lacaud G, Kouskoff V. 2012. ETV2 expression marks blood and endothelium precursors, including hemogenic endothelium, at the onset of blood development. Dev. Dyn. 241:1454–64.

Wareing S, Mazan A, Pearson S, Göttgens B, Lacaud G, Kouskoff V. 2012. The Flk1-cre Mediated Deletion of ETV2 Defines Its Narrow Temporal Requirement During Embryonic Hematopoietic Development. Stem Cells:1521–1531.

Warren AJ, Colledge WH, Carlton MB, Evans MJ, Smith AJ, Rabbitts TH. 1994. The oncogenic cysteine-rich LIM domain protein rbtn2 is essential for erythroid development. Cell 78:45–57.

Wesemann DR, Portuguese AJ, Magee JM, Gallagher MP, Zhou X, Panchakshari RA, Alt FW. 2012. Reprogramming IgH isotype-switched B cells to functional-grade induced pluripotent stem cells. Proc. Natl. Acad. Sci. U. S. A. 109:13745–50.

West AG. 2005. Remote control of gene transcription. Hum. Mol. Genet. 14:R101–R111.

Whyte WA, Bilodeau S, Orlando DA, Hoke HA, Frampton GM, Foster CT, Cowley SM, Young RA. 2012. Enhancer decommissioning by LSD1 during embryonic stem cell differentiation. Nature 482:221–5.

Wilson NK, Foster SD, Wang X, Knezevic K, Schütte J, Kaimakis P, Chilarska PM, Kinston S, Ouwehand WH, Dzierzak E, et al., 2010. Combinatorial transcriptional control in blood stem/progenitor cells: genome-wide analysis of ten major transcriptional regulators. Cell Stem Cell 7:532–44.

Xu C-R, Cole PA, Meyers DJ, Kormish J, Dent S, Zaret KS. 2011. Chromatin “prepattern” and histone modifiers in a fate choice for liver and pancreas. Science 332:963–6.

Yamada Y, Pannell R, Forster A, Rabbitts TH. 2000. The oncogenic LIM-only transcription factor Lmo2 regulates angiogenesis but not vasculogenesis in mice. Proc. Natl. Acad. Sci. U. S. A. 97:320–4.

Yamada Y, Warren AJ, Dobson C, Forster A, Pannell R, Rabbitts TH. 1998. The T cell leukemia

LIM protein Lmo2 is necessary for adult mouse hematopoiesis. Proc. Natl. Acad. Sci. U. S. A. 95:3890–5.

Yao H, Brick K, Evrard Y, Xiao T, Camerini-Otero RD, Felsenfeld G. 2010. Mediation of CTCF transcriptional insulation by DEAD-box RNA-binding protein p68 and steroid receptor RNA activator SRA. Genes Dev. 24:2543–55.

Yoder MC, Hiatt K, Dutt P, Mukherjee P, Bodine DM, Orlic D. 1997. Characterization of definitive lymphohematopoietic stem cells in the day 9 murine yolk sac. Immunity 7:335–44.

Zaret KS, Carroll JS. 2011. Pioneer transcription factors: establishing competence for gene expression. Genes Dev. 25:2227–41.

Zhao XD, Han X, Chew JL, Liu J, Chiu KP, Choo A, Orlov YL, Sung W-K, Shahab A, Kuznetsov VA, et al., 2007. Whole-Genome Mapping of Histone H3 Lys4 and 27 Trimethylations Reveals Distinct Genomic Compartments in Human Embryonic Stem Cells. Cell Stem Cell 1:286–298.

Zhou VW, Goren A, Bernstein BE. 2011. Charting histone modifications and the functional organization of mammalian genomes. Nat. Rev. Genet. 12:7–18.

Zovein AC, Turlo KA, Ponec RM, Lynch MR, Chen KC, Hofmann JJ, Cox TC, Gasson JC, Iruela-Arispe ML. 2010. Vascular remodeling of the vitelline artery initiates extravascular emergence of hematopoietic clusters. Blood 116:3435–44.

Chapter 2:

SCL binds to primed enhancers in mesoderm to regulate hematopoietic and cardiac fate divergence

Published online: January 6, 2015

Article

TRANSPARENT PROCESS OPEN ACCESS

THE EMBO JOURNAL

Scl binds to primed enhancers in mesoderm to regulate hematopoietic and cardiac fate divergence

Tõnis Org[1,†], Dan Duan[1,†], Roberto Ferrari[2,3], Amelie Montel-Hagen[1], Ben Van Handel[1], Marc A Kerényi[4], Rajkumar Sasidharan[1], Liudmilla Rubbi[1], Yuko Fujiwara[4], Matteo Pellegrini[1], Stuart H Orkin[4], Siavash K Kurdistani[2,3] & Hanna KA Mikkola[1,3,*]

Abstract

Scl/Tal1 confers hemogenic competence and prevents ectopic cardiomyogenesis in embryonic endothelium by unknown mechanisms. We discovered that Scl binds to hematopoietic and cardiac enhancers that become epigenetically primed in multipotent cardiovascular mesoderm, to regulate the divergence of hematopoietic and cardiac lineages. Scl does not act as a pioneer factor but rather exploits a pre-established epigenetic landscape. As the blood lineage emerges, Scl binding and active epigenetic modifications are sustained in hematopoietic enhancers, whereas cardiac enhancers are decommissioned by removal of active epigenetic marks. Our data suggest that, rather than recruiting corepressors to enhancers, Scl prevents ectopic cardiogenesis by occupying enhancers that cardiac factors, such as Gata4 and Hand1, use for gene activation. Although hematopoietic Gata factors bind with Scl to both activated and repressed genes, they are dispensable for cardiac repression, but necessary for activating genes that enable hematopoietic stem/progenitor cell development. These results suggest that a unique subset of enhancers in lineage-specific genes that are accessible for regulators of opposing fates during the time of the fate decision provide a platform where the divergence of mutually exclusive fates is orchestrated.

Keywords cardiac specification; enhancer; hematopoiesis; mesoderm diversification; transcriptional regulation

Subject Categories Chromatin, Epigenetics, Genomics & Functional Genomics; Development & Differentiation; Stem Cells

DOI 10.15252/embj.201490542 | Received 17 November 2014 | Revised 3 December 2014 | Accepted 5 December 2014

Introduction

Specification of cell types is dictated by few master regulators that activate lineage-specific transcriptional networks. This concept is underscored by studies in which overexpression of a small set of transcription factors can reprogram fibroblasts (or other cells) into a variety of cell types that closely resemble pluripotent cells, neurons, pancreatic beta cells, cardiomyocytes or hematopoietic cells (Takahashi & Yamanaka, 2006; Ieda *et al*, 2010; Huang *et al*, 2011; Kim *et al*, 2011; Pereira *et al*, 2013). Hematopoietic and cardiovascular systems are important targets for cell-based therapies due to the high morbidity and mortality associated with blood and heart diseases; however, so far, *in vitro* generation of transplantable cells for treating these diseases has not been successful. Blood cells, vasculature and the heart share not only an intimate functional relationship, but also a common origin in $Flk1^+$ mesoderm (Fehling *et al*, 2003; Huber *et al*, 2004; Iida *et al*, 2005; Kattman *et al*, 2006). Although many regulators of the blood and circulatory system have been discovered, it is unclear how the divergence of these lineages in multipotent cardiovascular mesoderm is orchestrated and how their cell identity is solidified. Although several specific epigenetic modifications have been associated with activation or repression of the regulatory regions of genes (Cui *et al*, 2009; Creyghton *et al*, 2010; Zentner *et al*, 2011), to what degree they cause, or are the consequence of, gene activation/repression by cell type-specific transcription factors is still unclear.

The embryonic hematopoietic system is established in multiple waves, starting with the generation of lineage-restricted progenitors in the yolk sac and culminating in the emergence of multipotent hematopoietic stem/progenitor cells (HS/PC) in the major vessels in the yolk sac (Li *et al*, 2005; Yoshimoto *et al*, 2011), aorta-gonad mesonephros (AGM) region (North *et al*, 1999; De Bruijn *et al*, 2000; Zovein *et al*, 2008; Chen *et al*, 2009; Bertrand *et al*, 2010; Boisset *et al*, 2010; Kissa & Herbomel, 2010) and the placenta (Rhodes *et al*, 2008). The Ets factor Etv2/ER71/Etsrp first distinguishes the hemato-vascular lineages from cardiac mesoderm by

1 Department of Molecular, Cell and Developmental Biology, University of California, Los Angeles, CA, USA
2 Department of Biological Chemistry, University of California, Los Angeles, CA, USA
3 Eli and Edythe Broad Stem Cell Research Center, University of California, Los Angeles, CA, USA
4 Department of Pediatric Oncology, Dana-Farber Cancer Institute and Division of Hematology/Oncology, Children's Hospital Boston, Howard Hughes Medical Institute, Harvard Stem Cell Institute, Harvard Medical School, Boston, MA, USA
*Corresponding author. Tel: +1 310 825 2565; E-mail: hmikkola@mcdb.ucla.edu
†These authors contributed equally to this work

specifying endothelium (Lee *et al*, 2008; Sumanas *et al*, 2008; Kataoka *et al*, 2011) and activates the bHLH factor Scl/Tal1, which confers hemogenic identity to endothelium (Van Handel *et al*, 2012). Scl also has a less well understood but important function in repressing the cardiac fate (Schoenebeck *et al*, 2007; Ismailoglu *et al*, 2008; Van Handel *et al*, 2012). Inducible overexpression of Scl during ES cell differentiation resulted in the expansion of hematopoietic lineage at the expense of cardiac and paraxial mesoderm (Ismailoglu *et al*, 2008), while the analysis of Scl knockout (Scl^{KO}) embryos revealed robust generation of ectopic cardiomyocytes in yolk sac vasculature, verifying a physiological role for Scl in cardiac repression (Van Handel *et al*, 2012). The requirement for Scl to repress cardiogenesis in hemogenic tissues was restricted to early midgestation of mouse development, suggesting the presence of epigenetic or other contributing mechanisms that solidify the fate choice. Scl also prevented misspecification of endocardium and cushion mesenchymal cells to cardiomyocytes. Although these studies pointed to a critical requirement for Scl in cardiac repression, it remained unknown whether Scl or its downstream targets repress cardiogenesis.

Scl functions in a multi-factor complex with Gata factors 1 or 2, E2A, Ldb1 and Lmo2 (Wadman *et al*, 1997) that promotes gene activation in hematopoietic cells (Tripic *et al*, 2009; Yu *et al*, 2009; Xu *et al*, 2012). Gata2 functions in HS/PC generation and survival (De Pater *et al*, 2013; Gao *et al*, 2013) whereas Gata1 regulates the maturation of erythroid, megakaryocytic and eosinophilic lineages (Bresnick *et al*, 2012), although there is redundancy between these factors (Takahashi *et al*, 2000). Embryos deficient for both Gata1 and Gata2 lack all blood cells, similar to Scl knockout embryos (Fujiwara *et al*, 2004). However, it is unknown whether hematopoietic Gata factors cooperate with Scl to repress cardiomyogenesis.

Here we show that Scl-dependent activation of hematopoietic fate and repression of cardiac fate during mesoderm diversification is accompanied by Scl binding to hematopoietic and cardiac enhancers that were epigenetically primed for activation in mesoderm. Our findings suggest that the accessibility and decommissioning of Scl-regulated enhancers is determined by modulation of active rather than repressive epigenetic modifications and is a major determinant of available fate choices and developmental stage specificity of target genes. We discovered a distinct subset of Scl-regulated enhancers that are also accessible for cardiac transcription factors in mesoderm, and propose that these enhancers serve as a platform where the fate choice between mutually exclusive fates is determined. Although hematopoietic Gata factors can bind with Scl to both activated and repressed enhancers, their function becomes critical only for activating genes required for HS/PC emergence from hemogenic endothelium. Elucidation of the stepwise process of how master regulators exploit the epigenetic landscape to establish hematopoietic or cardiovascular cell types from multipotent mesoderm provides new insights into improving directed differentiation and lineage reprogramming of stem/progenitor cells of these lineages for regenerative medicine.

Results

Scl specifies mesoderm by binding to genes encoding hematopoietic and cardiac regulators

To understand how Scl specifies hemogenic endothelium while simultaneously repressing the cardiac fate, we defined Scl target genes by combining gene expression and chromatin immunoprecipitation sequencing (ChIP-seq) analysis on $Flk1^+$ mesodermal cells differentiated from mouse ES cells (Supplementary Fig S1A). Scl binding associated genes (4,393 binding sites associated with 4,158 genes within 200 kb from transcriptional start sites) (Supplementary Table S1A) were intersected with Scl-dependent genes (592 and 553 genes that were significantly up- or down-regulated in mesoderm upon Scl expression (P-value < 0.05, fold change < 1.5, see details in Supplementary Fig S1A–C, Supplementary Table S1B and C, and Supplementary Materials and Methods). Integrated analysis showed Scl binding to 57% of the activated and 29% of the repressed genes in mesoderm (Fig 1A, Supplementary Table S1B and C), which is significantly higher than would be expected by random chance (P-values 4.08×10^{-103} and 3.91×10^{-10}, respectively). The genes in activated/bound group were enriched for GO term hematopoiesis, including key hematopoietic transcription factors *Runx1*, *Gata2*, *cMyb* and *Cfba2t3/Eto2* (Fig 1B–D). The genes in repressed/bound group were enriched for GO term heart development, including cardiac transcription

Figure 1. Scl binds to both its activated and repressed target genes in $Flk1^+$ mesoderm.

A Venn diagram showing the number of Scl binding sites and overlap with Scl activated and repressed genes in $Flk1^+$ MES (mesoderm) documents that Scl binds to both Scl-dependent activated and repressed genes.

B DAVID (Huang *et al*, 2007) GO enrichment analysis for Scl-bound and activated or Scl-bound and repressed genes shows enrichment of hematopoietic and heart-related terms, respectively.

C Gene expression heatmaps of selected genes from the bound and activated and bound and repressed groups show activation of key hematopoietic target genes and repression of key cardiac target genes in Scl-expressing mesoderm as compared to Scl-deficient mesoderm. Control [$Scl^{+/hCD4}$, divided into Scl-expressing (Scl^+) and non-expressing cells (Scl^-)] and Scl^{KO} EBs are shown.

D Scl and control IgG ChIP-seq tracks show examples of Scl binding sites near hematopoietic (*Runx1* and *Gata2*) and cardiac (*Gata4* and *Gata6*) genes in $Flk1^+$ mesoderm (MES).

E Verification of Scl binding sites marked with asterisks in (D) using ChIP-PCR, average enrichment of at least three independent biological experiments over negative control region (chr16: 92230219–92230338) with SEM are shown.

F Verification of Scl-dependent gene expression using qRT–PCR. Average of three biological replicates with SD are shown.

G Venn diagrams show the number of potential 'extended activated' and 'extended repressed' Scl target genes by intersecting genes associated with Scl binding in $Flk1^+$ MES with Scl activated and repressed genes from day 4 EBs, E9.5 yolk sac, placenta and endocardium (Van Handel *et al*, 2012).

H Heatmaps show Scl binding to majority of activated hematopoietic and repressed cardiac transcription factors and other proteins. See also Supplementary Fig S1 and Supplementary Table S1A–E.

factors *Gata4*, *Gata6* and *Tbx3* (Fig 1B–D). Quantitative RT–PCR and ChIP–PCR verified Scl-dependent expression and Scl binding with both activated and repressed genes (Fig 1E and F).

As the expression analysis in day 4 EB Flk1^{+} cells was limited to genes that were immediately activated or repressed upon Scl induction in mesoderm, we extended the analysis of Scl-dependent genes to those that became differentially expressed in endothelium in the yolk sac or the placenta, or endocardium in the heart in *Scl*^{KO} embryos (Van Handel *et al*, 2012). This analysis yielded an extended list of 3,709 Scl-dependent activated and 2,839 Scl-dependent repressed genes, of which 1,100 (29.6%) and 715 (25.2%) (Supplementary Fig S1A, Supplementary Table S1D

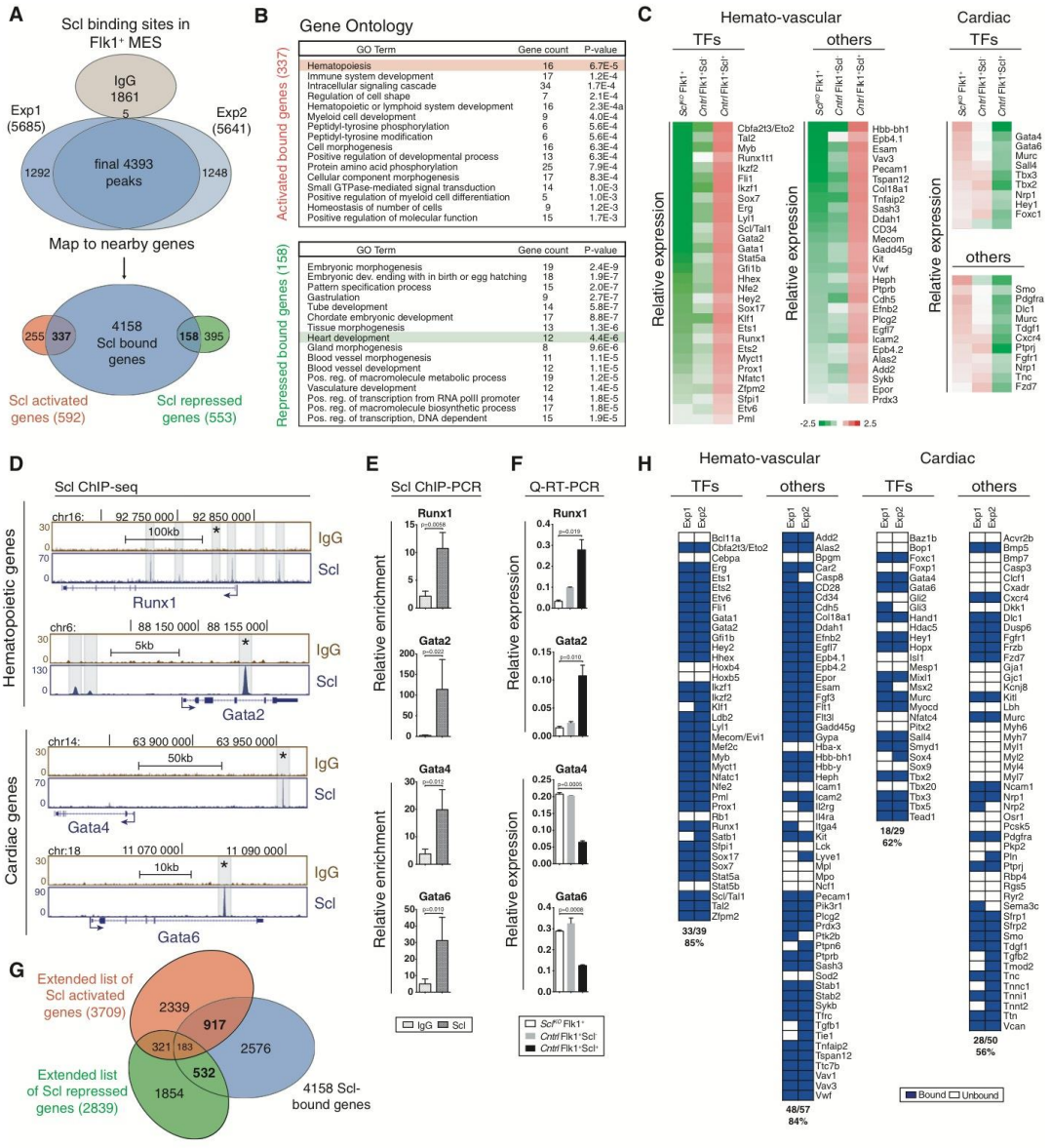

Figure 1.

and E) were bound by Scl in Flk1$^+$ mesoderm (Fig 1G), which is significantly higher than would be randomly expected (*P*-values 2.75×10^{-83} and 4.44×10^{-25}, respectively). Analysis of the 'extended activated' genes showed that Scl binds to regulatory regions of the majority (33/39) of known hematopoietic transcription factors, many (48/57) surface markers and other proteins characteristic of nascent HS/PCs and hemogenic endothelium such as *CD41* (*Itga2b*) and *Cdh5* (*VE-cadherin*) (Fig 1H). Scl binding was also associated with many (18/29) cardiac transcription factors (*Gata4*, *Gata6*, *Hand1* and *Tbx5*), *PDGFRα*, a marker for cardiogenic mesoderm and ectopic cardiomyogenic precursors in Scl^{KO} embryos (Van Handel *et al*, 2012), and cardiomyocyte contractile proteins (*Tnnc1*, *Tnnt2*, *Tnni1* and *Ttn*) (Fig 1H). These data showed that during mesoderm diversification, Scl binds to a broad network of genes that govern hematopoietic and cardiac development, including the master transcription factors of each lineage.

To verify that the ES cell *in vitro* differentiation system recapitulates ectopic cardiomyogenesis in Scl-deficient endothelial precursors, Scl^{KO} and wild-type ES cells were differentiated toward mesodermal lineages and assayed for differentiation potential and gene expression. Scl^{KO} ES cells with doxycycline-inducible Scl overexpression ($Scl^{KO}iScl$) were included to assess whether reintroduction of Scl is sufficient to reverse the phenotype. As expected, both wild-type and $Scl^{KO}iScl$ EBs, but not Scl^{KO} EBs, could generate CD41$^+$c-Kit$^+$ hematopoietic progenitors by day 7 (Supplementary Fig S1D). Likewise, Tie2$^+$CD31$^+$ endothelial precursors isolated from day 4.75 EBs from wild-type and $Scl^{KO}iScl$ cells, but not Scl^{KO} cells, robustly generated CD45$^+$CD11b$^{+/-}$ hematopoietic cells on OP9 stroma (Supplementary Fig S1E). Scl^{KO} Tie2$^+$CD31$^+$ endothelial precursors readily differentiated to troponin T-expressing cardiomyocytes, whereas re-expression of Scl abolished the ectopic cardiogenic potential in ES cell-derived endothelial cells (Supplementary Fig S1E). These data were reinforced by qRT–PCR analysis that verified the lack of expression of hematopoietic transcription factors and ectopic induction of cardiac factors in Scl-deficient endothelium, and rescue of these molecular defects by Scl overexpression (Supplementary Fig S1F). These data validate the ES cell *in vitro* differentiation system as a suitable model to study Scl-dependent cardiac repression and ectopic cardiogenesis from endothelial precursors.

Scl regulates mesodermal fate diversification via pre-established enhancers

Analysis of genomic locations of Scl binding showed that the majority of Scl binding sites in Flk1$^+$ mesoderm reside away from transcriptional start site (TSS) (Fig 2A), suggesting that Scl functions through enhancer elements. This was most pronounced in the repressed genes, where only 3% of Scl binding sites were found within 5 kb of TSS. We thus correlated Scl mesodermal binding sites with published datasets for cardiac enhancers, including the Vista Enhancer database that contains *in vivo* experimentally verified enhancers (Visel *et al*, 2007) and ChIP-seq analysis for co-activator p300, a marker of enhancers (Visel *et al*, 2009), in E11.5 mouse hearts (Blow *et al*, 2010). Intersecting these data with Scl binding sites in Flk1$^+$ mesoderm revealed Scl binding in 10–16% of all putative cardiac enhancers, which is significantly ($P = 8.6E{-}5$) higher than the overlap with enhancers in other tissues (Fig 2B and C). Analysis of well-established enhancers of cardiac transcription factors *Myocardin* and *Nkx2.5* (Fig 2D) (Lien *et al*, 1999; Creemers *et al*, 2006) and hematopoietic regulators *Runx1* (+23 enhancer) (Nottingham *et al*, 2007) and *Gata2* (+9.5 enhancer) (Wozniak *et al*, 2007; Gao *et al*, 2013) (Supplementary Fig S2A) showed clear overlap with Scl binding.

To assess the epigenetic state of Scl-bound enhancers, 4,393 Scl mesodermal binding sites were assessed for the average levels of histone modifications associated with enhancers (H3K4me1) and active enhancers (H3K4me1 and H3K27ac) (Creyghton *et al*, 2010; Wamstad *et al*, 2012) during ES cell differentiation to cardiomyocytes. In ES cells, Scl mesodermal binding sites were largely devoid of H3K4me1 and H3K27ac; however, in Flk1$^+$ mesoderm they had acquired high levels of H3K4me1 and some H3K27ac, which were in part retained during differentiation into cardiac progenitors and cardiomyocytes (Fig 2E and F). Analysis of the average H3K4me1 and H3K27ac levels around Scl binding sites in other mesodermal tissues (limb, fibroblasts) showed no enrichment (Fig 2F). This indicates that the regulatory regions to which Scl binds become epigenetically primed for activation specifically in Flk1$^+$ mesoderm.

We next asked whether Scl is required for depositing active histone marks at hematopoietic and/or cardiac enhancers or whether these enhancers have been epigenetically pre-established prior to Scl binding. ChIP-seq analysis for histone H3K4me1 and

Figure 2. Scl binds to enhancers that have been primed for activation in mesoderm.

A Distribution of Scl binding sites relative to TSS in Scl-bound activated or repressed genes shows that majority of Scl binding sites locate away from TSS. Chi-square test was used to assess differences in the distribution.

B Percent of tissue-specific enhancers validated by LacZ reporter mice (Vista enhancer browser) that overlap with Scl MES binding sites shows that Scl binds to experimentally verified heart enhancers more often compared to enhancers from other tissues.

C Percent of Scl MES binding sites that overlap with heart enhancers in E11.5 embryos defined by p300 binding (Blow *et al*, 2010) is higher than overlap with enhancers from other tissues.

D Scl MES binding sites overlap with experimentally verified heart-specific enhancers upstream of *Myocardin* and *Nkx2.5* genes and with hematopoietic enhancers within *Runx1* and *Gata2* genes.

E Percent of enhancers from different cardiac developmental stages identified by H3K4me1 (enhancers) and H3K4me1 combined with H3k27ac (active enhancers) (Wamstad *et al*, 2012) that overlap with Scl MES binding sites.

F Average H3K4me1 (left) and H3K27ac (right) profiles around all 4,393 Scl binding sites show tissue-specific enrichment in Flk1$^+$ mesoderm (MES), cardiac precursors (CP) and cardiomyocytes (CM) but not in ESC (mouse ES cells) mouse embryonic fibroblasts (MEF) and embryonic limbs (LIMB).

G Correlation analysis of H3K4me1 (left) and H3K27ac (right) levels between WT and Scl^{KO} MES and ES cells and MES (Wamstad *et al*, 2012) around 4,393 Scl binding sites shows that establishment of these marks occurs independently of Scl.

H Scl, H3K4me1 and H3K27ac ChIP-seq tracks show comparable levels of H3K4me1 and H3K27ac in WT and Scl^{KO} mesoderm around cardiac (*Gata6*, *Tbx5*) and hematopoietic (*Eto2*, *Gfi1b*) genes.

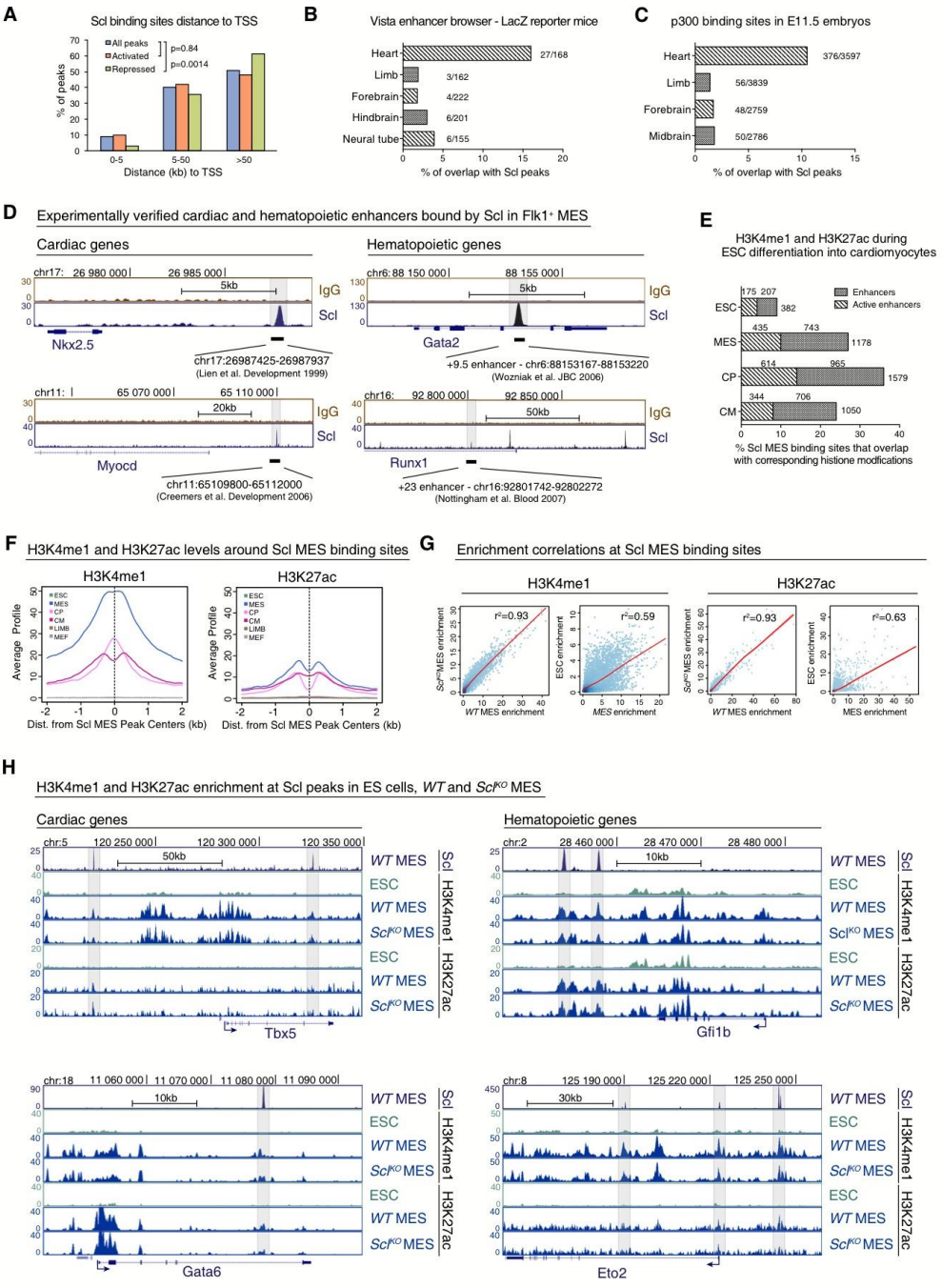

Figure 2.

H3K27ac in WT and Scl^{KO} Flk1$^+$ mesoderm evidenced co-localization of the active marks across all Scl binding sites (Fig 2G) including cardiac and hematopoietic genes (Fig 2H) in both cell lines. Although H3K27ac levels were generally lower and this mark was not present in all hematopoietic or cardiac enhancers, there was no significant difference in H3K27ac levels at Scl mesodermal binding sites in WT and Scl^{KO} Flk1$^+$ mesoderm (Fig 2G and H). These results show that Scl is not required for the establishment of active enhancer marks in mesoderm, suggesting that these enhancers have become primed for activation in multipotent cardiovascular mesoderm to pave the way for Scl action.

To investigate whether the epigenetically primed status of enhancers is necessary for Scl binding, we induced Scl expression ectopically in Scl^{KO}*iScl* ES cells and compared Scl binding in these cells to that in Flk1$^+$ mesoderm in wild-type and Scl^{KO}*iScl* cells. While inducible Scl was faithfully bound to the hematopoietic and cardiac enhancers in mesoderm, minimal binding was observed in ES cells (Supplementary Fig S2). Notably, the few binding sites where ectopically expressed Scl was able to bind in ES cells also harbored H3K4me1, whereas the key hematopoietic and cardiac enhancers were devoid of both Scl binding and H3K4me1 (Supplementary Fig S2). These data imply that Scl binding is tightly developmentally controlled, and at least in part determined by epigenetic status of the enhancers.

Repression of cardiac enhancers by Scl occurs transiently during mesoderm diversification

Since Scl is required only during a brief developmental window in midgestation to repress cardiogenesis in hemogenic tissues (Van Handel *et al*, 2012), we assessed whether Scl binding to cardiac enhancers is maintained in hematopoietic cells later in development. Intersecting Scl binding sites in Flk1$^+$ mesoderm with previously published Scl binding sites in ES cell-derived hematopoietic progenitor cell line (HPC7) (Wilson *et al*, 2010) or fetal liver erythroblasts (Kassouf *et al*, 2010) showed that many Scl binding sites are developmental stage specific (Fig 3A). GO enrichment analysis revealed enrichment of heart-related terms only with Flk1$^+$ mesoderm-specific peaks (Fig 3B) and genes (Supplementary Fig S3A). Analysis of Scl ChIP-seq tracks for cardiac regulators *Gata4, Nkx2-5* and *Myocardin* verified Scl binding only in Flk1$^+$ mesoderm (Fig 3C). To confirm that different methods for ChIP-seq analysis between labs did not account for the difference, we performed Scl ChIP-seq on MEL cells (mouse erythroleukemia line) and verified the absence of Scl binding in cardiac genes (Fig 3C, Supplementary Fig S3B). In comparison, Scl binding sites shared between different stages were enriched for hematopoiesis-related terms, and included major hematopoietic transcription factors (e.g. *Gata1, Gata2, Lyl1, Gif1b, Runx1* and *Myb*) (Fig 3C, Supplementary Fig S3A and B). While Flk1$^+$ mesoderm-specific peaks were rarely found within 5 kb of TSS (Fig 3D), 46% of the HPC7 or 34% of the erythroid cell-specific peaks were located within 5 kb to TSS. These data suggest that Scl binding extends from distant enhancers to promoters as hematopoiesis progresses.

Since Scl was no longer bound to cardiac enhancers in hematopoietic cells, we assessed whether the epigenetic landscape in Scl binding sites was modified upon differentiation of mesoderm to hematopoietic cells. Combinatorial clustering of Scl mesodermal binding sites based on H3K4me1 patterns in mesoderm, hematopoietic progenitors (HPC7) and erythroid cells (MEL) revealed two major clusters. Although the majority of Scl binding sites harbored H3K4me1 in mesoderm, this enhancer mark was lost in Scl binding sites in cluster L (= Loss of H3K4me1) but retained in cluster R (= Retention of H3K4me1) as hematopoietic development progressed. The gradual loss of H3K4me1 enrichment from HPC7 to MEL in cluster L strongly correlated with the loss of H3K27ac and Scl binding, while Scl binding sites in cluster R retained H3K4me1, H3K27ac and Scl binding (Fig 3E). The peaks in cluster L were enriched for cardiac GO terms and included key cardiac regulators *Gata4, Gata6* and *Myocardin* (Fig 3E, Supplementary Fig S3B), while Scl peaks in cluster R were enriched for hematopoietic-related GO terms and included hematopoietic regulators *Gata1, Gata2, Lyl*1 and *Runx1* (Fig 3E, Supplementary Fig S3B). The opposite was observed in the cardiomyocyte cell line HL1, in which the enhancers of key hematopoietic regulators lost H3K4me1 and H3K27ac, while the enhancers of regulators of cardiomyocyte differentiation maintained these active marks (Supplementary Fig S3B). These results imply that the epigenetic landscape becomes dynamically remodeled in unused enhancers upon mesodermal fate diversification to blood and heart.

Decommissioning of Scl-regulated cardiac enhancers is associated with loss of active epigenetic marks rather than gain of repressive marks

We next investigated whether the active epigenetic marks in Scl-regulated cardiac enhancers are replaced by repressive marks in

Figure 3. Scl binding to cardiac enhancers occurs transiently in mesoderm.

A Venn diagram showing overlaps of Scl binding sites in different developmental stages—Flk1$^+$ MES, fetal liver (FL) erythroblast cells (Kassouf *et al*, 2010) and hematopoietic progenitors (HPC7) (Wilson *et al*, 2010) (left)—shows that majority of Scl binding sites are developmental stage specific. Examples of developmental stage-specific Scl-bound genes are shown (right).

B GREAT (McLean *et al*, 2010) analysis of significantly enriched GO terms in Mouse Phenotype category for all common, Flk1$^+$ MES-specific, HPC7-specific and FL erythroblast-specific peaks shows enrichment of heart-related terms only among Flk1$^+$ MES-specific peaks.

C ChIP-seq tracks with Scl binding in Flk1$^+$ MES, HPC7, FL erythroblasts and MEL (mouse erythroleukemia) cells around cardiac (*Gata4*, *Myocd*, *Nkx2.5*) and hematopoietic (*Gata1*, *Gata2* and *Lyl1*) genes show that binding to cardiac genes occurs only in mesoderm, while binding to hematopoietic genes is maintained throughout hematopoietic development.

D Comparison of the location of developmental stage-specific Scl binding sites relative to TSS shows that Scl binding near TSS occurs more often in later hematopoietic development compared to mesoderm.

E Heatmaps of combinatorial clustering of H3K4me1 around Scl mesodermal binding sites in MES, HPC7 and MEL reveal two major clusters: Cluster L loses H3K4me1, H3K27ac and Scl binding during hematopoietic differentiation and is enriched for genes involved in heart development; cluster R retains H3K4me1, H3K27ac and Scl binding during hematopoietic differentiation and is enriched for hematopoiesis-related genes. Selected GO terms among top 10 most enriched are shown.

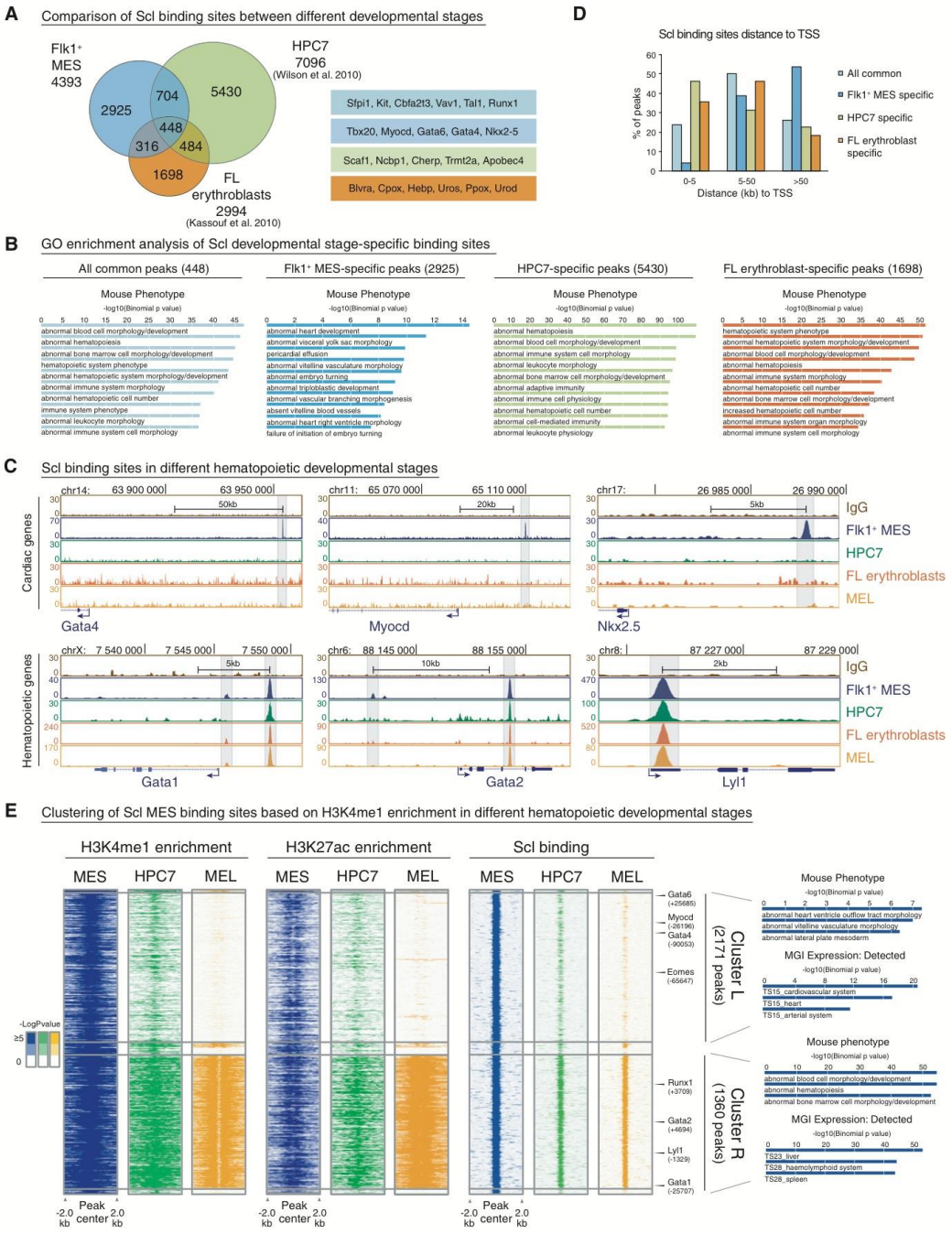

Figure 3.

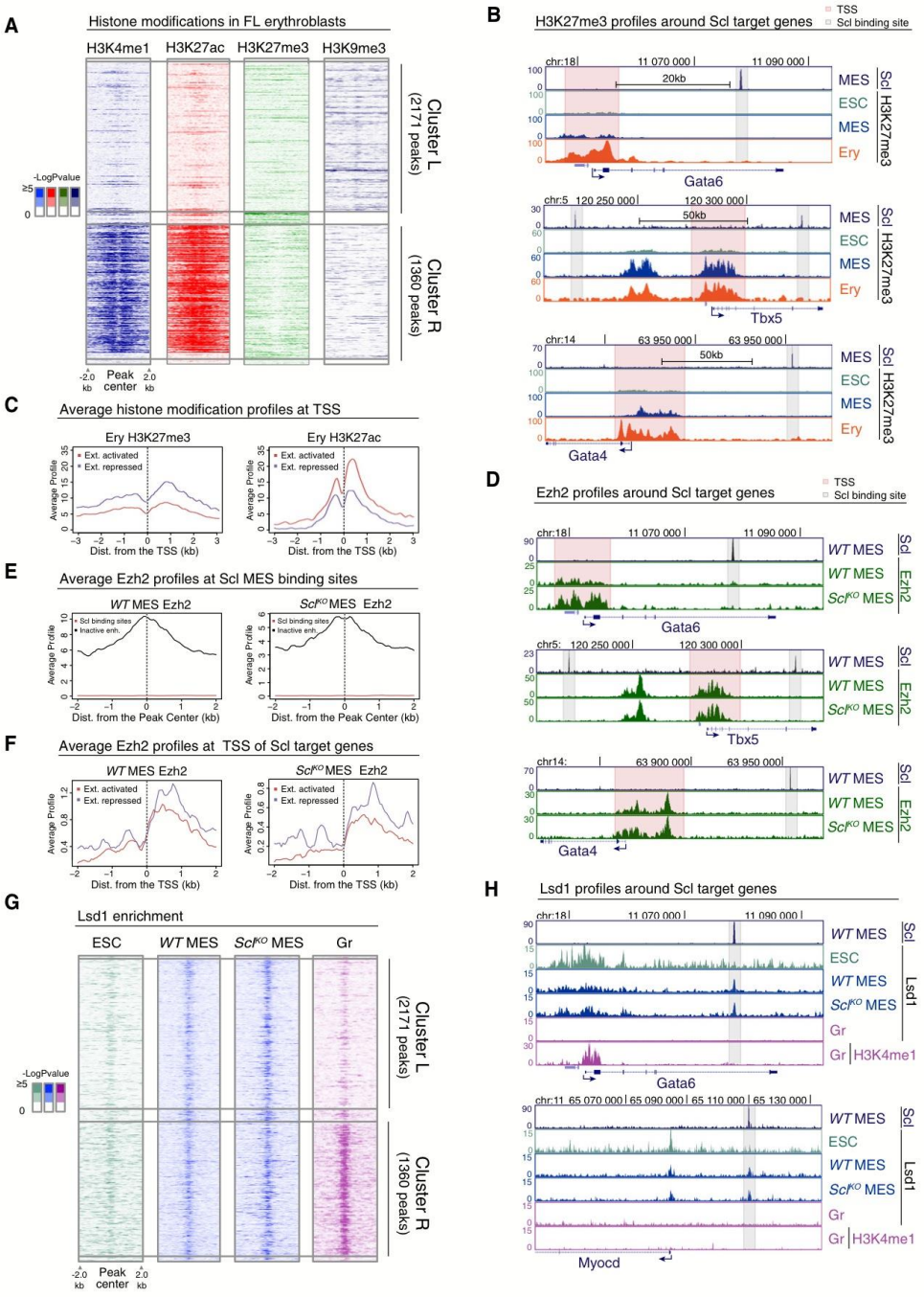

Figure 4.

Figure 4. Scl-mediated repression of cardiac genes cannot be explained by Scl-dependent corepressor recruitment.

A Heatmaps of H3K4me1, H3K27ac, H3K27me3 and H3K9me3 histone modifications in FL erythroblasts around Scl MES binding sites in cluster L and cluster R show no gain of common repressive histone marks in cluster L.

B H3K27me3 ChIP-seq tracks in ES cells (ESC), Flk1^{+} mesoderm (MES) and FL erythroblasts (Ery) show that cardiac genes *Gata6*, *Tbx5* and *Gata4* harbor H3K27me3 at the TSS (pink) but not at Scl binding sites (gray).

C Average H3K27me3 (left) and H3K27ac (right) levels in FL erythroblasts around the TSS of extended list of Scl activated and repressed genes show that Scl repressed genes have on average more H3K27me3 and less H3K27ac as compared to Scl activated genes.

D Ezh2 ChIP-seq tracks in WT and Scl^{KO} mesoderm showing that Ezh2 recruitment to the TSS of cardiac genes *Gata6*, *Tbx5* and *Gata4* is not Scl dependent.

E Average Ezh2 enrichment in WT (left) and Scl^{KO} mesoderm (right) for inactive enhancers (defined by having H3K4me1 and H3K27me3 modifications (Wamstad *et al*, 2012) and distance greater than 5 kb from TSS) and for Scl binding sites shows no Ezh2 enrichment at Scl binding sites.

F Average Ezh2 enrichment at the TSS of extended list of Scl activated and repressed genes is similar in WT (left) and Scl^{KO} mesoderm (right).

G Heatmaps of Lsd1 enrichment in ES cells, WT and Scl^{KO} mesoderm and in granulocytes (Gr) (Kerenyi *et al*, 2013) in cluster L and cluster R show co-localization of Lsd1 binding with Scl binding sites and reveal that recruitment of Lsd1 can happen independently of Scl.

H Lsd1 ChIP-seq tracks (ES cells, WT and Scl^{KO} Flk1^{+} mesoderm and granulocytes) and H3K4me1 ChIP-seq track (granulocytes) show that Lsd1 enrichment coincides with Scl MES binding sites nearby cardiac genes *Gata6* and *Myocd* in WT and Scl^{KO} Flk1^{+} mesoderm.

hematopoietic cells to solidify the fate choice. Analysis of Ter119 erythroid cells for several histone marks (ENCODE project and Kowalczyk *et al*, 2012) in Scl mesodermal binding sites confirmed a strong correlation between Scl binding and retention of the active histone marks H3K4me1 and H3K27ac in Cluster R, and loss of these marks in Cluster L (Fig 4A), also in erythroid cells *in vivo*. A candidate for a repression mechanism was Polycomb-mediated deposition of H3K27me3, which has been associated with silencing of both promoters and enhancers (Harmston & Lenhard, 2013). Moreover, Scl has been shown to interact with Ezh2, a core component of the Polycomb repressive complex 2 (PRC2) (Pinello *et al*, 2014). Analysis of H3K27me3 ChIP-seq data provided no evidence of H3K27me3 acquisition at Scl binding sites in erythroid cells in either Cluster R or L (Fig 4A). ChIP-seq tracks around cardiac genes *Gata4, Gata6* and *Tbx5* confirmed the lack of H3K27me3 at Scl binding sites in ES cells, mesoderm and erythroid cells (Fig 4B). However, H3K27me3 was observed at the TSS of some Scl-regulated genes (Fig 4B). Comparison of H3K27me3 levels in Scl-bound extended activated and extended repressed genes (see Fig 1, Supplementary Table S1D and E) in erythroid cells revealed an increase in H3K27me3 at the TSS of repressed genes, while H3K27ac was more enriched at the TSS of activated genes (Fig 4C). These data suggested that Polycomb may contribute to the silencing of Scl-regulated genes at promoters, and raised the question whether Scl binding at enhancers is required for bringing PRC2 complex to promoters via chromosomal looping. ChIP-seq analysis for Ezh2 in mesoderm showed strong correlation between Ezh2 binding and H3K27me3 at TSS; however, there was no enrichment of Ezh2 at Scl binding sites (Fig 4E). Moreover, there was no difference in the ability to recruit Ezh2 to the TSS of Scl-regulated genes in WT versus Scl^{KO} Flk1^{+} mesoderm (Fig 4D and F). Altogether, these data imply that although Polycomb-mediated repression may contribute to the silencing of cardiac genes in the blood lineage, it is not a major factor governing accessibility to Scl-bound enhancers in mesoderm or their derivatives, and the failure to repress cardiac genes in Scl-deficient mesoderm is not caused by lack of Ezh2 recruitment to these genes.

We next assessed whether the repressive histone modification H3K9me3 is acquired at the decommissioned enhancers during hematopoietic differentiation. The average levels of H3K9me3 were slightly higher in cluster L binding sites than in cluster R binding sites in three hematopoietic cell types (Ter119 erythroid cells, Fig 4A, Supplementary Fig S4B, and G1E embryonic erythroid cell line and Ch12 B lymphoid cells, Supplementary Fig S4A and B). However, analysis of H3K9me3 around key cardiac genes did not show specific enrichment for H3K9me3 at Scl-bound enhancers (Supplementary Fig S4C). These data imply that although regions around some Scl mesodermal binding sites acquire H3K9me3 during hematopoietic differentiation, deposition of H3K9me3 is unlikely the predominant mechanism that initiates Scl-mediated cardiac repression.

As DNA methylation can restrict transcription factor binding to its target DNA (Blattler & Farnham, 2013), we asked whether changes in DNA methylation mediate the inactivation of Scl-regulated cardiac enhancers in hematopoietic cells. Comparison of the average DNA methylation levels at Scl mesodermal binding sites associated with extended list of Scl activated or repressed genes in genome-wide methylation datasets from mouse ES cells (Habibi *et al*, 2013), bone marrow, heart, pancreas and skin (Hon *et al*, 2013), showed that Scl binding sites are on average hypomethylated compared to the surrounding regions (Supplementary Fig S4D). Nevertheless, both Scl's extended activated and repressed target genes showed a general increase in DNA methylation within 200 kb of Scl binding sites from ES cells to all adult cell types analyzed (Supplementary Fig S4E). The methylation levels in Scl extended activated genes were lower in the bone marrow compared to other tissues, while the extended repressed genes showed lower methylation in the heart (Supplementary Fig S4E).

To investigate whether Scl initiates differential methylation in mesoderm, we performed RRBS (reduced representation bisulfite sequencing) in ES cells, WT and Scl^{KO} Flk1^{+} mesodermal cells, and MEL cells. Global covariance analysis showed that major changes in DNA methylation occur later in hematopoietic development rather than in mesoderm (Supplementary Fig S4F). Intersection of RRBS data with Scl mesodermal binding sites showed no difference in methylation levels in ES cells and WT and Scl^{KO} Flk1^{+} mesoderm; only MEL cells had higher DNA methylation (Supplementary Fig S4G). Thus, while DNA methylation may contribute to the silencing of Scl target genes in differentiated cells, this occurs later in development and is not centered at Scl-bound enhancers. These data imply that DNA methylation is not a primary mechanism that silences Scl-regulated cardiac enhancers during hematopoietic specification.

Our analysis of known repressive histone marks did not provide evidence that Scl-regulated enhancers would be actively silenced during mesodermal lineage diversification, but rather implied that gain and loss of active epigenetic marks is the key determinant

that governs tissue-specific access to these enhancers. We thus assessed whether the recruitment of Lsd1, a lysine-specific demethylase 1 that decommissions enhancers by removing H3K4me1 (Whyte *et al*, 2012), to cardiac enhancers is interrupted in the absence of Scl. Comparison of ChIP-seq data of Lsd1 mesodermal binding to published Lsd1 binding datasets in ES cells and myeloid cells (Whyte *et al*, 2012; Kerenyi *et al*, 2013) showed robust co-localization of Lsd1 at Scl-bound enhancers (Fig 4G and H) in both cluster L and R in Flk1$^+$ mesoderm, which is a heterogenous population of cells committed to hemato-vascular or cardiac fates. In myeloid cells, cardiac enhancers were devoid of both Lsd1 and H3K4me1 (Fig 4H), documenting a short temporal window for Lsd1 action. Nevertheless, analysis of Lsd1 binding in Scl-deficient mesodermal cells did not show evidence of impaired Lsd1 binding in cardiac enhancers in Cluster L (Fig 4G and H). These results imply that, although Lsd1 is likely involved in the decommissioning of unused enhancers upon mesodermal lineage diversification, defective cardiac repression in Scl-deficient mesodermal derivatives is not caused by an inability to recruit Lsd1 to primed cardiac enhancers.

Binding by Scl and cardiac Gata4 and/or Hand1 define enhancer subgroups that may determine fate choice between opposing mesodermal fates

As the analysis of repressive marks and corepressors provided no evidence for direct Scl-dependent corepressor recruitment to enhancers or promoters in mesoderm, we considered the possibility that Scl inhibits cardiac fate by interfering with the activation of these genes by cardiac regulators. To identify candidate factors that could also bind to Scl-regulated enhancers, we performed DNA motif enrichment analysis for known transcription factor binding sites in Transfac and Jaspar databases. This analysis identified the composite Tal1(Scl)_Gata motif and Gata motifs as the most prevalent motifs in both activated and repressed genes (Fig 5A).

There are six known Gata factors, of which Gata1, 2 and 3 act in hematopoietic cells and Gata4, 5 and 6 regulate cardiac development (Chlon & Crispino, 2012). Gata4 can regulate cardiac development both indirectly via endoderm and directly by binding to cardiac genes in Flk1$^+$ mesoderm (Holtzinger *et al*, 2010; Oda *et al*, 2013). Analysis of a published dataset for Gata4 binding in Flk1$^+$ mesoderm revealed that Gata4 binding overlaps with a large fraction (41%) of Scl binding sites (Fig 5B). Moreover, as other bHLH factors can also bind to E-box motifs similar to Scl, we also performed ChIP-seq for Hand1, a key cardiac bHLH factor that can interact with cardiac Gata factors. 13.2% all Scl-bound enhancers were co-occupied by Scl and Hand1 in Flk1$^+$ mesoderm (9.7% Scl, Hand1 and Gata4 altogether, and 3.5% Scl and Hand1 alone). Analysis of the regulatory regions for key cardiac (*Gata6*, *Tbx5* and *Myocardin*) and hematopoietic (*Runx1*, *Gfi1b* and *Gata2*) transcription factors identified at least one enhancer in each gene bound by Scl, Hand1 and/or Gata4 (Fig 5C). The sites that can be occupied by all three factors (424 sites) included both that remain active (cluster R, 167 sites) and sites that become decommissioned during hematopoietic development (cluster L, 201 sites), and they associated with both Scl-dependent activated (128) and repressed (79) genes. Similar distribution was observed for Scl binding sites that were shared with Gata4 or Hand1 alone. These data suggest that a distinct subset of Scl-bound enhancers may be used by both hematopoietic and cardiac bHLH and Gata transcription factors to activate their own lineage or repress a competing lineage.

We next assessed whether there are any unique features that sets the 'dually accessible' enhancers apart from enhancers bound by Scl alone. The enhancers bound by both Scl and Gata4 and/or Hand1 were more evolutionarily conserved as compared to other Scl mesodermal binding sites (Fig 5D) and showed higher levels of Scl binding (Fig 5E), H3K4me1, H3K27ac (Fig 5F and G) and Lsd1 enrichment (Fig 5H). Moreover, Scl target genes that harbor an enhancer that can be bound by Scl and Gata4 and/or Hand1 showed higher average gene expression change in Scl-expressing WT versus Scl^{KO} Flk1$^+$ mesoderm as compared to Scl target genes that do not have a dually accessible enhancer (Fig 5I). The genes that contain a dually accessible enhancer included many hematopoietic (27/31, 87%) and cardiac (10/15, 67%) transcription factors (Fig 5J).

We next assessed whether similar developmental stage-specific binding observed with Scl is also seen with Gata4, for which several published datasets from fetal and adult stages are available (He *et al*, 2014). Analysis of Gata4 binding in different stages of heart development showed gradual loss of overlap between Scl mesodermal binding sites and Gata4 binding from Flk1$^+$ mesoderm to E12.5 hearts to adult hearts (Supplementary Fig S5A and B). While Gata4 binding was observed in both hematopoietic (Gfi1b and Myb) and cardiac enhancers (Tbx5 and Gata6) in mesoderm, hematopoietic enhancers had lost Gata4 binding in fetal hearts by E12.5. Many cardiac enhancers also lost Gata4

Figure 5. A subset of Scl-bound enhancers can be accessed by cardiac transcription factors.

A Scl DNA binding motif analysis shows enrichment of Tal1_Gata, Gata and Ets motifs in both Scl activated and repressed genes.

B Venn diagram showing overlaps between Scl, Hand1 and Gata4 (Oda *et al*, 2013) binding sites in Flk1$^+$ mesoderm documents that some of Scl MES binding sites are also bound by cardiac TFs.

C Gata4, Hand1 and Scl ChIP-seq tracks with cardiac and hematopoietic gene regions show examples of three subgroups of enhancers—those bound by Scl, Hand1 and Gata4 (gray), Scl and Gata4 (orange) and those bound only by Scl (blue).

D–H Scl binding sites that overlap with both Hand1 and Gata4 (gray) or with Hand1 (green) or Gata 4 (orange) alone show higher evolutionary conservation (D) and higher average enrichment of Scl (E), H3K4me1 (F), H3K27ac (G) and Lsd1 (H) in mesoderm compared to sites bound by Scl alone (blue).

I Average expression changes between Scl-expressing and Scl-deficient mesoderm shows that genes that are regulated by enhancers bound by all three (Scl, Hand1 and Gata4) factors or two factors (Scl and Hand1 or Scl and Gata4) show higher absolute expression changes compared to those bound by Scl alone.

J Analysis of Scl-regulated key hematopoietic and cardiac genes shows that many of them can be bound also by cardiac factors, Scl, Gata4 and Hand1 (orange); Scl and Hand1 binding (green); Scl and Gata4 binding (orange); and Scl binding alone (blue).

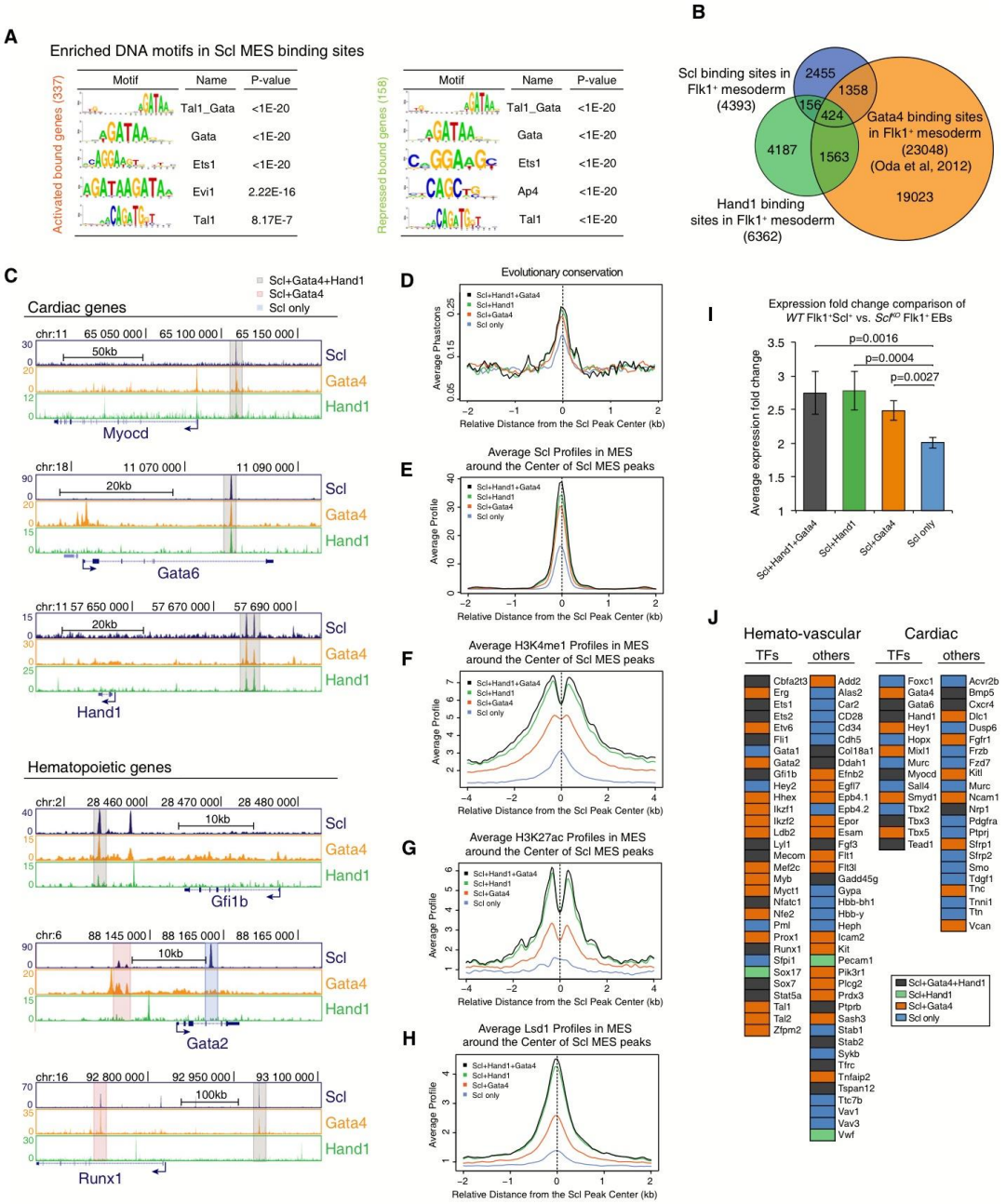

Figure 5.

binding in adult hearts (Supplementary Fig S5C). These data show that the key genes regulating cardiovascular fate determination harbor dually accessible enhancers that can be bound by both hematopoietic and cardiac factors in mesoderm, but are dynamically remodeled during lineage diversification and maturation. Our data propose that this subset of enhancers may be critical for initiating the fate choice between competing cardiovascular lineages.

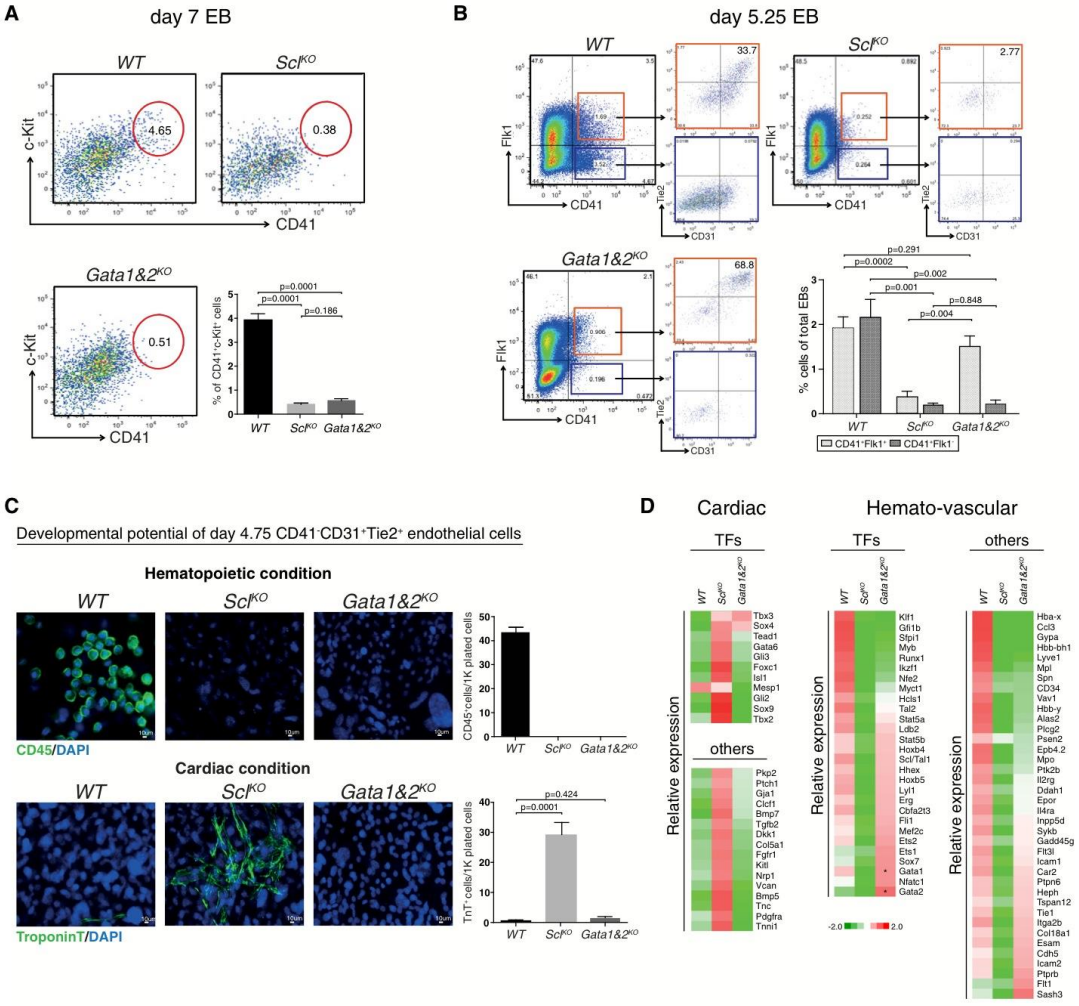

Figure 6. Gata1 and 2 are dispensable for cardiac repression, but essential for the emergence of HS/PCs from hemogenic endothelium.

A FACS analysis of day 7 EBs with markers CD41 and c-Kit shows efficient generation of HS/PCs from WT, but not *Scl*^{KO} or *Gata1&2*^{KO} cells. Average of six independent experiments with SEM is shown.

B FACS analysis of day 5.25 EBs with markers CD41, Flk1, Tie2 and CD31 shows the generation of hemogenic endothelial cells from WT and *Gata1&2*^{KO} cells, but not *Scl*^{KO} cells. Average of five independent biological experiments with SEM is shown.

C Assessment of the developmental potential of day 4.75 EB CD41^{-}CD31^{+}Tie2^{+} endothelial cells on OP9 for 14 days shows the generation of CD45^{+} hematopoietic cells from WT cells but not *Gata1&2*^{KO} or *Scl*^{KO} cells, and troponin T^{+} cardiomyocytes from *Scl*^{KO} cells, but not WT or *Gata1&2*^{KO} cells. Average of four independent experiments with SEM is shown.

D Heatmaps show gene expression differences in subsets of hematopoietic genes between *Gata1&2*^{KO} and WT or *Scl*^{KO} day 4.75 CD41^{-}CD31^{+}Tie2^{+} endothelial cells. Cardiac derepression is observed only in *Scl*^{KO} cells. *designates non-functional transcripts.

Gata1 and/or Gata2 are dispensable for cardiac repression but are essential for emergence of HS/PCs from hemogenic endothelium

Since Scl and Gata4 share common binding sites in both hematopoietic and cardiac enhancers and Scl acts together with hematopoietic Gata factors 1 and 2 in blood forming cells, we investigated whether hematopoietic Gata factors are required for Scl-induced gene activation and/or repression during mesoderm diversification. ChIP–PCR for Gata2 showed that, similar to Scl, Hand1 and Gata4, Gata2 binds to dually accessible enhancers in both hematopoietic and cardiac transcription factors that are activated or repressed by Scl (Supplementary Fig S5D).

To investigate whether hematopoietic Gata factors function in Scl-mediated gene activation and repression, we assessed the developmental potential of Gata1 and 2 double knockout (*Gata1&2^{KO}*) ES cells, which eliminates possible redundancy between Gata1 and 2. No c-Kit$^+$CD41$^+$ hematopoietic progenitors were detected in day 7 *Gata1&2^{KO}* EBs or *Scl^{KO}* EBs (Fig 6A). However, FACS analysis on day 5.25 EBs identified a subpopulation of cells in *Gata1&2^{KO}* EBs that expressed the early HS/PC marker CD41, while *Scl^{KO}* EBs were devoid of this population. Nevertheless, all CD41$^+$ cells in *Gata1&2^{KO}* EBs co-expressed Flk1 and the majority also expressed endothelial markers CD31 and Tie2, raising the hypothesis that HS/PC development becomes stalled at hemogenic endothelium in the absence of Gata1 and 2 (Fig 6B).

To assess the differentiation potential of Gata1- and 2-deficient endothelial cells, EBs were differentiated for 4.75 days, after which CD41$^-$CD31$^+$Tie2$^+$ endothelial cells were sorted and cultured for 14 days in hematopoietic and cardiac conditions on OP9 stroma. Neither *Gata1&2^{KO}* nor *Scl^{KO}* endothelial cells generated CD45$^+$ hematopoietic cells (Fig 6C). In contrast, only *Scl^{KO}*, but not *Gata1&2^{KO}* or WT endothelial cells, robustly differentiated into troponin T$^+$ cardiomyocytes. These data show that Gata1 and/or 2 is required for hematopoiesis, but not for the repression of cardiogenesis in endothelial precursors.

To investigate the effect of Gata1 and 2 on endothelial gene expression, CD41$^-$CD31$^+$Tie2$^+$ endothelial cells from day 4.75 EBs were sorted for RNA sequencing. No significant derepression of cardiac regulators was observed in *Gata1&2^{KO}* endothelial cells, unlike *Scl^{KO}* endothelial cells which showed induction of several cardiac genes (Fig 6D, Supplementary Table S2). Notably, expression of many hemato-vascular transcription factors that were down-regulated in *Scl^{KO}* endothelial cells (e.g. *Lyl1*, *Hhex*, *Cbfa2t3/Eto2*, *Erg*, *Fli1*, *Sox7*) was not significantly decreased in *Gata1&2^{KO}* endothelial cells. Likewise, many surface markers of hemogenic endothelium and HS/PCs (e.g. CD41/Itga2b, VE-cadherin/Cdh5, Esam, Icam2) were expressed in *Gata1&2^{KO}* endothelial cells, further supporting the notion that *Gata1&2^{KO}* cells can specify hemogenic endothelium. However, the expression of key HS/PC transcription factors *Runx1*, *Myb*, *Gfi1b*, *Pu.1/Sfpi1* and *Klf1* was down-regulated in *Gata1&2^{KO}* endothelial cells (Fig 6D), implying that Gata1 and/or 2 is required for the induction of the hematopoietic transcription factor network that enables the emergence of HS/PCs from hemogenic endothelium.

To exclude the possibility that Gata3, a hematopoietic Gata factor that functions in T cells (Hosoya *et al*, 2010) and HSC maintenance (Ku *et al*, 2012) compensates for Gata1 and 2 in cardiac repression, Gata1-, 2- and 3-deficient (*Gata1&2^{KO}Gata3^{KD}*) ES cells were generated using lentiviral knockdown of Gata3. Similar to *Gata1&2^{KO}*, *Gata1&2^{KO}Gata3^{KD}* endothelial cells showed neither up-regulation of cardiac program nor generation of ectopic cardiomyocytes in culture, and the hematopoietic program was similarly stalled at hemogenic endothelium with intact expression of many Scl-dependent hemato-vascular genes (*Hhex*, *Ets2*, *Lyl1*, *Itga2b/CD41*, *Cadh5/Ve-Cad* etc) and defective expression of key HS/PC transcription factors (e.g. *Runx1* and *Myb*) (Supplementary Fig S6). Collectively, these data show that hematopoietic Gata factors are critical for full activation of Scl-dependent hematopoietic transcriptional network, but not for cardiac repression.

Gata factors 1 and 2 recruit Scl to specific binding sites in key hematopoietic transcription factors

To investigate whether loss of Gata1 and Gata2 compromises Scl binding to its targets during mesoderm specification, we determined genome-wide Scl binding sites in Flk1$^+$ mesoderm from *Gata1&2^{KO}* EBs using ChIP-seq (Fig 7A, Supplementary Table S3). The GO terms enriched among the genes associated with overlapping Scl binding sites included both hematopoiesis and cardiogenesis, while the peaks lost in *Gata1&2^{KO}* cells were associated with genes related to hematopoiesis (Fig 7A). Analysis of the individual genes confirmed intact Scl binding to key cardiac enhancers (*Myocardin*, *Gata4* and *Gata6*) in the absence of Gata1 and 2 (Fig 7B, Supplementary Fig S7B). Likewise, a majority of hemato-vascular transcription factors (*Lyl1*, *Fli1*) that were expressed in *Gata1&2^{KO}* endothelium retained Scl binding (Fig 7C). The subset of genes that lost an Scl binding site in *Gata1&2^{KO}* Flk1$^+$ cells included transcription factors *Runx1*, *Myb*, *Pu.1/Sfpi1* and *Gfi1b*, whose expression in endothelium was Gata1 and 2 dependent (Fig 7D, Supplementary Fig S7B). Remarkably, while several other Scl binding sites were preserved near *Runx1* gene, the binding site that was lost in *Gata1&2^{KO}* cells corresponds to +23 enhancer that has been shown to be essential for *Runx1* regulation during HSC emergence (Nottingham *et al*, 2007) and becomes the strongest Scl binding site in HPC7 hematopoietic progenitor cells (Supplementary Fig S3B). These results imply that although Gata1 and 2 are not essential for Scl binding to the majority of its activated or repressed target genes, they are required for the recruitment of Scl to specific regulatory regions that govern the expression of key hematopoietic transcription factors. ChIP-PCR for *Gata1&2^{KO}Gata3^{KD}* mesoderm confirmed similar binding for Scl in key hematopoietic and cardiac enhancers in the absence of all three hematopoietic Gata factors (Supplementary Fig S7A).

We also assessed whether the hematopoietic Gata factors function by modifying the epigenetic landscape to enable access of Scl complex to key hematopoietic enhancers. Analysis of H3K4me1 and H3K27ac in Gata1- and 2-deficient mesodermal cells did not reveal differences in the establishment of primed state in key hematopoietic and cardiac enhancers, including those that could not be activated in *Gata1&2^{KO}* cells (Supplementary Fig S7B). Likewise, there was a strong correlation of global H3K4me1 and H3K27ac levels between WT and *Gata1&2^{KO}* Flk1$^+$ mesoderm (Supplementary Fig S7C). Collectively, these data show that Scl and hematopoietic Gata factors bind to enhancers that have been epigenetically primed for activation in mesoderm prior to their binding. While the repression of the cardiac fate by Scl can occur in the absence of hematopoietic

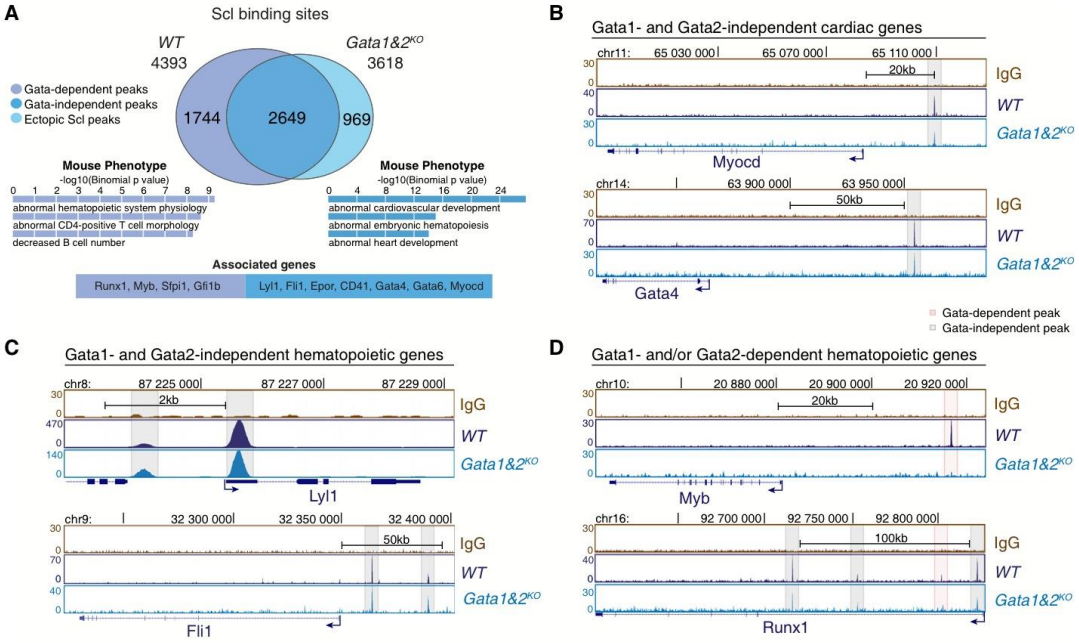

Figure 7. Gata1 and/or Gata2 modulates Scl binding in the enhancers of key hematopoietic transcription factors.

A Intersection of Scl binding sites in WT and *Gata1&2*^{KO} Flk1^{+} MES shows Gata1- and/or Gata2-dependent redistribution of Scl binding sites in a subset of target genes (two independent experiments). Selected GO terms among top 10 most enriched for Gata-independent (blue) and Gata-dependent (purple) Scl binding sites together with example genes reveal Gata1- and/or Gata2-dependent functions for Scl-mediated hematopoietic regulation.

B–D Scl ChIP-seq tracks in WT and *Gata1&2*^{KO} Flk1^{+} MES show Gata1- and 2-independent Scl binding to cardiac regulators (*Myocardin*, *Gata4*) (B), Gata1- and 2-independent Scl binding to key hemato-vascular regulators (*Lyl1*, *Fli1*) (C) and Gata1- and/or 2-dependent Scl binding to key HS/PC transcription factors (*Myb*, *Runx1*) (D).

Gata factors, they help recruit Scl to new regulatory regions to enable activation of key hematopoietic transcription factors that secure the emergence of HS/PCs from hemogenic endothelium.

Discussion

The ability to execute developmental fate decisions with proper temporal and spatial control is critical for embryonic development, as well as for harnessing the power of stem cell and reprogramming technologies for therapeutic applications. The bHLH factor Scl has emerged as a true master regulator of mesoderm fate as it not only governs the establishment of the entire hematopoietic system, but it also is critical for preventing ectopic cardiomyocyte development in hemogenic tissues (Van Handel *et al*, 2012). Here we show that Scl directly binds to enhancers regulating a broad network of hematopoietic and cardiac transcription factors to specify the hematopoietic lineage and override the cardiac fate and thus has a dual function in coordinating the segregation of multipotent cardiovascular mesoderm to downstream cell fates.

We discovered that Scl regulates mesodermal fates by binding to enhancers that have been primed for activation specifically in Flk1^{+} mesoderm. A previous study with DNA binding mutant of Scl showed that 80% of Scl peaks in erythroid cells were lost in the mutant and could neither be bound by Scl's interaction partner Gata1, raising the question whether Scl acts as a pioneer factor at these sites (Kassouf *et al*, 2010). Our finding that the establishment of the active histone modifications, H3K4me1 and H3K27ac, at the enhancers of Scl's hematopoietic and cardiac target genes occurs independent of Scl and its complex partners Gata1 and 2 implies that these factors do not act as a pioneer factors but rather exploit pre-established enhancers in mesoderm. These results suggest that yet another factor(s) is responsible for establishing primed enhancers that can attract Scl and Gata factors to their cell type-specific binding sites. Our data are consistent with a model that the acquisition of a primed, or provisionally activated, state at hematopoietic and cardiac enhancers precedes Scl and Gata1 and 2 binding and determines the available fate options in mesoderm. Our finding that overexpression of Scl in ES cells did not lead to Scl binding to hematopoietic or cardiac enhancers also supports this model.

Several recent studies have documented highly cell type-specific, functional Scl binding during later stages of hematopoietic development (Calero-Nieto *et al*, 2014; Pimkin *et al*, 2014; Wu *et al*, 2014). Our study documents the dynamic nature of Scl binding already in

mesoderm. In contrast to the key hematopoietic enhancers that retained Scl binding and active epigenetic marks throughout hematopoietic development, Scl binding to cardiac enhancers was restricted to Flk1$^+$ mesoderm and correlated with the transient presence of active histone marks. These data imply that Scl represses the cardiac fate during a brief window of developmental plasticity before mesodermal fates become solidified, providing a molecular basis for the inducible loss-of-function studies that narrowed down the temporal requirement for Scl function in cardiac repression to mesoderm/early angioblasts (Van Handel *et al*, 2012). Moreover, these data suggest enhancer decommissioning as a key mechanism that extinguishes the cardiac fate option in hematopoietic cells.

Our studies propose a model that Scl suppresses cardiogenesis by interfering with the activation of key cardiac genes until the 'window of opportunity' for their activation is closed, rather than directly recruiting corepressors. Analyses correlating Scl binding with major corepressors and repressive epigenetic marks (H3K27me3, H3K9me3 and DNA methylation) did not provide a mechanism by which transient Scl binding to these enhancers results in the repression of cardiac genes, but rather suggests that these repression mechanisms contribute to the overall gene silencing later, once the Scl-driven lineage choice decision has already been made.

Lsd1 emerged as a key candidate for modulating enhancer activity during mesoderm diversification as it decommissions cell type-specific enhancers by demethylating H3K4me1 in several developmental contexts including ES cells and myeloid cells (Whyte *et al*, 2012; Kerenyi *et al*, 2013), and interaction of Scl with Lsd1 has been implicated in erythroid progenitors and T-ALL (Hu *et al*, 2009a,b; Li *et al*, 2012). Our analysis verified a strong correlation between Lsd1 and Scl binding sites and H3K4me1 in mesoderm. However, Lsd1 binding to cardiac enhancers was not impaired in Scl-deficient cells. Thus, although Lsd1 is involved in decommissioning of unused enhancers during mesoderm diversification, its recruitment to cardiac enhancers is not Scl dependent. These data do not, however, exclude the possibility that the function of Lsd1, or the COREST complex Lsd1 is part of, may be influenced by Scl. As acetylation can impede Lsd1 function (Amente *et al*, 2013), it is plausible that Scl binding at hematopoietic enhancers reinforces a fully active state, possibly by chromosomal looping to promoter, and thereby indirectly impairs Lsd1 function. On the other hand, Scl binding at cardiac enhancers may interfere with chromosomal looping and/or the establishment of a proper cardiac activation complex, enabling Lsd1 to decommission cardiac enhancers. Future studies are required to directly test these hypotheses.

Our findings that there is substantial overlap with Scl and Hand1 and/or Gata4 mesodermal binding sites, and essentially all major hematopoietic and cardiac transcription factors that are regulated by Scl contain at least one enhancer that can also be bound by Hand1 and/or Gata4, support the model that repression of an alternative fate choice may be the result of preventing activation of these genes by competing lineage-specific regulators. The subset of Scl-bound enhancers that can also be bound by Hand1 and/or Gata4 showed higher evolutionary conservation, higher H3K4me1 and H3K27ac enrichment and Lsd1 binding in mesoderm, and stronger correlation with Scl-dependent gene expression change. We propose that these dually accessible enhancers that can be regulated by factors of two opposing lineages act as a platform where the fate choice is determined. Future studies will determine which cardiac factor(s) is most critical for activating these cardiac enhancers and whether they are also critical for suppressing the hematopoietic program.

We found that Gata2 can bind together with Scl to both hematopoietic and cardiac enhancers; however, we discovered that hematopoietic Gata factors (1, 2 and 3) are dispensable for Scl-mediated cardiac repression, and only necessary for recruiting Scl to specific binding sites to activate hematopoietic factors required for HS/PC emergence and differentiation (Runx1, Pu.1/Sfpi1, Klf1, Gfi1b). These data suggest that although the core Gata/Scl complex can bind to both activated and repressed genes, Gata/Scl interaction becomes critical principally in gene activation. Similar to hematopoietic Gata factors, Runx1 can redistribute Scl to new binding sites as development progresses from endothelium to HS/PCs (Lichtinger *et al*, 2012). Thus, Scl establishes the blood lineage by binding to a broad set of hematopoietic enhancers; it then induces downstream transcriptional network with the help of its target genes, which enable Scl to relocate to new binding sites to build a functional hematopoietic system.

The findings that Scl targets Gata1, Gata2 and Runx1 (Van Handel *et al*, 2012), which are critical for modulating Scl activity in hematopoietic genes, are not essential for cardiac repression underscore the unique role of Scl as a dual regulator of hematopoietic versus cardiac fate choice. Apart from the studies with Scl, ectopic cardiogenesis in hemato-vascular mesoderm has only been observed upon ablation of Etv2, the upstream regulator for Scl (Ren *et al*, 2010; Palencia-Desai *et al*, 2011; Rasmussen *et al*, 2011; Liu *et al*, 2012; Wareing *et al*, 2012). Future studies will be required to determine whether Etv2 has a specific function in silencing cardiac fate or whether it contributes indirectly by inducing Scl expression.

Our finding that Scl directs mesoderm diversification via enhancers is concordant with the data that transcription factor binding at enhancers is a key determinant of tissue-specific gene expression (Heintzman *et al*, 2009; Visel *et al*, 2009; Xu *et al*, 2012). Our discovery that Scl directly binds to enhancers of key transcription factors of two alternative fates suggests a mechanism by which lineage-specific transcription factors secure a mutually exclusive lineage choice by both activating their own lineage and preventing the establishment of alternative fates. Coordination of both processes by the same factor enables accurate fate specification and prevents the generation of a cell with mixed characteristics. As reprogramming of induced pluripotent stem cells is also initiated at enhancers (Soufi *et al*, 2012), understanding the repressive function of master regulators may have broader implications in regenerative medicine as the presence of a factor that could block lineage-specific enhancers during lineage reprogramming may influence the efficiency and outcome of reprogramming. Thus, better understanding of the prerequisites for gene activation and repression by master regulators, and how the epigenetic boundaries are created between cell types, will help develop more effective protocols for directing cell fates for therapeutic applications.

Materials and Methods

ES cell culture and differentiation

Standard ES cell culture conditions were used to maintain *Scl*^{hCD4} (Chung *et al*, 2002), *Scl*^{KO} (Porcher *et al*, 1996), *Scl*^{KO}*iScl*, WT,

Gata1&2^{KO} and *Gata1&2*^{KO}*Gata3*^{KD}ES cells. *Scl*^{KO}*iScl* cell line was generated by transduction of *Scl*^{KO} ES cells with rtTA and PNL1-Scl-GFP lentiviral vectors followed by clonal selection. *Gata1&2* ^{KO}*Gata3*^{KD} ES cells were generated by transducing *Gata1&2*^{KO} ES cells with Gata3 shRNA lentiviral vector (Santa Cruz). Flk1^{+} mesoderm and hemato-vascular derivatives were generated using EB differentiation as described (Mikkola *et al*, 2003). EBs were digested enzymatically and analyzed by FACS or enriched for desired populations by MACS or FACS sorting. For further details about cell culture, see Supplementary Materials and Methods.

Gene expression analysis

RNA preparation, hybridization to Mouse Genome 430 2.0 arrays, and analysis was conducted as described previously (Van Handel *et al*, 2012). Libraries for RNA sequencing were constructed using Encore Complete RNA-Seq DR Multiplex System 1-8 (Nugen). Libraries were sequenced using HIseq-2000 (Illumina). Reads were mapped to mouse genome (mm9) using TopHat v2.0.4 (Trapnell *et al*, 2009). Abundance estimations (FPKMs) were performed with Cufflinks v2.0.1 (Trapnell *et al*, 2010). Assemblies for all samples were merged using Cuffmerge, and differential expression ($P < 0.01$) was determined using Cuffdiff. Quantitative reverse-transcriptase polymerase chain reaction (qRT–PCR) was performed with LightCycler 480 SYBR Green I Master (Roche) using LightCycler 480 (Roche). Primer sequences are listed in Supplementary Table S4. For further details, see Supplementary Materials and Methods.

Chromatin immunoprecipitation sequencing analysis

ChIP with ES, Flk1^{+} mesodermal (MES), HPC7, MEL or HL1 cells were performed as described previously (Ferrari *et al*, 2012; Kerenyi *et al*, 2013). Libraries were generated using Nugen Ovation ultralow kit and sequenced using HIseq-2000 (Illumina). Mapping was performed using Bowtie (Langmead *et al*, 2009) as described (Ferrari *et al*, 2012). Peak identification was performed with MACS v1.3.7.1 (Zhang *et al*, 2008). For published ChIP-seq datasets used and more detailed methods, see Supplementary Materials and Methods.

Reduced representation bisulfite sequencing

RRBS libraries were generated from genomic DNA of mouse ES cells, WT and *Scl*^{KO} Flk1^{+} mesoderm (MES) and MEL cells as described previously (Meissner *et al*, 2005) with minor modifications. RRBS data were aligned with BS-Seeker2 (Guo *et al*, 2013). Differentially methylated cytosines were calculated with methylKit (Akalin *et al*, 2012). For detailed methods and the published genome-wide methylation datasets used in this study, see Supplementary Materials and Methods.

Analysis of endothelial differentiation potential

After 4.75 days of EB induction, CD41^{-}CD31^{+}Tie2^{+}cells were sorted from WT, *Scl*^{KO}, *Scl*^{KO}*iScl*, *Gata1&2*^{KO} and *Gata1&2*^{KO} *Gata3*^{KD} EBs and 20,000 cells were plated on irradiated OP9 stroma in 8-well chamber slides (354118 BD Falcon™). 1 mg/ml doxycycline (1:1,000) is added to *Scl*^{KO}*iScl* culture and is kept on since day 2 of EB induction. The media contained α-MEM, 20% FBS, 1% penicillin, streptomycin and 1% glutamine. For hematopoietic differentiation, 50 ng/ml SCF, 5 ng/ml IL3, 5 ng/ml IL6, 5 ng/ml TPO and 10 ng/ml Flt3L were added. For cardiac differentiation, 5 ng/ml hVEGF, 30 ng/ml mFGF, 50 ng/ml hBMP4 and 1 μM Wnt/Beta-Catenin Inhibitor XAV939 (Sigma) were added. After 14 days, FACS staining or immunostaining was performed as described (Van Handel *et al*, 2012). See Supplementary Materials and Methods for details.

Accession numbers

Microarray, ChIP-seq, RNA-seq and RRBS datasets have been deposited to the NCBI GEO database under the accession number GSE47085. All datasets used in this study are listed in Supplementary Table S5.

Supplementary information for this article is available online: http://emboj.embopress.org

Acknowledgements
The authors thank the Broad Stem Cell Research Center (BSCRC) Flow Cytometry Core for FACS sorting and BSCRC Sequencing core for next-generation sequencing. This work was funded by the California Institute for Regenerative Medicine (CIRM) New Faculty Award (RN1-00557), the Eli and Edythe Broad Center of Regenerative Medicine and Stem Cell Research at UCLA Research Award, American Heart Association (#14GRNT20480340), and Leukemia Lymphoma Society Scholar Award to HKAM (20103778). TO was supported by Leukemia Lymphoma Society postdoctoral fellowship (57537-13) and by the European Union through the European Social Fund (Mobilitas Grant No. MJD284). DD was supported by the government of P.R.C through the State Scholarship Fund (File No. 2011624028). AMH was supported by a fellowship from HFSP and American Society of Hematology. BVH was supported by the NIH/NHLBI T32 HL69766. Contributions of YF and SHO were supported by P30DK049216.

Author contributions
TO and DD were involved in project design, experimental work, data analysis and interpretation and manuscript preparation. RF and RS participated in data analysis and interpretation, and manuscript editing. AM-H, BVH and MAK were involved in experimental work and manuscript editing. LR was involved in experimental work. YF and SHO provided essential reagents and edited the manuscript. MP and SKK interpreted the data and edited the manuscript. HKAM was involved in project design, data analysis and interpretation, and manuscript preparation.

Conflict of interest
The authors declare that they have no conflict of interest.

References

Akalin A, Kormaksson M, Li S, Garrett-Bakelman FE, Figueroa ME, Melnick A, Mason CE (2012) methylKit: a comprehensive R package for the analysis of genome-wide DNA methylation profiles. *Genome Biol* 13: R87

Amente S, Lania L, Majello B (2013) The histone LSD1 demethylase in stemness and cancer transcription programs. *Biochim Biophys Acta* 1829: 981 – 986

Bertrand JY, Chi NC, Santoso B, Teng S, Stainier DYR, Traver D (2010) Haematopoietic stem cells derive directly from aortic endothelium during development. *Nature* 464: 108 – 111

Blattler A, Farnham PJ (2013) Cross-talk between site-specific transcription factors and DNA methylation states. *J Biol Chem* 288: 34287 – 34294

Blow MJ, McCulley DJ, Li Z, Zhang T, Akiyama JA, Holt A, Plajzer-Frick I, Shoukry M, Wright C, Chen F, Afzal V, Bristow J, Ren B, Black BL, Rubin EM, Visel A, Pennacchio LA (2010) ChIP-Seq identification of weakly conserved heart enhancers. *Nat Genet* 42: 806 – 810

Boisset J-C, van Cappellen W, Andrieu-Soler C, Galjart N, Dzierzak E, Robin C (2010) In vivo imaging of haematopoietic cells emerging from the mouse aortic endothelium. *Nature* 464: 116 – 120

Bresnick EH, Katsumura KR, Lee H-Y, Johnson KD, Perkins AS (2012) Master regulatory GATA transcription factors: mechanistic principles and emerging links to hematologic malignancies. *Nucleic Acids Res* 40: 5819 – 5831

Calero-Nieto FJ, Ng FS, Wilson NK, Hannah R, Moignard V, Leal-Cervantes AI, Jimenez-Madrid I, Diamanti E, Wernisch L, Göttgens B (2014) Key regulators control distinct transcriptional programmes in blood progenitor and mast cells. *EMBO J* 33: 1212 – 1226

Chen MJ, Yokomizo T, Zeigler BM, Dzierzak E, Speck NA (2009) Runx1 is required for the endothelial to haematopoietic cell transition but not thereafter. *Nature* 457: 887 – 891

Chlon TM, Crispino JD (2012) Combinatorial regulation of tissue specification by GATA and FOG factors. *Development* 139: 3905 – 3916

Chung YS, Zhang WJ, Arentson E, Kingsley PD, Palis J, Choi K (2002) Lineage analysis of the hemangioblast as defined by FLK1 and SCL expression. *Development* 129: 5511 – 5520

Creemers EE, Sutherland LB, McAnally J, Richardson JA, Olson EN (2006) Myocardin is a direct transcriptional target of Mef2, Tead and Foxo proteins during cardiovascular development. *Development* 133: 4245 – 4256

Creyghton MP, Cheng AW, Welstead GG, Kooistra T, Carey BW, Steine EJ, Hanna J, Lodato MA, Frampton GM, Sharp PA, Boyer LA, Young RA, Jaenisch R (2010) Histone H3K27ac separates active from poised enhancers and predicts developmental state. *Proc Natl Acad Sci USA* 107: 21931 – 21936

Cui K, Zang C, Roh T-Y, Schones DE, Childs RW, Peng W, Zhao K (2009) Chromatin signatures in multipotent human hematopoietic stem cells indicate the fate of bivalent genes during differentiation. *Cell Stem Cell* 4: 80 – 93

De Bruijn MF, Speck NA, Peeters MC, Dzierzak E (2000) Definitive hematopoietic stem cells first develop within the major arterial regions of the mouse embryo. *EMBO J* 19: 2465 – 2474

De Pater E, Kaimakis P, Vink CS, Yokomizo T, Yamada-Inagawa T, van der Linden R, Kartalaei PS, Camper SA, Speck N, Dzierzak E (2013) Gata2 is required for HSC generation and survival. *J Exp Med* 210: 2843 – 2850

Fehling HJ, Lacaud G, Kubo A, Kennedy M, Robertson S, Keller G, Kouskoff V (2003) Tracking mesoderm induction and its specification to the hemangioblast during embryonic stem cell differentiation. *Development* 130: 4217 – 4227

Ferrari R, Su T, Li B, Bonora G, Oberai A, Chan Y, Sasidharan R, Berk AJ, Pellegrini M, Kurdistani SK (2012) Reorganization of the host epigenome by a viral oncogene. *Genome Res* 22: 1212 – 1221

Fujiwara Y, Chang AN, Williams AM, Orkin SH (2004) Functional overlap of GATA-1 and GATA-2 in primitive hematopoietic development. *Blood* 103: 583 – 585

Gao X, Johnson KD, Chang Y-I, Boyer ME, Dewey CN, Zhang J, Bresnick EH (2013) Gata2 cis-element is required for hematopoietic stem cell generation in the mammalian embryo. *J Exp Med* 210: 2833 – 2842

Guo W, Fiziev P, Yan W, Cokus S, Sun X, Zhang MQ, Chen P-Y, Pellegrini M (2013) BS-Seeker2: a versatile aligning pipeline for bisulfite sequencing data. *BMC Genom* 14: 774

Habibi E, Brinkman AB, Arand J, Kroeze LI, Kerstens HHD, Matarese F, Lepikhov K, Gut M, Brun-Heath I, Hubner NC, Benedetti R, Altucci L, Jansen JH, Walter J, Gut IG, Marks H, Stunnenberg HG (2013) Whole-genome bisulfite sequencing of two distinct interconvertible DNA methylomes of mouse embryonic stem cells. *Cell Stem Cell* 13: 360 – 369

Harmston N, Lenhard B (2013) Chromatin and epigenetic features of long-range gene regulation. *Nucleic Acids Res* 41: 7185 – 7199

He A, Gu F, Hu Y, Ma Q, Yi Ye L, Akiyama JA, Visel A, Pennacchio LA, Pu WT (2014) Dynamic GATA4 enhancers shape the chromatin landscape central to heart development and disease. *Nat Commun* 5: 4907

Heintzman ND, Hon GC, Hawkins RD, Kheradpour P, Stark A, Harp LF, Ye Z, Lee LK, Stuart RK, Ching CW, Ching KA, Antosiewicz-Bourget JE, Liu H, Zhang X, Green RD, Lobanenkov VV, Stewart R, Thomson JA, Crawford GE, Kellis M *et al* (2009) Histone modifications at human enhancers reflect global cell-type-specific gene expression. *Nature* 459: 108 – 112

Holtzinger A, Rosenfeld GE, Evans T (2010) Gata4 directs development of cardiac-inducing endoderm from ES cells. *Dev Biol* 337: 63 – 73

Hon GC, Rajagopal N, Shen Y, McCleary DF, Yue F, Dang MD, Ren B (2013) Epigenetic memory at embryonic enhancers identified in DNA methylation maps from adult mouse tissues. *Nat Genet* 45: 1198 – 1206

Hosoya T, Maillard I, Engel JD (2010) From the cradle to the grave: activities of GATA-3 throughout T-cell development and differentiation. *Immunol Rev* 238: 110 – 125

Hu X, Li X, Valverde K, Fu X, Noguchi C, Qiu Y, Huang S (2009a) LSD1-mediated epigenetic modification is required for TAL1 function and hematopoiesis. *Proc Natl Acad Sci USA* 106: 10141 – 10146

Hu X, Ybarra R, Qiu Y, Bungert J, Huang S (2009b) Transcriptional regulation by TAL1: a link between epigenetic modifications and erythropoiesis. *Epigenetics* 4: 357 – 361

Huang DW, Sherman BT, Tan Q, Kir J, Liu D, Bryant D, Guo Y, Stephens R, Baseler MW, Lane HC, Lempicki RA (2007) DAVID Bioinformatics Resources: expanded annotation database and novel algorithms to better extract biology from large gene lists. *Nucleic Acids Res* 35: W169 – W175

Huang P, He Z, Ji S, Sun H, Xiang D, Liu C, Hu Y, Wang X, Hui L (2011) Induction of functional hepatocyte-like cells from mouse fibroblasts by defined factors. *Nature* 475: 386 – 389

Huber TL, Kouskoff V, Fehling HJ, Palis J, Keller G (2004) Haemangioblast commitment is initiated in the primitive streak of the mouse embryo. *Nature* 432: 625 – 630

Ieda M, Fu J-D, Delgado-Olguin P, Vedantham V, Hayashi Y, Bruneau BG, Srivastava D (2010) Direct reprogramming of fibroblasts into functional cardiomyocytes by defined factors. *Cell* 142: 375 – 386

Iida M, Heike T, Yoshimoto M, Baba S, Doi H, Nakahata T (2005) T Identification of cardiac stem cells with FLK1, CD31, and VE-cadherin expression during embryonic stem cell differentiation. *FASEB J* 19: 371 – 378

Ismailoglu I, Yeamans G, Daley GQ, Perlingeiro RCR, Kyba M (2008) Mesodermal patterning activity of SCL. *Exp Hematol* 36: 1593 – 1603

Kassouf MT, Hughes JR, Taylor S, McGowan SJ, Soneji S, Green AL, Vyas P, Porcher C (2010) Genome-wide identification of TAL1's functional targets: insights into its mechanisms of action in primary erythroid cells. *Genome Res* 20: 1064 – 1083

Kataoka H, Hayashi M, Nakagawa R, Tanaka Y, Izumi N, Nishikawa S, Jakt ML, Tarui H, Nishikawa S-I (2011) Etv2/ER71 induces vascular mesoderm from Flk1+PDGFRα+ primitive mesoderm. *Blood* 118: 6975 – 6986

Kattman SJ, Huber TL, Keller GM (2006) Multipotent flk-1^{+} cardiovascular progenitor cells give rise to the cardiomyocyte, endothelial, and vascular smooth muscle lineages. *Dev Cell* 11: 723 – 732

Kerenyi MA, Shao Z, Hsu Y-J, Guo G, Luc S, O'Brien K, Fujiwara Y, Peng C, Nguyen M, Orkin SH (2013) Histone demethylase Lsd1 represses hematopoietic stem and progenitor cell signatures during blood cell maturation. *Elife* 2: e00633

Kim J, Efe JA, Zhu S, Talantova M, Yuan X, Wang S, Lipton SA, Zhang K, Ding S (2011) Direct reprogramming of mouse fibroblasts to neural progenitors. *Proc Natl Acad Sci USA* 108: 7838 – 7843

Kissa K, Herbomel P (2010) Blood stem cells emerge from aortic endothelium by a novel type of cell transition. *Nature* 464: 112 – 115

Kowalczyk MS, Hughes JR, Garrick D, Lynch MD, Sharpe JA, Sloane-Stanley JA, McGowan SJ, De Gobbi M, Hosseini M, Vernimmen D, Brown JM, Gray NE, Collavin L, Gibbons RJ, Flint J, Taylor S, Buckle VJ, Milne TA, Wood WG, Higgs DR (2012) Intragenic enhancers act as alternative promoters. *Mol Cell* 45: 447 – 458

Ku C-J, Hosoya T, Maillard I, Engel JD (2012) GATA-3 regulates hematopoietic stem cell maintenance and cell-cycle entry. *Blood* 119: 2242 – 2251

Langmead B, Trapnell C, Pop M, Salzberg SL (2009) Ultrafast and memory-efficient alignment of short DNA sequences to the human genome. *Genome Biol* 10: R25

Lee D, Park C, Lee H, Lugus JJ, Kim SH, Arentson E, Chung YS, Gomez G, Kyba M, Lin S, Janknecht R, Lim D-S, Choi K (2008) ER71 acts downstream of BMP, Notch, and Wnt signaling in blood and vessel progenitor specification. *Cell Stem Cell* 2: 497 – 507

Li W, Ferkowicz MJ, Johnson SA, Shelley WC, Yoder MC (2005) Endothelial cells in the early murine yolk sac give rise to CD41-expressing hematopoietic cells. *Stem Cells Dev* 14: 44 – 54

Li Y, Deng C, Hu X, Patel B, Fu X, Qiu Y, Brand M, Zhao K, Huang S (2012) Dynamic interaction between TAL1 oncoprotein and LSD1 regulates TAL1 function in hematopoiesis and leukemogenesis. *Oncogene* 31: 5007 – 5018

Lichtinger M, Ingram R, Hannah R, Müller D, Clarke D, Assi SA, Lie-A-Ling M, Noailles L, Vijayabaskar MS, Wu M, Tenen DG, Westhead DR, Kouskoff V, Lacaud G, Göttgens B, Bonifer C (2012) RUNX1 reshapes the epigenetic landscape at the onset of haematopoiesis. *EMBO J* 31: 4318 – 4333

Lien CL, Wu C, Mercer B, Webb R, Richardson JA, Olson EN (1999) Control of early cardiac-specific transcription of Nk2–5 by a GATA-dependent enhancer. *Development* 126: 75 – 84

Liu F, Kang I, Park C, Chang L-W, Wang W, Lee D, Lim D-S, Vittet D, Nerbonne JM, Choi K (2012) ER71 specifies Flk-1$^+$ hemangiogenic mesoderm by inhibiting cardiac mesoderm and Wnt signaling. *Blood* 119: 3295 – 3305

McLean CY, Bristor D, Hiller M, Clarke SL, Schaar BT, Lowe CB, Wenger AM, Bejerano G (2010) GREAT improves functional interpretation of cis-regulatory regions. *Nat Biotechnol* 28: 495 – 501

Meissner A, Gnirke A, Bell GW, Ramsahoye B, Lander ES, Jaenisch R (2005) Reduced representation bisulfite sequencing for comparative high-resolution DNA methylation analysis. *Nucleic Acids Res* 33: 5868 – 5877

Mikkola HKA, Fujiwara Y, Schlaeger TM, Traver D, Orkin SH (2003) Expression of CD41 marks the initiation of definitive hematopoiesis in the mouse embryo. *Blood* 101: 508 – 516

North T, Gu TL, Stacy T, Wang Q, Howard L, Binder M, Marín-Padilla M, Speck NA (1999) Cbfa2 is required for the formation of intra-aortic hematopoietic clusters. *Development* 126: 2563 – 2575

Nottingham WT, Jarratt A, Burgess M, Speck CL, Cheng J-F, Prabhakar S, Rubin EM, Li P-S, Sloane-Stanley J, Kong-A-San J, de Bruijn MFTR (2007) Runx1-mediated hematopoietic stem-cell emergence is controlled by a Gata/Ets/SCL-regulated enhancer. *Blood* 110: 4188 – 4197

Oda M, Kumaki Y, Shigeta M, Jakt LM, Matsuoka C, Yamagiwa A, Niwa H, Okano M (2013) DNA methylation restricts lineage-specific functions of transcription factor Gata4 during embryonic stem cell differentiation. *PLoS Genet* 9: e1003574

Palencia-Desai S, Kohli V, Kang J, Chi NC, Black BL, Sumanas S (2011) Vascular endothelial and endocardial progenitors differentiate as cardiomyocytes in the absence of Etsrp/Etv2 function. *Development* 138: 4721 – 4732

Pereira C-F, Chang B, Qiu J, Niu X, Papatsenko D, Hendry CE, Clark NR, Nomura-Kitabayashi A, Kovacic JC, Ma'ayan A, Schaniel C, Lemischka IR, Moore K (2013) Induction of a hemogenic program in mouse fibroblasts. *Cell Stem Cell* 13: 205 – 218

Pimkin M, Kossenkov A V, Mishra T, Morrissey CS, Wu W, Keller CA, Blobel GA, Lee D, Beer MA, Hardison RC, Weiss MJ (2014) Divergent functions of hematopoietic transcription factors in lineage priming and differentiation during erythro-megakaryopoiesis. *Genome Res* 24: 1932 – 1944

Pinello L, Xu J, Orkin SH, Yuan G-C (2014) Analysis of chromatin-state plasticity identifies cell-type-specific regulators of H3K27me3 patterns. *Proc Natl Acad Sci USA* 111: E344 – E353

Porcher C, Swat W, Rockwell K, Fujiwara Y, Alt FW, Orkin SH (1996) The T cell leukemia oncoprotein SCL/tal-1 is essential for development of all hematopoietic lineages. *Cell* 86: 47 – 57

Rasmussen TL, Kweon J, Diekmann MA, Belema-Bedada F, Song Q, Bowlin K, Shi X, Ferdous A, Li T, Kyba M, Metzger JM, Koyano-Nakagawa N, Garry DJ (2011) ER71 directs mesodermal fate decisions during embryogenesis. *Development* 138: 4801 – 4812

Ren X, Gomez GA, Zhang B, Lin S (2010) Scl isoforms act downstream of etsrp to specify angioblasts and definitive hematopoietic stem cells. *Blood* 115: 5338 – 5346

Rhodes KE, Gekas C, Wang Y, Lux CT, Francis CS, Chan DN, Conway S, Orkin SH, Yoder MC, Mikkola HKA (2008) The emergence of hematopoietic stem cells is initiated in the placental vasculature in the absence of circulation. *Cell Stem Cell* 2: 252 – 263

Schoenebeck JJ, Keegan BR, Yelon D (2007) Vessel and blood specification override cardiac potential in anterior mesoderm. *Dev Cell* 13: 254 – 267

Soufi A, Donahue G, Zaret KS (2012) Facilitators and impediments of the pluripotency reprogramming factors' initial engagement with the genome. *Cell* 151: 994 – 1004

Sumanas S, Gomez G, Zhao Y, Park C, Choi K, Lin S (2008) Interplay among Etsrp/ER71, Scl, and Alk8 signaling controls endothelial and myeloid cell formation. *Blood* 111: 4500 – 4510

Takahashi S, Shimizu R, Suwabe N, Kuroha T, Yoh K, Ohta J, Nishimura S, Lim KC, Engel JD, Yamamoto M (2000) GATA factor transgenes under GATA-1 locus control rescue germline GATA-1 mutant deficiencies. *Blood* 96: 910 – 916

Takahashi K, Yamanaka S (2006) Induction of pluripotent stem cells from mouse embryonic and adult fibroblast cultures by defined factors. *Cell* 126: 663 – 676

Trapnell C, Pachter L, Salzberg SL (2009) TopHat: discovering splice junctions with RNA-Seq. *Bioinformatics* 25: 1105 – 1111

Trapnell C, Williams BA, Pertea G, Mortazavi A, Kwan G, van Baren MJ, Salzberg SL, Wold BJ, Pachter L (2010) Transcript assembly and quantification by RNA-Seq reveals unannotated transcripts and isoform switching during cell differentiation. *Nat Biotechnol* 28: 511 – 515

Tripic T, Deng W, Cheng Y, Zhang Y, Vakoc CR, Gregory GD, Hardison RC, Blobel GA (2009) SCL and associated proteins distinguish active from repressive GATA transcription factor complexes. *Blood* 113: 2191 – 2201

Van Handel B, Montel-Hagen A, Sasidharan R, Nakano H, Ferrari R, Boogerd CJ, Schredelseker J, Wang Y, Hunter S, Org T, Zhou J, Li X, Pellegrini M,

Chen J-N, Orkin SH, Kurdistani SK, Evans SM, Nakano A, Mikkola HKA (2012) Scl represses cardiomyogenesis in prospective hemogenic endothelium and endocardium. *Cell* 150: 590 – 605

Visel A, Minovitsky S, Dubchak I, Pennacchio LA (2007) VISTA enhancer browser—a database of tissue-specific human enhancers. *Nucleic Acids Res* 35: D88 – D92

Visel A, Blow MJ, Li Z, Zhang T, Akiyama JA, Holt A, Plajzer-Frick I, Shoukry M, Wright C, Chen F, Afzal V, Ren B, Rubin EM, Pennacchio LA (2009) ChIP-seq accurately predicts tissue-specific activity of enhancers. *Nature* 457: 854 – 858

Wadman IA, Osada H, Grütz GG, Agulnick AD, Westphal H, Forster A, Rabbitts TH (1997) The LIM-only protein Lmo2 is a bridging molecule assembling an erythroid, DNA-binding complex which includes the TAL1, E47, GATA-1 and Ldb1/NLI proteins. *EMBO J* 16: 3145 – 3157

Wamstad JA, Alexander JM, Truty RM, Shrikumar A, Li F, Eilertson KE, Ding H, Wylie JN, Pico AR, Capra JA, Erwin G, Kattman SJ, Keller GM, Srivastava D, Levine SS, Pollard KS, Holloway AK, Boyer LA, Bruneau BG (2012) Dynamic and coordinated epigenetic regulation of developmental transitions in the cardiac lineage. *Cell* 151: 206 – 220

Wareing S, Mazan A, Pearson S, Göttgens B, Lacaud G, Kouskoff V (2012) The Flk1-Cre-mediated deletion of ETV2 defines its narrow temporal requirement during embryonic hematopoietic development. *Stem Cells* 30: 1521 – 1531

Whyte WA, Bilodeau S, Orlando DA, Hoke HA, Frampton GM, Foster CT, Cowley SM, Young RA (2012) Enhancer decommissioning by LSD1 during embryonic stem cell differentiation. *Nature* 482: 221 – 225

Wilson NK, Foster SD, Wang X, Knezevic K, Schütte J, Kaimakis P, Chilarska PM, Kinston S, Ouwehand WH, Dzierzak E, Pimanda JE, de Bruijn MFTR, Göttgens B (2010) Combinatorial transcriptional control in blood stem/progenitor cells: genome-wide analysis of ten major transcriptional regulators. *Cell Stem Cell* 7: 532 – 544

Wozniak RJ, Boyer ME, Grass JA, Lee Y, Bresnick EH (2007) Context-dependent GATA factor function: combinatorial requirements for transcriptional control in hematopoietic and endothelial cells. *J Biol Chem* 282: 14665 – 14674

Wu W, Morrissey CS, Keller CA, Mishra T, Pimkin M, Blobel GA, Weiss MJ, Hardison RC (2014) Dynamic shifts in occupancy by TAL1 are guided by GATA factors and drive large-scale reprogramming of gene expression during hematopoiesis. *Genome Res* 24: 1945 – 1962

Xu J, Shao Z, Glass K, Bauer DE, Pinello L, Van Handel B, Hou S, Stamatoyannopoulos JA, Mikkola HKA, Yuan G-C, Orkin SH (2012) Combinatorial assembly of developmental stage-specific enhancers controls gene expression programs during human erythropoiesis. *Dev Cell* 23: 796 – 811

Yoshimoto M, Montecino-Rodriguez E, Ferkowicz MJ, Porayette P, Shelley WC, Conway SJ, Dorshkind K, Yoder MC (2011) Embryonic day 9 yolk sac and intra-embryonic hemogenic endothelium independently generate a B-1 and marginal zone progenitor lacking B-2 potential. *Proc Natl Acad Sci USA* 108: 1468 – 1473

Yu M, Riva L, Xie H, Schindler Y, Moran TB, Cheng Y, Yu D, Hardison R, Weiss MJ, Orkin SH, Bernstein BE, Fraenkel E, Cantor AB (2009) Insights into GATA-1-mediated gene activation versus repression via genome-wide chromatin occupancy analysis. *Mol Cell* 36: 682 – 695

Zentner GE, Tesar PJ, Scacheri PC (2011) Epigenetic signatures distinguish multiple classes of enhancers with distinct cellular functions. *Genome Res* 21: 1273 – 1283

Zhang Y, Liu T, Meyer CA, Eeckhoute J, Johnson DS, Bernstein BE, Nusbaum C, Myers RM, Brown M, Li W, Liu XS (2008) Model-based analysis of ChIP-Seq (MACS). *Genome Biol* 9: R137

Zovein AC, Hofmann JJ, Lynch M, French WJ, Turlo KA, Yang Y, Becker MS, Zanetta L, Dejana E, Gasson JC, Tallquist MD, Iruela-Arispe ML (2008) Fate tracing reveals the endothelial origin of hematopoietic stem cells. *Cell Stem Cell* 3: 625 – 636

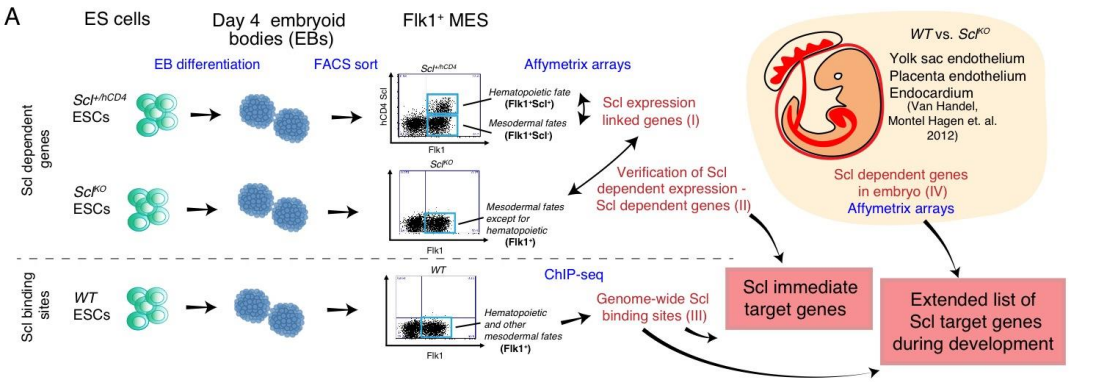
A
ES cells
Day 4 embryoid bodies (EBs)
Flk1+ MES
EB differentiation
FACS sort
Affymetrix arrays
Scl dependent genes
Scl+/hCD4 ESCs
SclKO ESCs
Hematopoietic fate (Flk1+Scl+)
Mesodermal fates (Flk1+Scl-)
Mesodermal fates except for hematopoietic (Flk1+)
Scl expression linked genes (I)
Verification of Scl dependent expression - Scl dependent genes (II)
WT vs. SclKO
Yolk sac endothelium
Placenta endothelium
Endocardium
(Van Handel, Montel Hagen et. al. 2012)
Scl dependent genes in embryo (IV)
Affymetrix arrays
Scl binding sites
WT ESCs
ChIP-seq
Hematopoietic and other mesodermal fates (Flk1+)
Genome-wide Scl binding sites (III)
Scl immediate target genes
Extended list of Scl target genes during development

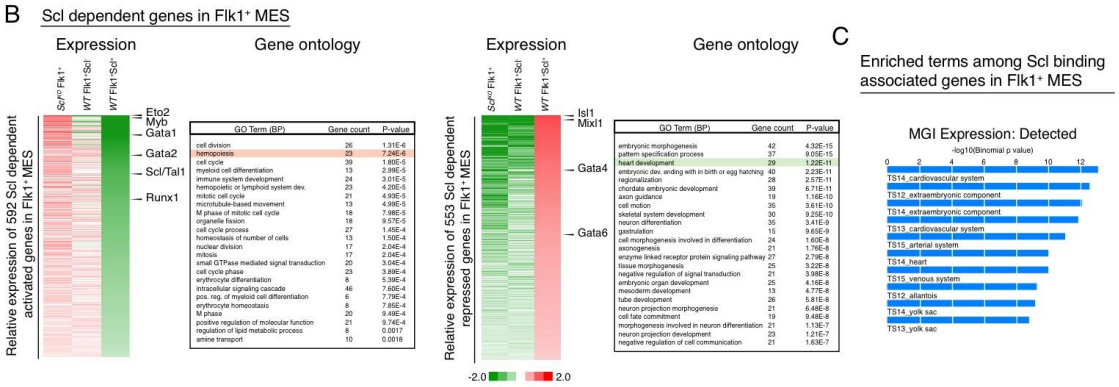
B
Scl dependent genes in Flk1+ MES
Expression
Gene ontology
Relative expression of 592 Scl dependent activated genes in Flk1+ MES
Eto2
Myb
Gata1
Gata2
Scl/Tal1
Runx1
GO Term (BP) Gene count P-value
cell division 26 1.31E-6
hemopoiesis 23 7.24E-6
cell cycle 39 1.80E-5
myeloid cell differentiation 13 2.99E-5
immune system development 24 3.01E-5
hemopoietic or lymphoid system dev. 23 4.20E-5
mitotic cell cycle 21 4.93E-5
microtubule-based movement 13 4.99E-5
M phase of mitotic cell cycle 18 7.98E-5
organelle fission 18 9.57E-5
cell cycle process 27 1.45E-4
homeostasis of number of cells 13 1.50E-4
nuclear division 17 2.04E-4
mitosis 17 2.04E-4
small GTPase mediated signal transduction 20 3.04E-4
cell cycle phase 23 3.89E-4
erythrocyte differentiation 8 5.39E-4
intracellular signaling cascade 46 7.60E-4
pos. reg. of myeloid cell differentiation 6 7.79E-4
erythrocyte homeostasis 8 7.85E-4
M phase 20 9.49E-4
positive regulation of molecular function 21 9.74E-4
regulation of lipid metabolic process 8 0.0017
amine transport 10 0.0018
Relative expression of 553 Scl dependent repressed genes in Flk1+ MES
Isl1
Mixl1
Gata4
Gata6
GO Term (BP) Gene count P-value
embryonic morphogenesis 42 4.32E-15
pattern specification process 37 9.05E-15
heart development 29 1.22E-11
embryonic dev. ending with in birth or egg hatching 40 2.23E-11
regionalization 28 2.57E-11
chordate embryonic development 39 6.71E-11
axon guidance 19 1.16E-10
cell motion 35 3.61E-10
skeletal system development 30 9.25E-10
neuron differentiation 35 3.41E-9
gastrulation 15 9.65E-9
cell morphogenesis involved in differentiation 24 1.60E-8
axonogenesis 21 1.76E-8
enzyme linked receptor protein signaling pathway 27 2.79E-8
tissue morphogenesis 25 3.22E-8
negative regulation of signal transduction 21 3.98E-8
embryonic organ development 25 4.16E-8
mesoderm development 13 4.77E-8
tube development 26 5.81E-8
neuron projection morphogenesis 21 6.48E-8
cell fate commitment 19 9.48E-8
morphogenesis involved in neuron differentiation 21 1.13E-7
neuron projection development 23 1.21E-7
negative regulation of cell communication 21 1.63E-7
-2.0
2.0
C
Enriched terms among Scl binding associated genes in Flk1+ MES
MGI Expression: Detected
-log10(Binomial p value)
TS14_cardiovascular system
TS12_extraembryonic component
TS14_extraembryonic component
TS13_cardiovascular system
TS15_arterial system
TS14_heart
TS15_venous system
TS12_allantois
TS14_yolk sac
TS13_yolk sac

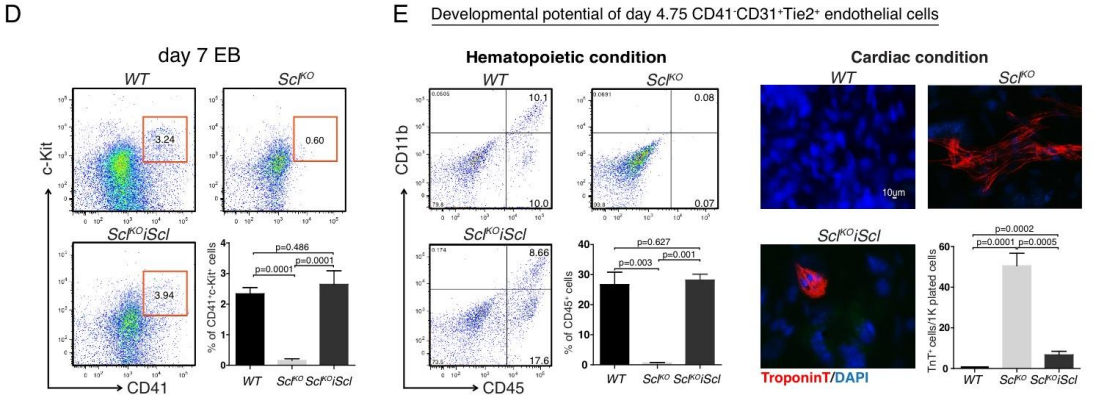
D
day 7 EB
WT
SclKO
SclKOiScl
c-Kit
CD41
3.24
0.60
3.94
% of CD41+c-Kit+ cells
p=0.486
p=0.0001
p=0.0001
p=0.0001
E
Developmental potential of day 4.75 CD41-CD31+Tie2+ endothelial cells
Hematopoietic condition
Cardiac condition
CD11b
CD45
10.1
10.0
0.08
0.07
8.66
17.6
% of CD45+ cells
p=0.627
p=0.003
p=0.001
10μm
TroponinT/DAPI
TnT+ cells/1K plated cells
p=0.0002
p=0.0001
p=0.0005

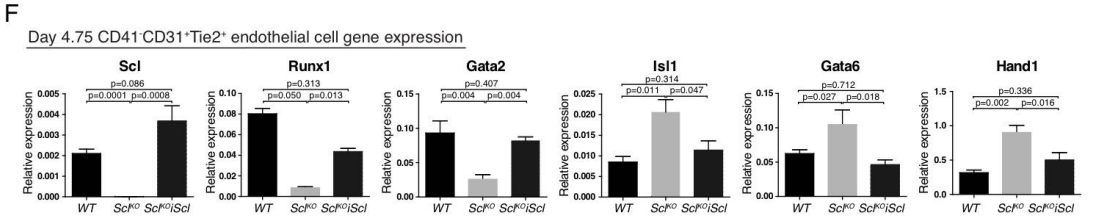
F
Day 4.75 CD41-CD31+Tie2+ endothelial cell gene expression
Scl
Runx1
Gata2
Isl1
Gata6
Hand1
Relative expression
p=0.086
p=0.0001
p=0.0008
p=0.313
p=0.050
p=0.013
p=0.407
p=0.004
p=0.004
p=0.314
p=0.011
p=0.047
p=0.712
p=0.027
p=0.018
p=0.336
p=0.002
p=0.016

Figure S1. Stepwise analysis of Scl target genes in ES cell derived Flk1^{+} mesoderm.

A Experimental workflow scheme for expression and ChIP-seq analysis to identify Scl target genes. To define genes that become induced upon Scl expression, *Scl^{hCD4}* reporter ES cells (Chung *et al*, 2002) were used to identify genes that become up-regulated in day 4 Scl-expressing mesoderm (Flk1^{+}Scl^{+}) as compared to Flk1^{+}Scl^{-} mesodermal precursors that give rise to other mesodermal lineages (I). To define the genes that also depend on Scl for their expression, Flk1^{+} mesoderm from *Scl^{KO}* ES cells (Porcher *et al*, 1996) were added in the comparison (II). Microarray analysis identified 592 and 553 annotated genes that were significantly up- or down-regulated in Flk1^{+}Scl^{+} mesoderm in *Scl^{hCD4}* embryoid bodies (EBs) as compared to both Flk1^{+}Scl^{-} mesoderm from *Scl^{hCD4}* EBs and Flk1^{+} mesoderm from *Scl^{KO}* EBs (Table S1B, C). ChIP-seq was used to determine genome-wide chromatin occupancy of Scl in Flk1^{+} mesoderm from day 4 EBs (III). Intersecting the data from two independent Scl ChIP-seq experiments identified 4,393 Scl binding sites, which associated with 4,158 genes within 200kb range from transcriptional start sites (TSS) (Table S1A). To identify Scl target genes later in development (Extended lists of Scl activated and repressed genes) Scl MES binding sites (III) were intersected with Scl dependent genes in yolk sac and placenta endothelium and endocardium (IV) (Van Handel *et al*, 2012) (Table S1D, E).

B Gene expression heatmaps and enriched DAVID (Huang *et al*, 2007) gene ontology (GO) terms for the Scl activated and repressed genes in day 4 Flk1^{+} MES show enrichment of hematopoietic and cardiac terms respectively.

C Genomic Regions Enrichment of Annotations Tool (GREAT) (McLean *et al*, 2010) enrichment analysis for 4393 Scl peaks in Flk1^{+} MES shows enrichment of heart related terms.

D FACS analysis of day 7 EBs from *WT, Scl*^{KO} and *Scl*^{KO}*iScl* ES cells for HS/PC markers CD41 and c-Kit shows that HS/PC generation is rescued upon induction of Scl expression. Average of eight independent experiments with SEM are shown.

E Developmental potential assay of CD41^{-}CD31^{+}Tie2^{+} endothelial cells from day 4.75 EBs by culturing them on OP9 for 14 days in hematopoietic and cardiac conditions followed by staining for CD45 (hematopoietic cells) and TroponinT (cardiomyocytes) shows that induction of Scl expression rescues hematopoietic cell generation and represses ectopic cardiomyogenesis. Average of four independent experiments with SEM are shown.

F q-RT-PCR in day 4.75 CD41^{-}CD31^{+}Tie2^{+} endothelial cells shows that, induced Scl expression rescues the expression of hematopoietic genes and represses the expression of cardiac genes. Average of four independent experiments with SEM are shown.

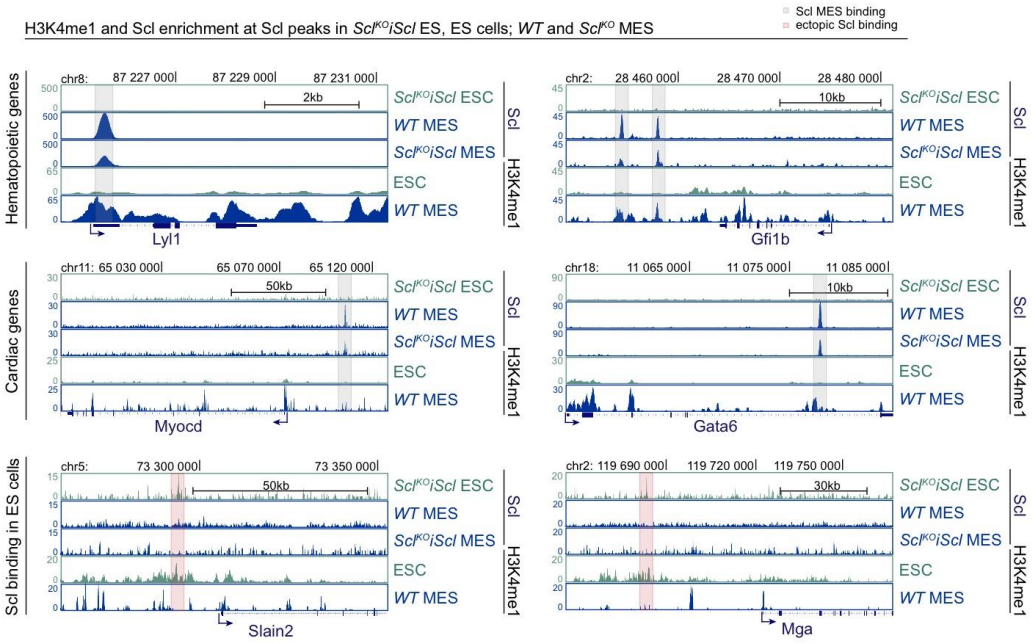

Figure S2. Scl overexpression in *Scl*^{KO} background restores Scl chromatin binding in mesoderm but not in ES cells.

Scl ChIP-seq tracks in *Scl*^{KO}*iScl* ES cells, *Scl*^{KO}*iScl* and WT mesoderm and H3K4me1 ChIP-seq tracks in ES cells and *WT* mesoderm around hematopoietic and cardiac genes, and genes ectopically bound by Scl in ES cells.

A

All common genes (655)

GO Term	Gene count	P-value
Protein amino acid phosphorylation	49	6.2E-8
Intracellular signaling cascade	62	6.7E-8
Phosphorylation	49	1.8E-6
Phosphate metabolic process	54	6.9E-6
Phosphorus metabolic process	54	6.9E-6
Positive regulation of cell proliferation	23	1.6E-4
Regulation of cell proliferation	34	3.8E-4
Hemopoiesis	20	6.0E-4
Activation of protein kinase activity	8	0.0012
Regulation of myeloid cell differentiation	8	0.0012
Regulation of small GTPase mediated signal transduction	18	0.0013
Protein kinase cascade	18	0.0019
Hemopoietic or lymphoid organ development	20	0.0022
Positive regulation of molecular function	21	0.0026
Programmed cell death	28	0.0035
Immune system development	20	0.0038
Induction of apoptosis by intracellular signals	6	0.0053
Positive regulation of catalytic activity	18	0.0055
DNA damage response, signal transduction resulting in induction of apoptosis	5	0.0061
Death	29	0.0066
Positive regulation of protein kinase activity	11	0.0074

Flk1$^+$ MES specific genes (2300)

GO Term	Gene count	P-value
Cell adhesion	105	3.0E-8
Biological adhesion	105	3.3E-8
Positive reg. of nitrogen compound metabolic process	99	5.9E-8
Positive reg. of nucleobase, nucleoside, nucleotide and nucleic acid metabolic process	96	9.6E-8
Reg. of transcription from RNA polymerase II promoter	109	3.1E-7
Positive reg. of RNA metabolic process	81	3.5E-7
Positive reg. of transcription, DNA-dependent	80	5.2E-7
Positive reg. of transcription	88	7.0E-7
Positive reg. of macromolecule biosynthetic process	95	1.1E-6
Positive reg. of gene expression	89	1.2E-6
Positive reg. of macromolecule metabolic process	109	1.2E-6
Tube development	56	1.6E-6
Positive reg. of biosynthetic process	98	1.7E-6
Positive reg. of cellular biosynthetic process	97	2.1E-6
Positive reg. of transcription from RNA polymerase II promoter	69	3.2E-6
Positive regulation of DNA binding	17	3.9E-6
Metal ion transport	80	5.9E-6
Heart development	48	6.5E-6
Positive regulation of binding	17	1.1E-5
Cell motion	68	1.4E-5

HPC7 specific genes (3158)

GO Term	Gene count	P-value
Translation	103	2.5E-15
RNA processing	115	2.1E-10
Apoptosis	115	1.0E-8
Programmed cell death	115	2.8E-8
Cell death	120	6.7E-8
Protein catabolic process	128	1.2E-7
Death	121	1.4E-7
Cellular macromolecule catabolic process	136	3.1E-7
Macromolecule catabolic process	144	3.3E-7
RNA splicing	58	3.9E-7
Cellular protein catabolic process	121	9.3E-7
ncRNA metabolic process	57	1.1E-6
Proteolysis involved in cellular protein catabolic process	120	1.2E-6
mRNA metabolic process	76	2.0E-6
mRNA processing	68	2.4E-6
Modification-dependent macromolecule catabolic process	112	7.1E-6
Modification-dependent protein catabolic process	112	7.1E-6
Protein localization	154	1.1E-5
Cell cycle	128	2.1E-5
Negative reg. of cyclin-dependent protein kinase activity	8	4.0E-5
Ribonucleoprotein complex biogenesis	39	5.5E-5
Regulation of apoptosis	115	7.9E-5

FL erythroblast specific genes (976)

GO Term	Gene count	P-value
Nucleosome assembly	15	5.4E-6
Chromatin assembly	15	7.5E-6
Protein-DNA complex assembly	15	8.8E-6
Nucleosome organization	15	8.8E-6
DNA packaging	17	1.5E-5
Cellular macromolecular complex assembly	25	7.0E-5
Macromolecular complex assembly	33	1.0E-4
Porphyrin metabolic process	8	1.3E-4
Tetrapyrrole metabolic process	8	1.3E-4
Chromatin assembly or disassembly	16	1.5E-4
Cellular macromolecular complex subunit organization	26	1.9E-4
Macromolecular complex subunit organization	33	4.6E-4
Protein catabolic process	43	0.001
Heme metabolic process	6	0.001
Macromolecule catabolic process	48	0.002
Chromosome organization	33	0.002
Response to metal ion	9	0.0029
Chromatin organization	27	0.0033
Cellular protein catabolic process	39	0.0065
Cellular macromolecule catabolic process	43	0.0067
Sphingolipid metabolic process	9	0.0076
Modification-dependent macromolecule catabolic process	37	0.0077

B

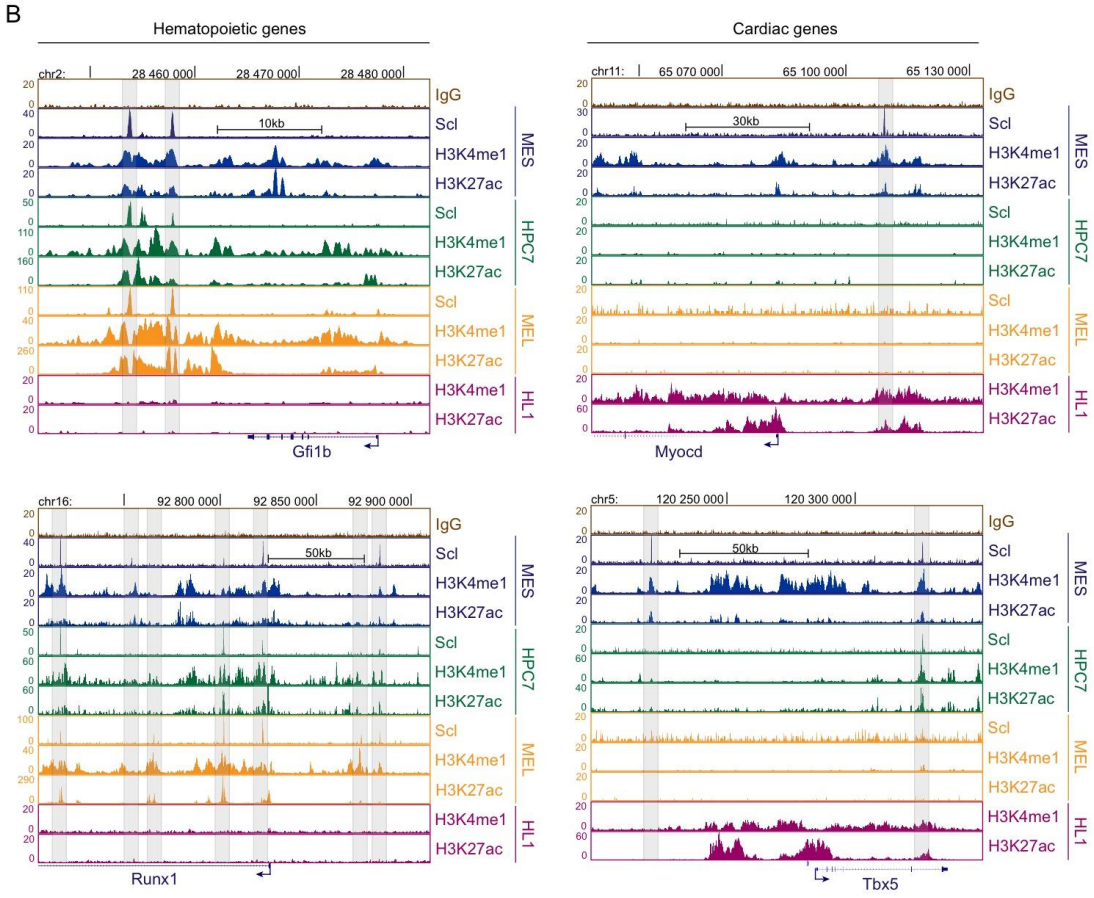

Figure S3. Scl binding shifts dynamically at different developmental stages.

A Significantly enriched DAVID GO Biological processes for 655 common, 2,300 $Flk1^{+}$ MES specific genes, 3,158 HPC7 specific genes and 976 Fetal Liver (FL) erythroblast specific genes shows enrichment of heart related terms only among $Flk1^{+}$ MES specific genes.

B ChIP-seq tracks showing that H3K4me1 and H3K27ac are enriched around Scl binding sites nearby cardiac genes (*Tbx5* and *Myocd*) in mesoderm and cardiomyocyte cell-line HL1, whereas H3K27ac around Scl binding nearby hematopoietic genes (*Gfi1b* and *Runx1*) is conserved in all hematopoietic developmental stages and is depleted in HL1 cells.

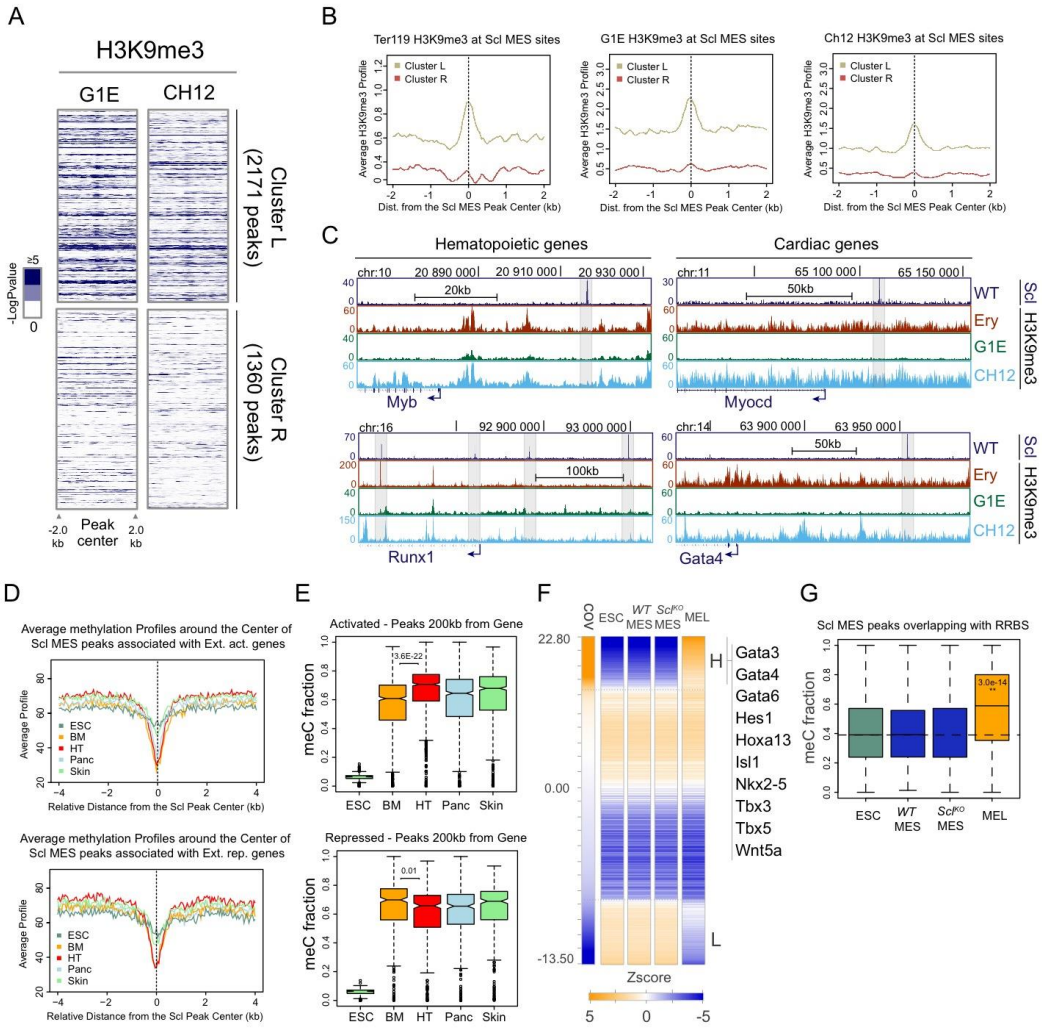
A
H3K9me3
G1E
CH12
Cluster L (2171 peaks)
Cluster R (1360 peaks)
-LogPvalue
≥5
0
-2.0 kb
Peak center
2.0 kb
B
Ter119 H3K9me3 at Scl MES sites
G1E H3K9me3 at Scl MES sites
Ch12 H3K9me3 at Scl MES sites
Cluster L
Cluster R
Average H3K9me3 Profile
Dist. from the Scl MES Peak Center (kb)
C
Hematopoietic genes
Cardiac genes
chr:10
20 890 000
20 910 000
20 930 000
20kb
Myb
chr:11
65 100 000
65 150 000
50kb
Myocd
chr:16
92 900 000
93 000 000
100kb
Runx1
chr:14
63 900 000
63 950 000
50kb
Gata4
WT
Ery
G1E
CH12
Scl H3K9me3
D
Average methylation Profiles around the Center of Scl MES peaks associated with Ext. act. genes
Average methylation Profiles around the Center of Scl MES peaks associated with Ext. rep. genes
Average Profile
ESC
BM
HT
Panc
Skin
Relative Distance from the Scl Peak Center (kb)
E
Activated - Peaks 200kb from Gene
Repressed - Peaks 200kb from Gene
meC fraction
3.6E-22
0.01
ESC
BM
HT
Panc
Skin
F
COV
ESC
WT MES
Scl^KO MES
MEL
22.80
0.00
-13.50
H
L
Gata3
Gata4
Gata6
Hes1
Hoxa13
Isl1
Nkx2-5
Tbx3
Tbx5
Wnt5a
Zscore
5
0
-5
G
Scl MES peaks overlapping with RRBS
meC fraction
3.0e-14
ESC
WT MES
Scl^KO MES
MEL

Figure S4. Analysis of H3K9me3 and DNA methylation do not provide a mechanism for Scl mediated gene repression.

A H3K9me3 heatmaps in Cluster L and Cluster R in G1E (erythroid) and CH12 (B-cell) cell-lines.

B H3K9me3 averages in Cluster L and Cluster R show that there is more H3K9me3 in Cluster L in Ter119^{+}, G1E and CH12 cells.

C ChIP-seq tracks with H3K9me3 enrichment at Scl MES binding sites around hematopoietic (*Myb* and *Runx1*) and cardiac (*Myocd* and *Gata4*) genes evidence little enrichment of H3K9me3 in Scl regulated enhancers.

D Average CpG methylation in ES cells (Habibi *et al*, 2013), Bone marrow (BM), Heart (HT), Pancreas (Panc) and Skin (Hon *et al*, 2013) show depletion of DNA methylation around Scl binding sites associated with Scl extended activated (upper) and repressed (lower) lists of genes.

E Analysis of fraction of meC in ES cells (Habibi *et al*, 2013), Bone marrow, Heart, Pancreas, and Skin (Hon *et al*, 2013) within 200kb from TSS of Scl extended activated (upper) and repressed (lower) lists of genes shows that Scl activated genes have less DNA methylation in bone marrow compared to heart, whereas Scl repressed genes have more DNA methylation

F Covariance analysis of RRBS data in ESC, *WT* and *Scl*^{KO} Flk1^{+} MES and MEL cells, show that differential methylation occurs later in hematopoietic development (MEL cells, H - hypermethylated sites, L - hypomethylated sites). Genes close to hypermethylated regions in MEL cells are shown.

G Fraction of meC among overlapping regions of Scl MES binding sites and RRBS data in ES cells, *WT* and Scl^{KO} $Flk1^{+}$ MES and MEL cells showing that DNA methylation is not Scl dependent in mesoderm.

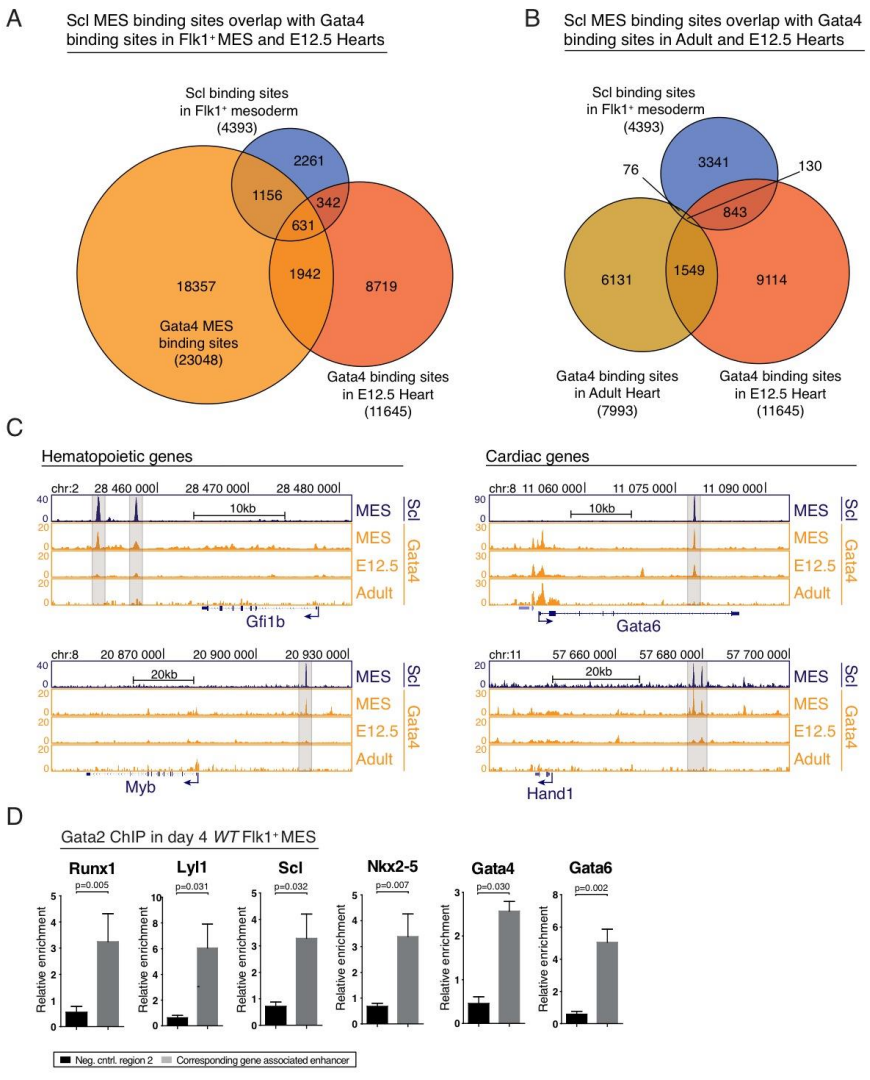
A
Scl MES binding sites overlap with Gata4 binding sites in Flk1+ MES and E12.5 Hearts
Scl binding sites in Flk1+ mesoderm (4393)
2261
1156
342
631
18357
1942
8719
Gata4 MES binding sites (23048)
Gata4 binding sites in E12.5 Heart (11645)
B
Scl MES binding sites overlap with Gata4 binding sites in Adult and E12.5 Hearts
Scl binding sites in Flk1+ mesoderm (4393)
3341
76
130
843
6131
1549
9114
Gata4 binding sites in Adult Heart (7993)
Gata4 binding sites in E12.5 Heart (11645)
C
Hematopoietic genes
Cardiac genes
chr:2 28 460 000 28 470 000 28 480 000
10kb
MES
Scl
MES
E12.5
Adult
Gata4
Gfi1b
chr:8 11 060 000 11 075 000 11 090 000
Gata6
chr:8 20 870 000 20 900 000 20 930 000
20kb
Myb
chr:11 57 660 000 57 680 000 57 700 000
Hand1
D
Gata2 ChIP in day 4 WT Flk1+ MES
Runx1
Lyl1
Scl
Nkx2-5
Gata4
Gata6
p=0.005
p=0.031
p=0.032
p=0.007
p=0.030
p=0.002
Relative enrichment
Neg. cntrl. region 2
Corresponding gene associated enhancer

Figure S5. Cardiac and hematopoietic Gata factors bind to Scl regulated cardiac and hematopoietic enhancers in mesoderm.

A, B Venn diagrams show that there is a gradual decrease in the number of overlapping binding sites when Scl mesodermal binding sites are compared to Gata4 binding in mesoderm (Oda *et al*, 2013), E12.5 hearts and adult hearts (He *et al*, 2014).

C Gata4 ChIP-seq tracks show the dynamics of Gata4 binding in different developmental stages (MES, E12.5 and adult hearts) (He *et al*, 2014; Oda *et al*, 2013) at sites that are also bound by Scl in mesoderm.

D ChIP-PCR analysis shows binding of Gata2 to Scl regulated enhancers in $Flk1^{+}$ mesoderm nearby *Runx1*, *Lyl1*, *Scl*, *Nkx2*-5, *Gata4* and *Gata6* genes. Data is shown as relative enrichment over negative control region (chr16: 92230219-92230338). Average of three experiments with SD are shown.

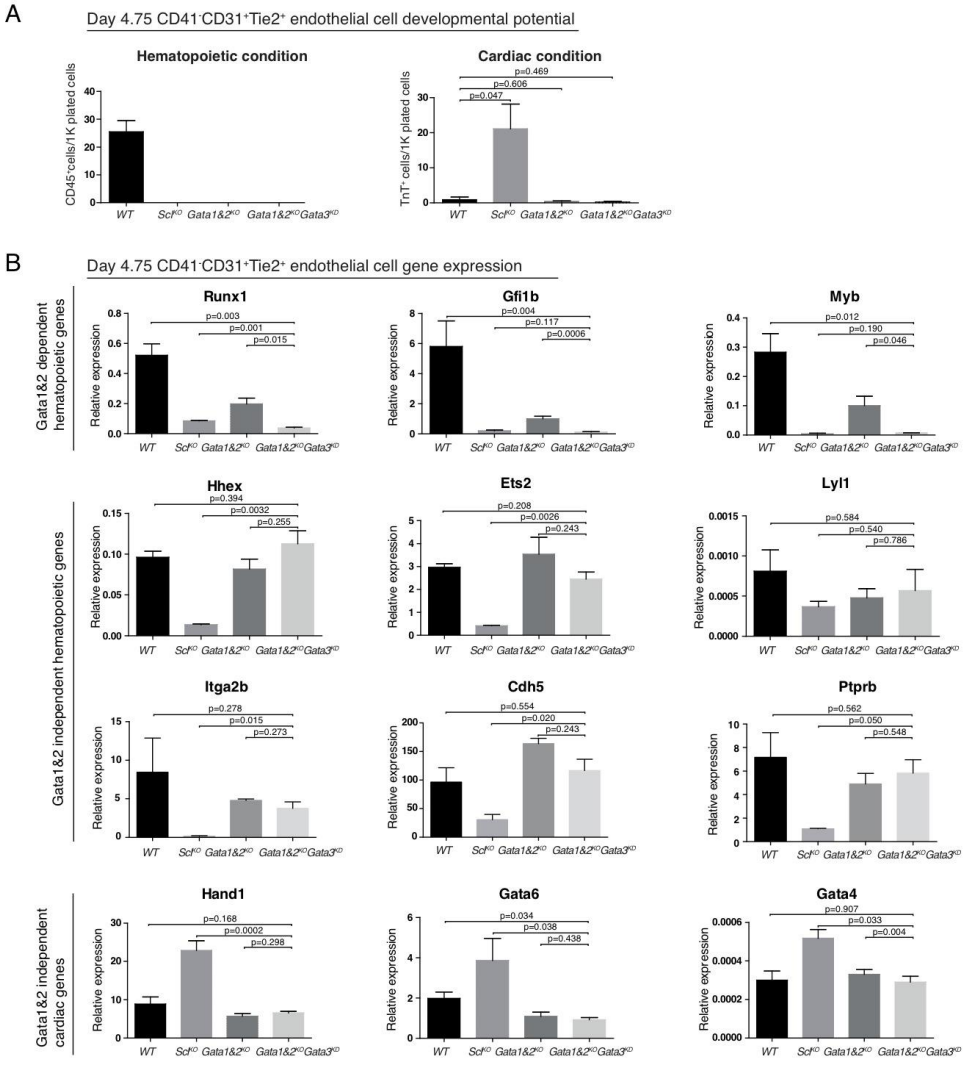
A
Day 4.75 CD41-CD31+Tie2+ endothelial cell developmental potential
Hematopoietic condition
Cardiac condition
CD45- cells/1K plated cells
TnT- cells/1K plated cells
p=0.469
p=0.606
p=0.047
WT
SclKO
Gata1&2KO
Gata1&2KOGata3KD
B
Day 4.75 CD41-CD31+Tie2+ endothelial cell gene expression
Gata1&2 dependent hematopoietic genes
Gata1&2 independent hematopoietic genes
Gata1&2 independent cardiac genes
Runx1
p=0.003
p=0.001
p=0.015
Gfi1b
p=0.004
p=0.117
p=0.0006
Myb
p=0.012
p=0.190
p=0.046
Hhex
p=0.394
p=0.0032
p=0.255
Ets2
p=0.208
p=0.0026
p=0.243
Lyl1
p=0.584
p=0.540
p=0.786
Itga2b
p=0.278
p=0.015
p=0.273
Cdh5
p=0.554
p=0.020
p=0.243
Ptprb
p=0.562
p=0.050
p=0.548
Hand1
p=0.168
p=0.0002
p=0.298
Gata6
p=0.034
p=0.038
p=0.438
Gata4
p=0.907
p=0.033
p=0.004
Relative expression

Figure S6. Hematopoietic Gata factors are dispensable for cardiac repression.

A Day 4.75 $CD41^{-}CD31^{+}Tie2^{+}$ endothelial cells cultured on OP9 in hematopoietic and cardiac conditions for 14 days show that, similar to *Gata1&2*^{KO} endothelial cells *Gata1&2*^{KO}*Gata3*^{KD} cells do not generate $CD45^{+}$ hematopoietic cells nor ectopic $TroponinT^{+}$ cardiomyocytes.

B q-RT-PCR in day 4.75 $CD41^{-}CD31^{+}Tie2^{+}$ endothelial cells shows that, similar to *Gata1&2*^{KO}, *Gata1&2*^{KO}*Gata3*^{KD} endothelial cells have reduced expression of *Runx1*, *Myb*, and *Gfi1b*. Expression of hemato-vascular regulators *Hhex*, *Lyl1*, *Ets2*, and hemato-vascular surface markers *Itga2b*, *Cdh5* and *Ptprb* is intact. Expression of cardiac regulators *Gata6*, *Hand1* and *Gata4* is not up-regulated compared to *WT* control.

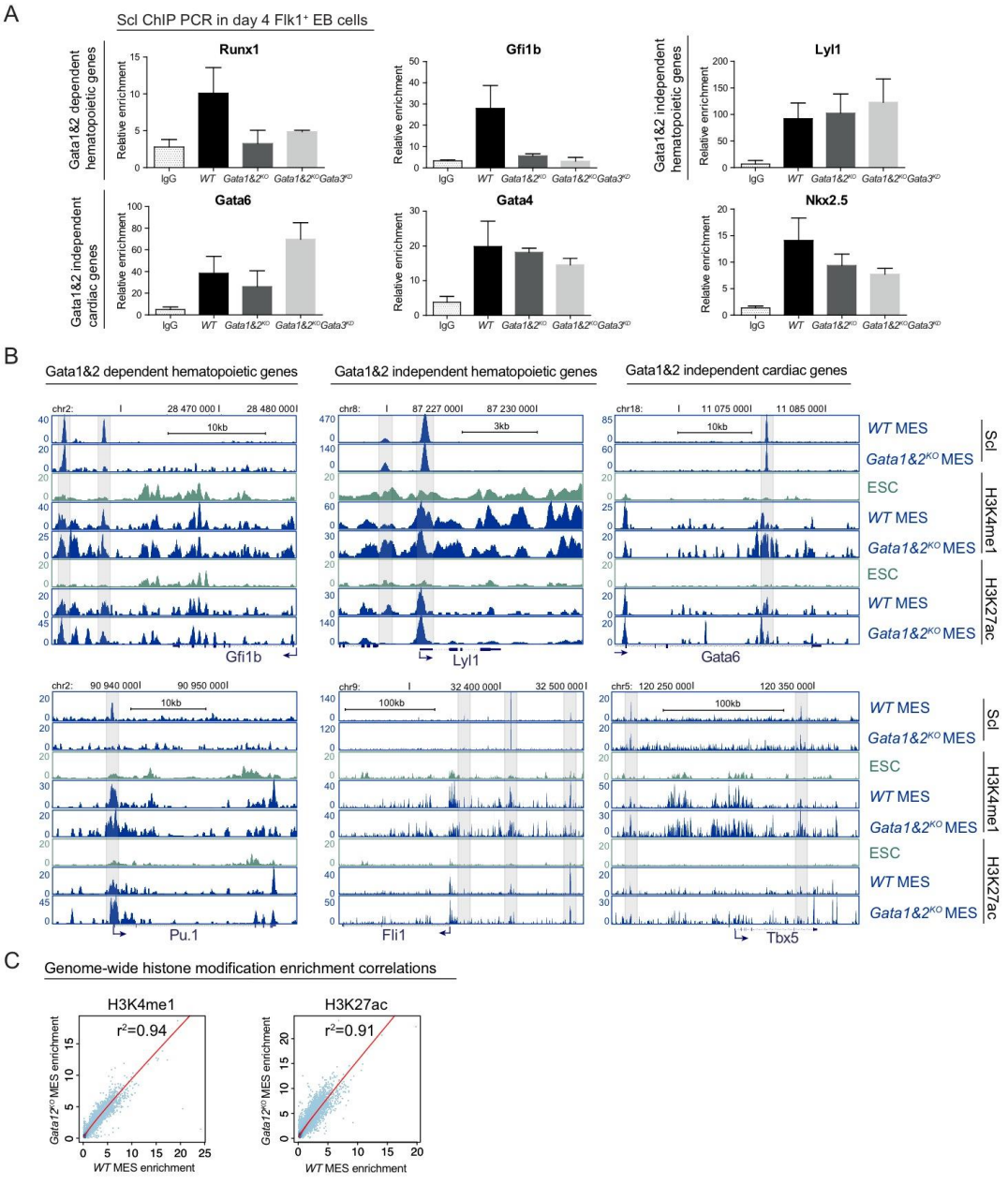
A
Scl ChIP PCR in day 4 Flk1+ EB cells
Gata1&2 dependent hematopoietic genes
Gata1&2 independent hematopoietic genes
Gata1&2 independent cardiac genes
Runx1
Gfi1b
Lyl1
Gata6
Gata4
Nkx2.5
Relative enrichment
IgG
WT
Gata1&2KO
Gata1&2KOGata3KD
B
Gata1&2 dependent hematopoietic genes
Gata1&2 independent hematopoietic genes
Gata1&2 independent cardiac genes
WT MES
Gata1&2KO MES
ESC
Scl
H3K4me1
H3K27ac
Gfi1b
Lyl1
Gata6
Pu.1
Fli1
Tbx5
C
Genome-wide histone modification enrichment correlations
H3K4me1
H3K27ac
r2=0.94
r2=0.91
Gata12KO MES enrichment
WT MES enrichment

Figure S7. Gata1 and 2 are dispensable for the establishment of H3K4me1 and H3K27ac in Scl boundenhancers in mesoderm.

A Scl ChIP-PCR shows that, similar to *Gata1&2*^{KO}, *Gata1&2*^{KO}*Gata3*^{KD} Flk1^{+} mesoderm cells show loss of Scl binding at *Runx1* and *Gfi1b* enhancers while binding is retained at *Lyl1* and cardiac *Gata4*, *Gata6* and *Nkx2.5* enhancers. Average of two experiments with SD are shown.

B ChIP-seq tracks for H3K4me1 and H3K27ac in ES cells, *WT* and *Gata1&2*^{KO} mesodermal cells show that establishment of active histone modifications in mesoderm around Scl binding sites is not dependent on Gata1 or 2.

C Genome-wide correlation analysis of H3K4me1 (left) and H3K27ac (right) levels between *WT* and *Gata1&2*^{KO} mesoderm (MES) shows that establishment of active histone modifications in mesoderm is not dependent on Gata1 or 2.

Supplementary materials and methods

Culture of ES, hematopoietic and cardiomyocyte cell lines

Standard ES cell culture media with DMEM (Cellgro), 15% serum (Hyclone or Omega) and 10ng/ml LIF (Millipore) and gelatin coated dishes were used to maintain mouse ES cells. Following lines were used: *WT, Scl*^{hCD4} knock-in (Chung *et al*, 2002), *Scl*^{KO} (Porcher *et al*, 1996), and *Gata1&2*^{KO} (Fujiwara *et al*, 1996). Of note, although the hCD4 knock-in disrupts one Scl allele, these ES cells recapitulate normal hematopoietic differentiation in culture (Chung *et al*, 2002), and Scl heterozygous embryos do not have a reported phenotype. *Gata1&2* ^{KO} *Gata3*^{KD} ES cell line was generated by infecting *Gata1&2*^{KO} ES cell line with Gata3 lentiviral shRNA (Santa Cruz, MOI=25), after which subclones of the infected cells were isolated using limiting dilution. Q-RT-PCR was performed to verify the knock-down of Gata3. *Scl*^{KO}*iScl* ES cell line was generated by infecting *Scl*^{KO} ES cell line with lentiviral vectors containing rtTA and Scl-IRES-GFP controlled by TRE, after which subclones of the infected cells were isolated using limiting dilution. Western Blot and FACS analysis of GFP was performed to verify the expression of Scl upon doxycycline induction. In functional assays Scl expression was induced with the addition of 1ug/ml doxycycline for 48h. MEL cells were grown in RPMI 1640 with L-Glutamine, 10% of FBS, 1% of penicillin and streptomycin. HPC7 cells (by professor L Carlsson, Umea University, Sweden) were grown in Iscove´s modified Dulbecco´s media (IMDM) (Gibco), supplemented with $NaHCO_3$, 1.5 x 10-4 M MTG (Sigma), 1% of penicillin and streptomycin, 10% of FBS and mouse Stem cell factor (SCF) at 100ng/mL (R&D Systems). HL1 cardiomyocyte cells were grown in Claycomb Medium with L-Glutamine plus 10% of FBS, 1% of penicillin and streptomycin and 0.1mM Norephinephrine (Claycomb *et al*, 1998).

Flk1^{+} mesodermal cells and hemato-vascular derivatives were generated by differentiating ES cells into embryoid bodies as described (Mikkola *et al*, 2003). For ChiP-seq and ChIP-PCR, day 4 Flk1^{+} mesodermal cells were digested with 0.25% trypsin (Gibco) and enriched using Flk1-PE antibody (clone Avas12a1, eBioscience), anti-PE microbeads and MACS LS columns (Miltenyi Biotech). For microarrays, day 4 EB cells were sorted on a BD FACS Aria II (BD Biosciences) using Flk1-PE and hCD4 (clone S3.5, Invitrogen) antibodies to collect distinct mesodermal cell populations. For RNA-seq and endothelial cell developmental potential assays day 4.75 EBs were digested with 2mg/ml collagenase (Worthington) and 0.5mg/ml dispase (Invitrogen), Tie2^{+}CD31^{+}CD41^{-} cells were sorted on a BD FACS Aria II (BD Biosciences) using Tie2-PE (clone TEK4), CD31-PECy7 (clone 390) and CD41-PerCPCy5.5 (clone MWReg30) antibodies (all from eBioscience).

Progression of hematopoietic development was assessed using the antibodies for CD41-PerCPCy5.5 or CD41-FITC (clone MWReg30), cKit-APC or PE-Cy7 (clone 2B8) Tie2-PE (clone TEK4), CD31-PECy7 (clone 390) (all from eBioscience) and Flk-1-APC (clone Avas 12alpha1) from BD Pharmingen. Dead cells were excluded with DAPI (Roche). Cell populations were analyzed using an LSR II or Fortessa flow cytometer or sorted using a FACSAria II cell sorter (BD Biosciences). Data were analyzed with FlowJo software, version 8.8.6 (TreeStar).

Affymetrix Microarray Analysis

RNA was isolated using the RNeasy Micro kit (Qiagen), amplified using the NuGEN Pico kit (Nugen, San Carlos CA), and hybridized on Affymetrix Mouse Genome 430 2.0 Array GeneChip microarrays. Differential expression was calculated using the R package Limma (Gentleman, 2005) from the open source Bioconductor project (Gentleman *et al*, 2004). Absolute

mRNA expression levels were calculated using, the RMA (Robust Multiarray Averaging (Bolstad *et al*, 2003)) method (provided through R library affy) resulting in background corrected, quantile normalized and probe level data summarized values for all probe sets. Bioconductor annotation database mouse4302.db was used to obtain official gene symbols for probe sets. PMA detection calls for each array sample were calculated with the mas5calls algorithm (Liu *et al*, 2006) within the R package affy. Probes with the 'Absent' designation for all samples were excluded from further analysis. Genes with p-value 0.05 and fold change at least 1.5 where designated as differentially expressed. Only genes that were differentially expressed in both: $Flk1^{+}Scl^{+}$ vs. $Flk1^{+}Scl^{-}$ day 4 EBs from *Cntrl* Scl^{hCD4} reporter ES cells, and *Cntrl* Scl^{hCD4} $Flk1^{+}Scl^{+}$ vs. $Flk1^{+}$ *SclKO* ES cell (Porcher et al.,, 1996) derived day 4 EBs were included in the final list of 592 up- and 553 down-regulated mesodermal genes. DAVID (Huang *et al*, 2007) tool was used to identify significantly over-represented functional GO biological process categories within differentially expressed genes.

To obtain the extended list of Scl dependent genes, expression profiles of Scl up- and down-regulated genes in day 4 EBs (see above) and previously published datasets of Scl (GSE27445) (Van Handel *et al*, 2012) up- and down-regulated genes in E9.25 yolk sac (*Cntrl* $CD31^{+}$ vs. Scl^{KO} $CD31^{+}$), placenta (*Cntrl* $CD31^{+}$ vs. Scl^{KO} $CD31^{+}$) and endocardium (*Cntrl* $CD31^{+}Pdgfra^{-}$ vs. Scl^{KO} $CD31^{+}Pdgfra^{-}$) were combined.

Chromatin immunoprecipitation and library preparation

Approximately $20x10^{6}$ and $2x10^{6}$ purified $Flk1^{+}$ mesodermal, ES cells, HPC7, MEL or HL1 cells were used per IP for ChIP-seq and ChIP-PCR, respectively. Cells were washed with PBS and crosslinked with 1% formaldehyde in PBS for 10 min at RT. After quenching with 0.125M

glycine cells were washed twice with PBS, and lysed in 400 µl of lysis buffer (1% SDS, 20 mM EDTA and 50 mM Tris-HCl (pH 8.0)) with protease inhibitors (Roche). Chromatin was sonicated on average 200bp fragments for ChIP-seq and 500bp fragments for ChIP-PCR using Misonix cup-horn sonicator, The lysate was diluted 10 times with ChIP dilution buffer containing 0.01% SDS, 1.1% Triton X-100, 1.2 mM EDTA and 16.7 mM Tris-HCl (pH 8.1) and immunoprecipitated anti-Scl (sc-12984X, Santa Cruz), anti-Gata2 (sc-9008X, Santa Cruz), anti-Hand1 (sc-9413X, Santa Cruz), anti-H3K4me1 (ab8895, Abcam), anti-H3K27ac (ab4729, Abcam), Ezh2 (39901, Active Motif) or control IgG (sc-2028**,** Santa Cruz) antibodies overnight at 4 degrees. 20 µl of the lysates were used as input. The immunoprecipitated complexes were captured using protein G Dynabeads (Invitrogen) and washed twice with the following buffers: low-salt immune complex wash buffer (0.1% SDS, 1% Triton X-100, 2 mM EDTA, 20 mM Tris-HCl (pH 8.1); high-salt immune complex wash buffer (0.1% SDS, 1% Triton X-100, 2 mM EDTA, 20 mM Tris-HCl (pH 8.1) and 500 mM NaCl); LiCl wash buffer (0.25 M LiCl, 1% NP40, 1% deoxycholate, 1 mM EDTA and 10 mM Tris-HCl (pH 8.1)) and TE (10 mM Tris-HCl and 1 mM EDTA (pH 8.0)). Chromatin complexes were eluted from the beads with 50 mM Tris-HCl, pH 8.0, 1 mM EDTA, and 1% SDS and reverse crosslinking was performed by overnight incubation at 65°C. Samples were treated with RNase A for 30 min at 37°C and proteinase K for 2 h at 56°C. DNA was subsequently purified using Qiagen MinElute Columns according to manufacturers instructions. DNA concentration was measured using a Qubit (Invitrogen).

ChIP with anti-Lsd1 antibody (ab17721, Abcam) in ***WT*** and Scl^{KO} $Flk1^{+}$ mesoderm was performed as described in (Kerenyi *et al*, 2013).

The library for sequencing was constructed using Ovation Ultralow IL or DR Multiplex System 1-8 kit according to manufacturer's instructions (Nugen). Libraries were sequenced using HIseq-

2000 (Illumina) to obtain 50 bp long reads.

Analysis of ChIP-seq data

Multiplexed runs were debarcoded using Fastx toolkit (http://hannonlab.cshl.edu/fastx_toolkit) or Unix shell scripts. Reads were mapped to the mouse genome (mm9) using bowtie v0.12.7 (Langmead *et al*, 2009) with (-m 1 –strata –best –v 2) parameters. Only reads that aligned to a unique position in the genome with no more than two sequence mismatches were retained for further analysis. Duplicate reads that mapped to the same exact location in the genome were counted only once to reduce clonal amplification effects.

Using mapped sam files as inputs bedgraph files were created using Homer with default parameters (Heinz et al.,, 2010), converted to bigwig format using bedGraphtoBigwig script (Kent *et al*, 2010) and visualized on UCSC genome browser (Kent *et al*, 2002) as custom tracks. Peak identification was performed with MACS v1.3.7.1 (Zhang *et al*, 2008) default parameters using respective input as a reference. Peaks form two independent experiments were intersected and IgG peaks were subtracted using Galaxy (Blankenberg *et al*, 2010) to obtain final list of 4393 Scl binding sites. To identify genes that are potential direct targets of Scl, peaks were mapped to nearby genes within 200kb range from TSS using Genomic Regions Enrichment of Annotations Tool (GREAT) (McLean *et al*, 2010). Top enriched terms for a given category are reported unless otherwise noted. Peak intersections, distance to TSS and overlaps with differentially expressed genes were determined using Galaxy (Blankenberg *et al*, 2010) and in house Unix shell scripts. Motif enrichment analysis was performed with Centdist (Zhang *et al*, 2011) using Transfac and Jaspar databases and 1000bp maximum comotif distance.

The following published ChIP-seq datasets were used for comparisons: p300 binding in E11.5

mouse tissues GSE22549 (Blow *et al*, 2010); histone modifications during ES cell step-wise differentiation into cardiomyocytes (ESC, MES - mesoderm, CP – cardiac progenitors, CM – cardiomyocytes) (Wamstad *et al*, 2012); H3K4me1 in MEL cells GSE31039 (ENCODE project), Ter119^{+} FL erythroblasts, GSM689846 (Kowalczyk *et al*, 2012), embryonic limbs GSE29184 (Shen *et al*, 2012), mouse embryonic fibroblasts GSE41440 (Herz *et al*, 2012), granulocytes GSM994230 (Kerenyi *et al*, 2013); H3K27ac in Ter119^{+} FL erythroblasts GSM802477 (Kowalczyk *et al*, 2012); H3K27me3 in Ter119^{+} FL erythroblasts GSM688811 (Wong *et al*, 2011) and GSM689847 (Kowalczyk *et al*, 2012); H3K9me3 in Ter119^{+} FL erythroblasts GSM946549 (ENCODE project), G1E cells GSM94654 (ENCODE project), Ch12 cells GSM946548 (ENCODE project); Lsd1 binding in ES cells GSM687282 (Whyte *et al*, 2012), granulocytes GSM994238 (Kerenyi *et al*, 2013); Gata4 binding in mesoderm GSM1015512 (Oda *et al*, 2013) and in E12.5 and adult hearts GSE52123 (He *et al*, 2014); Scl binding in HPC7 cells GSE22178 (Wilson *et al*, 2010) and in FL erythroblasts GSE21877 (Kassouf *et al*, 2010). All the datasets used in this study are listed in Table S5.

For the generation of the average histone profiles and heatmaps small variations to the protocol described in Ferrari et al., 2012 were applied. The genome was tiled into 50-bp windows. All windows with P-values less than 1.0 × 10−5 were considered to have significant peaks. A P-value < 1.0 × 10−5 was chosen to give a False Discovery Rate (FDR) of <1%. The FDR was calculated by applying the same statistic described above to the two halves of the same input library. The total number of significant peaks obtained this way was considered as an estimate of the number of false-positive peaks. Wiggle files (generated by the algorithm) containing significant counts were used for combinatorial binding analysis of histone modifications (Figure 3E). Combinatorial clustering signal for the significant counts was then substituted with –log

Poisson P-values. Sitepro, as part of the CEAS suite (http://cistrome.dfci.harvard.edu/ap/), was used to create tiling file of histone modifications for defined genomic intervals centered around Scl binding sites. This file was subsequently processed with Cluster 3.0 to obtain a CDT file for the generation of heatmaps with Java TreeView. Sitepro was also used for the generation of average histone modification profiles around Scl binding sites. Wiggle files of normalized tag density (Figures 2F, 4C, 4E, S2A, S4B) and bigwig files (Figure 5D-H) used for these analyses were generated as described in Ferrari et al.,, 2012 and above, respectively..

The correlation for *WT*, Scl^{KO}, $Gata12^{KO}$ H3K4me1 and H3K427ac ChIP-seq enrichments around Scl binding sites (Figure 2G, S2B) and genome-wide (Figure S7C) were calculated by correlation tool in Cistrome (Liu *et al*, 2011) using bigwig files generated as described above.

Reduced Representation Bisulfite Sequencing

RRBS libraries were generated starting from 240-450 ng of genomic DNA (measured by QUBIT, Life technology) as previously described by (Meissner *et al*, 2005) with minor modifications. Briefly, MspI- generated fragments were end-repaired and adenylated before ligation with Illumina TruSeq adapters. DNA purifications of each enzymatic reaction as well as size-selection of adapter-ligated fragments ranging from 200-350bp were carried out using AMPure XP beads (Beckman Coulter). Bisulfite conversion was performed twice with EpiTect kit (QIAGEN) in order to optimize the efficiency. Bisulfite-converted libraries were amplified using MyTaq Mix (Bioline) with the following program: 98°C for 2min, (98°C for 15sec, 60°C for 30sec, 72°C for 30sec) 12 cycles, 72°C for 5 min, 4°C indefinitely.

Analysis of RRBS data

RRBS data was aligned with bs-seeker2 (Guo *et al*, 2013). Differentially methylated cytosines were calculated with methyl-kit (Akalin *et al*, 2012). To identify DNA methylation changes that increased or decreased significantly, we focused on RRBS fragment CpG methylation levels and calculated the covariance between the fragment methylation and sample order (ordered by least to most differentiated). To determine the fragment CpG methylation score, we only considered CpG sites with a minimum coverage of four reads common to all the samples. The fragment methylation score is the Z score of the CpG methylation levels within the RRBS fragment standardized by the number of CpG sites within the fragment,

$$z = \frac{\bar{X} - \mu}{\sigma / \sqrt{N}}$$

where $\bar{X}$ is the average CG methylation within the fragment, μ is the mean CpG methylation of the sample methylome, σ is the standard deviation of the sample methylome, and N is the number of CpG sites within the fragment. DNA methylation fragments were ranked based on covariance and gene ontology determined with GREAT. For Fig S4G GCmap files for each sample were intersected (BEDtools) with coordinates of Scl peaks in mesoderm. All mapped cytosines were average for methylation fraction and plotted using R. Kolmogorov-Smirnov test p-value was calculated to compare the ESC and MEL distribution of methylated cytosines using matlab.

Genome-wide DNA methylation analysis

Published genome-wide DNA methylation datasets from various cell types (GSM1127953 – ES cells (Habibi *et al*, 2013); GSE42836 - Bone marrow, Heart, Pancreas and Skin (Hon *et al*,

2013)) (Figure S4D) were used to analyze average and differential DNA methylation. Average DNA methylation around 8kb regions centered at Scl mesodermal binding sites associated with extended lists of Scl activated or repressed genes was calculated in 50bp windows using Sitepro tool (Ji *et al*, 2006) within Cistrome integrative platfrom (Liu *et al*, 2011). For differential methylation analysis on Fig S4E raw data was reprocessed with BS-seeker2 and single GCmap files for each tissue were generated. BEDtools was used to generate the intersection between cytosines present within 200 kb from TSS of extended lists of Scl activated and repressed genes. Average methylation fraction was plotted for each tissue as boxplot using R.

Library preparation for RNA-seq

Total RNA was extracted using the RNeasy Mini kit (Qiagen) and library was constructed using an Encore Complete RNA-Seq DR Multiplex System 1-8 (Nugen). Libraries were sequenced using HIseq-2000 (Illumina) to obtain paired end 50 bp long reads.

Analysis of RNA-seq data

Debarcoding of the multiplex runs was performed using in house Unix shell script. Splice junction mapping to the mouse genome (mm9) was performed using TopHat v2.0.4 (Trapnell *et al*, 2009) with default parameters. For abundance estimations (FPKMs) the aligned read files were further processed with Cufflinks v2.0.1 (Trapnell *et al*, 2010). Assemblies for all samples were merged using Cuffmerge and differential expression was determined using Cuffdiff. Genes with a p-value smaller than 0.01 where considered as differentially expressed. All transcripts where the FPKM values for all the samples were lower than 0.5 were excluded from further analysis. For the calculation of fold change and heatmap generation FPKM value of 0.1 was used if no transcripts were detected for a given sample. For the generation of heatmaps with relative

expression each genes log2 ratio of a given sample FPKM was divided with the average of the all samples FPKM's and visualized using Java TreeView (Saldanha, 2004).

Statistical analysis

For ChIP-PCR on Figure 1E, 2I and S5D paired ratio t-test was used to calculate significance between shown pairs. Student's t-test was used to calculate if changes in expression detected with q-RT-PCR and if Scl binding overlaps with cardiac enhancers (Figure 2B, C) are significant and if there is a significant difference between absolute fold change between the groups in Figure 5I. Hypergeometric probability calculation in Geneprof software (Halbritter *et al*, 2012) (population size was set to 23148, that corresponds to the number of mouse genes in mm9 assembly) was used to assess if overlaps on Figures 1A and 1G are significant. In Figure 2A, chi-square test was used to calculate if differences between observed and expected are significant. Kolmogorov-Smirnov test was used to test differences in methylation levels (Figure S4E and S4G).

FACS staining and Immunostaining for hematopoietic and cardiac cells

Hematopoietic differentiation potential of sorted endothelial cells was assessed using the antibodies for CD11b-PE (cloneM1/70) from BD Pharmingen and CD45-PECy7 (clone30-F11) from eBioscience. Dead cells were excluded with DAPI (Roche). Cell populations were analyzed using an LSR II or Fortessa flow cytometer. Endothelial cells cultured in chamber slides were fixed with 4% PFA for 15min at room temperature and then permeabilized for 10min with PBS containing 0.25% Triton. After permeabilization, cells were blocked in with PBS containing 1% BSA and 0.05% Tween20 for 30 min. Primary antibody cardiac Troponin T (1:400, MS-295-P1, Thermo Scientific) and CD45 (1:300, 550539, BD Biosciences) were applied to the cells

overnight at 4 °C. After washing 3 times with PBS (0.05% Tween20), secondary antibody and DAPI were applied for 1h. Images were obtained on a Zeiss LSM 510 equipped with 405 nm, 488 nm, 543 nm, and 633 nm lasers after mounting.

Supplementary Bibliography

Akalin A, Kormaksson M, Li S, Garrett-Bakelman FE, Figueroa ME, Melnick A & Mason CE (2012) methylKit: a comprehensive R package for the analysis of genome-wide DNA methylation profiles. *Genome Biol.* **13:** R87

Blankenberg D, Von Kuster G, Coraor N, Ananda G, Lazarus R, Mangan M, Nekrutenko A & Taylor J (2010) Galaxy: a web-based genome analysis tool for experimentalists. *Curr. Protoc. Mol. Biol.* **Chapter 19:** Unit 19.10.1–21

Blow MJ, McCulley DJ, Li Z, Zhang T, Akiyama JA, Holt A, Plajzer-Frick I, Shoukry M, Wright C, Chen F, Afzal V, Bristow J, Ren B, Black BL, Rubin EM, Visel A & Pennacchio LA (2010) ChIP-Seq identification of weakly conserved heart enhancers. *Nat. Genet.* **42:** 806–10

Bolstad BM, Irizarry RA, Astrand M & Speed TP (2003) A comparison of normalization methods for high density oligonucleotide array data based on variance and bias. *Bioinformatics* **19:** 185–93

Chung YS, Zhang WJ, Arentson E, Kingsley PD, Palis J & Choi K (2002) Lineage analysis of the hemangioblast as defined by FLK1 and SCL expression. *Development* **129:** 5511–20

Claycomb WC, Lanson NA, Stallworth BS, Egeland DB, Delcarpio JB, Bahinski A & Izzo NJ (1998) HL-1 cells: a cardiac muscle cell line that contracts and retains phenotypic characteristics of the adult cardiomyocyte. *Proc. Natl. Acad. Sci. U. S. A.* **95:** 2979–84

Ferrari R, Su T, Li B, Bonora G, Oberai A, Chan Y, Sasidharan R, Berk AJ, Pellegrini M & Kurdistani SK (2012) Reorganization of the host epigenome by a viral oncogene. *Genome Res.* **22:** 1212–21

Fujiwara Y, Browne CP, Cunniff K, Goff SC & Orkin SH (1996) Arrested development of embryonic red cell precursors in mouse embryos lacking transcription factor GATA-1. *Proc. Natl. Acad. Sci. U. S. A.* **93:** 12355–8

Gentleman R (2005) Bioinformatics and computational biology solutions using R and Bioconductor New York: Springer Science+Business Media

Gentleman RC, Carey VJ, Bates DM, Bolstad B, Dettling M, Dudoit S, Ellis B, Gautier L, Ge Y, Gentry J, Hornik K, Hothorn T, Huber W, Iacus S, Irizarry R, Leisch F, Li C, Maechler M, Rossini AJ, Sawitzki G, et al (2004) Bioconductor: open software development for computational biology and bioinformatics. *Genome Biol.* **5:** R80

Guo W, Fiziev P, Yan W, Cokus S, Sun X, Zhang MQ, Chen P-Y & Pellegrini M (2013) BS-Seeker2: a versatile aligning pipeline for bisulfite sequencing data. *BMC Genomics* **14:** 774

Habibi E, Brinkman AB, Arand J, Kroeze LI, Kerstens HHD, Matarese F, Lepikhov K, Gut M, Brun-Heath I, Hubner NC, Benedetti R, Altucci L, Jansen JH, Walter J, Gut IG, Marks H & Stunnenberg HG (2013) Whole-genome bisulfite sequencing of two distinct interconvertible DNA methylomes of mouse embryonic stem cells. *Cell Stem Cell* **13:** 360–9

Halbritter F, Vaidya HJ & Tomlinson SR (2012) GeneProf: analysis of high-throughput sequencing experiments. *Nat. Methods* **9:** 7–8

Van Handel B, Montel-Hagen A, Sasidharan R, Nakano H, Ferrari R, Boogerd CJ, Schredelseker J, Wang Y, Hunter S, Org T, Zhou J, Li X, Pellegrini M, Chen J-N, Orkin SH, Kurdistani SK, Evans SM, Nakano A & Mikkola HKA (2012) Scl represses cardiomyogenesis in prospective hemogenic endothelium and endocardium. *Cell* **150:** 590–605

He A, Gu F, Hu Y, Ma Q, Yi Ye L, Akiyama JA, Visel A, Pennacchio LA & Pu WT (2014) Dynamic GATA4 enhancers shape the chromatin landscape central to heart development and disease. *Nat. Commun.* **5:** 4907

Herz H-M, Mohan M, Garruss AS, Liang K, Takahashi Y-H, Mickey K, Voets O, Verrijzer CP & Shilatifard A (2012) Enhancer-associated H3K4 monomethylation by Trithorax-related, the Drosophila homolog of mammalian Mll3/Mll4. *Genes Dev.* **26:** 2604–20

Hon GC, Rajagopal N, Shen Y, McCleary DF, Yue F, Dang MD & Ren B (2013) Epigenetic memory at embryonic enhancers identified in DNA methylation maps from adult mouse tissues. *Nat. Genet.* **45:** 1198–206

Huang DW, Sherman BT, Tan Q, Kir J, Liu D, Bryant D, Guo Y, Stephens R, Baseler MW, Lane HC & Lempicki RA (2007) DAVID Bioinformatics Resources: expanded annotation database and novel algorithms to better extract biology from large gene lists. *Nucleic Acids Res.* **35:** W169–75

Ji X, Li W, Song J, Wei L & Liu XS (2006) CEAS: cis-regulatory element annotation system. *Nucleic Acids Res.* **34:** W551–4

Kassouf MT, Hughes JR, Taylor S, McGowan SJ, Soneji S, Green AL, Vyas P & Porcher C (2010) Genome-wide identification of TAL1's functional targets: insights into its mechanisms of action in primary erythroid cells. *Genome Res.* **20:** 1064–83

Kent WJ, Sugnet CW, Furey TS, Roskin KM, Pringle TH, Zahler AM & Haussler D (2002) The human genome browser at UCSC. *Genome Res.* **12:** 996–1006

Kent WJ, Zweig AS, Barber G, Hinrichs AS & Karolchik D (2010) BigWig and BigBed: enabling browsing of large distributed datasets. *Bioinformatics* **26:** 2204–7

Kerenyi MA, Shao Z, Hsu Y-J, Guo G, Luc S, O'Brien K, Fujiwara Y, Peng C, Nguyen M & Orkin SH (2013) Histone demethylase Lsd1 represses hematopoietic stem and progenitor cell signatures during blood cell maturation. *Elife* **2:** e00633

Kowalczyk MS, Hughes JR, Garrick D, Lynch MD, Sharpe JA, Sloane-Stanley JA, McGowan SJ, De Gobbi M, Hosseini M, Vernimmen D, Brown JM, Gray NE, Collavin L, Gibbons RJ, Flint J, Taylor S, Buckle VJ, Milne TA, Wood WG & Higgs DR (2012) Intragenic enhancers act as alternative promoters. *Mol. Cell* **45:** 447–58

Langmead B, Trapnell C, Pop M & Salzberg SL (2009) Ultrafast and memory-efficient alignment of short DNA sequences to the human genome. *Genome Biol.* **10:** R25

Liu T, Ortiz JA, Taing L, Meyer CA, Lee B, Zhang Y, Shin H, Wong SS, Ma J, Lei Y, Pape UJ, Poidinger M, Chen Y, Yeung K, Brown M, Turpaz Y & Liu XS (2011) Cistrome: an integrative platform for transcriptional regulation studies. *Genome Biol.* **12:** R83

Liu W, Li R, Sun JZ, Wang J, Tsai J, Wen W, Kohlmann A & Williams PM (2006) PQN and DQN: algorithms for expression microarrays. *J. Theor. Biol.* **243:** 273–8

McLean CY, Bristor D, Hiller M, Clarke SL, Schaar BT, Lowe CB, Wenger AM & Bejerano G (2010) GREAT improves functional interpretation of cis-regulatory regions. *Nat. Biotechnol.* **28:** 495–501

Meissner A, Gnirke A, Bell GW, Ramsahoye B, Lander ES & Jaenisch R (2005) Reduced representation bisulfite sequencing for comparative high-resolution DNA methylation analysis. *Nucleic Acids Res.* **33:** 5868–77

Mikkola HKA, Fujiwara Y, Schlaeger TM, Traver D & Orkin SH (2003) Expression of CD41 marks the initiation of definitive hematopoiesis in the mouse embryo. *Blood* **101:** 508–16

Oda M, Kumaki Y, Shigeta M, Jakt LM, Matsuoka C, Yamagiwa A, Niwa H & Okano M (2013) DNA methylation restricts lineage-specific functions of transcription factor Gata4 during embryonic stem cell differentiation. *PLoS Genet.* **9:** e1003574

Porcher C, Swat W, Rockwell K, Fujiwara Y, Alt FW & Orkin SH (1996) The T cell leukemia oncoprotein SCL/tal-1 is essential for development of all hematopoietic lineages. *Cell* **86:** 47–57

Saldanha AJ (2004) Java Treeview--extensible visualization of microarray data. *Bioinformatics* **20:** 3246–8

Shen Y, Yue F, McCleary DF, Ye Z, Edsall L, Kuan S, Wagner U, Dixon J, Lee L, Lobanenkov V V & Ren B (2012) A map of the cis-regulatory sequences in the mouse genome. *Nature* **488:** 116–20

Trapnell C, Pachter L & Salzberg SL (2009) TopHat: discovering splice junctions with RNA-Seq. *Bioinformatics* **25:** 1105–11

Trapnell C, Williams BA, Pertea G, Mortazavi A, Kwan G, van Baren MJ, Salzberg SL, Wold BJ & Pachter L (2010) Transcript assembly and quantification by RNA-Seq reveals unannotated transcripts and isoform switching during cell differentiation. *Nat. Biotechnol.* **28:** 511–5

Wamstad JA, Alexander JM, Truty RM, Shrikumar A, Li F, Eilertson KE, Ding H, Wylie JN, Pico AR, Capra JA, Erwin G, Kattman SJ, Keller GM, Srivastava D, Levine SS, Pollard KS, Holloway AK, Boyer LA & Bruneau BG (2012) Dynamic and coordinated epigenetic regulation of developmental transitions in the cardiac lineage. *Cell* **151:** 206–20

Whyte WA, Bilodeau S, Orlando DA, Hoke HA, Frampton GM, Foster CT, Cowley SM & Young RA (2012) Enhancer decommissioning by LSD1 during embryonic stem cell differentiation. *Nature* **482:** 221–5

Wilson NK, Foster SD, Wang X, Knezevic K, Schütte J, Kaimakis P, Chilarska PM, Kinston S, Ouwehand WH, Dzierzak E, Pimanda JE, de Bruijn MFTR & Göttgens B (2010) Combinatorial transcriptional control in blood stem/progenitor cells: genome-wide analysis of ten major transcriptional regulators. *Cell Stem Cell* **7:** 532–44

Wong P, Hattangadi SM, Cheng AW, Frampton GM, Young RA & Lodish HF (2011) Gene induction and repression during terminal erythropoiesis are mediated by distinct epigenetic changes. *Blood* **118:** e128–38

Zhang Y, Liu T, Meyer CA, Eeckhoute J, Johnson DS, Bernstein BE, Nusbaum C, Myers RM, Brown M, Li W & Liu XS (2008) Model-based analysis of ChIP-Seq (MACS). *Genome Biol.* **9:** R137

Zhang Z, Chang CW, Goh WL, Sung W-K & Cheung E (2011) CENTDIST: discovery of co-associated factors by motif distribution. *Nucleic Acids Res.* **39:** W391–9

Chapter 3:

ETV2 cooperates with SCL for timely gene activation during hemogenic endothelium specification

Abstract

The ETS transcription factor *Etv2* and its target *Scl* are critical for establishing blood and vascular lineages from cardiovascular mesoderm and repressing ectopic cardiac differentiation. However, their respective functions in these cell fate decisions are unknown. Overexpression of SCL in *Etv2* deficient mesoderm (*Etv2*^{KO}iSCL) was sufficient to bypass the functional requirement for ETV2 in both hemato-vascular specification and cardiac repression. However, although *Etv2*^{KO}iSCL endothelial cells showed timely induction of most hematopoietic transcription factors and suppression of cardiac regulators, there was a delayed rescue of several vascular genes. ChIP-sequencing showed direct binding by ETV2, often together with SCL at the same or different sites, in genes that were rescued with delay in *Etv2*^{KO}iSCL endothelium. ATAC-sequencing of *Etv2*^{KO}iSCL endothelial cells showed that ETV2 is required for opening of chromatin at ETV2 binding sites. The co-operation of ETV2 and SCL is thus essential for timely activation of hemato-vascular genes during mesoderm diversification to blood and vascular lineages.

Introduction

Cardiovascular and blood systems are closely related both functionally and by their developmental origin. Serious problems will be caused when these organ systems become dysfunctional during development or post-natal life, and thus there are extensive efforts to develop cell-based therapies to help regenerate these organ systems. Although hematopoietic, endothelial and cardiomyocytic cells can be differentiated from pluripotent stem cells, and reprogrammed from fibroblasts (Margariti et al., 2012; Morita et al., 2015; Levenberg et al., 2002; Adams et al., 2013; Wang et al., 2005), it has not been possible to generate fully functional and long lasting stem/progenitor cells for these tissues. Thus, it is important to develop a more detailed molecular map of how cardiovascular and hematopoietic cells are generated during development.

Hematopoietic, endothelial and cardiac cells are all derived from $Flk1^{+}$ cardiovascular mesoderm (Chung et al., 2002; Ema et al., 2003; Ema et al., 2006). Although several transcription factors that are required for blood or cardiovascular development have been identified, how the various cardiovascular and blood lineages diverge from a common precursor is poorly understood. ETV2 specifies hemangioblast that gives rise to hematopoietic and endothelial progenitors, from $Flk1^{+}PDGFRa^{+}$ primitive mesoderm (Kataoka et al., 2011; Sakurai et al., 2006). *Etv2* deficient mouse embryos die around E9.0 due to complete failure of vasculature and blood development (Lee et al., 2008). *Etv2* expression also demarcates the establishment of hemogenic endothelium and the onset of blood development (Wareing et al., 2012). ETV2 activates the hematopoietic master regulator SCL, which is critical for specification of hemogenic endothelium and hematopoietic cells (Ren et al., 2010; Wareing et al., 2012; Lancrin et al., 2009; Liu et al., 2015).

Scl^{KO} embryos die around E9.5 due to lack of all blood cells (Shivdasani et al., 1995). Thus, both ETV2 and SCL are indispensable for establishing the hematopoietic system.

Recent studies suggest that both ETV2 and SCL are also involved in repressing the cardiac fate as the vascular endothelial and hematopoietic lineages diverge from common mesodermal precursor (Ismailoglu et al., 2008; Gering et al., 2003). In addition to failing to activate hematopoiesis (Van Handel et al., 2012), *Scl* deficient endothelium in the yolk sac became misspecified to cardiac fate and generated fully functional, beating cardiomyocytes. Misspecification to cardiac fate was also observed in *Scl* deficient endocardium in the heart. SCL directs this dual fate decision by binding to epigenetically primed cardiac and hemato-vascular enhancers in mesoderm. While cardiac enhancers lose the enhancer mark H3K4me1 upon hematopoietic development, hematopoietic enhancers generally retain an active state and SCL binding. These data suggest that SCL directly represses cardiac fate during a specific temporal window in mesoderm by silencing epigenetically primed enhancers, while it converts the hematopoietic genes into fully active state (Org et al., 2015). Notably, SCL complex partners GATA1 and 2, and its downstream target RUNX1, are only required for hematopoietic activation, and not for cardiac repression.

In addition to SCL, the only other transcription factor whose loss has been associated with ectopic cardiac development is ETV2. The lack of ETV2 in mice leads to increased Flk1^{+}PDGFRa^{+} cardiogenic mesoderm as well as upregulation of cardiac genes (Lee et al., 2008; Liu et al., 2012). Furthermore, the precursors for vascular endothelial and endocardial cells ectopically differentiate into cardiomyocytes in *Etv2* deficient zebrafish embryos(Palencia-Desai et al., 2011; Liu et al., 2013). On the other hand, failure to repress ETV2 expression in fish embryos results in expansion of endocardial cells at the expense of myocardial population

(Schupp et al., 2014). These results imply that ETV2 expression has to be precisely regulated to enable the divergence of cardiomyocytic and vascular lineages during development. However, whether ETV2 is directly involved in cardiac repression, or merely does so by inducing SCL, is not known.

Here we show that SCL can specify hemogenic endothelium and repress ectopic cardiogenesis in mesodermal precursors independent of ETV2. However, ETV2 co-operates with SCL to ensure timely activation of hemato-vascular genes by promoting chromatin accessibility at its binding sites. In contrast, ETV2 function in cardiac repression is indirect and mediated by its downstream target genes, such as SCL. SCL thus has a unique role in regulating mutually the exclusive fate decision between hematopoietic and cardiac lineages by directing both gene activation and repression.

Results

ETV2 and SCL co-regulate one another

Our goal was to dissect the individual functions of ETV2 and SCL in the divergence of vascular, hematopoietic and cardiac fates. ETV2 has been shown to directly activate SCL expression through 5' enhancer (Wareing, et al., 2012; Gottgens et al., 2004). Analysis of published ETV2 binding data verified that ETV2 directly binds to *Scl* upstream regulatory regions in mesoderm to activate the expression of *Scl* (Liu et al., 2015) (Supplementary Figure S1A). In concordance with the finding that *Scl* is a direct target gene for ETV2, *Scl* expression could not be detected in $Etv2^{KO}$ D4.75 $Flk1^{+}$ mesodermal cells (Fig1A).

Analysis of published SCL binding data in $Flk1^{+}$ mesoderm showed that SCL directly binds to an upstream regulatory region of *Etv*2 (Org et al., 2015)(Supplementary Figure S1A) that is responsible for driving *Etv2* expression (Ferdous et al., 2009; Rasmussen et al., 2011). Indeed, Scl^{KO} ES cell derived day 4.75 $CD41^{-}CD31^{+}Tie2^{+}$ endothelial cells showed increased Etv2 expression. The overexpression of *Etv2* was suppressed to levels comparable to WT upon restoration of *Scl* expression during Scl^{KO} ES cell differentiation (Fig1B). These data suggest that SCL may regulate the timely repression of *Etv2* expression through a negative feedback loop. Notably, although *Etv2* is expressed robustly in Scl^{KO} endothelial cells both *in vitro* and *in vivo* (Supplementary Figure S1B), Scl^{KO} endothelial cells cannot generate hematopoietic cells, or prevent misspecification to cardiac fate (Org et al., 2015 Jan 6). These data indicate that ETV2 is not sufficient to repress cardiac fate and specify hematopoiesis in endothelium in the absence of SCL.

SCL can functionally restore the development of hemato-vascular lineages and repress ectopic cardiogenesis in the absence of ETV2

Prior studies have shown that induction of SCL expression in *Etv2* deficient cells can rescue the generation of VECAD^{+} endothelial cells (Kataoka et al., 2011), CD41^{+} hematopoietic progenitor population as well as precursors for primitive erythropoiesis and transient definitive hematopoiesis (Wareing et al., 2012). To investigate how SCL can rescue hemato-vascular development in the absence of *Etv2,* and to assess the function of ETV2 in cardiac repression, SCL expression was induced in *Etv2* deficient cells using the doxycycline inducible *Etv2*^{KO}iSCL ES cell line where doxycycline-inducible Scl-2A-GFP transgene was introduced into *Etv2*-deficient ESCs. Rescue of *Etv2* expression in *Etv2*^{KO}iETV2 cell line was used as a control. Since ETV2 is only transiently expressed during development (Ferdous et al., 2009; Kataoka et al., 2011; Lee et al., 2008) ETV2 was induced transiently by limiting doxycycline administration from day 2 to day 4.75 of EB differentiation, while SCL expression was induced from day 2 of EB differentiation and maintained throughout the assays, mimicking its known expression pattern (Fig1C). Real-time PCR and FACS analysis of GFP was performed to verify the expression of *Scl* and *Etv2* upon doxycycline induction (Supplementary Figure S1D).

Whereas *Etv2*^{KO} EBs failed to generate CD31^{+}TIE2^{+} endothelial population, promiscuous activation of SCL in *Etv2*^{KO}iSCL cells was sufficient to enable the generation of CD31^{+}TIE2^{+} endothelial cells in day 7 EBs to frequency comparable to WT and *Etv2*^{KO}iETV2 cells. Whereas no c-KIT^{+}CD41^{+} hematopoietic progenitors were detected in day7 *Etv2*^{KO} EBs or *Scl*^{KO} EBs, the hematopoietic progenitor population was rescued in *Etv2*^{KO}iSCL EBs to frequency comparable to WT and *Etv2*^{KO} iETV2 cells (Fig1D).

To examine the differentiation potential of endothelial cells derived from the various genetically modified ES cells, EBs were differentiated for 4.75 days when hematovascular precursors are first specified and sorted $CD31^{+}TIE2^{+}$ endothelial cells were subjected to *in vitro* differentiation assays. Although the population of *Etv2*^{KO}iSCL CD41-$CD31^{+}TIE2^{+}$ endothelial cells was rescued to similar frequency as WT in day 7 EBs (Fig 1D), the day 4.75 *Etv2*^{KO}iSCL CD41-$CD31^{+}TIE2^{+}$ endothelial cell population was significantly smaller than in WT (Supplementary Figure S1C). This was mainly due to reduced Tie2 expression, as the $CD31^{+}$ population in *Etv2*^{KO}iSCL cells was comparable to, if not higher, than WT and *Etv2*^{KO}iETV2 cells.

To test whether day 4.75 *Etv2*^{KO}iSCL endothelial cells are hemogenic, $CD41^{-}CD31^{+}TIE2^{+}$ cells were sorted and cultured for 14 days with hematopoietic growth factors on OP9 stroma (Fig1C). In contrast to *Scl*^{KO} endothelial cells that could not give rise to any $CD45^{+}$ hematopoietic cells, induction of SCL expression in *Etv2*^{KO}iSCL ES cells rescued the generation of $CD45^{+}$ hematopoietic population (Fig1E). These data confirm that SCL is capable of functionally restoring the generation of hemato-vascular populations, the specification of hemogenic endothelium and its subsequent differentiation to hematopoietic cells in EBs in the absence of ETV2.

To investigate whether SCL can prevent the misspecification of endothelium to cardiac fate in the absence of ETV2, EBs were differentiated for 4.75 days, after which $CD41^{-}CD31^{+}Tie2^{+}$ endothelial cells were sorted and cultured for 14 days in cardiomyocyte-promoting conditions on OP9 stroma (Fig1C). In *Etv2*^{KO}iSCL day 4.75 endothelial cells, SCL expression was induced from day 2 onward, while in *Etv2*^{KO}iETV2 cells, ETV2 was transiently induced between D2-D4.75. Whereas *Scl*^{KO} endothelial cells gave rise to TroponinT expressing cardiomyocytes in culture, no significant ectopic cardiogenic differentiation from *Etv2*^{KO}iSCL endothelial cells was

observed (Fig1F). These data imply that *Etv2* expression is not essential for cardiac repression in the endothelium, as SCL can represses cardiogenesis in endothelial cells that have never expressed ETV2.

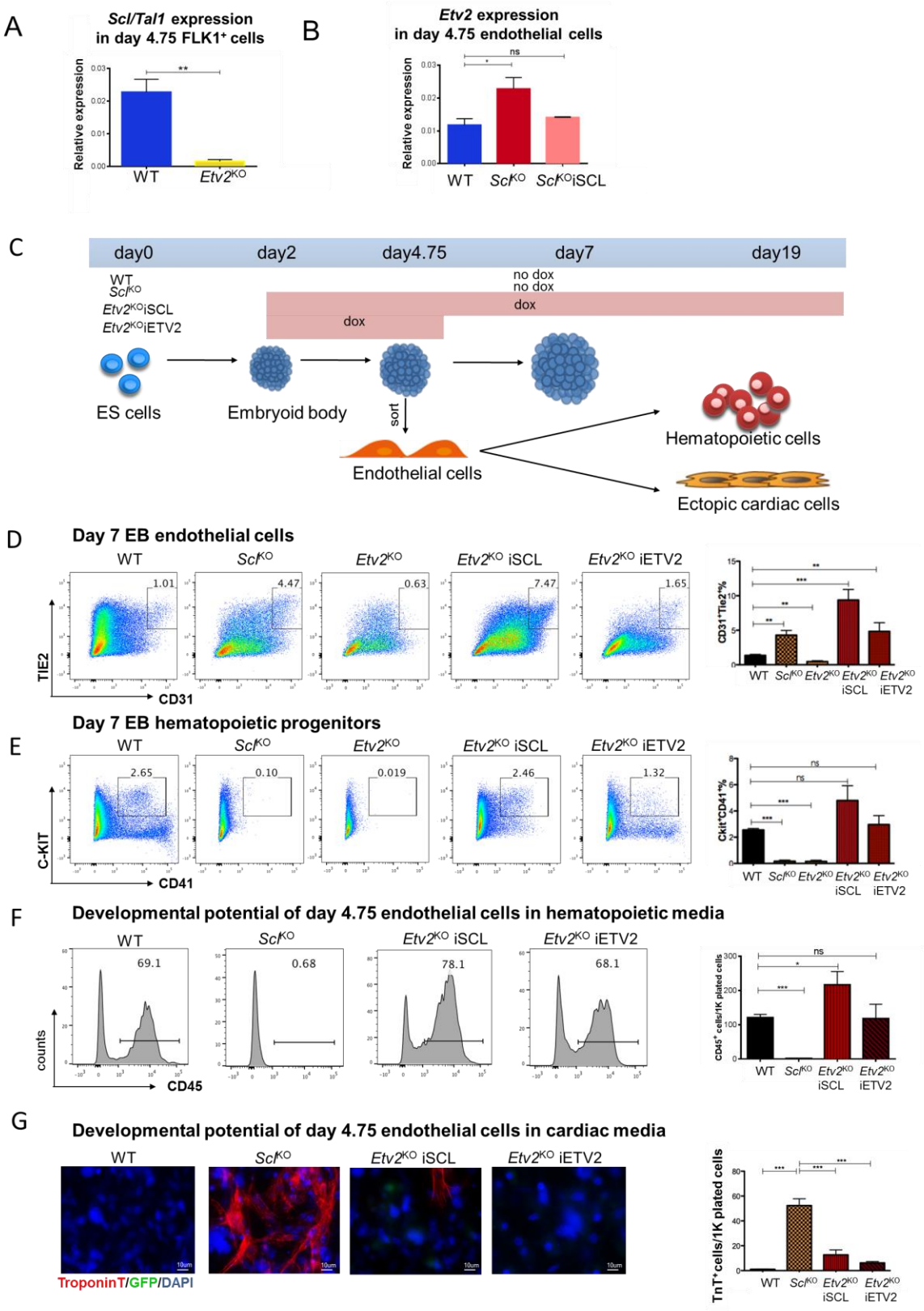
A
Scl/Tal1 expression in day 4.75 FLK1+ cells
Relative expression
WT
Etv2KO
B
Etv2 expression in day 4.75 endothelial cells
Relative expression
WT
SclKO
SclKOiSCL
C
day0
day2
day4.75
day7
day19
WT
SclKO
Etv2KOiSCL
Etv2KOiETV2
no dox
dox
dox
ES cells
Embryoid body
sort
Endothelial cells
Hematopoietic cells
Ectopic cardiac cells
D
Day 7 EB endothelial cells
WT
SclKO
Etv2KO
Etv2KO iSCL
Etv2KO iETV2
1.01
4.47
0.63
7.47
1.65
TIE2
CD31
CD31+Tie2+%
E
Day 7 EB hematopoietic progenitors
2.65
0.10
0.019
2.46
1.32
C-KIT
CD41
Ckit+CD41+%
F
Developmental potential of day 4.75 endothelial cells in hematopoietic media
69.1
0.68
78.1
68.1
counts
CD45
CD45+ cells/1K plated cells
G
Developmental potential of day 4.75 endothelial cells in cardiac media
TroponinT/GFP/DAPI
TnT+cells/1K plated cells

Figure 1

Figure 3.1: *Scl* overexpression functionally rescues endothelial and hematopoietic populations and represses ectopic cardiogenesis in *Etv2*^{KO} cells

A. qRT-PCR of *Scl* expression relative to *GAPDH* in day 4.75 Flk1^{+} WT and *Etv2*^{KO} cells. Average of 3 biological replicates with SD is shown.

B. qRT-PCR of *Etv2* expression relative to *GAPDH* in day 4.75 CD41^{-}CD31^{+}TIE2^{+} WT, *Scl*^{KO} and *Scl*^{KO}iSCL endothelial cells. Average of 3 biological replicates with SD is shown.

C. Schematic of WT, *Scl*^{KO}, *Etv2*^{KO}iSCL, *Etv2*^{KO}iETV2 ES cell differentiation strategy to EBs and differentiation of sorted endothelial cells to hematopoietic cells or ectopic cardiomyocytes.

D. Flow cytometry analysis of day 7 EBs with CD31 and TIE2 shows efficient generation of endothelial cells from WT, *Scl*^{KO}, *Etv2*^{KO}iSCL and *Etv2*^{KO}iETV2, but not *Etv2*^{KO} cells. Average of 4 biological replicates with SD is shown.

E. Flow cytometry analysis of day 7 EBs with c-KIT and CD41 shows efficient generation of hematopoietic progenitors from WT, *Etv2*^{KO}iSCL and *Etv2*^{KO}iETV2, but not *Scl*^{KO} *and* *Etv2*^{KO} cells. Average of 4 biological replicates with SD is shown.

F. Flow cytometry analysis of day 4.75 CD41^{-}CD31^{+}TIE2^{+} endothelial cells cultured on OP9 for 14 days in hematopoiesis promoting media, stained for CD45 shows efficient generation of hematopoietic cells from WT, *Etv2*^{KO}iSCL and *Etv2*^{KO}iETV2, but not *Scl*^{KO} cells. Average of 6 independent experiments with SD is shown.

G. Immunostaining of day 4.75 CD41^{-}CD31^{+}TIE2^{+} endothelial cells on OP9 for 14 days in cardiac promoting media with TroponinT shows robust generation of ectopic cardiomyocytes from *Scl*^{KO} cells, significantly fewer in *Etv2*^{KO}iSCL and *Etv2*^{KO}iETV2 cells, and not in WT cells. Average of 4 independent experiments with SD is shown.

Molecular rescue in *Etv2*^{KO}iSCL endothelial cells is incomplete at day 4.75

Despite the ability of *Etv2*^{KO}iSCL endothelial cells to functionally rescue hematopoiesis and repress ectopic cardiogenesis, the observed delay in inducing TIE2 expression raised the hypothesis that lack of ETV2 in *Etv2*^{KO}iSCL endothelial cells somehow impacts the specification or maturation of hemato-vascular precursors. To define at the molecular level whether SCL can properly specify the hemato-vascular precursors in the absence of ETV2, CD41^{-}CD31^{+}TIE2^{+} endothelial cells from day 4.75 EBs were sorted for RNA sequencing. Direct comparison of CD31^{+}TIE2^{+} endothelial cells by RNA sequencing identified 149 genes that were significantly downregulated in day4.75 *Etv2*^{KO}iSCL endothelial cells compared to WT and *Etv2*^{KO}iETV2 cells (Fig2A). These poorly activated genes were enriched in gene ontology categories involving vascular development and hematopoietic development (Fig2B). Among them, many HSC and endothelial transcriptional regulators (e.g. *Sox17, Erg, Ets1, Ets2, JunB*) and HSC/hemogenic endothelium surface markers (e.g. *Esam, Cdh5*) failed to be activated in day 4.75 *Etv2*^{KO}iSCL CD31^{+}TIE2^{+} endothelium (Fig2D,2E). The poor induction of endothelial /HSC marker ESAM in day 4.75 *Etv2*^{KO}iSCL CD31^{+} cells was confirmed by flow cytometry (Fig2L). In contrast, many of the hematopoietic regulators that are known SCL targets (e.g.*Runx1, Lyl1, Gata2, Myb, Hhex, Cbfa2t3/Eto2,*) were induced in *Etv2*^{KO}iSCL endothelial cells to levels comparable to WT and *Etv2*^{KO}iETV2 endothelial cells (Fig2D,2E).

153 genes (which were rescued in *Etv2*^{KO}iETV2 cells to levels similar to WT) failed to be repressed by Scl in day 4.75 *Etv2*^{KO}iSCL CD31^{+}TIE2^{+} cells (Fig2A). These genes were enriched in chordate embryonic development, RNA processing and heart development (Fig2C). Analysis of the individual cardiac genes showed that some genes involved in embryonic morphogenesis and early cardiac development (e.g. *Hand1, Fgf8, Foxh1, Tpm1, Bmp4, Lef1*) were upregulated

in day 4.75 *Etv2*^{KO}iSCL CD31^{+}TIE2^{+} endothelial cells (Fig2F, 2G). However, most cardiac genes were not significantly derepressed in *Etv2*^{KO}iSCL endothelial cells (e.g. *Gata6, Isl1, FoxC1, Pdgfra*) (Fig2F, 2G). These data imply that although SCL can functionally rescue the generation of hematovascular populations and repress ectopic cardiogenesis from endothelium, the molecular rescue of hemogenic endothelium specification is incomplete in day 4.75 endothelial cells, as evidenced by poor induction of vascular genes, and persistent activation of early cardiac mesoderm genes.

Molecular rescue of *Etv2*^{KO}iSCL endothelium occurs with delay

Flow cytometry analysis of *Etv2*^{KO}iSCL EBs at day 7 showed that although ESAM surface expression was minimal in CD31^{+} endothelial cells in day 4.75 EBs, its expression was comparable to WT in day 7 CD31^{+} endothelial cells (Fig2L). This raised the question of whether the poor activation of hematovascular genes in day 4.75 in the absence of *Etv2* could be rescued by SCL at later stage.

To assess at a genome-wide level the degree of molecular rescue in day 7 endothelial cells, CD31^{+}TIE2^{+}CD41^{-} cells from day7 WT, *Scl*^{KO}, *Etv2*^{KO}iSCL and *Etv2*^{KO}iETV2 EBs were sorted for RNA sequencing. The majority of genes that were rescued at day 4.75 retained stable expression also in day 7 *Etv2*^{KO}iSCL endothelial cells. Most of the hematovascular genes that were not activated in day 4.75 in *Etv2*^{KO}iSCL endothelial had reached expression level comparable to WT and *Etv2*^{KO}iETV2 cells cells by day 7 (e.g *Sox17*, *Junb*) (Fig2H,2I). Similarly, most of the genes associated with heart and mesoderm development that failed to be repressed by *Scl* overexpression in day 4.75 *Etv2*^{KO}iSCL endothelial cells were downregulated by day7 (e.g. Hand1, Tpm1, Bmp4), unlike *Scl*^{KO} endothelial cells in which cardiac gene

expression level remained high (Fig2J,2K). Intersection of genes that could not be activated or repressed properly in day 4.75 and day 7 endothelial cells showed only 13 genes remained suppressed and 4 remained derepressed at both stages (Fig2M). These data imply that although the molecular maturation from cardiovascular mesoderm to hematovascular precursors in *Etv2* deficient cells appears delayed, forced SCL activation alone is sufficient to induce hematopoiesis and repress cardiogenesis independent of *Etv2*. However, these data imply that *Etv2* is necessary for the properly timed activation of a subset of hemato-vascular genes and repression of cardiac mesoderm genes during development.

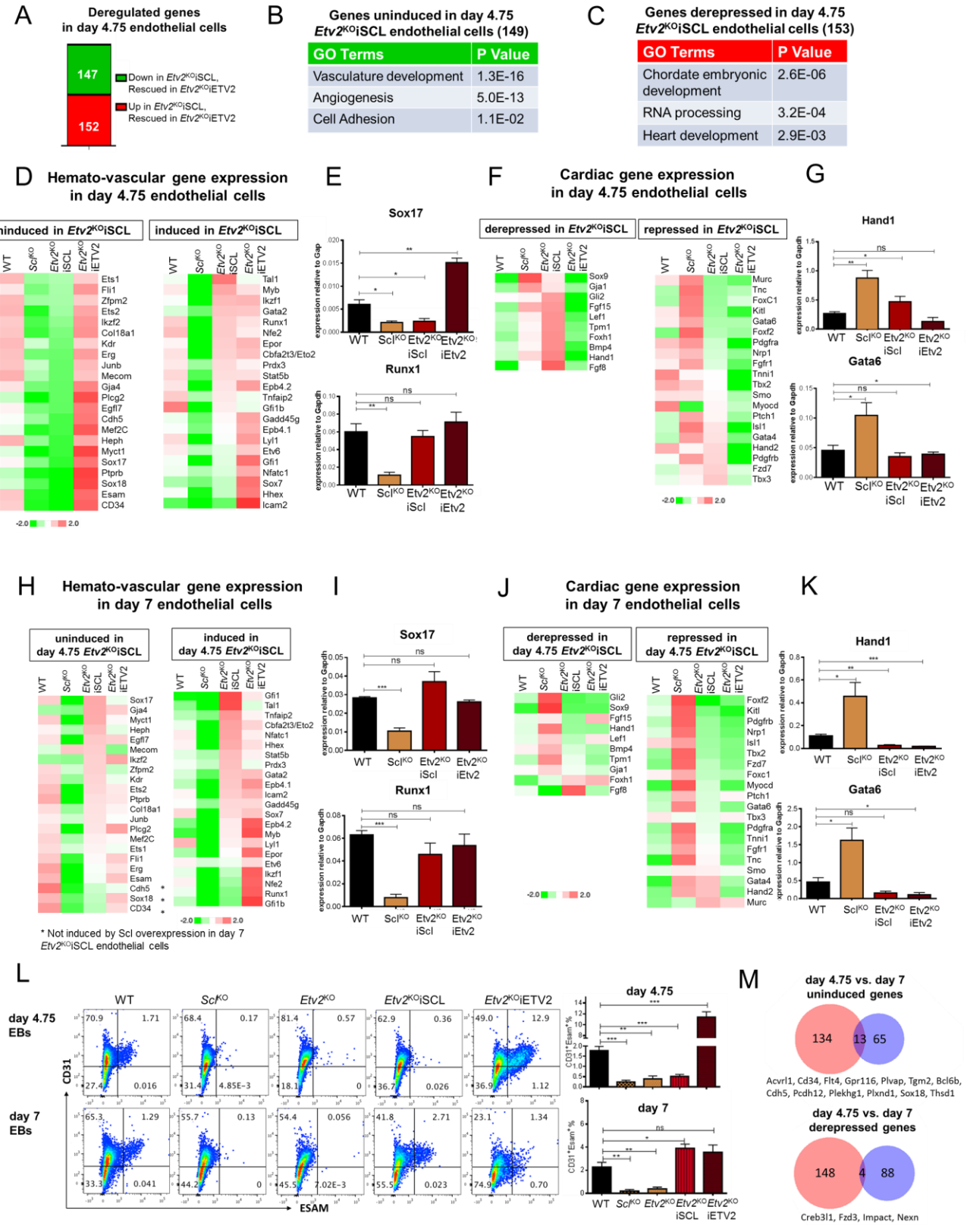
A
Deregulated genes in day 4.75 endothelial cells
147
152
Down in Etv2KOiSCL, Rescued in Etv2KOiETV2
Up in Etv2KOiSCL, Rescued in Etv2KOiETV2
B
Genes uninduced in day 4.75 Etv2KOiSCL endothelial cells (149)
GO Terms | P Value
Vasculature development | 1.3E-16
Angiogenesis | 5.0E-13
Cell Adhesion | 1.1E-02
C
Genes derepressed in day 4.75 Etv2KOiSCL endothelial cells (153)
GO Terms | P Value
Chordate embryonic development | 2.6E-06
RNA processing | 3.2E-04
Heart development | 2.9E-03
D
Hemato-vascular gene expression in day 4.75 endothelial cells
uninduced in Etv2KOiSCL
induced in Etv2KOiSCL
E
Sox17
Runx1
F
Cardiac gene expression in day 4.75 endothelial cells
derepressed in Etv2KOiSCL
repressed in Etv2KOiSCL
G
Hand1
Gata6
H
Hemato-vascular gene expression in day 7 endothelial cells
uninduced in day 4.75 Etv2KOiSCL
induced in day 4.75 Etv2KOiSCL
* Not induced by Scl overexpression in day 7 Etv2KOiSCL endothelial cells
I
Sox17
Runx1
J
Cardiac gene expression in day 7 endothelial cells
derepressed in day 4.75 Etv2KOiSCL
repressed in day 4.75 Etv2KOiSCL
K
Hand1
Gata6
L
WT
SclKO
Etv2KO
Etv2KOiSCL
Etv2KOiETV2
day 4.75 EBs
day 7 EBs
CD31
ESAM
day 4.75
day 7
M
day 4.75 vs. day 7 uninduced genes
134
13
65
Acvrl1, Cd34, Flt4, Gpr116, Plvap, Tgm2, Bcl6b, Cdh5, Pcdh12, Plekhg1, Plxnd1, Sox18, Thsd1
day 4.75 vs. day 7 derepressed genes
148
4
88
Creb3l1, Fzd3, Impact, Nexn

Figure 2

Figure 3.2: Molecular rescue in *Etv2*^{KO}iSCL endothelial cells is partially delayed

A. Bar graph of RNA seq analysis shows 147 genes uninduced and 152 derepressed in day 4.75 *Etv2*^{KO}iSCL endothelial cells compared to WT and *Etv2*^{KO}iETV2 cells.

B. DAVID GO analysis for genes uninduced in day 4.75 *Etv2*^{KO}iSCL CD41^{-}CD31^{+}TIE2^{+} endothelial cells shows enrichment of vascular development and angiogenesis categories.

C. DAVID GO analysis for genes derepressed in day 4.75 CD41^{-}CD31^{+}TIE2^{+} *Etv2*^{KO}iSCL endothelial cells shows enrichment of embryonic and heart development categories.

D. Heatmaps assessing gene expression differences between WT, *Scl*^{KO}, *Etv2*^{KO}iSCL and *Etv2*^{KO}iETV2 day 4.75 CD41^{-}CD31^{+}TIE2^{+} endothelial cells show poor induction of a subset of hemato-vascular genes in *Etv2*^{KO}iSCL cells, while others are induced to levels comparable to controls

E. qRT-PCR verification of *Sox17* (uninduced) *Runx1* (induced) expression in WT, *Scl*^{KO}, *Etv2*^{KO}iSCL and *Etv2*^{KO}iETV2 day 4.75 CD41^{-}CD31^{+}TIE2^{+} endothelial cells. Average of 3 biological replicates with SD is shown.

F. Heatmaps assessing gene expression differences between WT, *Scl*^{KO}, *Etv2*^{KO}iSCL and *Etv2*^{KO}iETV2 day 4.75 CD41^{-}CD31^{+}TIE2^{+} endothelial cells show poor repression of a subset of cardiac and mesodermal genes, whereas others are derepressed to levels comparable to controls.

G. qRT-PCR verification of *Hand1* and *Gata6* expression in WT, *Scl*^{KO}, *Etv2*^{KO}iSCL and *Etv2*^{KO}iETV2 day 4.75 CD41^{-}CD31^{+}TIE2^{+} endothelial cells. Average of 3 biological replicates with SD is shown.

H. Heatmaps assessing gene expression differences between WT, *Scl*^{KO}, *Etv2*^{KO}iSCL and *Etv2*^{KO}iETV2 day 7 CD41^{-}CD31^{+}TIE2^{+} endothelial cells in the same subsets of hemato-vascular genes uninduced and induced in day 4.75 *Etv2*^{KO}iSCL endothelial cells.

I. qRT-PCR verification of *Sox17* and *Runx1* expression in WT, *Scl*^{KO}, *Etv2*^{KO}iSCL and *Etv2*^{KO}iETV2 day 7 CD41^{-}CD31^{+}TIE2^{+} endothelial cells. Average of 3 biological replicates with SD is shown.

J. Heatmaps assessing gene expression differences between WT, *Scl*^{KO}, *Etv2*^{KO}iSCL and *Etv2*^{KO}iETV2 day 7 CD41^{-}CD31^{+}TIE2^{+} endothelial cells show subsets of cardiac and mesodermal genes that are derepressed or repressed in day 4.75 *Etv2*^{KO}iSCL endothelial cells.

K. qRT-PCR verification of *Hand1* and *Gata6* expression in WT, *Scl*^{KO}, *Etv2*^{KO}iSCL and *Etv2*^{KO}iETV2 day 4.75 CD41^{-}CD31^{+}TIE2^{+} endothelial cells. Average of 3 biological replicates with SD is shown.

L. Flow cytometry analysis of day 4.75 and day 7 EBs with ESAM and CD31 shows ESAM expression in day 4.75 WT and *Etv2*^{KO}iETV2, but not in *Scl*^{KO}, *Etv2*^{KO} and *Etv2*^{KO}iSCL CD31^{+} cells. Esam^{+} becomes expressed in CD31^{+} cells in day 7 WT, *Etv2*^{KO}iSCL and *Etv2*^{KO}iETV2, but not in *Scl*^{KO} and *Etv2*^{KO} EBs. Average of 4 biological replicates with SD is shown.

M. Venn diagram shows intersection of genes uninduced or derepressed in day 4.75 and day 7 CD41^{-}CD31^{+}TIE2^{+} endothelial cells. 13 and 4 genes remained uninduced and derepressed in both day 4.75 and day 7 CD41^{-}CD31^{+}TIE2^{+} endothelial cells, respectively

ETV2 and SCL cooperate by binding to the same or different regulatory sites of hemato-vascular genes to induce timely activation

To understand how ETV2 and SCL cooperate to regulate gene expression during mesoderm specification to hemato-vascular lineages, published SCL binding data (Org et al., 2015) and ETV2 binding data (Liu et al., 2015) in Flk1+ mesodermal cells were analyzed together. SCL binding was associated with 4158 genes, and ETV2 binding with 2287 genes. Intersection of SCL and ETV2 bound genes yielded 1101 genes that were bound by both SCL and ETV2 (Fig3A). Gene ontology analysis showed that these genes were enriched in both vasculature development and heart development. However, comparison of the exact SCL and ETV2 binding sites showed that out of 4373 SCL binding sites and 2729 ETV2 binding sites, only 393 sites were bound by both SCL and ETV2 (Fig3B). These common binding sites were enriched in gene ontology categories related to hematopoiesis and vascular development (Fig3B, C). The regulatory sites that were uniquely bound by either SCL or ETV2 were also enriched in genes associated with cardiovascular development, implying that ETV2 may co-operate with SCL in gene regulation by binding to different sites than SCL (Fig3B, C).

In contrast to SCL binding sites, which typically reside away from transcription start site (TSS), more than 20% of ETV2 binding sites located within 5kb of TSS (Fig3D). These data support the hypothesis that SCL and ETV2 may function at different regulatory regions to co-ordinate gene expression. Analysis of selected hemato-vascular genes shows that ETV2 can bind to regulatory sites of the same genes as SCL binds to (e.g. *Gata2, Scl/Tal1*). Particularly, ETV2 binds to the same sites as SCL does which include many vascular transcription factors whose activation was delayed (e.g. *Fli1*, *Sox17*) in $Etv2^{KO}$iSCL endothelium (Fig3C). In comparison, ETV2 binds to few cardiac and mesodermal genes (Fig3C).

To correlate ETV2 and SCL binding with gene expression, the genes that could not be induced by SCL overexpression in day 4.75 *Etv2* deficient endothelial cells were categorized in subcategories based on whether they were bound by ETV2 and/or SCL. 53.7% of the genes that could not be activated in a timely manner were bound by ETV2, and 46.3% were co-bound by SCL at the same or different regulatory sites (Fig3E). 29.5% genes whose rescue was delayed in *Etv2*^{KO}iSCL endothelium were bound by SCL alone, whereas 16.8% of the genes were not bound either by ETV2 or SCL. As an example of ETV2 and SCL co-regulated genes, *Esam*, whose expression in *Etv2*^{KO}iSCL cells was delayed, contained both ETV2 binding sites that were ETV2 specific, as well as common with SCL. *Cdh5*, which was not activated in day 4.75 or day 7 endothelium, harbored different SCL and ETV2 binding sites (Fig3F).

In contrast to the genes whose activation was delayed in *Etv2*^{KO}iSCL, only 15.7% of the genes that could not be repressed in a timely manner were bound by ETV2 (7.8% ETV2 alone, or 3.3% and 4.6% together with SCL in the same or different regulatory sites, respectively). This binding pattern was similar to that of genes whose expression was not significantly different between WT, *Etv2*^{KO}iSCL and *Etv2*^{KO}iETV2 day 4.75 endothelial cells (Fig3E). Compared to genes activated with delay in *Etv2*^{KO}iSCL endothelial cells, of which only 16.8% were bound by neither ETV2 nor SCL, 59.5% of genes repressed with delay did not harbor any ETV2 or SCL binding sites, suggesting most of the genes repressed with delay in *Etv2*^{KO}iSCL endothelial cells are indirect targets of ETV2 or SCL. 24.8% genes that were repressed with delay in *Etv2*^{KO}iSCL endothelium were bound by SCL only, suggesting these may represent genes that are directly repressed by SCL. Examples to these were the cardiac regulator *Hand1,* the repression of which was delayed, that was bound only by SCL, whereas *Sox9,* whose expression was also not repressed timely in *Etv2*^{KO} iSCL endothelial cells, was neither bound by ETV2 nor SCL (Fig3G)

This analysis implies that ETV2 cooperates with SCL by binding to the same or different regulatory sites to activate hemato-vascular genes, while the repression of cardiac genes occurs via ETV2 induced genes, including SCL.

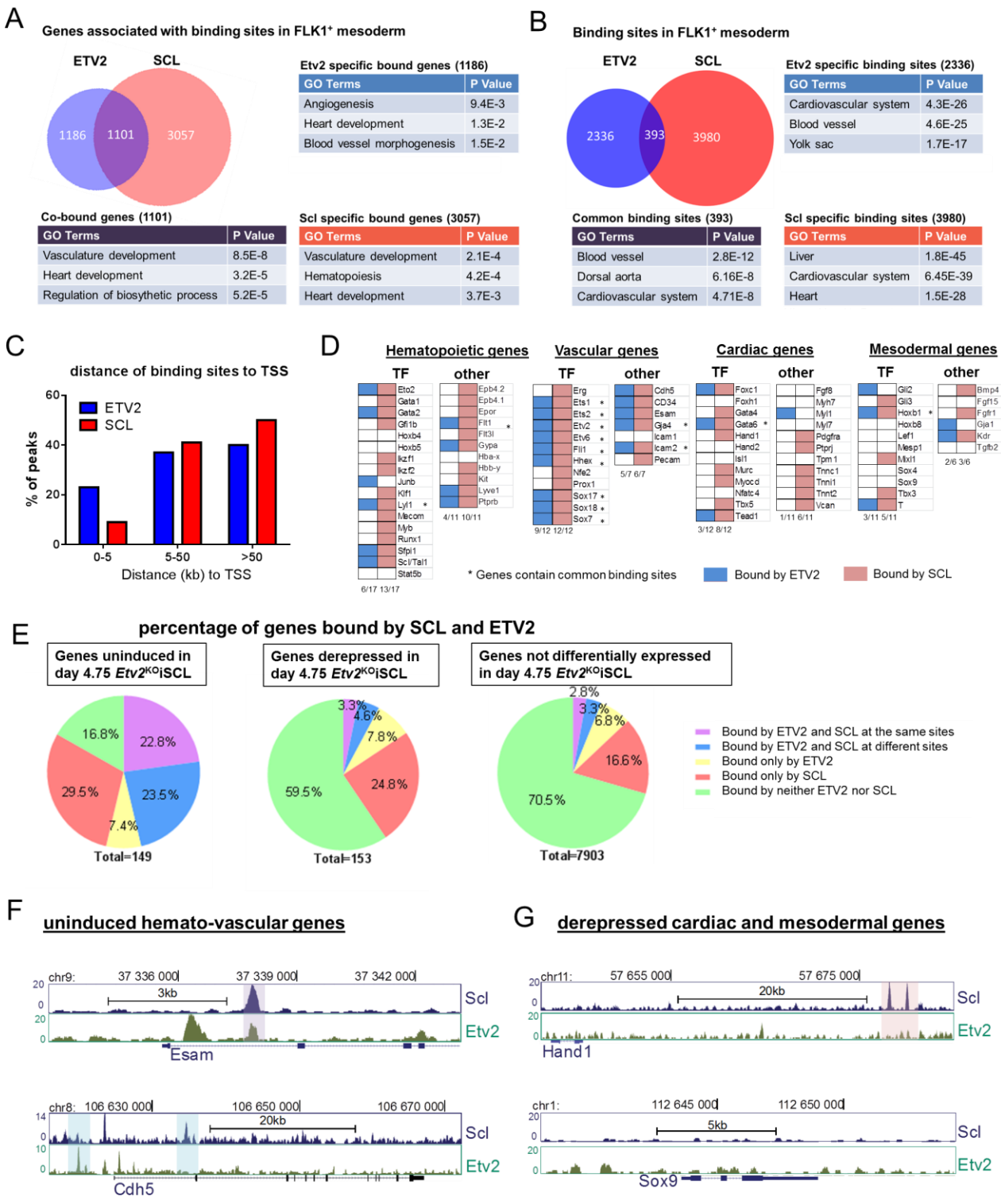
A
Genes associated with binding sites in FLK1+ mesoderm
ETV2
SCL
1186
1101
3057
Etv2 specific bound genes (1186)
GO Terms | P Value
Angiogenesis | 9.4E-3
Heart development | 1.3E-2
Blood vessel morphogenesis | 1.5E-2
Co-bound genes (1101)
GO Terms | P Value
Vasculature development | 8.5E-8
Heart development | 3.2E-5
Regulation of biosythetic process | 5.2E-5
Scl specific bound genes (3057)
GO Terms | P Value
Vasculature development | 2.1E-4
Hematopoiesis | 4.2E-4
Heart development | 3.7E-3
B
Binding sites in FLK1+ mesoderm
ETV2
SCL
2336
393
3980
Etv2 specific binding sites (2336)
GO Terms | P Value
Cardiovascular system | 4.3E-26
Blood vessel | 4.6E-25
Yolk sac | 1.7E-17
Common binding sites (393)
GO Terms | P Value
Blood vessel | 2.8E-12
Dorsal aorta | 6.16E-8
Cardiovascular system | 4.71E-8
Scl specific binding sites (3980)
GO Terms | P Value
Liver | 1.8E-45
Cardiovascular system | 6.45E-39
Heart | 1.5E-28
C
distance of binding sites to TSS
% of peaks
ETV2
SCL
0-5
5-50
>50
Distance (kb) to TSS
D
Hematopoietic genes
TF
other
Eto2
Gata1
Gata2
Gfi1b
Hoxb4
Hoxb5
Ikzf1
Ikzf2
Junb
Klf1
Lyl1 *
Mecom
Myb
Runx1
Sfpi1
Scl/Tal1
Stat5b
6/17 13/17
Epb4.2
Epb4.1
Epor
Flt1 *
Flt3l
Gypa
Hba-x
Hbb-y
Kit
Lyve1
Ptprb
4/11 10/11
Vascular genes
TF
other
Erg
Ets1 *
Ets2 *
Etv2 *
Etv6 *
Fli1 *
Hhex *
Nfe2
Prox1
Sox17 *
Sox18 *
Sox7 *
9/12 12/12
Cdh5
CD34
Esam
Gja4 *
Icam1
Icam2 *
Pecam
5/7 6/7
Cardiac genes
TF
other
Foxc1
Foxh1
Gata4
Gata6 *
Hand1
Hand2
Isl1
Murc
Myocd
Nfatc4
Tbx5
Tead1
3/12 8/12
Fgf8
Myh7
Myl1
Myl7
Pdgfra
Ptprj
Tpm1
Tnnc1
Tnni1
Tnnt2
Vcan
1/11 6/11
Mesodermal genes
TF
other
Gli2
Gli3
Hoxb1 *
Hoxb8
Lef1
Mesp1
Mixl1
Sox4
Sox9
Tbx3
T
3/11 5/11
Bmp4
Fgf15
Fgfr1
Gja1
Kdr *
Tgfb2
2/6 3/6
* Genes contain common binding sites
Bound by ETV2
Bound by SCL
E
percentage of genes bound by SCL and ETV2
Genes uninduced in day 4.75 Etv2KOiSCL
16.8%
22.8%
29.5%
23.5%
7.4%
Total=149
Genes derepressed in day 4.75 Etv2KOiSCL
3.3%
4.6%
7.8%
59.5%
24.8%
Total=153
Genes not differentially expressed in day 4.75 Etv2KOiSCL
2.8%
3.3%
6.8%
16.6%
70.5%
Total=7903
Bound by ETV2 and SCL at the same sites
Bound by ETV2 and SCL at different sites
Bound only by ETV2
Bound only by SCL
Bound by neither ETV2 nor SCL
F
uninduced hemato-vascular genes
chr9: 37 336 000 37 339 000 37 342 000
3kb
Scl
Etv2
Esam
chr8: 106 630 000 106 650 000 106 670 000
20kb
Scl
Etv2
Cdh5
G
derepressed cardiac and mesodermal genes
chr11: 57 655 000 57 675 000
20kb
Scl
Etv2
Hand1
chr1: 112 645 000 112 650 000
5kb
Scl
Etv2
Sox9

Figure 3

Figure 3.3: ETV2 and SCL cooperate by binding to the same or different regulatory sites of hemato-vascular genes to induce timely activation

A. Venn diagram shows intersection of genes associated with ETV2 and SCL binding sites in $Flk1^{+}$ mesoderm. 1101 genes are bound by both ETV2 and SCL. DAVID GO analysis for genes bound by both ETV2 and SCL, genes specifically bound by ETV2 and genes specifically bound by SCL all show enrichment in hemato-vascular and heart development.
B. Venn diagram shows intersection of sites bound by ETV2 and SCL in $Flk1^{+}$ mesoderm. 393 genomic sites are bound by both ETV2 and SCL. GREAT analysis of significantly enriched GO terms for ETV2 and SCL common binding sites, ETV2 specific binding sites and SCL specific binding sites all show enrichment of hemato-vascular system.
C. Bar graph shows distribution of the distance of ETV2 and SCL binding sites relative to TSS. 23% of ETV2 binding sites and 9% of SCL binding sites locate within 5kb to TSS.
D. Heatmaps show ETV2 and SCL binding to selected hemato-vascular, cardiac and mesodermal transcription factors and other genes. Asterisk indicates genes containing ETV2 and SCL common binding sites.
E. Pie chart shows percent of genes bound by ETV2 and/or SCL in genes uninduced, genes derepressed and genes not differentially expressed in day 4.75 *Etv2*^{KO}iSCL endothelial cells.
F. ChIP-seq genome browser tracks with ETV2 and SCL binding in $Flk1^{+}$ mesodermal cells around uninduced genes (*Esam*, *Cdh5*) in day 4.75 *Etv2*^{KO}iSCL endothelial cells are shown. ETV2 and SCL common binding site is shadowed in purple, ETV2 and SCL different binding sites to the same gene is shadowed in blue. SCL specific binding site is shadowed in red.

G. ChIP-seq genome browser tracks with ETV2 and SCL binding in Flk1^{+} mesodermal cells around derepressed genes (*Hand1*, *Sox9*) in day 4.75 *Etv2*^{KO}iSCL endothelial cells are shown.

ETV2 facilitates SCL mediated timely activation of hematovascular genes by increasing chromatin accessibility

To understand how ETV2 assists SCL in timely hemato-vascular gene activation, we investigated whether lack of ETV2 in *Etv2*^{KO}iSCL mesoderm impairs SCL's ability to bind to its target genes. 65% of genes that were poorly induced in day 4.75 *Etv2*^{KO}iSCL endothelial cells and bound by SCL in WT mesoderm retained SCL binding in *Etv2*^{KO}iSCL mesodermal cells. 73% of derepressed genes that were bound by SCL in WT mesoderm were also bound by SCL in *Etv2*^{KO}iSCL mesodermal cells. Similarly, 69% of the not differentially expressed genes retained SCL binding in *Etv2*^{KO}iSCL mesodermal cells (Supplementary Figure S3A, B). These data indicate that SCL binding to its target genes occur largely independent of ETV2, and that the delayed activation and repression of genes in *Etv2*^{KO}iSCL endothelial cells is not explained by loss of SCL binding.

To assess whether ETV2 assists SCL in gene activation by preparing the chromatin configuration suitable for gene activation, assay for transposes accessible chromatin (ATAC) sequencing was performed on day 4.75 endothelial cells. Changes in chromatin accessibility were identified by intersecting ATAC sequencing peaks between WT, *Etv2*^{KO}iSCL and *Etv2*^{KO}iETV2 endothelial cells. 6067 sites were less accessible in *Etv2*^{KO}iSCL cells compared to WT and *Etv2*^{KO}iETV2 cells. These sites were enriched in gene ontology terms related to arterial system and blood

island. In contrast, only 176 sites were more accessible in *Etv2*^{KO}iSCL endothelial cells than WT and *Etv2*^{KO}iETV2 cells. These sites were not enriched for any specific gene ontology categories. Correlating gene expression, chromatin accessibility and binding, 99 out of 149 genes (66%) that could not be activated in day 4.75 *Etv2*^{KO}iSCL endothelial cells contained less accessible sites, and 36 (24%) of them were bound by ETV2 (Fig4A). Only 2 of 149 uninduced genes in day 4.75 *Etv2*^{KO}iSCL endothelial cells contained more accessible sites, and none of them was bound by ETV2 (Fig 4B).

76 out of 153 (49%) of genes that were derepressed in day 4.75 Etv2^{KO}iSCL endothelial cells harbored less accessible sites, but only 5 (3%) of them were bound by ETV2, which is comparable to the percentage of genes that were not differentially expressed in WT, *Etv2*^{KO}iSCL and *Etv2*^{KO}iETV2 endothelial cells (30% and 2%). 1% of genes that could not be repressed timely harbored more accessible sites, which is comparable to genes not differentially expressed (1%)

Quantification of average ATAC sequencing signal around ETV2 specific binding sites showed a drop in chromatin accessibility in *Etv2*^{KO}iSCL endothelial cells compared to WT and *Etv2*^{KO}iETV2 cells. The decrease became more obvious at ETV2 and SCL co-binding sites. In contrast, average ATAC seq signal around SCL specific binding sites showed no significant change in chromatin accessibility in the absence of ETV2 (Fig4C). Genome browser shots showed example genes (*CD34, Cdh5, Ets1, Fli1*) whose activation was delayed in day 7 endothelial cells harboring ETV2 binding sites that are less accessible in *Etv2*^{KO} iSCL compared to WT or *Etv2*^{KO} iETV2 day 4.75 endothelial cells. The reduction of chromatin accessibility was not obvious at sites specifically bound by SCL or sites bound by neither ETV2 nor SCL (Fig4D).

These data suggest that ETV2 may be responsible for opening chromatin at its binding sites related to hemato-vascular genes, enabling SCL mediated gene activation.

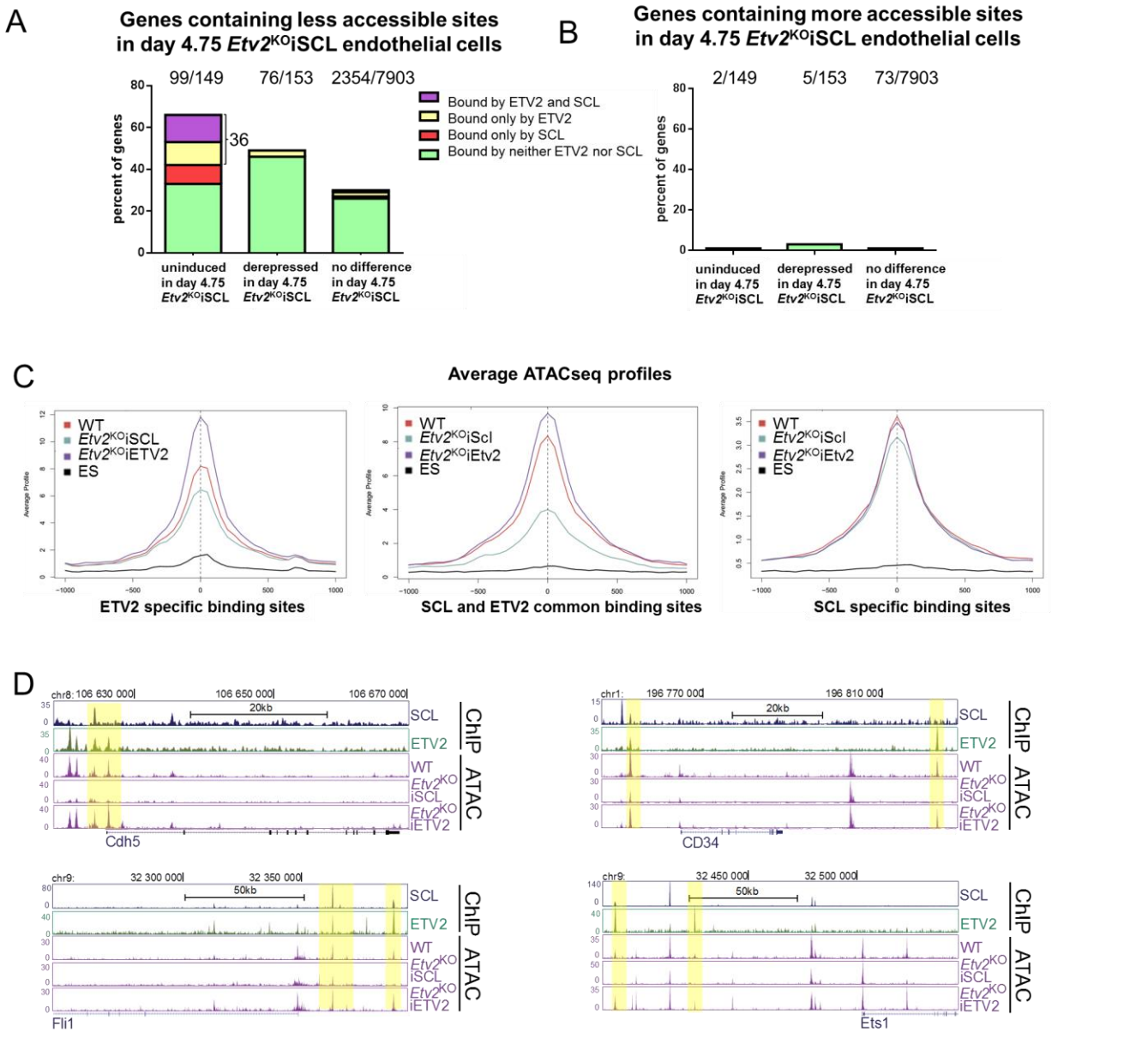

Figure 4

Figure 3.4: ETV2 facilitates SCL mediated timely activation of hemato-vascular genes by increasing chromatin accessibility

A. Bar graph shows the percentage of genes bound by ETV2 and/or SCL among uninduced, derepressed and not differentially expressed genes that harbor less accessible regulatory sites in day 4.75 *Etv2*^{KO}iSCL endothelial cells.

B. Bar graph shows the percentage of genes bound by ETV2 and/or SCL among uninduced, derepressed and not differentially expressed genes that harbor sites that are more accessible in day 4.75 *Etv2*^{KO}iSCL endothelial cells.

C. Average ATAC seq profiles of WT ES cells, WT, *Etv2*^{KO}iSCL and *Etv2*^{KO}iETV2 day 4.75 endothelial cells around ETV2 specific binding sites, ETV2 and SCL common binding sites and SCL specific binding sites show reduction of ATAC seq signal around ETV2 binding sites, especially ETV2 and SCL common binding sites in *Etv2*^{KO}iSCL compared to WT and *Etv2*^{KO}iETV2 day 4.75 endothelial cells.

D. ChIP-seq and ATAC-seq genome browser tracks show ETV2 and SCL binding in Flk1^{+} mesodermal cells and ATAC-seq peaks in WT, *Etv2*^{KO}iSCL and *Etv2*^{KO}iETV2 day 4.75 endothelial cells around uninduced genes (*Cdh5*, *Fli1*, *CD34* and *Ets1*). Sites that are bound by ETV2 and are less open in *Etv2*^{KO}iSCL endothelial cells are shadowed in yellow.

Discussion

One of the first challenges in embryonic development is to establish functional cardiovascular and blood systems to support the growth and survival of the fetus. Although individual factors regulating cardiac, hematopoietic and vascular lineages have been identified, how these regulators cooperate to execute the precisely timed fate decisions is poorly understood. The bHLH factor SCL is critical for activating hematopoiesis while repressing cardiac fate. SCL complex partners GATA1 and GATA2, or its target gene *Runx1*, are not needed for SCL mediated cardiac repression but are essential for hemogenic endothelial to hematopoietic stem/progenitor cell transition (Org et al., 2015). The only factor in addition to SCL that has been shown to repress cardiogenesis during mesoderm specification to cardiovascular and blood lineages is ETV2, the upstream regulator of SCL (Palencia-Desai et al., 2011; Rasmussen et al., 2011; Schupp et al., 2014). Whether ETV2 is directly involved in cardiac repression process remained to be addressed.

Here we show that ETV2 is not directly involved in or critical for repression of cardiac transcriptional programs, but rather does so by inducing SCL. SCL overexpression in *Etv2* deficient mesoderm was sufficient to functionally repress ectopic cardiogenesis in endothelial cells. In agreement with previous studies, SCL induction in *Etv2* deficient mesoderm was also sufficient to rescue hematopoietic progenitors and endothelial cells in the absence of *Etv2* (Kataoka et al., 2011; Wareing et al., 2012). Most genes associated with cardiac development were properly repressed in day 4.75 *Etv2*^{KO}iSCL endothelial cells although some early cardiac genes and mesodermal genes were repressed with delay, suggesting that mesoderm divergence to hemato-vascular and cardiac lineages was inefficient in the absence of *Etv2*. There was minimal binding of ETV2 to the genes that were repressed with delay, suggesting that ETV2 does not

have a direct repressive function at this stage but that it does so through its downstream transcriptional targets. In support of this model, a recent study showed that ETV2 mediated activation of miRNA130a is required to enable cardiac gene repression and endothelial gene activation (Singh et al., 2015).

Although previous work had shown that SCL overexpression in *Etv2* deficient mesoderm is sufficient to generate hematopoietic and endothelial cells, it was unknown how complete the rescue of the hemato-vascular molecular program was in the absence of the key endothelial specification factor *Etv2*. Analysis of endothelial gene expression profile at 2 different stages (day 4.75 and day 7) identified a subset of hemato-vascular genes whose activation in *Etv2*^{KO}iSCL endothelial cells was not complete until day7, implying that ETV2 facilitates timely gene activation during mesoderm specification to endothelial and hematopoietic lineages. Genes activated with delay include known transcription factors and cell surface markers for endothelial cells, hemogenic endothelium and HSCs, such as *Ets1*, *Fli1*, *Sox17*, *Junb*, *Esam*. Although most of these genes were rescued in day 7 endothelial cells, a different subset of genes enriched in cell adhesion, blood vessel development including *Itga6*, *Stab1* etc. were deregulated (Supplementary FigureS2). 13 genes that were not activated in day4.75 *Etv2*^{KO}iSCL endothelial cells remained suppressed in day7, including *Cdh5, CD34, Sox18*. These data raise the questions whether the failure to properly coordinate the activation of these genes compromises hematovascular differentiation. This is in particular relevant to the question of generating HSCs, as many of the hemato-vascular genes that are induced with delay are genes involved in specification of definitive HSCs from specialized hemogenic endothelium. Although hematopoietic progenitors can be readily generated from *Etv2*^{KO}iSCL cells, the generation of true self-renewing HSCs cannot be assessed in the ES cell differentiation system. Although it is

generally thought that *Etv2* expression declines after vessel specification (Lee et al., 2008; Kataoka et al., 2011), recent studies suggested that ETV2 may be expressed and function in mouse adult hematopoietic stem cells and post-natal vascular regeneration (Lee et al., 2011; Park et al., 2016). Further studies are needed to understand how ETV2 functions in HSC development and maintenance, and governs vessel formation under stress condition such as irradiation, infection or injury.

It is well established that ETV2 and SCL act serially to regulate hematovascular differentiation (Sumanas et al., 2008; Chan et al., 2013; Ciau-Uitz et al., 2013). However, how ETV2 and SCL cooperate to facilitate precise gene regulation during mesodermal lineage specification is not known. By combining the analysis of RNA sequencing gene expression and published ChIP sequencing data for ETV2 and SCL, we found that ETV2 may cooperate with SCL for timely gene activation of hemato-vascular genes through the same or different regulatory sites. It is likely that ETV2 also brings other factors to enhance SCL mediated gene activation. This is supported by multiple studies which showed that ETV2 can form complexes with other proteins to coordinate gene regulation. FOXC2 and GATA2 interact with ETV2 to synergistically activate hematopoietic and endothelial gene expression (De Val et al., 2008; Shi et al., 2014). In addition, the recent study showed that Etv2 interacts with a C2H2 zinc finger protein OVOL2 which enhances ETV2 mediated hematovascular lineage development (Kim et al., 2014). Notably, we found that ETV2 binds more often to the promoter than SCL, which generally binds to the enhancers of genes in mesoderm. These data raise the hypothesis that ETV2 may prepare the promoter for SCL mediated gene activation.

Previous studies have shown that *Etv2* expression alone is sufficient to reprogram fibroblast to endothelial cells (Morita et al., 2015; Veldman et al., 2013). Additionally, prolonged *Etv2*

expression forces abnormal endothelial program in hematopoietic cells (Hayashi et al., 2012). However, the mechanism for the strong reprogramming power of ETV2 is unknown. We have shown that SCL binds to pre-established enhancers to regulate gene expression, but the factor that establishes the epigenetic landscape remain to be identified (Org et al., 2015). Our data indicate that ETV2 binding correlates with chromatin accessibility. The chromatin is less open at ETV2 binding sites in *Etv2*^{KO}iScl endothelial cells, suggesting that ETV2 may prepare the open sites for SCL or other factors to bind and regulate gene expression. ETV2 may not be absolutely required for, but it can facilitate timely gene activation by SCL. For example, *Esam* whose ETV2 binding sites are less open at day 4.75 in *Etv2*^{KO}iSCL endothelial cells are deregulated in day 4.75, but rescued at day 7. The strong power of ETV2 could be explained by its function in establishing epigenetic landscape for other factors to function.

In summary, these data solidify that ETV2 is an activator rather than a repressor of gene expression during hemato-vascular specification, and reinforce that SCL is the key factor that is responsible for activating hematopoietic genes while repressing cardiac program in hemogenic endothelium. Furthermore, for the first time we show that cooperates with SCL to ensure the timely activation of many critical hemato-vascular genes by increasing chromatin accessibility at its binding sites. Further studies are needed to understand how ETV2 modifies the chromatin and which factors it activates to cooperate with SCL for cardiac and mesodermal gene repression.

Methods

ES cell culture and EB differentiation

Standard ES cell culture conditions were used to maintain WT, *Scl*^{KO}, *Etv2*^{KO}iSCL and Etv2^{KO}iETV2 cell lines. Dr. Kouskoff kindly shared their *Etv2*^{KO}iSCL and *Etv2*^{KO}iETV2 ES cell lines where doxycycline-inducible Scl-2A-GFP transgene or Etv2-2A-GFP transgene was introduced into *Etv2*-deficient ESCs. Flk1^{+} cardiovascular mesoderm and hemato-vascular derivatives were generated using EB differentiation as described (Mikkola et al., 2003). EBs were digested enzymatically and analyzed by flow cytometry or enriched for desired populations by MACS or FACS sorting. Real-time PCR and FACS analysis of GFP was performed to verify the expression of *Scl* and *Etv2* upon doxycycline induction (Supplementary Figure S1D). For RNA-seq and endothelial cell developmental potential assays, day 4.75 and day 7 EBs were digested with 2mg/ml collagenase (Worthington) and 0.5mg/ml dispase (Invitrogen), and Tie2^{+}CD31^{+}CD41^{-} cells were sorted on a BD FACS Aria II (BD Biosciences) using Tie2-PE (clone TEK4), CD31-PECy7 (clone 390) and CD41-PerCPCy5.5 (clone MWReg30) antibodies (all from eBioscience).

Analysis of endothelial cell differentiation potential

After 4.75 days of EB induction, CD41^{-}CD31^{+}Tie2^{+}cells were sorted from WT, *Scl*^{KO}, *Etv2*^{KO}iSCL, *Etv2*^{KO}iETV2 EBs and 20,000 cells were plated on irradiated OP9 stroma in 8 well chamber slides (354118 BD FalconTM). 1mg/ml Doxycycline (1:1000) was added to *Etv2*^{KO}iETV2 culture from EB day 2 to day 4.75, and to *Etv2*^{KO}iSCL culture at day2 EB induction throughout the culture. The differentiation media contained α-MEM, 20% FBS, 1% Penicillin, Streptomycin and 1% Glutamine. For hematopoietic differentiation, 50ng/ml SCF,

5ng/ml IL3, 5ng/ml IL6, 5ng/ml TPO and 10ng/ml Flt3L were added. For cardiac differentiation, 5ng/ml hVEGF, 30ng/ml mFGF, 50ng/ml hBMP4 and 1 μM Wnt/Beta-Catenin Inhibitor XAV939 (Sigma) were added. After 14 days, FACS staining or immunostaining was performed as described (Van Handel et al., 2012).

Immunostaining

Endothelial cells cultured in chamber slides were fixed with 4% PFA for 15min at room temperature and permeabilized for 10min with PBS containing 0.25% Triton. After permeabilization, cells were blocked in PBS containing 1% BSA and 0.05% Tween20 for 30 min. Primary antibody cardiac Troponin T (1:400, MS-295-P1, Thermo Scientific) was applied to the cells overnight at 4 °C. After washing 3 times with PBS (0.05% Tween20), secondary antibody and DAPI were applied for 1h. Images were obtained on a Zeiss LSM 510 equipped with 405 nm, 488 nm, 543 nm, and 633 nm lasers after mounting.

Flow cytometry for hematopoietic and endothelial cells

Progression of hematopoietic development was assessed using the antibodies for CD41-PerCPCy5.5 or CD41-FITC (clone MWReg30), cKit-APC or PE-Cy7 (clone 2B8) Tie2-PE (clone TEK4), CD31-PECy7 (clone 390) (all from eBioscience), Esam-APC (clone 1G8, Biolengend). Dead cells were excluded with DAPI (Roche). Cell populations were analyzed using an LSR II or Fortessa flow cytometer or sorted using a FACSAria II cell sorter (BD Biosciences). Data were analyzed with FlowJo software, version 8.8.6 (TreeStar).

Quantitative reverse transcription PCR (qRT–PCR)

Total RNA was isolated from sorted cells using RNeasy Mini kit (QIAGEN). cDNAs were prepared by the Quantitect reverse transcription kit (QIAGEN), and quantitative polymerase chain reaction (qPCR) was performed with LightCycler 480 SYBR Green I Master (Roche) using the LightCycler 480 real-time PCR system (Roche). All samples were normalized to GAPDH unless otherwise noted. All primer sequences can be found in Supplementary Table1.

RNAseq library preparation and date analysis

Total RNA was extracted using RNeasy Mini kit (Qiagen) and library was constructed using Ovation RNA-seq System 1-16 for Model Organisms (0348, Nugen). Libraries were sequenced using HIseq-2000 (Illumina) to obtain paired end 50 bp long reads.

Debarcoding of the multiplex runs was performed using in house Unix shell script. Splice junction mapping to the mouse genome (mm9) was performed using TopHat v2.0.4 (Trapnell et al., 2009) with default parameters. For abundance estimations (FPKMs), the aligned read files were further processed with Cufflinks v2.0.1 (Trapnell et al., 2010). Assemblies for all samples were merged using Cuffmerge and differential expression was determined using Cuffdiff. Genes with a q-value smaller than 0.05 where considered as differentially expressed. Relative expression of each gene was calculated by dividing FPKM with average FPKM of all samples. Heatmap was generated with log2 ratio of relative expression of genes by Java TreeView(Saldanha 2004). An online tool DAVID Bioinformatics Resources 6.7 (Huang et al., 2009) was used for Gene ontology (GO) analysis.

Criteria for differentially expressed genes in *Etv2*^{KO}iSCL endothelial cells

2 replicates of RNAseq were performed from day4.75 WT, *Scl*^{KO}, *Etv2*^{KO}iSCL and *Etv2*^{KO}iETV2 endothelial cells. Cuffdiff was used to calculate significant difference for gene expression between different cell lines. Genes with a q-value smaller than 0.05 where considered as differentially expressed. The expression of uninduced genes in day4.75 *Etv2*^{KO}iSCL endothelial cells was significantly lower in *Etv2*^{KO}iSCL, but higher or not significantly different in *Etv2*^{KO}iETV2 than in WT. To exclude genes that are repressed by Etv2, genes upregulated in *Etv2*^{KO} Flk1^{+} mesoderm microarray data (Liu et al., 2012) were intersected and 2 (Egr1, Fstl1) overlapping genes were taken out of the list. The expression of genes derepressed in day 4.75 *Etv2*^{KO}iSCL endothelial cells was significantly higher in *Etv2*^{KO}iSCL, but lower or not significantly different in *Etv2*^{KO}iETV2 than WT. To exclude genes that are activated by Etv2, genes downregulated in *Etv2*^{KO} Flk1^{+} mesoderm microarray data(Liu et al., 2012) were intersected and only 1 overlapping gene (*Scl*) was taken out of the list. Finally, genes not differentially expressed in day 4.75 *Etv2*^{KO}iSCL endothelial cells were expressed and the expression was not significantly different in *Etv2*^{KO}iSCL and *Etv2*^{KO}iETV2 compared to WT.

Assay for transposase accessible chromatin (ATAC) seq

ATAC-seq libraries were constructed by adapting a published protocol(Buenrostro et al., 2015). In brief, ES cells were grown and differentiated to day4.75 EBs. 50,000 CD41-CD31+Tie2+ endothelial cells were sorted, washed with cold PBS and resuspended in 50µl of ES buffer (10mM Tris, pH 7.4, 10mM NaCl, 3mM $MgCl_2$). Permeabilized cells were resuspended in 50µl transposase reaction (1× tagmentation buffer, 1.0–1.5µl Tn5 transposase enzyme (Illumina)) and incubated for 30min at 37°C. Subsequent steps of the protocol were performed as previously described (Buenrostro et al., 2015). Libraries were purified using a Zymo Research DNA Clean

& Concentrator kit. Each library was then paired-end sequenced (2×50bp) on a HiSeq instrument (Illumina).

Analysis of ATAC-seq data

Reads were mapped to the mouse genome (mm9) using Bowtie v0.12.7 (Langmead et al., 2009) with (-m 1 –strata –best –v 2) parameters. Only reads that aligned to a unique position in the genome with no more than two sequence mismatches were retained for further analysis. Duplicate reads that mapped to the same exact location in the genome were counted only once to reduce clonal amplification effects. Using mapped sam files as inputs, bedgraph files were created using Homer with default parameters (Heinz et al., 2010), converted to bigwig format using bedGraphtoBigwig script (Kent et al., 2010) and visualized on UCSC genome browser (Kent et al., 2002) as custom tracks. Peak identification was performed with MACS v1.3.7.1 (Zhang et al., 2008) default parameters. Peaks from WT, *Scl*^{KO}, *Etv2*^{KO}iSCL and *Etv2*^{KO}iETV2 endothelial cells were intersected using Galaxy(Blankenberg et al., 2010). To identify genes associated with ATAC peaks, peaks were mapped to nearby genes within 200kb range from TSS using Genomic Regions Enrichment of Annotations Tool (GREAT) (McLean et al., 2010). Top enriched terms for a given category are reported unless otherwise noted. Peak intersections, distance to TSS and overlaps with differentially expressed genes were determined using Galaxy (Blankenberg et al., 2010), GREAT and in house Unix shell scripts. ATAC seq average signal profiles were generated using Galaxy Cistrome Sitepro.

Analysis of ChIP-seq data

Raw data of ETV2 and SCL ChIP sequencing in mesodermal cells were accessed from GEO (Liu et al., 2015; Org et al., 2015). Reads were mapped to the mouse genome (mm9) using

bowtie v0.12.7 (Langmead et al., 2009) with (-m 1 –strata –best –v 2) parameters. Only reads that aligned to a unique position in the genome with no more than two sequence mismatches were retained for further analysis. Duplicate reads that mapped to the same exact location in the genome were counted only once to reduce clonal amplification effects. Mapped sam files were analyzed the same way as described in ATAC-seq data descried earlier.

Statistical analysis

Student's t-test (Prism5, GraphPad Software, La Jolla, CA) was used for statistical analysis. * indicates 0.01< p value < 0.05, ** indicates 0.001 < p value < 0.01, *** indicates 0.0001 < p value < 0.001, **** indicates p value < 0.0001

Acknowledgement

We would like to thank Dr. Kouskoff (Cambridge University, United Kingdom) for kindly sharing *Etv2*^{KO}iSCL and *Etv2*^{KO}iETV2 ES cell lines. We would also like to thank the UCLA BSCRC Flow Cytometry Core for the assistance in FACS sorting and the UCLA Stem Cells Sequencing core for the assistance in ChIP sequencing, RNA sequencing and ATAC sequencing. This work was funded by the California Institute for Regenerative Medicine (CIRM) New Faculty Award (RN1-00557), the Eli and Edythe Broad Center of Regenerative Medicine and Stem Cell Research at UCLA Research Award, American Heart Association (#14GRNT20480340), and Leukemia Lymphoma Society Scholar Award (20103778) to H.K.A.M. D.D was supported by the government of P.R.C through the State Scholarship Fund (File No.2011624028) and 2016 UCLA Dissertation Year Fellowship. T.O was supported by Leukemia Lymphoma Society postdoctoral fellowship (57537-13) and by the European Union through the European Social Fund (Mobilitas Grant No. MJD284).

Authorship contributions:

D.D and H.K.A.M designed experiments, interpreted the data, and wrote the manuscript, D.D. performed experiments. T.O discussed the idea, provided suggestions and edited the manuscript.

Disclosure of conflicts of interests:

No conflict of interest

Bibliography:

Adams WJ, Zhang Y, Cloutier J, Kuchimanchi P, Newton G, Sehrawat S, Aird WC, Mayadas TN, Luscinskas FW, García-Cardeña G. 2013. Functional vascular endothelium derived from human induced pluripotent stem cells. Stem cell reports 1:105–13.

Blankenberg D, Von Kuster G, Coraor N, Ananda G, Lazarus R, Mangan M, Nekrutenko A, Taylor J. 2010. Galaxy: a web-based genome analysis tool for experimentalists. Curr. Protoc. Mol. Biol. Chapter 19:Unit 19.10.1–21.

Buenrostro JD, Wu B, Chang HY, Greenleaf WJ. 2015. ATAC-seq: A Method for Assaying Chromatin Accessibility Genome-Wide. Curr. Protoc. Mol. Biol. 109:21.29.1–9.

Chan SS-K, Shi X, Toyama A, Arpke RW, Dandapat A, Iacovino M, Kang J, Le G, Hagen HR, Garry DJ, et al., 2013. Mesp1 patterns mesoderm into cardiac, hematopoietic, or skeletal myogenic progenitors in a context-dependent manner. Cell Stem Cell 12:587–601.

Chung YS, Zhang WJ, Arentson E, Kingsley PD, Palis J, Choi K. 2002. Lineage analysis of the hemangioblast as defined by FLK1 and SCL expression. Development 129:5511–20.

Ciau-Uitz A, Pinheiro P, Kirmizitas A, Zuo J, Patient R. 2013. VEGFA-dependent and -independent pathways synergise to drive Scl expression and initiate programming of the blood stem cell lineage in Xenopus. Development 140:2632–42.

Ema M, Faloon P, Zhang WJ, Hirashima M, Reid T, Stanford WL, Orkin S, Choi K, Rossant J. 2003. Combinatorial effects of Flk1 and Tal1 on vascular and hematopoietic development in the mouse. Genes Dev. 17:380–93.

Ema M, Takahashi S, Rossant J. 2006. Deletion of the selection cassette, but not cis-acting elements, in targeted Flk1-lacZ allele reveals Flk1 expression in multipotent mesodermal progenitors. Blood 107:111–7.

Etsrp/Etv2 is directly regulated by Foxc1a/b in the zebrafish angioblast. - PubMed - NCBI. [accessed 2016 Mar 29]. http://www.ncbi.nlm.nih.gov/pubmed/22135404

Ferdous A, Caprioli A, Iacovino M, Martin CM, Morris J, Richardson JA, Latif S, Hammer RE, Harvey RP, Olson EN, et al., 2009. Nkx2-5 transactivates the Ets-related protein 71 gene and specifies an endothelial/endocardial fate in the developing embryo. Proc. Natl. Acad. Sci. U. S.

A. 106:814–9.

Gering M, Yamada Y, Rabbitts TH, Patient RK. 2003. Lmo2 and Scl/Tal1 convert non-axial mesoderm into haemangioblasts which differentiate into endothelial cells in the absence of Gata1. Development 130:6187–99.

Gottgens B, Broccardo C, Sanchez M-J, Deveaux S, Murphy G, Gothert JR, Kotsopoulou E, Kinston S, Delaney L, Piltz S, et al., 2004. The scl +18/19 Stem Cell Enhancer Is Not Required for Hematopoiesis: Identification of a 5' Bifunctional Hematopoietic-Endothelial Enhancer Bound by Fli-1 and Elf-1. Mol. Cell. Biol. 24:1870–1883.

Van Handel B, Montel-Hagen A, Sasidharan R, Nakano H, Ferrari R, Boogerd CJ, Schredelseker J, Wang Y, Hunter S, Org T, et al., 2012. Scl represses cardiomyogenesis in prospective hemogenic endothelium and endocardium. Cell 150:590–605.

Hayashi M, Pluchinotta M, Momiyama A, Tanaka Y, Nishikawa S-I, Kataoka H. 2012. Endothelialization and altered hematopoiesis by persistent Etv2 expression in mice. Exp. Hematol. 40:738–750.e11.

Huang DW, Sherman BT, Lempicki RA. 2009. Systematic and integrative analysis of large gene lists using DAVID bioinformatics resources. Nat. Protoc. 4:44–57.

Ismailoglu I, Yeamans G, Daley GQ, Perlingeiro RCR, Kyba M. 2008. Mesodermal patterning activity of SCL. Exp. Hematol. 36:1593–603.

Kataoka H, Hayashi M, Nakagawa R, Tanaka Y, Izumi N, Nishikawa S, Jakt ML, Tarui H, Nishikawa S-I. 2011a. Etv2/ER71 induces vascular mesoderm from Flk1+PDGFRα+ primitive mesoderm. Blood 118:6975–86.

Kataoka H, Hayashi M, Nakagawa R, Tanaka Y, Izumi N, Nishikawa S, Jakt ML, Tarui H, Nishikawa S-I. 2011b. Etv2/ER71 induces vascular mesoderm from Flk1+PDGFRα+ primitive mesoderm. Blood 118:6975–86.

Kent WJ, Sugnet CW, Furey TS, Roskin KM, Pringle TH, Zahler AM, Haussler D. 2002. The human genome browser at UCSC. Genome Res. 12:996–1006.

Kent WJ, Zweig AS, Barber G, Hinrichs AS, Karolchik D. 2010. BigWig and BigBed: enabling browsing of large distributed datasets. Bioinformatics 26:2204–7.

Kim JY, Lee RH, Kim TM, Kim D-W, Jeon Y-J, Huh S-H, Oh S-Y, Kyba M, Kataoka H, Choi K, et al., 2014. OVOL2 is a critical regulator of ER71/ETV2 in generating FLK1+, hematopoietic, and endothelial cells from embryonic stem cells. Blood 124:2948–52.

Lancrin C, Sroczynska P, Stephenson C, Allen T, Kouskoff V, Lacaud G. 2009. The haemangioblast generates haematopoietic cells through a haemogenic endothelium stage. Nature 457:892–5.

Langmead B, Trapnell C, Pop M, Salzberg SL. 2009. Ultrafast and memory-efficient alignment of short DNA sequences to the human genome. Genome Biol. 10:R25.

Lee D, Kim T, Lim D-S. 2011. The Er71 is an important regulator of hematopoietic stem cells in adult mice. Stem Cells 29:539–48.

Lee D, Park C, Lee H, Lugus JJ, Kim SH, Arentson E, Chung YS, Gomez G, Kyba M, Lin S, et al., 2008. ER71 acts downstream of BMP, Notch, and Wnt signaling in blood and vessel progenitor specification. Cell Stem Cell 2:497–507.

Levenberg S, Golub JS, Amit M, Itskovitz-Eldor J, Langer R. 2002. Endothelial cells derived from human embryonic stem cells. Proc. Natl. Acad. Sci. U. S. A. 99:4391–6.

Liu F, Bhang SH, Arentson E, Sawada A, Kim CK, Kang I, Yu J, Sakurai N, Kim SH, Yoo JJW, et al., 2013. Enhanced hemangioblast generation and improved vascular repair and regeneration from embryonic stem cells by defined transcription factors. Stem cell reports 1:166–82.

Liu F, Kang I, Park C, Chang L-W, Wang W, Lee D, Lim D-S, Vittet D, Nerbonne JM, Choi K. 2012. ER71 specifies Flk-1+ hemangiogenic mesoderm by inhibiting cardiac mesoderm and Wnt signaling. Blood 119:3295–305.

Liu F, Li D, Yu YYL, Kang I, Cha M-J, Kim JY, Park C, Watson DK, Wang T, Choi K. 2015. Induction of hematopoietic and endothelial cell program orchestrated by ETS transcription factor ER71/ETV2. EMBO Rep. 16:654–69.

Margariti A, Winkler B, Karamariti E, Zampetaki A, Tsai T, Baban D, Ragoussis J, Huang Y, Han J-DJ, Zeng L, et al., 2012. Direct reprogramming of fibroblasts into endothelial cells capable of angiogenesis and reendothelialization in tissue-engineered vessels. Proc. Natl. Acad. Sci. U. S. A. 109:13793–8.

McLean CY, Bristor D, Hiller M, Clarke SL, Schaar BT, Lowe CB, Wenger AM, Bejerano G.

2010. GREAT improves functional interpretation of cis-regulatory regions. Nat. Biotechnol. 28:495–501.

Morita R, Suzuki M, Kasahara H, Shimizu N, Shichita T, Sekiya T, Kimura A, Sasaki K, Yasukawa H, Yoshimura A. 2015. ETS transcription factor ETV2 directly converts human fibroblasts into functional endothelial cells. Proc. Natl. Acad. Sci. U. S. A. 112:160–5.

Org T, Duan D, Ferrari R, Montel-Hagen A, Van Handel B, Kerenyi MA, Sasidharan R, Rubbi L, Fujiwara Y, Pellegrini M, et al., 2015 Jan 6. Scl binds to primed enhancers in mesoderm to regulate hematopoietic and cardiac fate divergence. EMBO J.

Palencia-Desai S, Kohli V, Kang J, Chi NC, Black BL, Sumanas S. 2011. Vascular endothelial and endocardial progenitors differentiate as cardiomyocytes in the absence of Etsrp/Etv2 function. Development 138:4721–32.

Park C, Lee T-J, Bhang SH, Liu F, Nakamura R, Oladipupo SS, Pitha-Rowe I, Capoccia B, Choi HS, Kim TM, et al., 2016. Injury-Mediated Vascular Regeneration Requires Endothelial ER71/ETV2. Arterioscler. Thromb. Vasc. Biol. 36:86–96.

Rasmussen TL, Kweon J, Diekmann M a, Belema-Bedada F, Song Q, Bowlin K, Shi X, Ferdous A, Li T, Kyba M, et al., 2011. ER71 directs mesodermal fate decisions during embryogenesis. Development 138:4801–12.

Ren X, Gomez GA, Zhang B, Lin S. 2010. Scl isoforms act downstream of etsrp to specify angioblasts and definitive hematopoietic stem cells. Blood 115:5338–46.

Sakurai H, Era T, Jakt LM, Okada M, Nakai S, Nishikawa S, Nishikawa S. 2006. In vitro modeling of paraxial and lateral mesoderm differentiation reveals early reversibility. Stem Cells 24:575–86.

Saldanha AJ. 2004. Java Treeview--extensible visualization of microarray data. Bioinformatics 20:3246–8.

Schupp M-O, Waas M, Chun C-Z, Ramchandran R. 2014. Transcriptional inhibition of etv2 expression is essential for embryonic cardiac development. Dev. Biol. 393:71–83.

Shi X, Richard J, Zirbes KM, Gong W, Lin G, Kyba M, Thomson JA, Koyano-Nakagawa N, Garry DJ. 2014. Cooperative interaction of Etv2 and Gata2 regulates the development of endothelial and hematopoietic lineages. Dev. Biol. 389:208–18.

Shivdasani RA, Mayer EL, Orkin SH. 1995. Absence of blood formation in mice lacking the T-cell leukaemia oncoprotein tal-1/SCL. Nature 373:432–4.

Singh BN, Kawakami Y, Akiyama R, Rasmussen TL, Garry MG, Gong W, Das S, Shi X, Koyano-Nakagawa N, Garry DJ. 2015. The Etv2-miR-130a Network Regulates Mesodermal Specification. Cell Rep. 13:915–23.

Sumanas S, Gomez G, Zhao Y, Park C, Choi K, Lin S. 2008. Interplay among Etsrp/ER71, Scl, and Alk8 signaling controls endothelial and myeloid cell formation. Blood 111:4500–10.

Trapnell C, Pachter L, Salzberg SL. 2009. TopHat: discovering splice junctions with RNA-Seq. Bioinformatics 25:1105–11.

Trapnell C, Williams BA, Pertea G, Mortazavi A, Kwan G, van Baren MJ, Salzberg SL, Wold BJ, Pachter L. 2010. Transcript assembly and quantification by RNA-Seq reveals unannotated transcripts and isoform switching during cell differentiation. Nat. Biotechnol. 28:511–5.

De Val S, Chi NC, Meadows SM, Minovitsky S, Anderson JP, Harris IS, Ehlers ML, Agarwal P, Visel A, Xu S-M, et al., 2008. Combinatorial regulation of endothelial gene expression by ets and forkhead transcription factors. Cell 135:1053–64.

Veldman MB, Zhao C, Gomez GA, Lindgren AG, Huang H, Yang H, Yao S, Martin BL, Kimelman D, Lin S. 2013. Transdifferentiation of fast skeletal muscle into functional endothelium in vivo by transcription factor Etv2. PLoS Biol. 11:e1001590.

Wang Y, Yates F, Naveiras O, Ernst P, Daley GQ. 2005. Embryonic stem cell-derived hematopoietic stem cells. Proc. Natl. Acad. Sci. U. S. A. 102:19081–6.

Wareing S, Eliades A, Lacaud G, Kouskoff V. 2012. ETV2 expression marks blood and endothelium precursors, including hemogenic endothelium, at the onset of blood development. Dev. Dyn. 241:1454–64.

Wareing S, Mazan A, Pearson S, Göttgens B, Lacaud G, Kouskoff V. 2012. The Flk1-cre Mediated Deletion of ETV2 Defines Its Narrow Temporal Requirement During Embryonic Hematopoietic Development. Stem Cells:1521–1531.

Zhang Y, Liu T, Meyer CA, Eeckhoute J, Johnson DS, Bernstein BE, Nusbaum C, Myers RM, Brown M, Li W, et al., 2008. Model-based analysis of ChIP-Seq (MACS). Genome Biol. 9:R137.

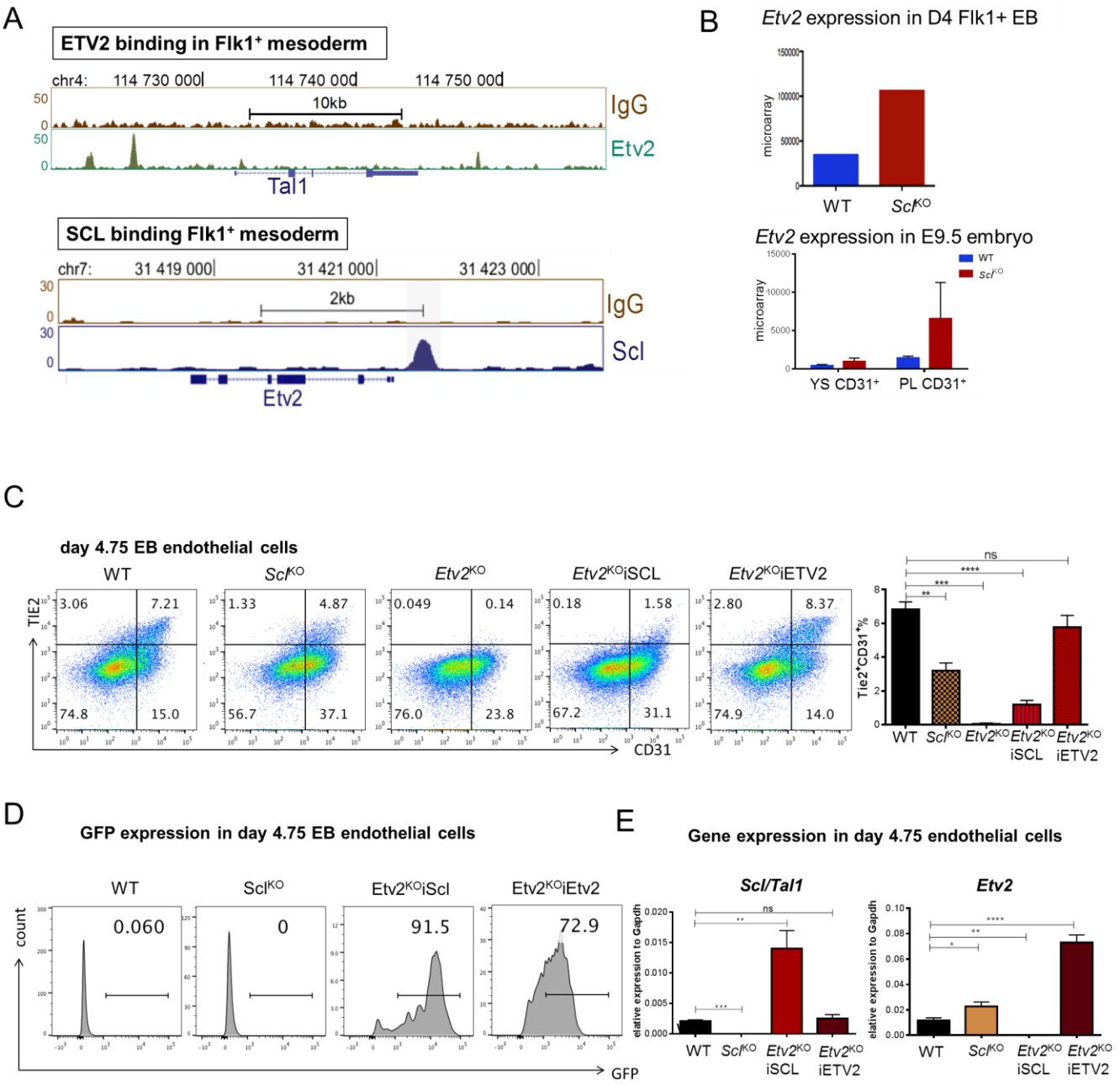

Supplementary Figure 1

Supplementary Figure S1: Differentiation of day 4.75 CD41^{-}CD31^{+}TIE2^{+} endothelial cells is delayed in *Etv2*^{KO}iSCL EBs

A. Genome browser tracks show ETV2 binding to Scl upstream regulatory sites and SCL binding to Etv2 regulatory site in Flk1^{+} mesoderm cells

B. Microarray data shows *Etv2* expression is upregulated in *Scl*^{KO} day 4 Flk1^{+} mesoderm cells and yolk sac and placenta CD31^{+} population compared to WT.

C. Flow cytometry analysis of day 4.75 EBs with markers CD31 and TIE2 shows efficient generation of endothelial population from WT, *Scl*^{KO} and *Etv2*^{KO}iETV2, but not *Etv2*^{KO} cells. The population is reduced in *Etv2*^{KO}iSCL EBs. Average of 4 biological replicates with SD is shown.

D. Flow cytometry analysis of GFP in day 4.75 CD41^{-}CD31^{+}TIE2^{+} population show efficient gene induction by doxycycline

E. qRT-PCR verification of *Scl* and *Etv2* expression in WT, *Scl*^{KO}, *Etv2*^{KO}iSCL and *Etv2*^{KO}iETV2 day 4.75 CD41^{-}CD31^{+}TIE2^{+} endothelial cells. Average of 3 biological replicates with SD is shown.

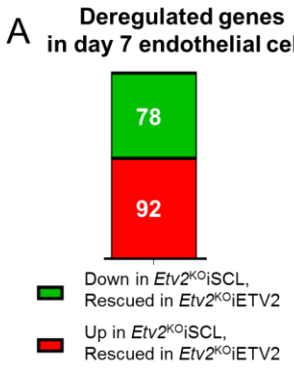

B

Genes uninduced in day 7 Etv2^{KO}iSCL endothelial cells(78)

GO Terms	P Value
Cell adhesion	6.50E-08
Hemostasis	9.60E-06
Vasculature development	1.80E-05

C

Genes derepressed in day 7 Etv2^{KO}iSCL endothelial cells (92)

GO Terms	P Value
Heart development	7.20E-04
Muscle organ development	4.10E-03
Regulation of system process	4.50E-03

Supplementary Figure 2

Supplementary Figure S2: Deregulated genes in day 7 CD41^{-}CD31^{+}TIE2^{+} *Etv2*^{KO}iSCL endothelial cells

A. Bar graph of RNA seq analysis shows 78 genes uninduced and 92 genes derepressed in day 7 *Etv2*^{KO}iSCL endothelial cells compared to WT and *Etv2*^{KO}iETV2 cells.

B. DAVID GO analysis for genes uninduced in day 7 *Etv2*^{KO}iSCL CD41^{-}CD31^{+}TIE2^{+} endothelial cells shows enrichment of cell adhesion and vascular development .

C. DAVID GO analysis for genes derepressed in day 7 CD41^{-}CD31^{+}TIE2^{+} *Etv2*^{KO}iSCL endothelial cells shows heart and muscle development.

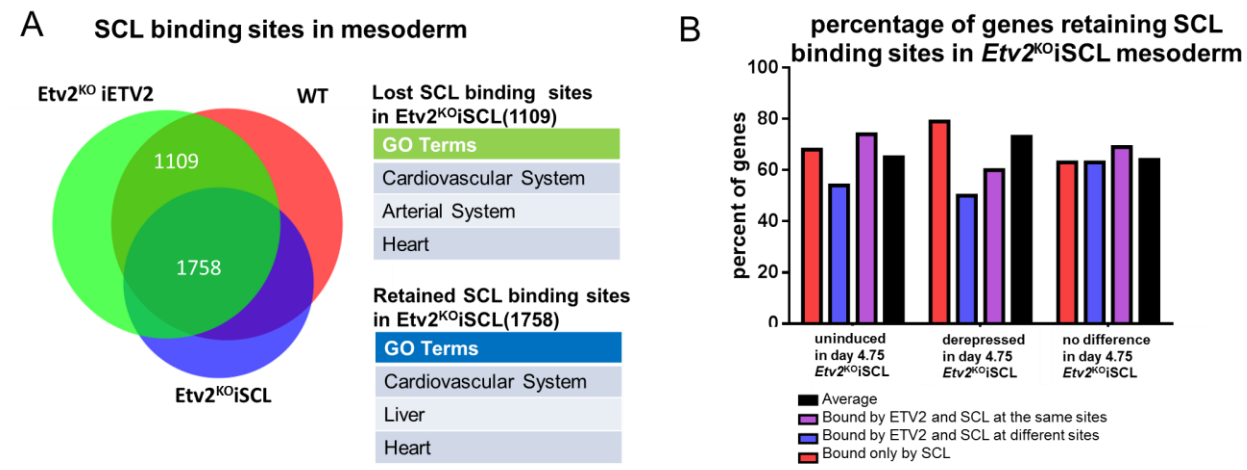

Supplementary Figure 3

Supplementary Figure S3: Rescue of SCL binding in day 4 Flk1^{+} *Etv2*^{KO}iSCL cells

A. Venn diagram shows intersection of sites bound by SCL in Flk1^{+} mesoderm of WT, *Etv2*^{KO}iSCL and *Etv2*^{KO}iETV2 EBs. 1758 sites retain SCL binding while 1109 genomic sites are lost in *Etv2*^{KO}iSCL cells. GREAT analysis of significantly enriched GO terms for SCL both lost and retained sites show enrichment of cardiovascular system and heart.

B. Bar graph shows the percentage of genes retaining SCL binding sites in *Etv2*^{KO}iSCL mesoderm in genes that were uninduced, derepressed and not differentially expressed.

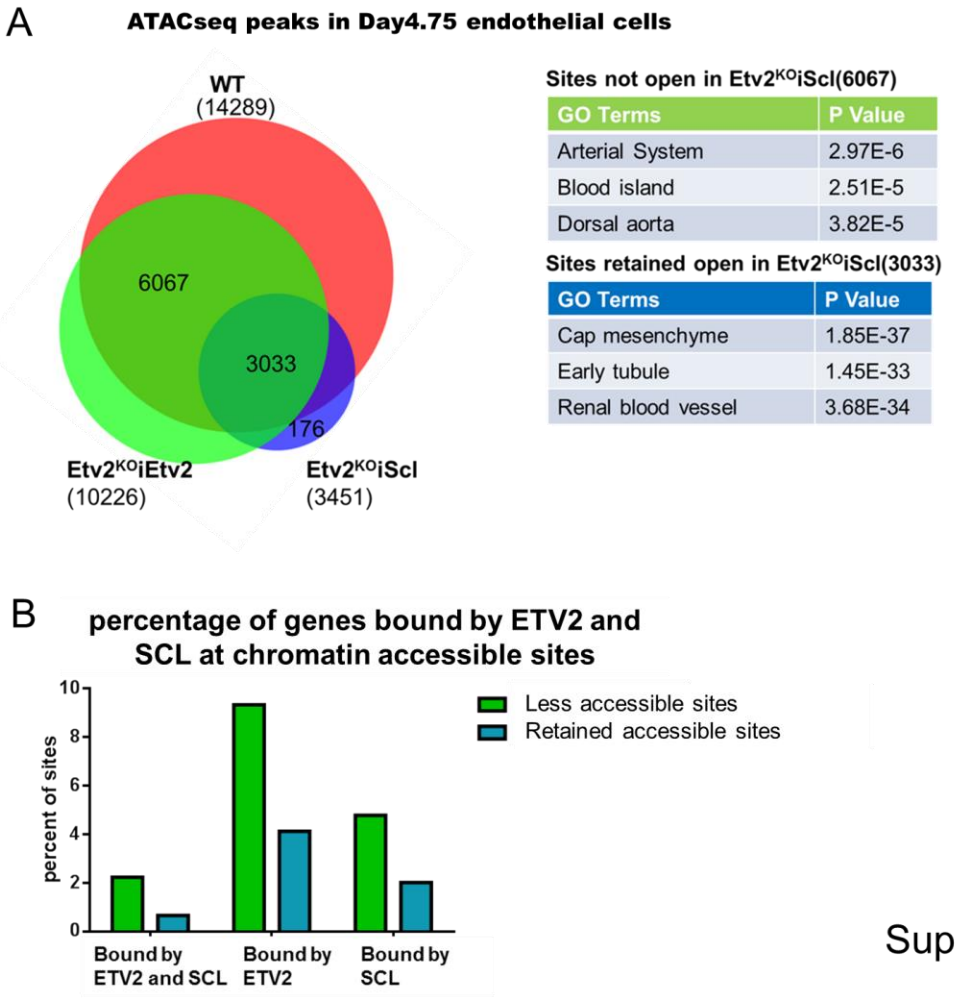

Supplementary Figure 4

Supplementary Figure S4: ATAC seq in day 4.75 WT, *Etv2*^{KO}iSCL, and *Etv2*^{KO}iETV2 endothelial cells

A. Venn diagram of intersection of peaks called from ATACseq in WT, *Etv2*^{KO}iSCL and *Etv2*^{KO}iETV2 day 4.75 endothelial cells shows 6067 and 176 sites that are more accessible or less accessible in *Etv2*^{KO}iSCL cells compared to WT and *Etv2*^{KO}iETV2 cells. GREAT analysis of significantly enriched GO terms for less accessible sites shows enrichment of arterial system.

B. Bar graph shows the percentage of sites that are more accessible or less accessible, out of sites bound by both ETV2 and SCL, bound by ETV2 only and bound by SCL only.

Table S1. Primers used in q-RT-PCR assays

Name	Forward primer	Reverse primer	
mGapdh	AGGTCGGTGTGAACGGATTTG	TGTAGACCATGTAGTTGAGGTCA	
mEtv2	CAGAGTCCAGCATTCACCAC	AGGAATTGCCACAGCTGAAT	
mTal1/Scl	GACCCGCAACTAGAGGGACAG	CGCTCCTAGCTCGATGACG	
mRunx1	TGGTAGGTAACGCAGCAATG	AAGGGAAGGAGCCAGGTATG	
mSox17	ACTTGTAGTTGGGGTGGTCC	GAACCCAGATCTGCACAACG	
mGata6	CCAGATGGCAGCAAAAAT	GCAGAGTCAGAGGCAGGAAG	
mHand1	CCTCTTCCGTCCTCTTAC	GGGGCTGCGAGTGGTCA	

Chapter 4:

Summary and Discussion

Cardiovascular and blood systems are the first functioning organ systems during development, dysfunction of which during embryogenesis or post-natal life can be life-threatening. Understanding how mesoderm gives rise to hematopoietic or cardiac stem/progenitor cells is an important step in advancing cell-based therapies for blood and heart disease.

In this work, we have:

1. Discovered that SCL acts via enhancers that have been epigenetically primed for activation in mesoderm. SCL transiently binds to cardiac enhancers and possibly represses cardiogenesis by preventing gene activation through these enhancers by cardiac regulators.
2. Shown that GATA1 and GATA2 are dispensable for hematopoietic vs. cardiac fate choice, but are essential for endothelial to hematopoietic transition.
3. Discovered that ETV2 is not directly required for cardiac fate repression in mesoderm during hemato-vascular specification, but it cooperates with SCL for timely hemato-vascular gene activation by increasing chromatin accessibility at its binding sites.

Chapter 2: SCL binds to primed enhancers in mesoderm to regulate hematopoietic and cardiac fate divergence

Although SCL was known to specify hematopoietic fate while repressing the competing cardiac fate during mesoderm diversification, how SCL exploits the epigenetic landscape and regulates gene expression for the fate choice has been unknown

In this work (Org et al., 2015), We discovered that SCL dictates mesodermal diversification by binding to enhancers that have been primed for activation with active histone modifications, H3K4me1 and H3K27ac, specifically in mesoderm (Figure 4.1). Moreover, epigenetic priming

of the enhancers is a prerequisite for SCL binding to these regulatory regions. In contrast to the key hematopoietic enhancers that retained SCL binding and active epigenetic marks throughout hematopoietic development, SCL binding and the presence of active marks at cardiac enhancers were restricted to $Flk1^{+}$ mesoderm, and gradually disappeared during hematopoietic development. These data imply that hematopoietic enhancers remain open to ensure the activation of hematopoietic genes while cardiac enhancers become inactive and SCL is no longer needed for cardiac gene repression at later stages of hematopoietic development. This provides a molecular explanation for why SCL is only required for cardiac fate repression during a temporal developmental window (Van Handel et al., 2012).

No direct correlation between SCL binding and gain of "classical" repressive epigenetic marks (H3K27me3, H3K9me3 and DNA methylation) was detected in this study. This suggests that SCL represses cardiac fate through a "passive" mechanism rather than "active" recruitment of co-repressors. We identified substantial overlap with SCL and cardiac transcription factor HAND1 and/or GATA4 mesodermal binding sites, including at least one enhancer in the genes encoding essentially all major hematopoietic and cardiac transcription factors. This supports the hypothesis that repression of an alternative fate choice may be the result of SCL preventing the activation of these genes by competing lineage specific regulators. These dually accessible enhancers that can be regulated by factors of two opposing lineages act as a platform where the fate choice is determined. Future studies will determine which cardiac factor(s) are most critical for activating these cardiac enhancers, and if they are also critical for suppressing the hematopoietic program. Other complementary hypotheses for how SCL regulates gene expression are: 1. SCL binding at enhancers may lead to or block enhancer RNA transcription which is required for gene activation or repression. 2. SCL mediates or blocks enhancer-

promoter looping for gene activation or repression. Interestingly, DNA binding domain of SCL is not required for early hematopoietic development (Kassouf et al., 2008; Kassouf et al., 2010), but whether SCL DNA binding capability is essential for cardiac repression remains elusive. These important questions require further studies to address.

We found that GATA2 can bind together with SCL to both hematopoietic and cardiac enhancers (Figure 4.1). However, hematopoietic GATA factors (1, 2 and 3) are dispensable for SCL mediated cardiac repression, and only necessary for recruiting SCL to specific binding sites to activate hematopoietic factors required for HS/PC emergence and differentiation (*Runx1, Pu.1/Sfpi1, Klf1, Gfi1b*). These data suggest that although the core SCL/GATA complex can bind to both activated and repressed genes, SCL and GATA interaction becomes critical only in gene activation. Moreover, we have shown that SCL loses its binding at regulatory sites for the key hematopoietic genes which cannot be induced in the absence of GATA1 and 2. Similar to hematopoietic GATA factors, RUNX1 can also redistribute SCL to new binding sites as development progresses from endothelium to HS/PCs (Lichtinger et al., 2012). Apart from GATA1 and GATA2, LDB1 and LMO2 are also part of the SCL complex, serving as bridging molecules and have been implicated in hematopoietic development (Schlaeger et al., 2004; Mukhopadhyay et al., 2003; Lécuyer et al., 2007; Warren et al., 1994). Whether LDB1 and/or LMO2 are required for SCL mediated cardiac repression remains to be elucidated.

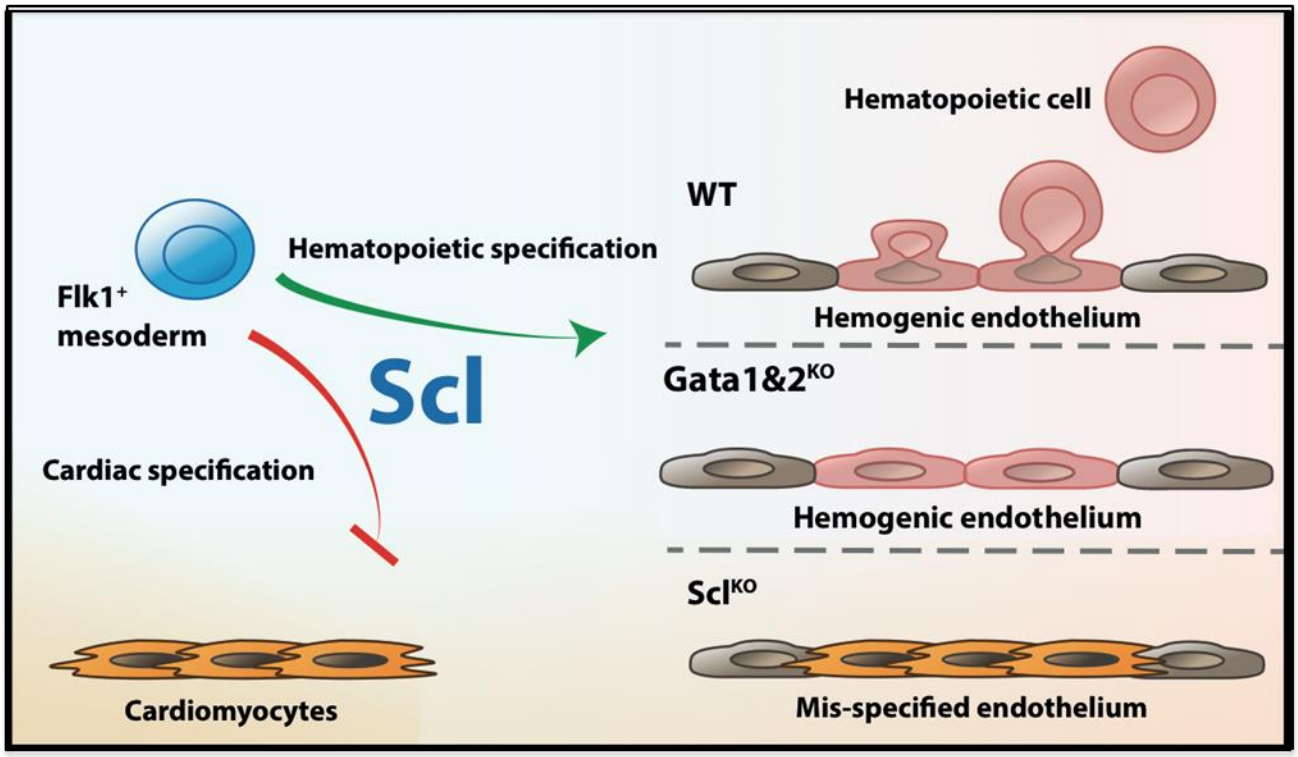

Figure 4.1 SCL dictates hematopoietic fate while repressing cardiogenesis

SCL is critical for hematopoiesis, in the absence of which ectopic cardiomyocytes are mis-specified in hemogenic endothelium. GATA1 and GATA2 are not required for hematopoietic vs. cardiac fate choice but are essential for endothelial to hematopoietic transition.

Chapter3: ETV2 cooperates with SCL for timely gene activation during hemogenic endothelium specification

Our data in Chapter 3 show that SCL can specify hemogenic endothelium, HS/PCs and repress ectopic cardiogenesis in hemogenic endothelium independent of ETV2 (Figure 4.2). Our finding that SCL overexpression is sufficient to repress ectopic cardiogenesis in ETV2 deficient endothelial cells implies that ETV2 is not directly involved in cardiac repression, but rather does so by inducing SCL. While SCL can bind directly to most cardiac genes in *Etv2* deficient mesoderm and repress their expression in day 4.75 *Etv2*^{KO}iSCL endothelial cells, some early

cardiac/mesodermal genes are repressed with delay. This suggests that other ETV2 target genes may also contribute to timely gene repression during mesoderm diversification to cardiac and hemato-vascular fates. One such candidate is miRNA130a, which was recently shown to be activated by ETV2, and regulate both cardiac repression and endothelial activation (Singh et al., 2015).

SCL induction is sufficient to rescue endothelial cells, hematopoietic progenitors, primitive erythroid cells and myeloid cells in ETV2 deficient cells (Kataoka et al., 2011; Wareing et al., 2012) (Chapter 3). However, the degree to which the molecular program is rescued during endothelial differentiation is unknown. By assessing gene expression profile at two different stages (day 4.75 and day 7) of endothelial differentiation, we identified a subset of genes, the activation of which in *Etv2*^{KO}iSCL endothelial cells is not complete until day 7, implying that ETV2 cooperates with SCL to enable timely gene activation. Genes activated with delay include known transcription factors and cell surface markers for endothelial cells, hemogenic endothelium and HSCs, such as *Ets1, Fli1, Sox17, Esam, Junb*, etc. The timely activation of these genes may ensure the proper hematovascular differentiation during development and in particular affect correct specification of hemogenic endothelium to HSCs. Moreover, while most of these genes were rescued in day 7 endothelial cells, yet, a different subset of genes enriched in cell adhesion and blood vessel development were still deregulated, such as *Itga6, Stab1*. However, only 13 genes that were not activated in day 4.75 *Etv2*^{KO}iSCL endothelial cells remained suppressed in day 7 endothelium, including *Cdh5, CD34, Sox18.* These data indicate that lack of ETV2 may affect different programs at different stages of endothelial cell specification and maturation. Although ETV2 is generally thought as a developmentally expressed vascular gene (Lee et al., 2008; Kataoka et al., 2011), recent studies suggested that

ETV2 may be expressed and function in mouse adult hematopoietic stem cells and post-natal vascular regeneration (Lee et al., 2011; Park et al., 2016). Further studies are needed to understand how ETV2 functions in HSC development and maintenance, and governs vessel formation under stress condition such as irradiation, infection or injury.

Previous studies have shown that ETV2 alone is sufficient to reprogram fibroblast to endothelial cells (Morita et al., 2015; Veldman et al., 2013). Additionally, prolonged ETV2 expression forces abnormal endothelial program in hematopoietic cells (Hayashi et al., 2012). However, the molecular mechanism underlying the strong reprogramming power of ETV2 are unknown. Our data indicate that ETV2 binding correlate with chromatin accessibility, as critical regulatory sites bound by ETV2 in hemato-vascular genes are less open in *Etv2*^{KO}iSCL endothelial cells. Moreover, ETV2 binding sites that lose chromatin accessibility are enriched in genes whose expression cannot be timely activated in *Etv2*^{KO}iSCL endothelial cells. This implies that ETV2 may prepare chromatin for SCL or other factors to regulate gene expression. The strong reprogramming power of ETV2 could be explained by its function in establishing epigenetic landscape that is exploited by other factors. Further investigation is needed to understand the mechanisms by which ETV2 increases the chromatin accessibility to facilitate timely gene activation.

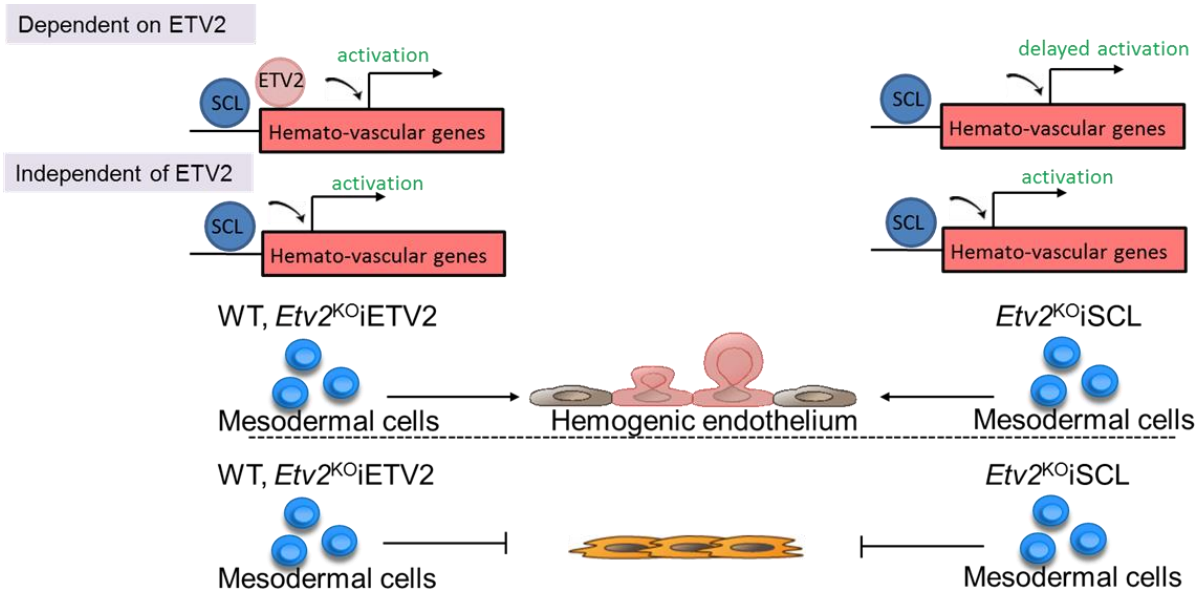

Figure 4.2 ETV2 cooperates with SCL for timely hemato-vascular gene activation in hemogenic endothelium

SCL can functionally restore the development of hemato-vascular lineages and repress ectopic cardiogenesis independent of ETV2. ETV2 cooperates with SCL for timely activation of some hemato-vascular genes by increasing chromatin accessibility at its binding sites.

Bibliography:

Van Handel B, Montel-Hagen A, Sasidharan R, Nakano H, Ferrari R, Boogerd CJ, Schredelseker J, Wang Y, Hunter S, Org T, et al., 2012. Scl represses cardiomyogenesis in prospective hemogenic endothelium and endocardium. Cell 150:590–605.

Hayashi M, Pluchinotta M, Momiyama A, Tanaka Y, Nishikawa S-I, Kataoka H. 2012. Endothelialization and altered hematopoiesis by persistent Etv2 expression in mice. Exp. Hematol. 40:738–750.e11.

Kassouf MT, Chagraoui H, Vyas P, Porcher C. 2008. Differential use of SCL/TAL-1 DNA-binding domain in developmental hematopoiesis. Blood 112:1056–67.

Kassouf MT, Hughes JR, Taylor S, McGowan SJ, Soneji S, Green AL, Vyas P, Porcher C. 2010. Genome-wide identification of TAL1's functional targets: insights into its mechanisms of action in primary erythroid cells. Genome Res. 20:1064–83.

Kataoka H, Hayashi M, Nakagawa R, Tanaka Y, Izumi N, Nishikawa S, Jakt ML, Tarui H, Nishikawa S-I. 2011. Etv2/ER71 induces vascular mesoderm from Flk1+PDGFRα+ primitive mesoderm. Blood 118:6975–86.

Lécuyer E, Larivière S, Sincennes M-C, Haman A, Lahlil R, Todorova M, Tremblay M, Wilkes BC, Hoang T. 2007. Protein stability and transcription factor complex assembly determined by the SCL-LMO2 interaction. J. Biol. Chem. 282:33649–58.

Lee D, Kim T, Lim D-S. 2011. The Er71 is an important regulator of hematopoietic stem cells in adult mice. Stem Cells 29:539–48.

Lichtinger M, Ingram R, Hannah R, Müller D, Clarke D, Assi SA, Lie-A-Ling M, Noailles L, Vijayabaskar MS, Wu M, et al., 2012. RUNX1 reshapes the epigenetic landscape at the onset of haematopoiesis. EMBO J. 31:4318–33.

Morita R, Suzuki M, Kasahara H, Shimizu N, Shichita T, Sekiya T, Kimura A, Sasaki K, Yasukawa H, Yoshimura A. 2015. ETS transcription factor ETV2 directly converts human fibroblasts into functional endothelial cells. Proc. Natl. Acad. Sci. U. S. A. 112:160–5.

Mukhopadhyay M, Teufel A, Yamashita T, Agulnick AD, Chen L, Downs KM, Schindler A, Grinberg A, Huang S-P, Dorward D, et al., 2003. Functional ablation of the mouse Ldb1 gene results in severe patterning defects during gastrulation. Development 130:495–505.

Org T, Duan D, Ferrari R, Montel-Hagen A, Van Handel B, Kerenyi MA, Sasidharan R, Rubbi L, Fujiwara Y, Pellegrini M, et al., 2015 Jan 6. Scl binds to primed enhancers in mesoderm to regulate hematopoietic and cardiac fate divergence. EMBO J.

Park C, Lee T-J, Bhang SH, Liu F, Nakamura R, Oladipupo SS, Pitha-Rowe I, Capoccia B, Choi HS, Kim TM, et al., 2016. Injury-Mediated Vascular Regeneration Requires Endothelial ER71/ETV2. Arterioscler. Thromb. Vasc. Biol. 36:86–96.

Schlaeger TM, Schuh A, Flitter S, Fisher A, Mikkola H, Orkin SH, Vyas P, Porcher C. 2004. Decoding hematopoietic specificity in the helix-loop-helix domain of the transcription factor SCL/Tal-1. Mol. Cell. Biol. 24:7491–502.

Singh BN, Kawakami Y, Akiyama R, Rasmussen TL, Garry MG, Gong W, Das S, Shi X, Koyano-Nakagawa N, Garry DJ. 2015. The Etv2-miR-130a Network Regulates Mesodermal Specification. Cell Rep. 13:915–23.

Veldman MB, Zhao C, Gomez GA, Lindgren AG, Huang H, Yang H, Yao S, Martin BL, Kimelman D, Lin S. 2013. Transdifferentiation of fast skeletal muscle into functional endothelium in vivo by transcription factor Etv2. PLoS Biol. 11:e1001590.

Wareing S, Mazan A, Pearson S, Göttgens B, Lacaud G, Kouskoff V. 2012. The Flk1-cre Mediated Deletion of ETV2 Defines Its Narrow Temporal Requirement During Embryonic Hematopoietic Development. Stem Cells:1521–1531.

Warren AJ, Colledge WH, Carlton MB, Evans MJ, Smith AJ, Rabbitts TH. 1994. The oncogenic cysteine-rich LIM domain protein rbtn2 is essential for erythroid development. Cell 78:45–57.

Appendix:

Endothelial cells provide an instructive niche for the differentiation and functional polarization of M2-like macrophages

2012 120: 3152-3162
doi:10.1182/blood-2012-04-422758 originally published online August 23, 2012

Endothelial cells provide an instructive niche for the differentiation and functional polarization of M2-like macrophages

Huanhuan He, Jingying Xu, Carmen M. Warren, Dan Duan, Xinmin Li, Lily Wu and M. Luisa Iruela-Arispe

Blood (print ISSN 0006-4971, online ISSN 1528-0020), is published weekly by the American Society of Hematology, 2021 L St, NW, Suite 900, Washington DC 20036.

Endothelial cells provide an instructive niche for the differentiation and functional polarization of M2-like macrophages

Huanhuan He,[1] Jingying Xu,[2] Carmen M. Warren,[3] Dan Duan,[3] Xinmin Li,[4] Lily Wu,[2,5] and M. Luisa Iruela-Arispe[3,5,6]

Departments of [1]Human Genetics, [2]Medical and Molecular Pharmacology, [3]Molecular, Cell and Developmental Biology, and [4]Pathology and Laboratory Medicine; [5]Jonsson Comprehensive Cancer Center; and [6]Molecular Biology Institute, University of California, Los Angeles, Los Angeles, CA

Endothelial cells and macrophages are known to engage in tight and specific interactions that contribute to the modulation of vascular function. Here we show that adult endothelial cells provide critical signals for the selective growth and differentiation of macrophages from several hematopoietic progenitors. The process features the formation of well-organized colonies that exhibit progressive differentiation from the center to the periphery and toward an M2-like phenotype, characterized by enhanced expression of Tie2 and CD206/Mrc1. These colonies are long-lived depending on the contact with the endothelium; removal of the endothelial monolayer results in rapid colony dissolution. We further found that Csf1 produced by the endothelium is critical for the expansion of the macrophage colonies and that blockade of Csf1 receptor impairs colony growth. Functional analyses indicate that these macrophages are capable of accelerating angiogenesis, promoting tumor growth, and effectively engaging in tight associations with endothelial cells in vivo. These findings uncover a critical role of endothelial cells in the induction of macrophage differentiation and their ability to promote further polarization toward a proangiogenic phenotype. This work also highlights some of the molecules underlying the M2-like differentiation, a process that is relevant to the progression of both developmental and pathologic angiogenesis. (*Blood.* 2012;120(15):3152-3162)

Introduction

The link between the hematopoietic and the endothelial cell lineages is rooted early in development. In fact, definitive hematopoietic stem cells (HSCs) first emerge in the embryo from a specialized endothelial intermediate that holds hemogenic capacity.[1-4] Although the process of hematopoietic cells (HCs) budding from hemogenic endothelium is no longer present in the adult, the interactions between HCs and the endothelium continue to be critical for the trafficking and homing of HCs, as well as for activation and recruitment of inflammatory cells to specific tissue sites.[5]

More recently, sinusoidal endothelial cells were shown to be essential for the self-renewal capacity of hematopoietic stem/progenitor cells (HSPCs) through the production of specific angiocrine factors.[6,7] Intriguingly, bone marrow sinusoidal endothelial cells can also constitute a platform for the differentiation of HSPCs. This dual role of endothelial cells has been best exemplified by findings communicated by Kobayashi and colleagues, where the coculture of genetically modified human umbilical vein endothelial cells (HUVECs) with HSPCs supported both self-renewal and lineage-specific differentiation of HSPCs.[8] Notably, the mechanisms by which endothelial cells mediate regeneration or differentiation of HCs depend largely on organ-specific determinants. Overall, mounting evidence supports the concept that the crosstalk between endothelial cells and HCs impacts the differentiation and stem cell properties of hematopoietic progenitors.

The consequences of endothelial-hematopoietic cell interactions are not unidirectional toward the latter; endothelial cells have also shown to benefit. In fact, macrophages have been demonstrated to associate tightly with capillaries and aid in the progression of angiogenesis. Specifically, during development, tissue-resident macrophages facilitate vascular morphogenesis by bridging the neighboring tip cells and mediating anastomosis of adjacent capillaries.[9-11] In pathologic situations, such as carcinogenesis, Tie2-expressing macrophages (TEMs) are actively involved in promoting tumor neovascularization. Selective depletion of TEMs significantly impairs angiogenesis and tumor growth.[12,13]

To further dissect the impact of the crosstalk between adult endothelial cells and HCs, we established a long-term coculture system. Here we show that adult endothelial cells of diverse origins provide critical niches for the selective growth and differentiation of macrophages from hematopoietic progenitor cells. This process involves the formation of colonies that exhibit progressive differentiation toward an M2-like phenotype. The formation and maintenance of these colonies require direct contact with endothelial cells. Overall, the findings provide novel insights into the broad impact of the endothelium on HCs and further define the interactions that are critical for angiogenesis in both physiologic and pathologic settings.

Methods

Mice

DsRed mice, B6.Cg-Tg(CAG-DsRed*MST)1Nagy/J, were purchased from The Jackson Laboratory. Immortalized mouse endothelial cells (IMECs) were isolated from Immortomice, CBA;B10-Tg(H2K^{b}-tsA58)6Kio/Crl, that were purchased from Charles River. Animal protocols were conducted

Submitted April 11, 2012; accepted August 8, 2012. Prepublished online as *Blood* First Edition paper, August 23, 2012; DOI 10.1182/blood-2012-04-422758.

The online version of this article contains a data supplement.

The publication costs of this article were defrayed in part by page charge payment. Therefore, and solely to indicate this fact, this article is hereby marked "advertisement" in accordance with 18 USC section 1734.

in accordance with University of California, Los Angeles (UCLA) Department of Laboratory Animal Medicine's Animal Research Committee guidelines.

Isolation and purification of IMECs

Mice were perfused with PBS, followed by 500 μg/mL collagenase (c0130; Sigma-Aldrich). Liver, lung, and adipose tissue were homogenized and incubated with collagenase at room temperature for 30 minutes. Samples were mixed with MCDB-131 medium (VEC Tech) containing 20% FBS (FB-11; Omega Sci), centrifuged at 200 rcf for 5 minutes, and then resuspended in MCDB-131 medium with 20% FBS. The suspension was passed through a 40-μm filter (352340; BD Biosciences), and plated onto gelatin-coated culture dishes. After 2 hours, cells were washed extensively to remove nonadherent cells, then cultured at 33°C (for induction of the oncogene). For purification, confluent endothelial cells were washed with cold DMEM (10-017-CV; Cellgro) twice then incubated with rat anti–mouse CD31 (553370; BD Biosciences) in DMEM for 15 minutes under agitation at room temperature. Cells were washed twice with cold DMEM and incubated with anti–rat-IgG magnetic beads (Invitrogen) for 15 minutes at room temperature, followed by washes, trypsinization, and magnetic purification. After several washes, purified endothelial cells were resuspended in DMEM with 10% FBS and 20 U/mL IFNgamma and cultured at 33°C. Characterization of the IMECs confirmed the expression of Vegfr2 and VE-Cadherin and their functional activation by Vegfa (supplemental Figure 1A, available on the *Blood* Web site; see the Supplemental Materials link at the top of the online article). Purity of the IMECs was evaluated by the expression of CD31 via flow cytometry (supplemental Figure 1B).

Isolation of bone marrow cells

Bone marrow cells were isolated from DsRed mice. Briefly, tibia and femur were obtained then bone marrow was flushed using DPBS (21-031-CV; Cellgro). Red blood cells were lysed. Cell suspension was passed through a 40-μm filter (BD Biosciences, 352340) and seeded on the top of the IMEC monolayer. Cells were cultured in HSC media (α-MEM; 12 000-022; Gibco) with 20% fetal bovine serum (SH30070.03E; Hyclone), penicillin-streptomycin (100 U/mL; Cellgro), β-mercaptoethanol (55μM; Gibco), murine SCF (40 ng/mL), Flt3-L (20 ng/mL), IL-6 (10 ng/mL), IL-3 (10 ng/mL), thrombopoietin (TPO; 10 ng/mL), and vascular endothelial growth factor A (VEGFA; 10 ng/mL). All cytokines were purchased from PeproTech. Culture media were changed weekly. Cultures were observed under Axiovert 200M microscope (Carl Zeiss) for phase contrast and fluorescent imaging twice every week at room temperature.

Colony cell harvesting

Cocultures of indicated days were washed twice with DPBS (21-031-CV; Cellgro) then incubated with Versene for 5 minutes. IMECs were separated from colonies by incubating with Versene at 37°C until they detached from the plate as a thin layer. Attached cells were rinsed with DPBS and collected by cell lifter. The purity of colony cells being $F4/80^+$ and $Mac1^+$ was evaluated by flow cytometry, as shown in Figure 1D.

May-Grünwald-Giemsa staining

Cytospin slides of bone marrow and colony cells were prepared by Shandon Cytospin 4 cytocentrifuge (Thermo Electric) following standard procedures. To identify nuclear and cytoplasmic characteristics of each cell, cytospin specimens were stained with 100% May-Grünwald solution (Merck) for 5 minutes, followed by phosphate buffer wash, and then stained with 5% Giemsa solution (Merck) in deionized water for 15 minutes. All staining procedures were performed at room temperature. Staining was analyzed with Olympus BX40 microscope (Olympus).

Flow cytometry and cell sorting

Colony cells were isolated, counted, and incubated with fluorophore-conjugated antibodies at 4°C for 30 minutes, then resuspended in FACS buffer [(HBSS; Cellgro, 21-022-CV) with 2% FBS (Omega Sci; FB-11) and 10mM HEPES (Gibco; 15 630)]. Antibodies used were APC-eFluor780-F4/80 (eBio; 47-4801), eFluor450-Ly6C (eBio; 48-5932), AlexFluor700-MHCII (eBio; 56-5321), APC-Tie2 (Biolegend; 124009), PE-Gr-1 (eBio; 12-5931), PE-Cy7-Sca1 (eBio; 25-5981), FITC-cKit (eBio; 11-1171), APC-lineage cocktail (BD Biosciences; 51-9003632), APC-CD31 (eBio, 17-0311), FITC–Mac-1 (eBio; 11-0112), APC-CD206 (Biolegend; 141707), APC-CD36 (eBio; 17-0361), FITC-iNOS (BD; 610330), and PerCP-eFluor710-CD115 (eBio; 46-1152). DAPI (Invitrogen; D1306) was used as cell viability dye. LSRII Analytic Flow Cytometer (BD Biosciences) was used for acquisition. For progenitor sorting, DsRed bone marrow cells were isolated and immunofluorescently labeled with indicated markers. FACSAriaII High-Speed Cell Sorter (BD Biosciences) was used. Data were analyzed with FlowJo Version 9.5 (TreeStar). Triplicates were analyzed for quantification.

Immunofluorescent staining

For cocultured cells, colony cells were fixed with 2% PFA after removal of the IMEC layer. Immunofluorescent labeling was performed using standard procedures. Antibodies used were anti–mouse Csf1r (eBio; 14-1152), anti–mouse F4/80 (Serotech; MCA497R), anti–mouse CD206 (Santa Cruz Biotechnology; sc-34577), and anti–mouse CD31 (BD Biosciences; 553370). DAPI (Invitrogen; D1306) was used to stain nuclei. Fluorescent microscopy was performed using confocal microscope, LSM710 (Carl Zeiss) at room temperature.

BrdU assay

BrdU (Sigma-Aldrich; B5002) was added to the coculture for 6 hours before cells were fixed with Carnoys fixative. DNA was then denatured with 2M HCl (Sigma-Aldrich) and neutralized with borate buffer (pH 8.5; Sigma-Aldrich). Immunofluorescent labeling was performed using standard procedures with anti–mouse BrdU (Pierce, MA3-071) and anti–mouse F4/80 (Serotech; MCA497R) antibodies. DAPI (Invitrogen; D1306) was used to stain nuclei. Fluorescent microscopy was performed using confocal microscope, LSM710 (Carl Zeiss) at room temperature.

DiI-Ac-LDL assay

Cells were labeled with 10 μg/mL DiI-Ac-LDL (Invitrogen; L3484) for 4 hours at 37°C, then washed with PBS, trypsinized and passed through a 40-μm filter (BD; 352340) to produce single-cell suspension. LSRII Analytic Flow Cytometer (BD Biosciences) was used. APC-CD31 (eBio; 17-0311) was used to exclude IMEC contamination.

Ultrastructural analysis

For transmission electronic microscopic (TEM) analysis, cells were cultured on Thermanox Coverslips (Ted Pella; 26028) and fixed in Karnovsky glutaraldehyde. Ultrathin sections were prepared by UCLA Electron Microscopy Core Facility and examined under transmission electron microscope (JEOL 100CX) at room temperature.

Transwell assay

All transwell assays were performed with HSC media (see "Isolation of bone marrow cells"). IMECs were seeded in the cell culture inserts (BD Biosciences; 353090) and HCs were seeded into the 6-well plate. For direct contact transwell experiment, IMECs were seeded with inserts (BD Biosciences; 353090 and 353091) upside-down, incubated with medium for 2 hours, and then place into a 6-well plate as regular cultures. Cultures were observed under Axiovert 200M microscope (Carl Zeiss) for phase contrast and fluorescent imaging at room temperature.

Real-time PCR

Total RNA was extracted using RNeasy Kit (QIAGEN; 74106). RNA was reverse transcribed to cDNA using SuperScript First-strand Synthesis System (Invitrogen; 18080-051) according to the manufacturer's instructions. Quantitative real-time PCR was performed using SYBR Green system (QIAGEN; 330509) and detected on Opticon2 PCR machine (MJ

Research) by 3-stage program parameters provided by the manufacturer. Each sample was tested in triplicates and samples obtained from 2 independent experiments were used. Analysis of relative gene expression data used the $2^{-\Delta\Delta CT}$ method. Primers used are provided in supplemental Table 1.

GW2580 treatment and annexin V/PI staining

GW2580 (a gift from Dr Lily Wu, UCLA) was dissolved in dimethyl sulfoxide and added to the coculture from day 1 at the concentration of 2μM. For cell-cycle analysis, GW2580 treated colony cells and control were fixed with 75% ethanol (Gold Shield Chem) for 1 hour at 4°C. Cells were then washed twice with PBS. Propidium iodide staining solution (0.5 mL; BD Biosciences, 556463) and 0.1 mg/mL RNase A (Sigma-Aldrich; R4875) were added to the cell pellet and incubated for 1 hour at room temperature. Histogram of PE (for PI detection) was obtained using LSRII Analytic Flow Cytometer (BD Biosciences) and analyzed with FlowJo Version 9.5 (TreeStar). For annexin V/PI staining, colony cells were washed twice with cold PBS and resuspended in FACS Buffer (see "Flow cytometry and cell sorting") at a concentration of 1×10^6 cells/mL. The solution (100 μL) was added with FITC–annexin V (BD Biosciences; 556419) and PI (BD Biosciences; 556463), and then incubated for 30 minutes at room temperature in the dark and washed before flow cytometric analysis.

Microarray hybridization and data analysis

Total RNA was extracted using RNeasy Mini Kit (Invitrogen). Integrity of the RNA was evaluated using an Agilent 2100 Bioanalyzer (Agilent Technologies) and purity/concentration was determined by NanoDrop 8000 Spectrophotometer (Thermo Scientific). Agilent mouse 8×60 k array hybridizations were performed by UCLA Clinical Microarray Core following standard Agilent Expression Analysis protocol (GSE39660). The acquisition of array image was undertaken by Agilent Scan Control and Feature Extraction 10.7 software. Raw data were analyzed using Partek genomics Suite 6.4. Data were normalized by RMA algorithm. Thresholds for selecting significant genes were set at $>= 2$-fold and FDR corrected $P < .05$. Genes met both criteria were considered as significant changes.

Tumor growth and angiogenesis model

RM1 cells (1×10^5) alone or with colony cells (2×10^4) were injected subcutaneously on the flank of C57BL/6 mice. Tumor size was determined by caliper measurements when tumors were palpable from day 6. Tumor volume was calculated by a rational ellipse formula ($m1 \times m1 \times m2 \times 0.5236$, where m1 is the shorter axis and m2 is the longer axis). Thin sections (~ 4 μm) were prepared from PFA-fixed paraffin-embedded tumor tissues. To quantify vessels, 3 sections from 2 to 3 tumors of each group were immunostained for CD31 (BD Biosciences; 553370) and scanned by a confocal microscope (Carl Zeiss; LSM710) at room temperature. Three high-power fields from each slide were examined using ImageJ Version 1.46d software (National Institutes of Health; NIH). In all studies, values were expressed as mean ± SEM.

Matrigel assay

Cocultured colony cells (5×10^4) and IMECs (1×10^4) were resuspended in DMEM (Cellgro, 10-017-CV) and mixed with Matrigel (BD Biosciences; 354248) at the ratio of 1:1 by volume. The mixture was injected subcutaneously on the flank of nude mice. As control, DMEM was mixed with Matrigel and injected on the other side of the flank. Animals were killed at day 7 after injection and Matrigel implants were dissected out. The implants were fixed and processed as regular histologic tissue. Matrigel sections were immunostained for anti–MECA-32 (Santa Cruz Biotechnology; sc-19603) and anti-DsRed (MBL; PM005) antibodies and scanned by a confocal microscope (Carl Zeiss; LSM710) at room temperature. 3D rendering of z-stack images were acquired by Volocity Version 5.5 software (Improvision).

Results

Endothelial cells instruct the differentiation of macrophages

To determine the effect of heterotypic endothelial-hematopoietic cell interactions, we established an in vitro coculture system where these 2 types of cells could engage in direct contact and the impact could be investigated over time at both cellular and molecular level. Liver sinusoidal endothelial cells (IMECs) were used to support the growth of HCs isolated from the bone marrow of DsRed mice (Figure 1A). Upon coculture, a subset of HCs transmigrated across endothelium, took residence under the endothelial monolayer, and formed colonies that were visible under the fluorescent microscope 5 days after coculture. The number and size of the colonies expanded quickly (Figure 1B). Cells comprising the colonies were evaluated by cytospin. These cells were morphologically homogeneous compared with the original mixture of the bone marrow cells (Figure 1C). Further characterization revealed that the large majority of these cells were positive for F4/80 and Mac-1 (Figure 1D), markers for the macrophage lineage. Cells within the colonies were engaged in active proliferation, as shown by BrdU incorporation analysis (Figure 1E). Colony cells were also able to endocytose Dil-Ac-LDL providing further support to the macrophage identity of these cells (Figure 1F). Adult endothelial cells isolated from lung and adipose tissue were also able to induce and support macrophage differentiation (supplemental Figure 1C-D). Emergence of colonies did not occur when bone marrow was cultured alone or in the presence of OP9 stromal cells (supplemental Figure 2A-B).

Endothelial cell contact is essential for the emergence and maintenance of macrophage colonies

Given the intimate association between the endothelium and the colonies (Figure 2A-B), we next investigated whether the emergence and maintenance of the colonies were dependent on the physical contact with endothelium. Ultrastructural analysis confirmed the physical association between IMECs and colony cells (Figure 2C). Careful removal (peeling) of the endothelial monolayer from cultures containing colonies resulted in quick disaggregation of underlying colonies within 24 hours (Figure 2D). Furthermore, cocultures using transwells, which prevent cell-cell contact but enable exchange of secreted factors, did not support the growth of colonies, revealing that colony formation required direct contact with the endothelium (Figure 2E). Through modification of the transwell assay whereby minimal contact with the endothelium was enabled, we further determined that contact with endothelial cell processes was sufficient to elicit organization of colonies (supplemental Figure 2C). Several cell adhesion molecules were significantly expressed in both cell types. We found that VCAM1 and VE-Cadherin were present in colony macrophages with low but detectable levels of ICAM1 (Figure 2F, supplemental Figure 2D). Interestingly, contact with bone marrow cells induced an up-regulation of ICAM1 and VE-Cadherin in the endothelial monolayer (Figure 2G).

CSF1 signaling is critical for the expansion but not for the initiation of macrophage colonies

Macrophage colony-stimulating factor (MCSF; or CSF1) is a chemokine shown to stimulate proliferation, differentiation, and survival of macrophages.[14] To determine whether it plays a role in

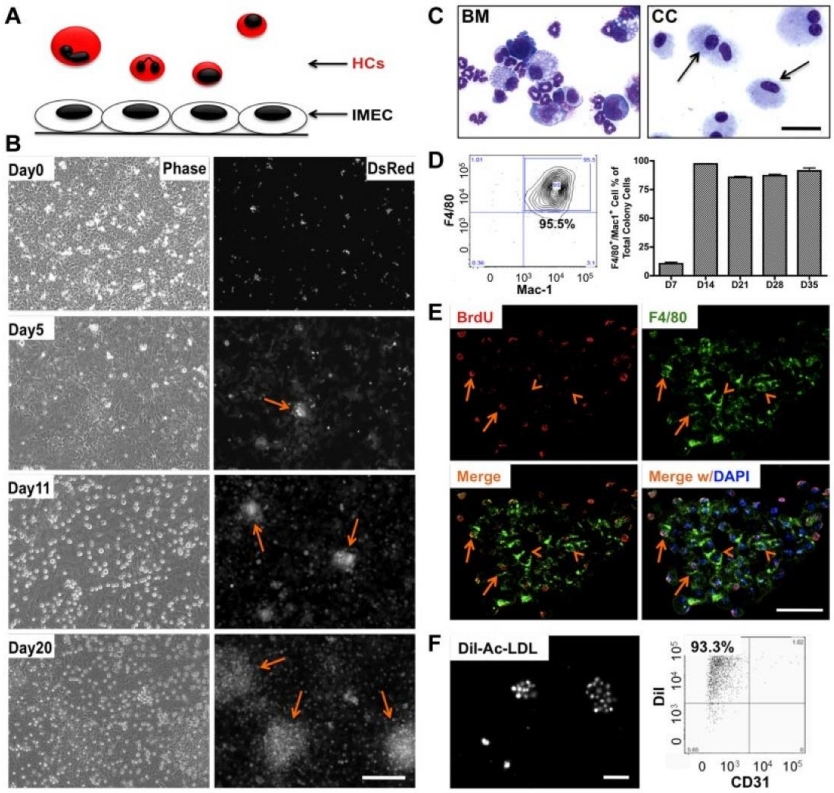

Figure 1. Endothelial cells induce differentiation and expansion of macrophages in vitro. (A) Schematic representation of the coculture system that includes murine hematopoietic cells (HCs) and immortalized mouse endothelial cells (IMECs). All HCs express DsRed fluorescent protein. (B) Phase contrast (left) and fluorescent (right) micrographs depict the formation of DsRed$^+$ colonies (arrow) during coculture. Note that the colonies were phase-dim or invisible under phase view. Scale bar, 200 μm. (C) Photomicrographs of isolated bone marrow (BM) cells and cells from day 27 colonies (CC, arrow) after May-Grünwald-Giemsa staining. Scale bar, 50 μm. (D) FACS profile (left) indicates that the large majority of cells in the colonies were F4/80$^+$/Mac-1$^+$ (n = 3). (E) Fluorescent micrographs of bromodeoxyuridine (BrdU) staining indicating active proliferation within the colony. Day 10 colonies were pulse-labeled with BrdU for 8 hours and then costained for anti-BrdU (red) and anti-F4/80 (green) antibodies. Arrow, cells positive for both F4/80 and BrdU. Arrowhead indicates F4/80$^+$ cells not stained for BrdU. DAPI indicates staining for nucleus (blue). Scale bar, 50 μm. (F) Colony cells uptake DiI-ac-LDL. Cells were incubated with 10 μg/mL DiI-ac-LDL for 4 hours, followed by fluorescent microscopy (left). (Right) FACS profile shows the majority colony cells take up DiI-ac-LDL. CD31, to exclude possible IMEC contamination. Scale bar, 200 μm.

endothelial-induced colony formation, we first determined transcriptional levels of both secreted and membrane-bound forms of *Csf1* in cocultured IMECs. Interestingly, membrane-bound *Csf1*, the less dominant isoform, was prevalent in IMECs (Figure 3A). Transcripts for the *Csf1* receptor (*Csf1r*) were highly expressed by colony macrophages with the peak at day 21, time of maximal expansion of the colonies (Figure 3B). Expression of Csf1r in the macrophage colonies was also confirmed by immunostaining (Figure 3C) and flow cytometry (supplemental Figure 3A-B).

To further ascertain the functional contribution of CSF1 in the formation and expansion of the colonies, we applied a CSF1R exclusive inhibitor, GW2580, to the cocultures. GW2580 is a selective small molecule kinase inhibitor that was shown to completely prevent CSF1R-dependent growth of macrophages in vitro and in vivo at therapeutically relevant doses.[15] Exposure to GW2580 (2μM) from the onset of the coculture drastically impaired colony formation (Figure 3D-E). Small colonies were present in GW2580–treated culture, but these never expanded. Evaluation with propidium iodide indicated an increase in the early apoptotic and dead cells on treatment (Figure 3F-G) and an alteration in cell cycle (supplemental Figure 3C). Together, these findings demonstrate that the CSF1 pathway is certainly involved in the expansion and the survival of the colonies. However, blockage of CSF1 pathway does not alter the initiation of the macrophage differentiation program, as the percentage of F4/80$^+$ cells was unaltered on the exposure to GW2580 albeit the colony size was much smaller (data not shown).

Macrophages in colonies are polarized toward the M2 subtype and express high levels of VEGFA

Th1 (eg, LPS and IFN-γ) and Th2 (eg, IL-4, IL-13, and IL-10) cytokines can differentially polarize macrophages to M1 (or classically activated) or M2 (or alternatively activated) phenotype, respectively. M1-polarized macrophages produce high levels of IL-1β, IL-12, IL-23, TNFα, and CXCL10, and are markedly

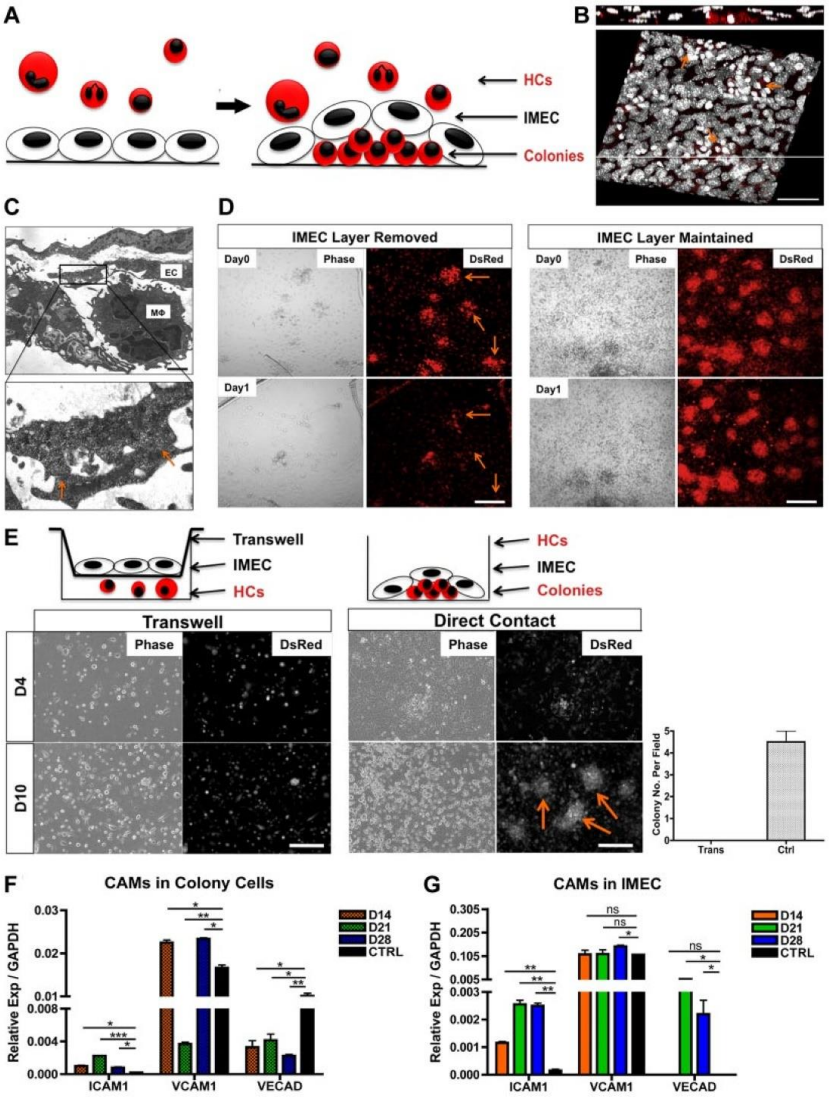

Figure 2. Direct contact with the endothelium is required for the formation and maintenance of macrophage colonies. (A) Schematic representation of the colonies as they take residence under the endothelial monolayer. (B) Confocal 3D reconstruction of the DsRed colonies (arrows) growing underneath the IMEC layer. Composite x-y sections and a single z-section are shown. Scale bar, 50 μm. (C) Ultrastructural analysis of cells cocultured for 28 days by transmission electron microscopy. (Bottom) Magnified micrograph reveals direct contact (arrows) between the 2 cell types. EC indicates endothelial cell; and MΦ, macrophage-like cell. Scale bar, 4 μm. (D) Colonies disaggregate (arrow) after the removal of IMEC layer for 1 day, depicted by phase contrast and fluorescent micrographs (left). Colonies with IMECs were maintained (right). Scale bar, 200 μm. (E) Colonies failed to form via transwells. (Left) Cocultures of HCs and IMECs separated by the transwell (0.4-μm pore size). (Middle) Cocultures through direct contact. Arrows indicate colonies. (Right) Quantification of colony number at day 10 of coculture (n = 3). Scale bar, 200 μm. (F) Real time PCR quantification of ICAM1, VCAM1, and VE-Cadherin in colonies. Ctrl indicates bone marrow–derived macrophages with 5 ng/mL IL-4 stimulated for 24 hours (n = 6). (G) Corresponding cell adhesion molecules (CAMs) expression in IMECs. Ctrl indicates IMECs in the absence of coculture (n = 6; $*P < .05$; $**P < .01$; $***P < .001$; unpaired Student *t* test).

proinflammatory and angiostatic, whereas M2 macrophages secrete IL-10, CCL17, and CCL22, which are known to promote tissue repair and angiogenesis.[16-18]

To determine whether the polarization of macrophages occurs in the colonies, we evaluated levels of MHCII, a phenotypic marker for inflammatory/M1–polarized macrophages. Flow cytometric overlay graphs at progressive time points of cocultures showed a continuous reduction of MHCII expression on colony macrophages (Figure 4A) indicating that the colony macrophages were not M1-polarized.

To evaluate M2-associated markers, we first determined Tie2 levels. Tie2, a tyrosine kinase receptor for angiopoietin, is also

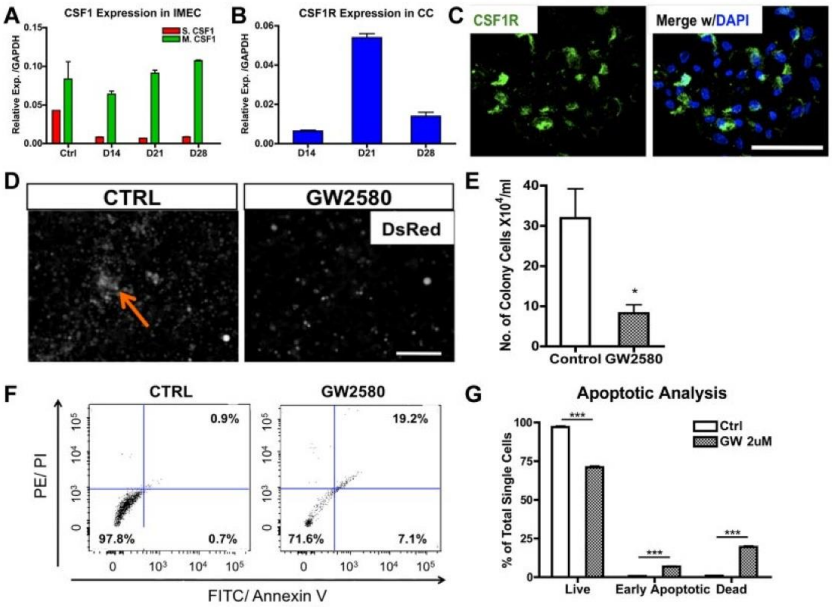

Figure 3. CSF1 is essential for the expansion of macrophage colonies. (A) Membrane-bound *Csf1* but not secreted *Csf1* is prevalently expressed in IMECs by real-time PCR analysis. Ctrl, IMECs in the absence of coculture (n = 6). (B) *Csf1* receptor (*Csf1r*) transcripts are highly expressed in colony cells (n = 6). (C) Immunolocalization of Csf1r (green) on a representative colony from day 10 coculture. DAPI indicates staining for nucleus (blue). Scale bar, 50 μm. (D) GW2580, a CSF1R inhibitor, significantly impairs colony emergence and growth. Coculture was treated with GW2580 (2μM) for 7 days. Ctrl indicates coculture exposed to vehicle. Arrow indicates a colony. Scale bar, 200 μm. (E) Quantification of colony cell number at day 14 of coculture in the presence or absence of GW2580 treatment (n = 3). (F) Representative dot plots showing increased apoptotic activity on GW2580 treatment. Colony cells from day 14 coculture treated with GW2580 (2μM) or vehicle were stained for propidium iodide (PI) and annexin V. (G) Apoptotic analysis of colony cells on GW2580 or vehicle treatment (n = 3; $^*P < .05$; $^{***}P < .001$; unpaired Student *t* test).

considered to be a marker associated with M2-like, proangiogenic macrophages in tumors.[12,19] Interestingly, the expression of Tie2 rose significantly in colony macrophages over time (Figure 4B), suggesting that the endothelial-induced macrophages were polarized toward the M2 fate.

Additional transcripts associated with M1 and M2 polarization were measured. We consistently found that colony macrophages expressed high levels of M2 markers, *Arg1, CD206/Mrc1*, and *CD36*. In contrast, levels for *IL-12, IL-1β*, and *Tnfα* (M1 markers) were not detectable in these macrophages (Figure 4C). Additional phenotypic markers for M1 and M2-associated markers were examined by flow cytometry (supplemental Figure 4A-C). Combined, the data indicate that the colony macrophages were M2 polarized, which is also confirmed by microarray data (GSE39660; supplemental Figure 5A-D). We were also able to detect M2–like macrophages in the supernatant of the cocultures (supplemental Figure 4D-E). We further found that the macrophages expressed high levels of *Vegfa* (Figure 4D), which may explain why the endothelial monolayer is able to be retained under the coculture conditions for longer periods of time (up to 2 months), compared with in the absence of the coculture (1-2 weeks).

We further confirmed the M2-like polarization of macrophages by immunofluorescence and noticed a hierarchical organization within the colonies. Expression of the pan-macrophage marker F4/80 was concentrated in the center of the colonies; whereas levels of CD206/Mrc1 were gradually increased toward the periphery of the colony (Figure 4E). This indicates that maturation toward an M2-skewed phenotype occurred as the cells migrated toward the edge of the colony.

Endothelial cells induce M2-like macrophage differentiation regardless of the developmental stage of the initiating myeloid progenitor

To identify the progenitor cell that could induce the generation of the M2-like macrophages on contact with the endothelium, we sorted HSPCs, G/CMPs (granulocyte-macrophage and common myeloid progenitors), and MEPs (megakaryocyte-erythroid progenitors) from whole bone marrow and proceeded to test their ability to generate colonies on coculture with endothelial cells. These 3 populations were sorted based on lineage markers, c-Kit, Sca1, and CD34 expression (supplemental Figure 6A). We found that all of the progenitor populations were able to generate colonies on coculture, but at different times. Colonies from MEP culture emerged first at day 7, followed by G/CMP at day 14. Cocultures with HSPCs were the last to show emergence of colonies, at day 25 (Figure 5A).

Although unsorted bone marrow gave rise to the highest number of colonies (supplemental Figure 6D), normalization to the original number of seeded cells revealed that HSPCs had the greatest fold of expansion (Figure 5B). The findings imply that on contact with endothelium, HSPCs were able to survive, self-renew, and further differentiate into the M2-like subtype more effectively than other progenitors. These results also showed that the adult endothelium is able to directly program the differentiation of macrophages from any hematopoietic progenitors. Similar to the effect of Csf1r inhibition on whole bone marrow, GW2580 also impaired the expansion of colony cells from all progenitors (data not shown).

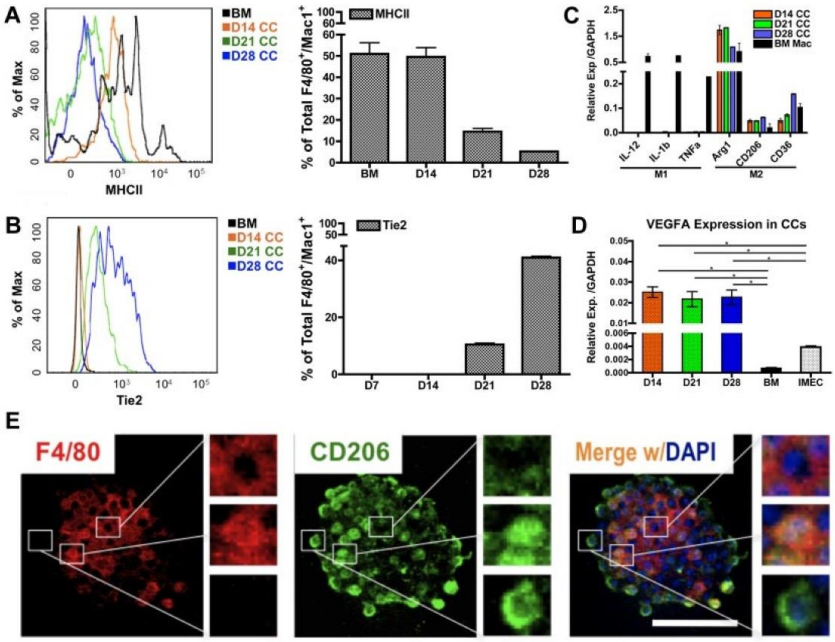

Figure 4. Endothelial cells impart M2 polarity on colony macrophages. (A) MHCII expression in colony cells is reduced on coculture, as determined by FACS overlay graph (left) and quantification (right; n = 3). (B) Tie2 expression in colony cells is gradually increased over time as shown by FACS overlay graph (left) and quantification (right; n = 3). (C) Colony cells exhibit M2 macrophage markers but not M1 markers, as detected by real-time PCR analysis. Ctrl indicates bone marrow–derived macrophages stimulated with 50 ng/mL LPS (for M1 control) or with 5 ng/mL IL-4 (for M2 control) for 24 hours (n = 6). (D) Colony cells express high level of *Vegfa* transcripts. (E) Immunolocalization of F4/80 (pan macrophage marker, red) and CD206/Mrc1 (M2 macrophage marker, green) in a macrophage colony. Note that cells in the center of the colony are F4/80$^+$ and CD206$^-$; cells on the periphery are F4/80$^-$ and CD206$^+$; cells in between are positive for both markers. Colony shown is from day 14 coculture. DAPI indicates staining for nucleus (blue). Scale bar, 50 μm (*$P < .05$; unpaired Student *t* test).

Evaluation of transcripts and immunofluorescence for M2-associated markers confirmed that the colony macrophages emerging from the coculture with each progenitor population were also alternatively activated (Figure 5C-D). This suggested that IMECs were able to support M2-like macrophage colony differentiation from all hematopoietic progenitors.

We also demonstrated that the colonies could be promptly induced from CD45$^+$ cells rather than CD45$^-$ cells. Surprisingly, Gr-1$^+$/Mac-1$^+$ cells were not able to induce colony formation on coculture, yet the Gr-1$^-$ population was able to generate macrophages on exposure to endothelial cells (supplemental Figure 6B-C).

Macrophages from colonies promote tumor growth and angiogenesis

Tumor associated macrophages (TAMs) have been generally considered as M2-polarized.[19] These cells have been shown to promote tumor growth and angiogenesis.[12,19] To test whether the colony macrophages could function as M2 macrophages in the tumor microenvironment, we coinjected these cells together with RM1 cells (murine prostate cancer cells) into wild type C57BL/6 mice. Resulting subcutaneous tumors were palpable by 6 days after injection and reached terminal point around day 12.

Tumors injected with colony macrophages exhibited faster growth kinetics compared with the control group. Although tumors from both groups were similar by day 7, the tumors coinjected with macrophages showed higher tumor volume at subsequent time points (Figure 6A). The proangiogenic function of colony macrophages in the tumors was also evaluated. CD31 staining revealed greater vascular density in the tumors that were injected with colony macrophages (Figure 6B-C). Quantification of the vascular area and vessel numbers also supported the proangiogenic role of these macrophages in vivo (Figure 6D-E).

The association of colony macrophages with capillaries was clearly noted in matrigel assays. Macrophages isolated from the cocultures were coinjected with IMECs in matrigel plugs. After 7 days, vascular networks were found highly decorated with macrophages (Figure 6F) simulating the intimate interaction between macrophages and blood vessels described in vivo.[20]

Discussion

In the last decade, interactions between endothelial cells and macrophages have been characterized in detail and their biologic consequences have started to be understood. Yet, as we gain further appreciation of the physical and functional relationships between macrophages and endothelial cells, additional questions arise. In particular: How do these interactions take place and what are the relevant molecular players? How and when does macrophage polarization occur? And does proliferation/expansion of macrophages take place in situ or does it require individual cell recruitment and differentiation? The work presented here demonstrates that endothelial cells can provide a selective niche for the

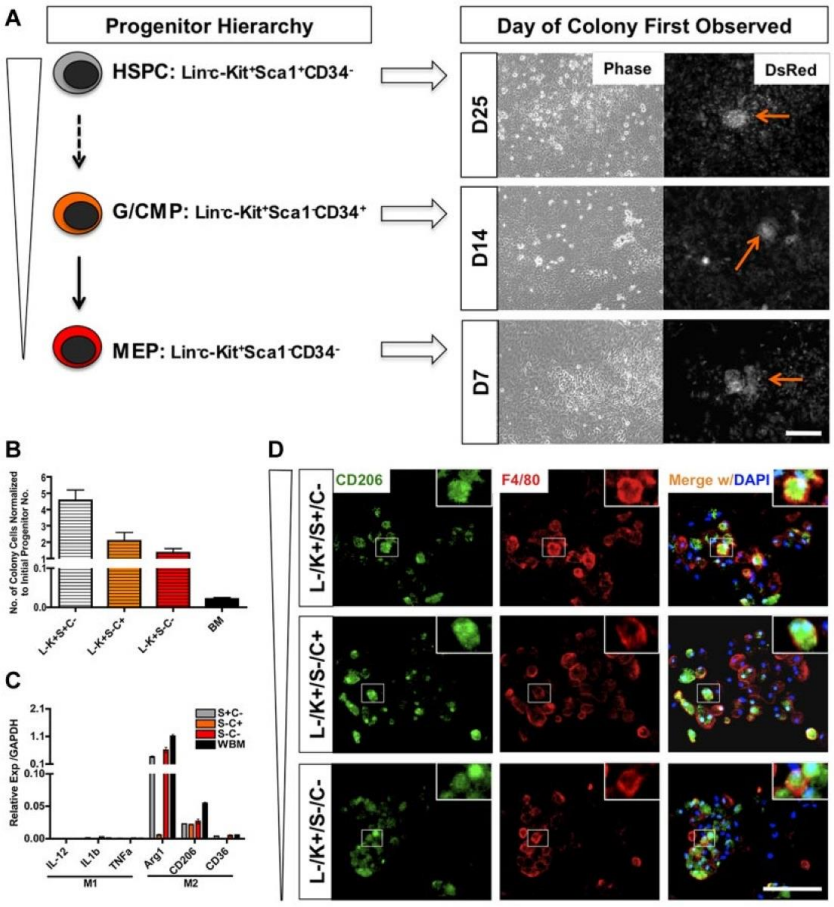

Figure 5. IMECs support macrophage differentiation from hematopoietic progenitors. (A) Schematic representation of hematopoietic progenitors evaluated and the time of emergence of macrophage colonies (right). HSPC indicates hematopoietic stem/progenitor cell; G/CMP, granulocyte-macrophage and common myeloid progenitor; and MEP, megakaryocyte-erythroid progenitor. Arrows indicate colonies. Scale bar, 200 μm. (B) Colony cell number at day 28 of cocultures was normalized to the initial number of progenitor cells plated (n = 6). (C) Colony cells from all progenitors moderately display M2 macrophage markers but lack M1 markers. Ctrl indicates colony cells from the coculture of whole bone marrow (WBM) cells and IMECs (n = 6). (D) Colonies from all progenitors expressed CD206/Mrc1 (M2 macrophage marker, green) and F4/80 (pan macrophage marker, red). Colonies shown are from d14 coculture. DAPI indicates staining for nucleus (blue). Scale bar, 100 μm.

differentiation and functional polarization of M2-like macrophages. We found that several types of adult endothelial cells shared this capacity and that endothelial-mediated macrophage differentiation could be triggered in hematopoietic progenitors at several stages of developmental progression. The growth-mediated properties imparted by endothelial cells were greatly dependent on their ability to activate CSF1R through production of CSF1. In turn, colony macrophages increased the stability of endothelial cell monolayers and provided a local source of VEGFA. We also found that macrophage colonies were M2-polarized and that the colonies exhibited a well-organized structure with poorly differentiated cells in the center and M2-polarized cells in the periphery (Figure 6G). More importantly, these endothelial-induced macrophages were able to associate with blood vessels and promote angiogenesis and tumor growth similarly to M2-like macrophages in vivo. These findings imply that the differentiation of macrophages, particularly M2-polarized cells such as TEMs, might be mediated by cell-cell interactions with the endothelium as these cells extravasate and gain residence in the vessel wall. Such instructive role of the vascular niche in promoting macrophage differentiation toward an M2-like, proangiogenic phenotype may well explain the reported association of $Tie^{2+}CD206/Mrc1^{+}$ TEMs with tumors blood vessels.[12,19]

The recent realization that the diversity of macrophage phenotypes also impacts their interaction and functional relationship with the endothelium has resolved some ongoing controversies.[21] In particular, there is increasing evidence that M1-like macrophages have angiostatic properties and do not necessarily associate with vessels. In contrast, M2-like macrophages tightly associate with endothelial cells and promote angiogenesis.[20] In this context, our findings that endothelial cells could effectively induce macrophage differentiation and M2-like polarization in vitro is consistent with a

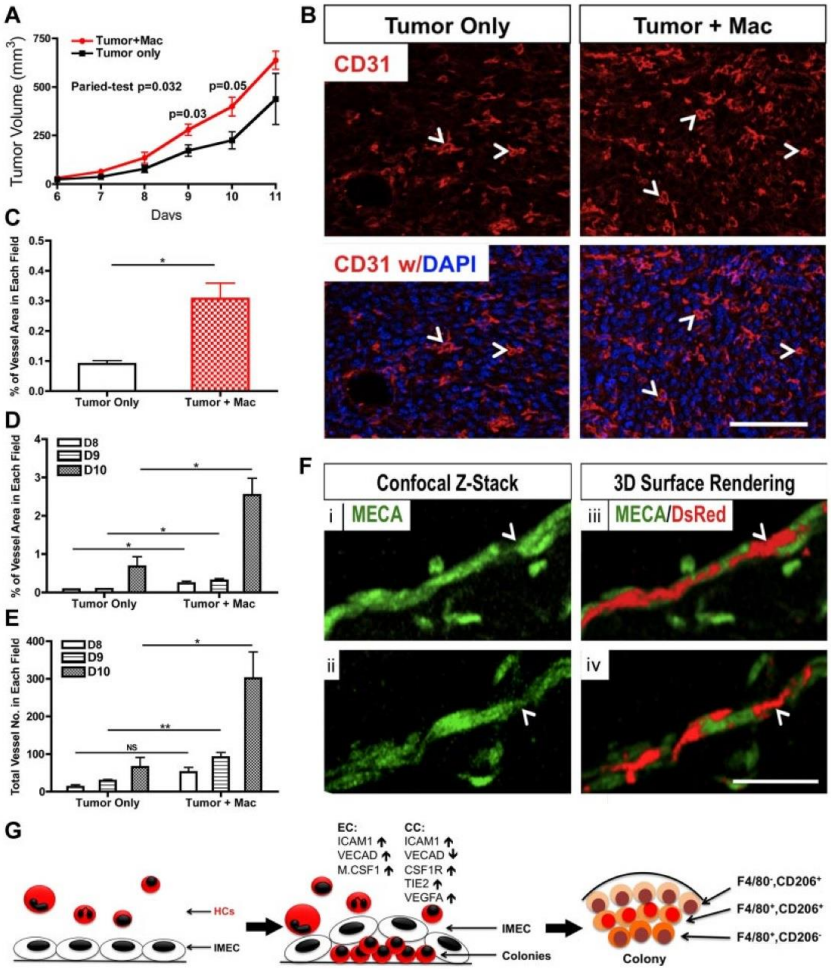

Figure 6. Macrophages derived from coculture promote tumor growth and angiogenesis. (A) Colony cells promote tumor growth in wild-type C57BL/6 mice. Mice were injected with RM1 tumor cells (1×10^5) alone or with colony cells (1×10^4; n = 3–5). (B) Representative pictures of tumor sections stained for CD31 (red). Tumors that were co-injected with colony cells showed a higher vascular density. Arrowhead indicates representative vessel. DAPI indicates staining for nuclei (blue). Scale bar, 100 μm. (C) Quantification (percentage) of vascular area in tumor sections shown in (B; n = 3). (D) Quantification of vessel area in tumor sections from indicated days (n = 3). (E) Quantification of vessel number in tumor sections from indicated days (n = 3). (F) Immunolabeling (i,ii) and 3D surface rendering (iii,iv) of colony cells (DsRed) and vessels (MECA, green) after colony cells and IMECs were injected with matrigel for 7 days. Colony cell (arrowhead) is bridging 2 endothelial cells. Scale bar, 50 μm. (G) Model of IMEC-induced M2 macrophage differentiation (*$P < .05$; **$P < .01$; unpaired Student *t* test).

productive and symbiotic relationship between these 2 cell types. The present studies now raise the question as to whether endothelial contact is largely (or solely) responsible for the induction of the M2 phenotype, whereas the M1 phenotype might be induced by different cells or through distinct mechanisms. Furthermore, if vessel-associated M2 macrophages continuously promote angiogenesis, what is the counteracting factor that inhibits the abnormal angiogenic response? In addition, it is unknown, at present, whether these macrophages are constitutively associated with the vasculature or only recruited by the endothelium under pathologic settings. If constitutively associated, are they inactive in their proangiogenic capacity during normal conditions?

Our understanding of macrophage heterogeneity is only rudimentary. The topic has been on the spotlight because of the widely diverse and important effects that each different subset of macrophages has on autoimmune disorders, microbial infections, and cancer.[22-24] The initial inflammatory response is typically conducted by classically activated (M1-like) macrophages.[23] In contrast, the resolution phase is driven by alternatively activated (M2-like) macrophages. The latter are known to be hyporesponsive to inflammatory stimuli, to drive tissue remodeling, promote wound healing, and accelerate angiogenesis.[20] Previous studies have shown that M2 polarization can be induced by specific cytokines and exposure of adherent macrophages to IL4.[25-27] Our

findings indicate that direct contact with the endothelium was necessary and sufficient for the induction of macrophage colonies and M2-like polarization; therefore it is unlikely that in this setting secreted factors alone would be sufficient. Instead, our findings demonstrate that endothelial cell contact is essential to initiate, support, and maintain M2-like macrophage colonies. Nonetheless, the identity of the cell adhesion molecules that drive the process is still unclear and subject to current investigations.

Cell-surface interactions between endothelial and HCs play essential roles in immune function and homeostasis.[5] In fact, heterotypic molecular activation plays a pivotal role in hematopoietic homing and in the inflammatory response. More recently endothelial cells have been proposed to constitute the bone marrow niche and support stem cell maintenance; as well as to regulate their differentiation.[6-8,28,29]Although soluble factors have been shown to promote HSCs, a rapid attrition is shown to occur in cell-free cultures.[30-35] On the other hand, the direct interaction of HSCs with stroma, and in particularly with endothelial cells has shown to be necessary to support long-term self-renewal and maintenance of these hematopoietic progenitors,[36-39] and more recently of HSCs.[7] Consistent with the latter, our data provided solid evidence to support that endothelial cells were able to capture, retain, and regulate the differentiation of macrophages through direct cell contact.

Our findings also indicate that in addition to cell contact, CSF1 is required for the expansion of the macrophage colonies. CSF1 is a key cytokine to support the differentiation of expansion of monocyte lineages. Deletion of Csf1 in mice (*op/op* mutant) greatly reduces the number of monocytes[40]; interestingly, macrophages are still present in various organs of *op/op* mice, such as liver, lung, and brain.[41] This has provoked the speculation as to the presence of alternative factors that could partially compensate for the crucial role of Csf1 in macrophage formation. In our study, the administration of GW2580, a small molecule that blocks CSF1R function, significantly reduced the expansion of macrophage colonies but did not inhibit their formation. Together the findings indicate that CSF1 is necessary for robust proliferation of macrophages but it does not appear to affect the process of differentiation.

The question as to whether macrophages proliferate while at the tissue of residence or are terminally differentiated without proliferative capacity has been subject to discussion. Several studies have provided support to the concept that tissue-resident macrophages proliferate locally.[42-44] In particular, a recent paper demonstrated that in response to IL-4, macrophages can replicate in situ in the absence of recruitment from the hematopoietic pool.[44] Interestingly, this is the same cytokine known to promote polarization toward the M2-like phenotype. Along these lines, the coculture system described here shows that endothelial-induced M2-like macrophages had proliferative capacity.

Finally, the actual source of macrophages is also an interesting puzzle. Although macrophages are believed to differentiate directly from monocytes during (or shortly after) extravasation from the blood stream, macrophages do exist in the embryo before the production of monocytes in the fetal liver.[45] This opens the argument: What is the origin of these macrophages? Can other progenitors give rise to macrophages? Is this only developmental or can it occur in adult settings? And can macrophage differentiation be "programmed" by the surrounding cells, particularly endothelial cells, on angiogenic sites? In this study, we have shown that in fact, monocytes ($Gr\text{-}1^+/Mac\text{-}1^+$) are not largely responsible for the formation of M2-polarized macrophage colonies; but rather, other progenitors at prior stages of differentiation gave rise to macrophage colonies when in contact with endothelium.

Acknowledgments

The authors thank Howard Lo and Ryan Freshman for their technical assistance, Calvin Pan for his bioinformatic assistance, the Tissue Procurement Core Laboratory Shared Resource, the Electron Microscopy Core Facility, the FACSCalibur Flow Cytometric Facility at the University of California, Los Angeles.

This work was supported by the California Institute for Regenerative Medicine Award (RB1-01328), CTSI (NIH/NCATS Grant UL1TR000124) and the grant from the Jonsson Cancer Center Foundation.

Authorship

Contribution: H.H., J.X., L.W., and M.L.I.A. designed the research; H.H., C.M.W., D.D., J.X., and X.L. performed the experiments; H.H., X.L., L.W., and M.L.I.A. analyzed the data; and H.H. and M.L.I.A. wrote the paper.

Conflict-of-interest disclosure: The authors declare no competing financial interests.

Correspondence: M. Luisa Iruela-Arispe, Department of Molecular, Cell, and Developmental Biology, Biomedical Sciences, Rm 447, UCLA, Los Angeles, CA; e-mail: arispe@mcdb.ucla.edu.

References

1. Zovein AC, Hofmann JJ, Lynch M, et al. Fate tracing reveals the endothelial origin of hematopoietic stem cells. *Cell Stem Cell.* 2008;3(6):625-636.
2. Chen M, Yokomizo T, Zeigler B, Dzierzak E, Speck N. Runx1 is required for the endothelial to haematopoietic cell transition but not thereafter. *Nature.* 2009;457(7231):887-891.
3. Eilken H, Nishikawa S, Schroeder T. Continuous single-cell imaging of blood generation from haemogenic endothelium. *Nature.* 2009;457(7231): 896-900.
4. Lancrin C, Sroczynska P, Stephenson C, Allen T, Kouskoff V, Lacaud G. The haemangioblast generates haematopoietic cells through a haemogenic endothelium stage. *Nature.* 2009; 457(7231):892-895.
5. Ley K, Laudanna C, Cybulsky MI, Nourshargh S. Getting to the site of inflammation: the leukocyte adhesion cascade updated. *Nat Rev Immunol.* 2007;7(9):678-689.
6. Heissig B, Hattori K, Dias S, et al. Recruitment of stem and progenitor cells from the bone marrow niche requires MMP-9 mediated release of kit-ligand. *Cell.* 2002;109(5):625-637.
7. Butler J, Nolan D, Vertes E, et al. Endothelial cells are essential for the self-renewal and repopulation of Notch-dependent hematopoietic stem cells. *Cell Stem Cell.* 2010;6(3):251-264.
8. Kobayashi H, Butler J, O'donnell R, et al. Angiocrine factors from Akt-activated endothelial cells balance self-renewal and differentiation of haematopoietic stem cells. *Nat Cell Biol.* 2010; 12(11):1046-1056.
9. Espinosa-Heidmann DG, Suner IJ, Hernandez EP, Monroy D, Csaky KG, Cousins SW. Macrophage depletion diminishes lesion size and severity in experimental choroidal neovascularization. *Invest Ophthalmol Vis Sci.* 2003;44(8):3586-3592.
10. Sakurai E, Anand A, Ambati BK, van Rooijen N, Ambati J. Macrophage depletion inhibits experimental choroidal neovascularization. *Invest Ophthalmol Vis Sci.* 2003;44(8):3578-3585.
11. Fantin A, Vieira JM, Gestri G, et al. Tissue macrophages act as cellular chaperones for vascular anastomosis downstream of VEGF-mediated endothelial tip cell induction. *Blood.* 2010;116(5): 829-840.
12. De Palma M, Venneri M, Galli R, et al. Tie2 identifies a hematopoietic lineage of proangiogenic monocytes required for tumor vessel formation and a mesenchymal population of pericyte progenitors. *Cancer Cell.* 2005;8(3):211-226.
13. Lin EY, Li JF, Bricard G, et al. Vascular endothelial growth factor restores delayed tumor progression in tumors depleted of macrophages. *Mol Oncol.* 2007;1(3):288-302.
14. Auffray C, Sieweke MH, Geissmann F. Blood monocytes: development, heterogeneity, and relationship with dendritic cells. *Annu Rev Immunol.* 2009;27:669-692.

15. Conway JG, McDonald B, Parham J, et al. Inhibition of colony-stimulating-factor-1 signaling in vivo with the orally bioavailable cFMS kinase inhibitor GW2580. *Proc Natl Acad Sci U S A*. 2005; 102(44):16078-16083.
16. Gordon S. Alternative activation of macrophages. *Nat Rev Immunol*. 2003;3(1):23-35.
17. Mosser DM. The many faces of macrophage activation. *J Leukoc Biol*. 2003;73(2):209-212.
18. Mantovani A, Sica A, Sozzani S, Allavena P, Vecchi A, Locati M. The chemokine system in diverse forms of macrophage activation and polarization. *Trends Immunol*. 2004;25(12):677-686.
19. Mazzieri R, Pucci F, Moi D, et al. Targeting the ANG2/TIE2 axis inhibits tumor growth and metastasis by impairing angiogenesis and disabling rebounds of proangiogenic myeloid cells. *Cancer Cell*. 2011;19(4):512-526.
20. Ruhrberg C, De Palma M. A double agent in cancer: deciphering macrophage roles in human tumors. *Nat Med*. 2010;16(8):861-862.
21. Lamagna C, Aurrand-Lions M, Imhof BA. Dual role of macrophages in tumor growth and angiogenesis. *J Leukoc Biol*. 2006;80(4):705-713.
22. Allavena P, Sica A, Garlanda C, Mantovani A. The Yin-Yang of tumor-associated macrophages in neoplastic progression and immune surveillance. *Immunol Rev*. 2008;222:155-161.
23. Martinez FO, Sica A, Mantovani A, Locati M. Macrophage activation and polarization. *Front Biosci*. 2008;13:453-461.
24. Sica A, Larghi P, Mancino A, et al. Macrophage polarization in tumour progression. *Semin Cancer Biol*. 2008;18(5):349-355.
25. Munder M, Eichmann K, Modolell M. Alternative metabolic states in murine macrophages reflected by the nitric oxide synthase/arginase balance: competitive regulation by CD4+ T cells correlates with Th1/Th2 phenotype. *J Immunol*. 1998;160(11):5347-5354.
26. Raes G, De Baetselier P, Noël W, Beschin A, Brombacher F, Hassanzadeh Gh G. Differential expression of FIZZ1 and Ym1 in alternatively versus classically activated macrophages. *J Leukoc Biol*. 2002;71(4):597-602.
27. Nair MG, Cochrane DW, Allen JE. Macrophages in chronic type 2 inflammation have a novel phenotype characterized by the abundant expression of Ym1 and Fizz1 that can be partly replicated in vitro. *Immunol Lett*. 2003;85(2):173-180.
28. Kiel MJ, Yilmaz OH, Iwashita T, Yilmaz OH, Terhorst C, Morrison S. SLAM family receptors distinguish hematopoietic stem and progenitor cells and reveal endothelial niches for stem cells. *Cell*. 2005;121(7):1109-1121.
29. Ding L, Saunders T, Enikolopov G, Morrison S. Endothelial and perivascular cells maintain haematopoietic stem cells. *Nature*. 2012; 481(7382):457-462.
30. Miller CL, Eaves CJ. Expansion in vitro of adult murine hematopoietic stem cells with transplantable lympho-myeloid reconstituting ability. *Proc Natl Acad Sci U S A*. 1997;94(25):13648-13653.
31. Varnum-Finney B, Xu L, Brashem-Stein C, et al. Pluripotent, cytokine-dependent, hematopoietic stem cells are immortalized by constitutive Notch1 signaling. *Nat Med*. 2000;6(11):1278-1281.
32. Antonchuk J, Sauvageau G, Humphries RK. HOXB4-induced expansion of adult hematopoietic stem cells ex vivo. *Cell*. 2002;109(1):39-45.
33. Krosl J, Austin P, Beslu N, et al. In vitro expansion of hematopoietic stem cells by recombinant TAT-HOXB4 protein. *Nat Med*. 2003;9(11):1428-1432.
34. Willert K, Brown JD, Danenberg E, et al. Wnt proteins are lipid-modified and can act as stem cell growth factors. *Nature*. 2003;423(6938):448-452.
35. Zhang CC, Kaba M, Ge G, et al. Angiopoietin-like proteins stimulate ex vivo expansion of hematopoietic stem cells. *Nat Med*. 2006;12(2):240-245.
36. Yildirim S, Boehmler AM, Kanz L, Möhle R. Expansion of cord blood CD34+ hematopoietic progenitor cells in coculture with autologous umbilical vein endothelial cells (HUVEC) is superior to cytokine-supplemented liquid culture. *Bone Marrow Transplant*. 2005;36(1):71-79.
37. Freund D, Bauer N, Boxberger S, et al. Polarization of human hematopoietic progenitors during contact with multipotent mesenchymal stromal cells: effects on proliferation and clonogenicity. *Stem Cells Dev*. 2006;15(6):815-829.
38. Wagner W, Wein F, Roderburg C, et al. Adhesion of hematopoietic progenitor cells to human mesenchymal stem cells as a model for cell-cell interaction. *Exp Hematol*. 2007;35(2):314-325.
39. Alakel N, Jing D, Muller K, Bornhauser M, Ehninger G, Ordemann R. Direct contact with mesenchymal stromal cells affects migratory behavior and gene expression profile of CD133+ hematopoietic stem cells during ex vivo expansion. *Exp Hematol*. 2009;37(4):504-513.
40. Cecchini MG, Dominguez MG, Mocci S, et al. Role of colony stimulating factor-1 in the establishment and regulation of tissue macrophages during postnatal development of the mouse. *Development*. 1994;120(6):1357-1372.
41. Witmer-Pack MD, Hughes DA, Schuler G, et al. Identification of macrophages and dendritic cells in the osteopetrotic (op/op) mouse. *J Cell Sci*. 1993;104(4):1021-1029.
42. Chorro L, Sarde A, Li M, et al. Langerhans cell (LC) proliferation mediates neonatal development, homeostasis, and inflammation-associated expansion of the epidermal LC network. *J Exp Med*. 2009;206(13):3089-3100.
43. Davies LC, Rosas M, Smith PJ, Fraser DJ, Jones SA, Taylor PR. A quantifiable proliferative burst of tissue macrophages restores homeostatic macrophage populations after acute inflammation. *Eur J Immunol*. 2011;41(8):2155-2164.
44. Jenkins SJ, Ruckerl D, Cook PC, et al. Local macrophage proliferation, rather than recruitment from the blood, is a signature of TH2 inflammation. *Science*. 2011;332:1284-1288.
45. Pucci F, Venneri M, Biziato D, et al. A distinguishing gene signature shared by tumor-infiltrating Tie2-expressing monocytes, blood "resident" monocytes, and embryonic macrophages suggests common functions and developmental relationships. *Blood*. 2009;114(4):901-914.